Edited by:

**UNIVERSITY POLITEHNICA TIMISOARA**



with kindly supported by:

**THE GENERAL ASSOCIATION OF ROMANIAN ENGINEERS (AGIR)
– branch of HUNEDOARA**



Editor / Technical preparation / Cover design:

Assoc. Prof. Eng. KISS Imre, PhD.
UNIVERSITY POLITEHNICA TIMISOARA,
FACULTY OF ENGINEERING HUNEDOARA

Commenced publication year:
2008

# ASSOCIATE EDITORS and
# REGIONAL COLLABORATORS

The Editor and editorial board members do not receive any remuneration. These positions are voluntary. The members of the Editorial Board may serve as scientific reviewers.

We are very pleased to inform that our journal ACTA TECHNICA CORVINIENSIS – Bulletin of Engineering is going to complete its ten years of publication successfully. In a very short period it has acquired global presence and scholars from all over the world have taken it with great enthusiasm. We are extremely grateful and heartily acknowledge the kind of support and encouragement from you.

ACTA TECHNICA CORVINIENSIS – Bulletin of Engineering seeking qualified researchers as members of the editorial team. Like our other journals, ACTA TECHNICA CORVINIENSIS – Bulletin of Engineering will serve as a great resource for researchers and students across the globe. We ask you to support this initiative by joining our editorial team. If you are interested in serving as a member of the editorial team, kindly send us your resume to redactie@fih.upt.ro.

# INTERNATIONAL SCIENTIFIC COMMITTEE MEMBERS and SCIENTIFIC REVIEWERS

## MANAGER & CHAIRMAN

**ROMANIA** **Imre KISS**, University Politehnica TIMISOARA, Faculty of Engineering HUNEDOARA, Department of Engineering & Management, General Association of Romanian Engineers (AGIR) – branch HUNEDOARA

## INTERNATIONAL SCIENTIFIC COMMITTEE MEMBERS & SCIENTIFIC REVIEWERS from:

**ROMANIA**
**Viorel–Aurel ŞERBAN**, University Politehnica TIMIŞOARA – TIMIŞOARA
**Teodor HEPUŢ**, University Politehnica TIMIŞOARA – HUNEDOARA
**Caius PĂNOIU**, University Politehnica TIMIŞOARA – HUNEDOARA
**Mircea BEJAN**, Tehnical University of CLUJ-NAPOCA – CLUJ-NAPOCA
**Liviu MIHON**, University Politehnica TIMIŞOARA – TIMIŞOARA
**Ilare BORDEAŞU**, University Politehnica TIMIŞOARA – TIMIŞOARA
**Corneliu CRĂCIUNESCU**, University Politehnica TIMIŞOARA – TIMIŞOARA
**Liviu MARŞAVIA**, University Politehnica TIMIŞOARA – TIMIŞOARA
**Nicolae HERIŞANU**, University Politehnica TIMIŞOARA – TIMIŞOARA
**Dumitru TUCU**, University Politehnica TIMIŞOARA – TIMIŞOARA
**Valer DOLGA**, University Politehnica TIMIŞOARA – TIMIŞOARA
**Ioan VIDA-SIMITI**, Technical University of CLUJ-NAPOCA – CLUJ-NAPOCA
**Csaba GYENGE**, Technical University of CLUJ-NAPOCA – CLUJ-NAPOCA
**Sava IANICI**, "Eftimie Murgu" University of REŞIŢA – REŞIŢA
**Ioan SZÁVA**, "Transilvania" University of BRASOV – BRASOV
**Liviu NISTOR**, Technical University of CLUJ-NAPOCA – CLUJ-NAPOCA
**Sorin VLASE**, "Transilvania" University of BRASOV – BRASOV
**Horatiu TEODORESCU DRĂGHICESCU**, "Transilvania" University of BRASOV – BRASOV
**Maria Luminiţa SCUTARU**, "Transilvania" University of BRASOV – BRASOV
**Iulian RIPOŞAN**, University Politehnica BUCUREŞTI – BUCUREŞTI
**Ioan DZITAC**, Agora University of ORADEA – ORADEA
**Daniel STAN**, University Politehnica TIMIŞOARA – TIMIŞOARA
**Adrian STUPARU**, University Politehnica TIMIŞOARA – TIMIŞOARA
**Corina GRUESCU**, University Politehnica TIMIŞOARA – TIMIŞOARA
**Carmen ALIC**, University Politehnica TIMIŞOARA – HUNEDOARA

**SLOVAKIA**
**Štefan NIZNIK**, Technical University of KOŠICE – KOŠICE
**Karol VELIŠEK**, Slovak University of Technology BRATISLAVA – TRNAVA
**Juraj ŠPALEK**, University of ŽILINA – ŽILINA
**Ervin LUMNITZER**, Technical University of KOŠICE – KOŠICE
**Miroslav BADIDA**, Technical University of KOŠICE – KOŠICE
**Milan DADO**, University of ŽILINA – ŽILINA
**Ladislav GULAN**, Slovak University of Technology – BRATISLAVA
**Ľubomir ŠOOŠ**, Slovak University of Technology in BRATISLAVA – BRATISLAVA
**Miroslav VEREŠ**, Slovak University of Technology in BRATISLAVA – BRATISLAVA
**Milan SAGA**, University of ŽILINA – ŽILINA
**Imrich KISS**, Institute of Economic & Environmental Security – KOŠICE
**Michal CEHLÁR**, Technical University KOSICE – KOSICE
**Pavel NEČAS**, Armed Forces Academy of General Milan Rastislav Stefanik – LIPTOVSKÝ MIKULÁŠ
**Vladimir MODRAK**, Technical University of KOSICE – PRESOV
**Michal HAVRILA**, Technical University of KOSICE – PRESOV

**CROATIA**
**Drazan KOZAK**, Josip Juraj Strossmayer University of OSIJEK – SLAVONKI BROD
**Predrag COSIC**, University of ZAGREB – ZAGREB
**Milan KLJAJIN**, Josip Juraj Strossmayer University of OSIJEK – SLAVONKI BROD
**Miroslav CAR**, University of ZAGREB – ZAGREB
**Antun STOIĆ**, Josip Juraj Strossmayer University of OSIJEK – SLAVONKI BROD
**Ivo ALFIREVIĆ**, University of ZAGREB – ZAGREB

**GREECE**
**Nicolaos VAXEVANIDIS**, University of THESSALY – VOLOS

The Scientific Committee members and Reviewers do not receive any remuneration. These positions are voluntary.

We are extremely grateful and heartily acknowledge the kind of support and encouragement from all contributors and all collaborators!

ACTA TECHNICA CORVINIENSIS – Bulletin of Engineering is dedicated to publishing material of the highest engineering interest, and to this end we have assembled a distinguished Editorial Board and Scientific Committee of academics, professors and researchers.

ACTA TECHNICA CORVINIENSIS – Bulletin of Engineering publishes invited review papers covering the full spectrum of engineering. The reviews, both experimental and theoretical, provide general background information as well as a critical assessment on topics in a state of flux. We are primarily interested in those contributions which bring new insights, and papers will be selected on the basis of the importance of the new knowledge they provide.

ACTA TECHNICA CORVINIENSIS – Bulletin of Engineering encourages the submission of comments on papers published particularly in our journal. The journal publishes articles focused on topics of current interest within the scope of the journal and coordinated by invited guest editors. Interested authors are invited to contact one of the Editors for further details.

ACTA TECHNICA CORVINIENSIS – Bulletin of Engineering accept for publication unpublished manuscripts on the understanding that the same manuscript is not under simultaneous consideration of other journals. Publication of a part of the data as the abstract of conference proceedings is exempted.

Manuscripts submitted (original articles, technical notes, brief communications and case studies) will be subject to peer review by the members of the Editorial Board or by qualified outside reviewers. Only papers of high scientific quality will be accepted for publication. Manuscripts are accepted for review only when they report unpublished work that is not being considered for publication elsewhere. The evaluated paper may be recommended for:

✓ **Acceptance without any changes** – in that case the authors will be asked to send the paper electronically in the required .doc format according to authors' instructions;
✓ **Acceptance with minor changes** – if the authors follow the conditions imposed by referees the paper will be sent in the required .doc format;
✓ **Acceptance with major changes** – if the authors follow completely the conditions imposed by referees the paper will be sent in the required .doc format;
✓ **Rejection** – in that case the reasons for rejection will be transmitted to authors along with some suggestions for future improvements (if that will be considered necessary).

The manuscript accepted for publication will be published in the next issue of ACTA TECHNICA CORVINIENSIS – Bulletin of Engineering after the acceptance date.

# TABLE of CONTENTS

The **ACTA TECHNICA CORVINIENSIS – Bulletin of Engineering, Tome XI [2018], Fascicule 3 [July – September]** include original papers submitted to the Editorial Board, directly by authors or by the regional collaborators of the Journal.

[1.]A. ABDULKARIM, [2.]S.M. ABDELKADER, [3.]D.J. MORROW, [4.]SAY AMUDA, [5.]I.S. MADUGU,
[6.]A.J. FALADE, [7.]S. SAMINU, [8.]Y.A. ADEDIRAN

# EFFECTS OF PV AND BATTERY STORAGE TECHNOLOGIES ON THE OPTIMAL SIZING OF RENEWABLE ENERGY MICROGRID

[1,6,8.]Department of Electrical & Electronics Engineering, University of Ilorin, NIGERIA
[2.]Department of Electrical Engineering, Mansoura University, Mansoura, EGYPT
[3.]School of Electronics, Electrical Engineering and Computer Science, Queen's University, Belfast, UNITED KINGDOM
[4.]Department of Computer Engineering, University of Ilorin, NIGERIA
[5.]Department of Electrical Engineering, Kano University of Science and Technology, Wudil, NIGERIA
[4.]Department of Biomedical Engineering, University of Ilorin, NIGERIA

**Abstract:** This paper presents analyses of the model for the optimum design of standalone hybrid microgrid. The model is developed with the aim of optimizing system component sizing that can reliably satisfy isolated loads. The objective function is to minimize the annual cost of the plant while taking all constraints into consideration. Mixed integer linear programming technique is used to solve the optimization problem. By applying some approximations, the output power of the wind energy conversion system is expressed as a linear function of wind speed. Effects of different PV technologies and the rated power of each unit have been investigated. The results have shown the ability of the proposed model by reducing the cost of energy by 89.35%, 90.26%, 88.3530%, and 89.99% for AP120, ASE 300, KC120 and SAPC165 respectively. In the same way the carbon dioxide emission is reduced by 83%, 82.82%, 82.51% and 73.48 in the same order of the PV modules. Also, the optimal design is sensitive to the rated power of the WECS and SECS. In addition, the benefit-to-cost ratio, payback period are sensitive to the storage technology.
**Keywords:** Renewable Energy, Wind, PV, Battery Storage and diesel generator

## GENERAL INTRODUCTION

Isolated loads and rural communities rely on the use of diesel generators for their daily energy needs. Fortunately, some of these places are blessed with renewable energy resources such as wind and solar power [1]. It has been suggested that these renewable energy resources be used to support the existing diesel generator. Due to the nature of the output power of the renewable energy resources, there is a need to add storage unit. Therefore, in order to achieve continuous, economical and reliable energy supply to these loads, there is a need to use all the mentioned resources together. Also, it is necessary to supply isolated loads with constant frequency and continuous electricity. These requirements make the design of a standalone microgrid very complex. In order to achieve these it is paramount to design all the parts correctly; therefore proper sizing methodology of the hybrid microgrid system is required [2]. The design of the proposed system is site-specific and depends on the amount of renewable energy generation, cost prices of diesel and load [3].

Several efforts have been done in the optimum design of hybrid microgrid. Particle swarm optimizations have been proposed in [4]- [5]. In [4], the system designed considered uncertainty in load, wind and solar radiation by modifying the particle swarm optimization. Optimum design of hybrid system consisting of wind, diesel generator and battery storage system has been proposed in [5], the design determines the reliability of the system considering component failures. Generally are three main approaches in the optimal configuration of hybrid system technically and

economically. This includes iterative, the probabilistic and trade-off approaches [11].

Also, other factors such as PV technology, temperature, customer damage functions that may affect the optimum configurations have not been given the expected attention. For realistic planning, there is the need to analyse the effects of these factors on the optimal design of microgrid. Hence the need for the development of another methodology that could be used in order to analysed effects of some of them in the optimal design of a standalone microgrid. This paper presents the optimal design of standalone microgrid considering the penalty as a result of carbon emission into the atmosphere. In addition, the effects of different types of PV systems and the rated power of each unit on the optimal system configuration have been investigated. In distinct to other literatures, the effects of different PV technology on the the optimum design of microgrids is considered in this work using AP120, ASE300, KC120 and SAPC145 [12]- [13]. Also, the effect of storage technology on the cost of energy for optimum design which has not been given the necessary attention was investigated using lead acid battery, nickel-cadmium battery, Sodium-polysilfied batteries, electrochemical capacitor, SMES, Flywheel energy storage, Sodium-Sulpur batteries, Zinc-Bromine batteries, VRB and batteries.

## SYSTEM CONFIGURATION AND OPERATIONS

In this section, a schematic diagram of the proposed hybrid system is presented in Figure 1. It can be seen that the

proposed system has five major building blocks. These include Wind Energy Conversion System (WECS), Solar Energy Conversion System (SECS), Storage system, Diesel Generator (DG) and Static Energy Conversion System (STECS). These components operate in parallel to guarantee continuous power supply to the load. The storage system is connected to reduce the fluctuations and store the excess power produced by the renewable energy sources. When the power produced by the two renewable energy sources is less than the demand, the battery supply the deficit. On the other hand, when the power supplies by both renewable energy sources and the battery is less than the demand, the diesel generator operates to supply the deficit.
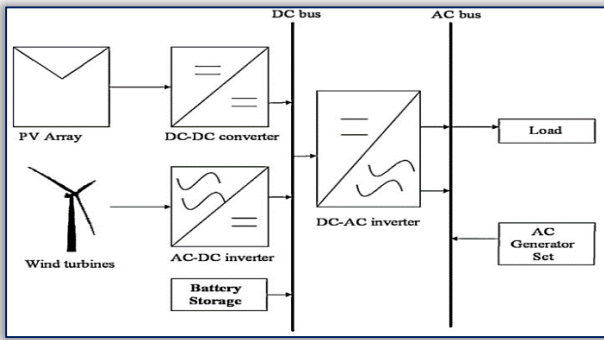


Figure 1: Proposed hybrid Microgrid

## ⊞ Output power of WECS

The power output of wind energy conversion system is a function of the wind speed, these results in different design alternatives [14]- [15]. Therefore, the power output of wind energy conversion system is expressed as a function of rated capacity and a variable that is a function of the wind speed. Modelling using this approach, the number of the wind turbine generator is modelled as a decision variable, such that, the model decides on the capacity for each design. This presentation enables to linearly approximate the wind speed and output power in the range cut-In velocity and the rated velocity of the wind turbine generator ($V_{ci} < V < V_r$) [16]. After the random distribution is obtained, the power output of the WECS is expressed as a function of wind speed and determined using equation (1),

$$P(v) = \propto P_r \qquad (1)$$

$$\propto = \begin{cases} \frac{V_i - V_{ci}}{V_r - V_{ci}} & V_{ci} < V < V_r \\ 1.0 & V_r \leq V < V_{co} \\ 0 & V \leq V_{ci} \text{ or } V \geq V_{co} \end{cases} \qquad (2)$$

$\propto_{i,k}$ is a constant, and it can be observed that the output power can be determined as a piecewise linear relationship of the rated capacity ($P_r$). Therefore, the rated capacity of the WECS can be used as a decision variable. Hence, the model decides on the number of wind turbines for each design.

## ⊞ Output power of SECS

This section presents the model used for the determination of the output power of the SECS. In [17]- [8], many models are proposed depending on the application. The proposed model utilized factors such as temperature, number of series and parallel connected cells. Also, it operates under standard test condition, light intensity, and the ambient temperature. This presentation enables to study the effects of other factor that were not analyzed in the literature [12]. The model used in the analysis is expressed according to the following expressions. Initially, the short circuit current of the PV module is defined [13]. Models presented in [18] are combined together formulated the expression of the output power of the SECS as

$$\text{PSEC}(T) = I_{MP}(T) * V_{MP}(T) * N_{PV} \qquad (3)$$

where, $\text{PSEC}$ : PV output power: solar radiation of the operating point, $I_{mp}$ and $V_{mp}$ are the maximum point current and voltage.

Equation (3) enables to use the number of the PV panels as part of the design variable. The output of the SECS is made of a number of the PV panels connected in series ($N_{PV}$) and parallel ($N_{PV.P}$). Therefore, the model determines the total number of connected PV panels. Depending on the application the PV panels may be connected in parallel for higher current or in series for higher voltage.

## OBJECTIVE FUNCTION

The objective function is developed to minimize the annual cost of the system. Therefore, objective function $F_{min}(X)$ to be minimized is defined as follows,

$$F_{min}(X) = ACC(x) + AOM(x) + ARC(x)$$
$$+AFC(x) + AEC(x) \qquad (4)$$

where, $ACC(x), AOM(x), ARC(x), \ AFC(x)$ and $AEC(x)$ are the Annual Capital Cost, Annual Operating and Maintenance, Annual Recovery Cost Annual Fuel Cost and Annual Carbon emission costs respectively [14].

In this arrangement, the diesel generator operates only when the energy supply of the renewable resources and the battery cannot meet demand. Therefore, for every interval, the penalty; as a result of carbon emission is determined. The emission factor is assumed to be in the range of 30-50 $/Ton [19]. The expression of the determination of the AEC is defined in equation (5),

$$AEC(x) = \sum_{t=1}^{T} \frac{E_f * E_{cf} * P_{DG}(t)}{1000} \qquad (5)$$

## CONSTRAINTS

The constraints in this optimization maintain a balance between the power generation and system demand. In this case, the constraints are classified under three main sub headings. These include power balance, energy balance and component rating constraints as defined in eqs. (6)-(13).

$$PD_i + PWR_i + PSR_i + \eta_D \times q_{Di} - {q_{ci}}/{\eta_c} = P_{Li} \qquad (6)$$

$$\sum_{i=1}^{T} q_{Di} \times \Delta t_i = \sum_{i=1}^{T} q_{ci} \times \Delta t_i \qquad (7)$$

$$ES_i + q_{Di} \times \Delta t_i - ES_{i-1} - q_{ci} \times \Delta t_i = 0 \qquad (8)$$

$$ES_i - QS \leq 0 \qquad (9)$$

$$ES_i - \gamma . QS \geq 0 \qquad (10)$$

$$PD_r - PD_i \geq 0 \qquad (11)$$

$$PINV - PWR_i \times +PSR_i \times +\eta_D \times q_{Di} \geq 0 \qquad (12)$$

$$PINV - PD_i + P_L \geq 0 \qquad (13)$$

where, PDr, PWR, PSR, PINV and QS are the rated power per units for diesel generator, wind turbine generator, PV system and battery storage respectively, $q_{Di}$, $q_{ci}$, $\eta_c$: charging,

discharging power and efficiency of the storage unit, $\mathbf{ES}$: energy stored in the storage unit and $\mathbf{P_L}$: load demand. The model thereby, determined the optimal number of PV panels, wind turbine generators, diesel generators, storage and the inverter-rectifier units. In addition, the model also, decides on the output powers of the diesel generator and the storage levels at each interval. Due to the nature of the objective function, constraints and the expected output of the model, Mixed Integer Programming (MIP) is used to solve the optimization problem.

## APPLICATION OF THE MODEL

In order to test the application of the proposed design procedure, the assumed rated power of each unit are presented in Tables 1. In addition, more details on the PV module specifications are can be found in [13]- [20]. In addition, the cost data of each unit can be found in [9]-[10].

Table 1: Rate power of the base case

| Number | Rated power |
|---|---|
| WT | 100 kW |
| PV | 8 kW |
| DG | 100 kW |
| Battery | 185 kWh |
| Inverter-Rectifier | 100 kW |

The output of the optimization procedure is shown in Table 2. According to the AP120 module, the system contained 3x100 kW WT, 12x8 kW PV, 2x100 kW diesel generator, 1x185 kWh storage and 1x100kW rectifier-inverter unit. In the same way, the optimal configuration for the ASE300 module is 3x100 kW, 1x8 kW, 1x100 kW and 1x185 kWh, 1x100kW of WECS, SECS, diesel generator, storage system and 1x100kW of rectifier-inverter unit respectively. KC120 module configuration include 3x100 kW, 2x8 kW, 1x100 kW, 1x185 kWh, and 1x100 kW of rectifier-inverter. Finally, SAPC145 has 3x100 kW of WECS, 1x8 kW SECS, 2x100 kW DG and 1x100 kW inverter-rectifier unit.

Table 2: Output of the optimization

| Type of PV | AP120 | ASE300 | KC120 | SAPC165 |
|---|---|---|---|---|
| WT | 3 | 3 | 3 | 3 |
| PV | 12 | 1 | 2 | 1 |
| DG | 1 | 1 | 1 | 2 |
| Battery | 1 | 1 | 1 | 0 |
| Inverter-Rectifier | 2 | 1 | 1 | 1 |
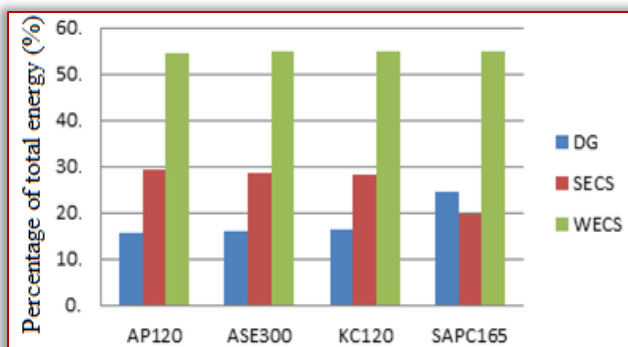


Figure 2: Energy contribution of each PV technology

Critical examination of the results have shown that PV module technology affects the optimal design of standalone microgrid. In terms of energy contribution, WECS contributes more, followed by SECS and DG has the least contribution in all the PV modules analysed. The energy contribution of the SECS depends on the PV technology. In Figure 2, the energy contributions of SECS of each PV module is 29.4014%, 28.6885%, 28.3491% and 19.9344% for AP120, ASE300, KC120 and SAPC14 respectively. AP120 module is best for the environment due to the low power output of the DG unit.

Table 3: Cost of energy

| Energy cost | AP120 | ASE300 | KC120 | SAPC165 |
|---|---|---|---|---|
| DG | 0.1099 | 0.1099 | 0.1099 | 0.1099 |
| Hybrid | 0.0117 | 0.0107 | 0.0128 | 0.0110 |

The energy cost of each technology is shown in Table 3. It can be observed that ASE300 has the least energy cost, followed by SAPC145, AP120 and KC120 offers typo expansive. The result in Figure 4 shows that the annual carbon penalty cost is 3590$, 3639 $, 3995 $ and 3703$ for AP120, ASE300, KC120 and SAPC165 respectively. On the other hand, the penalty cost due to carbon emission as a result of the DG operation is 21,174$/yr. These have shown an 83.0%, 82.82%, 82.51% and 73.48 carbon savings for the AP120, ASE300, KC120 and SAPC165 respectively. It can be observed that the penalty cost is also sensitive to the PV module technology. Therefore, AP120 module is the most suitable for the environment.
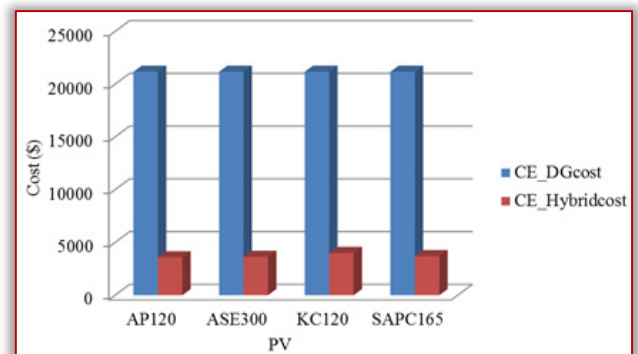


Figure 3: Annual carbon emission for each technology

## ⊞ Effects of the rated power of each unit

The proposed method is suitable to study the effects of the rated power of each unit in the optimal design. In order to achieve this, the rated power of each unit is increased by 25%, 50% and 75%. The effects of this variation on the optimal design of the system have been studied in this section. The results are presented in Figures 4-7 for AP120 technology. Variations of the optimal design with rated power of WECS are shown in Figures 4. The effects of the rated power of SECS on the optimal design are also presented in Figure 5. Similarly, Figure 6 shows the optimal configuration considering rated power of DG. Optimal design considering increases in the rated power of the storage system is also shown in Figure 7. In general, the variation depends on the PV technologies. It has been observed that as the rated power increased, the number of energy units decreased. The result shows that in addition to the PV technology, the optimal design is sensitive to the rated power of the WECS and SECS.
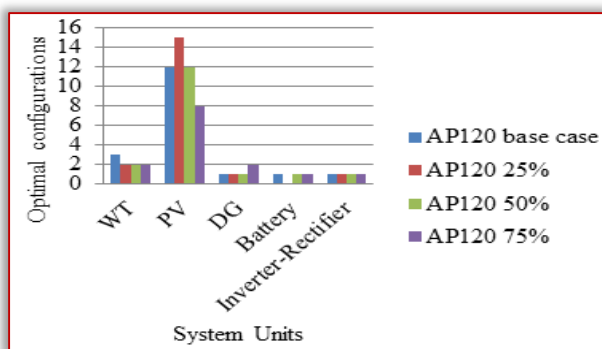
Figure 4: Variation of the rated power of WECS
for the AP120 module
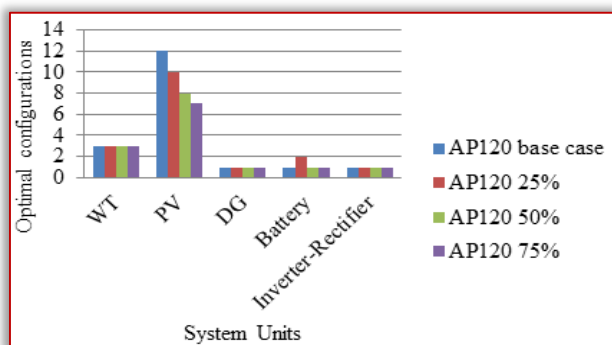


Figure 5: Variation of the rated power of SECS
for the AP120 module
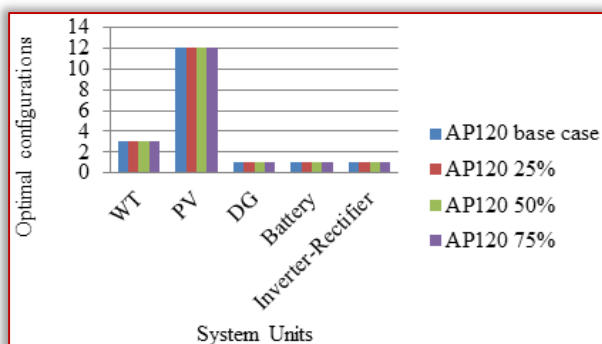


Figure 6: Variation of the rated power of DG
for the AP120 module
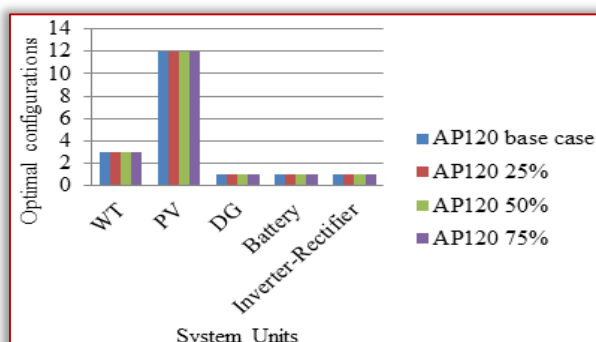


Figure 7: Variation of the rated power of storage
for the AP120 module

On the other hand, the optimal design is not sensitive to the rated power of the storage and the DG generator. The result shows the case of AP120 PV module only, other modules analyzed are not shown here. Other PV modules analyzed are not shown here for the sake of brevity.

## ⊞ Effects of storage technology on the optimum design

In this section, the effects of different energy technology on the optimum system configuration is considered. Some of the literature in the storage for the stand-alone microgrid were presented in [21] and [22]. In [21], the optimal ratings of different battery technology were analysed for minimizing the energy cost of wind-diesel microgrid. In [22], scheduling of a storage connected to isolated microgrid based on the knowledge expert system is proposed. Due to the result in the section 7.0, the analysis in this section is based on the AP120 PV module alone. Hence, more details about the storage technologies can be found in [21].

The data of each battery storage is shown in Table 4 and the results of different opimizations are presented in Table 5. The most sensitive component is the cost of energy ($/kWh), it actually changes with technology. It can be observed that lead acid, Sodium Polysulfide, ZBB and VRB batteries have lower cost of energy. This is followed by PSB, LI-ion, NI-Cad and Na-S in that order. Battery storages that have a lifespan greater than the project life are not considered. These include Electrochemical Capacitors, SMES and Flywheel energy storage systems. Also, their capital cost is very high compared to project cost, therefore it is assumed not suitable for the proposed application.

Table 4: Specifications of the battery

|  | Capital cost ($) | Energy rating (MW) | life (yrs) | energy eff. | charging eff. | Discharge eff. |
|---|---|---|---|---|---|---|
| Lead acid | 50-150 | 0.001-40 | 5-15 | 70-80 | 95 | 80 |
| Na-S | 200-600 | 0.4-244.8 | 10-20 | 75-89 | 99 | 88 |
| LI-ion | 900-1300 | 0.001-50 | 14-16 | 75-95 | 99 | 95 |
| VRB | 600 | 2-120 | 10-20 | 65-85 | 98 | 85 |
| PSB | 300-1000 | 0.005-120 | 15 | 60-75 | 90 | 75 |
| ZBB | 500 | 0.1-4 | 8-10 | 65-85 | 98 | 85 |
| NI-Cad | 1197 |  | 10-15 |  | 85 | 65 |

Table 5: Impacts of battery technology on the energy price

| Battery | Lead acid | Na-S | LI-ion | VRB |
|---|---|---|---|---|
| Energy cost ($/kWh) | 0.01228 | 0.01386 | 0.01336 | 0.01312 |
| Battery | PSB | ZBB | NI-Cad |  |
| Energy cost ($/kWh) | 0.0133 | 0.0131 | 0.0134 |  |
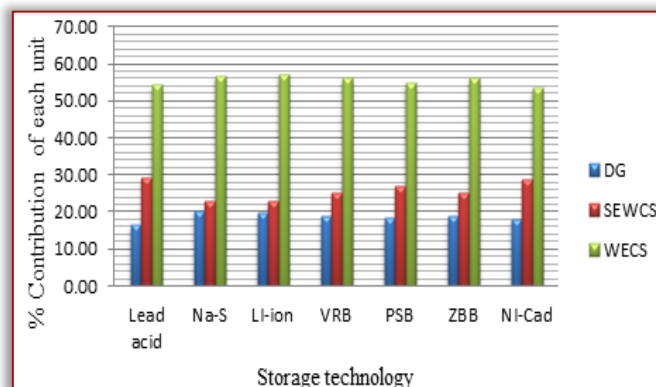


Figure 8: Energy contribution of different units
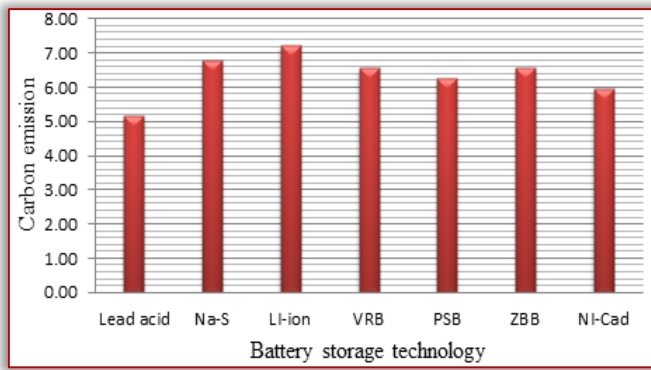
Figure 9: variation of Carbon emission with battery storage technology

In the same way, the energy contribution of each generating unit is presented in Figure 8 while the carbon emission effect is shown in Figure 9. It can be further affirmed that lead-acid battery is still the best for the standalone system. However, other battery storage technology might be suitable for higher application such as grid connected system due to high energy density and initial capital cost. The result further confirmed the dependence of the system performances on the storage technology. Therefore, it is critical for both the system operators and planners to know the suitable storage system economically and environmentally.

⊡ Economic Impact of the Proposed Microgrid

In this section, the benefit of the system is analyzed from the economic point of view. The main idea behind these assessments is to decide on whether the proposed microgrid is economically viable. This can be achieved by the use of economic indicators such as Net Present Value (NPV), Benefit-Cost Ratio (BCR) and Payback Period (PBP).

— Net Present Value (VPB)

This is defined as the net value of benefits (B) and cost of the project, discounted back at the beginning of the investment. The benefit in this case is the income from selling the generated power. On the other hand, the cost is the total capital investment cost and the accumulated annual operation and maintenance cost (A). In some cases it can be assumed to be about 2% of the total project cost. In this design the actual data is used and the mathematical expression for the determination of the NPV is given by

$$NPV = NPV(B) − [IC + NPV(A)] \qquad (14)$$

where, $NPV(B)$: the Net Present Value of Benefits
IC: the Initial Cost (total capital investment) and
$NPV(A)$: the Net Present Value of the Annual cost,

$$NPV(B) = B[(1 + I)^n − 1]/I(1 + I)^n \qquad (15)$$
$$NPV(A) = A[(1 + I)^n − 1]/I(1 + I)^n \qquad (16)$$

B: All benefits
A: Annual operation and maintenance cost
I: the real rate discount,
Using equations (14) to (16), the net present value of the proposed microgrid in the study area is obtained and used in sections 8. 2 and 8.3. The NPV is > 0, the project is economically possible, which means, it will bring more profit to the investor.

— Benefit Cost Ratio (BCR)

This index is defined as the ratio of the net present value of the total benefits to the net present value of all the cost plus the investment cost. The BCR of the project is obtained by using

$$BCR = NPV(B)/[IC + NPV(A)] \qquad (17)$$

The result presented in Figure 10 shows that BCR is > 0. The result further affirmed the NPV claim; therefore the project is also economically acceptable. It can be regarded as the profitability index interpreted by most investors easily. The result further confirmed the effects of the battery storage on the optimum design of microgrids. Therefore, Lithium ion battery is the best in terms of the profitability index.
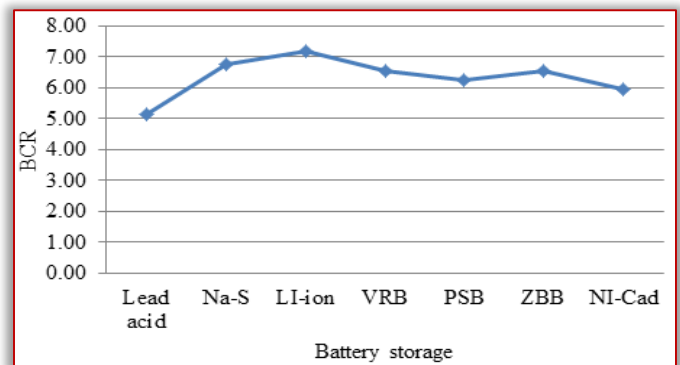


Figure 10: BCR of different battery

— Payback Period (PBP)

The payback period is the year (n) in which the net present value of all benefits will be equal to the net present value of all the costs plus capital investment, therefore at PBP; the equation (14) is then equated to zero, which gives;

$$NPV(B) = [IC + NPV(A)] \qquad (18)$$

Finally solving for n results in

$$n = −\ln(1 − \frac{(I×IC)}{(B−A)})/\ln(1 + I) \qquad (19)$$
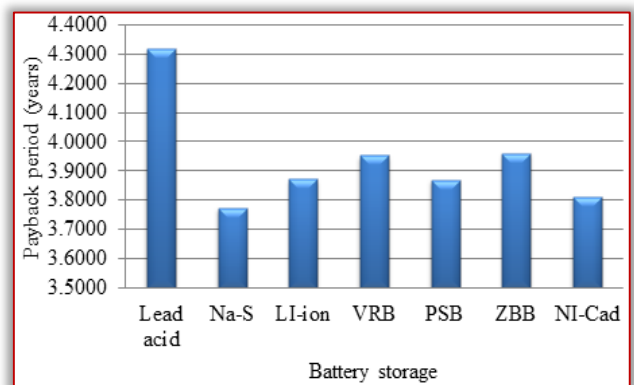


Figure 11: Payback period

According to the result obtained in Figure 11, it can observe that the project is economically possible because the payback period is less compared to the lifespan of the project. The result shows that, lead acid battery with less energy cost takes longer time to return the money invested. Therefore, from the investor point of view may not be the best for the chosen environment. Using this index, the project will be better using sodium sulphide battery storage.

## CONCLUSION

This paper presented another method for the optimal design of standalone microgrid based on mixed integer programming. The results have shown that realistic optimal planning of the system, the effects of PV module need to be considered. Optimal design of the proposed system is sensitive to the rated power of the each unit. According the PV technologies, AP120 is the most suitable due to the higher output power. This reduced the use of the DG connected to the system. However, ASE300 has the least energy cost due to the less number of series connected cells. Therefore, the energy cost is sensitive to the storage and PV module technology. Also neglecting the penalty cost due to the carbon emissions leads to underestimation of the annual cost of the plant.

## References

[1] A Abdulkarim, S.M Abdelkader, and D.J. Morow, "Reliability importance measures of componets for standalone hybrid renewable energy micogrid," in ENEFM, Oludeniz, 2014.

[2] S. Abdelkader, "Techno-Economic Design of a Stand-Alone Renewable Energy System," in International Conference on Renewable Energies and Power Quality (ICREPQ'15), La Coruña (Spain), 2015.

[3] R.K Ullah, R. Akikur, and K.R. Saidur, "Comparative study of stand-alone and hybrid solar energy systems suitable for off-grid electrification: A review," Elsevier, no. 27, pp. 738-752, November, 2013.

[4] Lingfeng Wang and C. Singh, "PSO-based Hybrid Generating System Design Incorporating Reliability Evaluation and Generation/Load Forecasting," in Power Tech, 2007 IEEE, Lausanne, 2007.

[5] F Riahy and G. H. Jahanbani, "Optimum design of hybrid renewable energy system," Renewable Energy Trend and application, vol. 11, no. 1, pp. 231-250, 2013.

[6] Bo Zhao, X. Zhang, J. Chen, C. Wang, and L. Guo, "Operation Optimization of Standalone Microgrids Considering Lifetime Characteristics of Battery Energy Storage System," , IEEE Transactions on Sustainable Energy, vol. 4, no. 4, pp. 934- 943, 2013.

[7] Lu Zhang, G. Barakat, and A. Yassine, "Design and optimal sizing of hybrid PV/wind/diesel system with battery storage by using DIRECT search algorithm," in Power Electronics and Motion Control Conference (EPE/PEMC), Novi Sad, 2012.

[8] Y. Yang, W. Pei, and Z. Qi, "Optimal sizing of renewable energy and CHP hybrid energy microgrid system," in Innovative Smart Grid Technologies - Asia (ISGT Asia), 2012 IEEE , Tianjin, 2012.

[9] W.D. Kellogg, M.H. Nehrir, G. Venkataramanan, and V. Gerez, "Generation unit sizing and cost analysis for stand-alone wind, photovoltaic, and hybrid/pv systems," IEEE Trans. Energy Conversion, vol. 13, no. 1, pp. 70-75, March 1998.

[10] K. Tanaka and K. Maeda, "Simulation-based design of microgrid system for a resort community," in International Conference on Clean Electrical Power (ICCEP), 2011, Ischia.

[11] A.A. Nafeh, "Optimal Economical Sizing Of A PV-Wind Hybrid Energy System Using Genetic Algorithm," International Journal of Green Energy, vol. 8, pp. 25-43, 2911.

[12] L. K. David, "Photovoltaic Module and Array Performance Characterization Methods for All System Operating Conditions," New York, 1997.

[13] H. Fanney, M. W. Davis, B. P. King, D. L. Dougherty, W. E. Boyson, and J. A. Kratochvil, "Comparison of Photovoltaic Module Performance Measurements," Journal of Solar Energy Engineering, ASME, vol. 128, pp. 153-159, 2006.

[14] L Zhang, G Barakat, and A. Yassine, "Deterministic Optimization and Cost Analysis of Hybrid PV/Wind/Battery/Diesel Power System," International journal of Renewable Energy Research, vol. 2, no. 4, pp. 687-696, 2012.

[15] Y. Yang, W. Pei, and Z. Qi, "Optimal sizing of renewable energy and CHP hybrid energy microgrid system," in Innovative Smart Grid Technologies - Asia (ISGT Asia), IEEE, Tianjin, 2012.

[16] A Abdulkarim, S. M. Abdelkader, and D.J Morrow, "Model for Optimum Design of Standalone Hybrid Renewable Energy Microgrids," Journal of Fundamental and Applied Sciences, vol. 9, no. 2, pp. 1074-1101, 2017.

[17] Q. Lei, "A Summary of Optimal Methods for the Planning of Stand-alone Microgrid System," Energy and Power Engineering, vol. 5, pp. 992-998, 2013.

[18] H Suryoatmojo, "Artificial Intelligence Based optimal Configuration of hybrid power Generation System," Kumamoto University, Japan, PhD Thesis 2010.

[19] R.W. Wies, R.A. Johnson, A.N. Agrawal, and T.J. Chubb, "Simulink Model for Economic Analysis and Environmental Impacts of a PV With Diesel-Battery System for Remote Villages," Power Systems, IEEE Transactions on , vol. 20, no. 2, pp. 692-700, 2005.

[20] D.L. King, W.E. Boyson, and J.A. Kratochvill, "Photovoltaic Array Performance Model ," California, 2004.

[21] M. Ross, R. Hidalgo, C. Abbey, and G. Joos, "Analysis of Energy Storage Sizing and Technologies," in Electric Power and Energy Conference (EPEC), IEEE, Halifax, NS, 2010.

[22] M Ross, R. Hidalgo, C. Abbey, and G. Joo´s, "Energy storage system scheduling for an isolated microgrid," IET Renewable Power Generation, vol. 5, no. 2, pp. 117–123, 2010.

[23] L. Wang and C. Singh, "Compromise Between Cost and Reliability in Optimum Design of an Autonomous Hybrid Power System Using Mixed-Integer PSO Algorithm," in International Conference on Clean Electrical Power, 2007. ICCEP '07., Capri, 2007.

[24] M. Meiqin, J. Meihong, D. Wei, and L. Chang, "Multi-objective economic dispatch model for a microgrid considering reliability," in 2nd IEEE International Symposium on Power Electronics for Distributed Generation Systems (PEDG), 2010 , Hefei, China, 2010.

[25] Zhang L, Barakat G, and Yassine A, "Deterministic Optimization and Cost Analysis of Hybrid PV/Wind?Battery/Diesel Power System," International journal of Renewable Energy Research, vol. 2, no. 4, 2012.

[26] A Abdulkarim, S.M Abdelkader, and D.J. Morow, "Statistical Analyses of Wind and Solar Energy Resources for the development of hybrid renewable energy system," in ENEFM, Oludeniz, 2014.

[27] Zhao, Z. Xuesong, C. Jian, W. Caisheng, and G. Li, "Operation Optimization of Standalone Microgrids Considering Lifetime Characteristics of Battery Energy Storage System," IEEE Transaction on Sustainable Energy, vol. 4, no. 4, pp. 934-942, 2013.

[28] J. Li, W. Wei, and J. Xiang, "A simple sizing algorithm for standalone-pv/wind/batter hybrid microgrids," Energies, vol. 5, pp. 5307-5323, 2012.

[29] M. Bashir and J. Sadeh, "Size optimization of new hybrid stand-alone renewable energy system considering a reliability index," in Environment and Electrical Engineering (EEEIC), 11th International Conference on, Venice, 2012.

[30] M. Mao, S. Sun, and C. Liuchen, "Economic analysis of the microgrid with multi-energy and electric vehicles," in Power Electronics and ECCE Asia (ICPE & ECCE), IEEE 8th International Conference on, Jeju, 2011

[1.]A.P. VIJAYAKUMAR, [2.]N.R. DEVI

# CLOSED LOOP CONTROLLED FORWARD CONVERTER ANALYSIS USING PI, FUZZY LOGIC AND ANN CONTROLLER

[1.]Department of Electrical and Electronics Engineering, JNTU, Hyderabad, Telangana, INDIA
[2.]Department of Computer Science and Engineering, Panimalar Engineering College, Chennai, INDIA

**Abstract:** Closed loop controlled model is developed for the determination of time domain specifications, transient response and steady state analysis. Simulation of DC to DC modified forward converter using active clamp-Neutral Point Connected Auxiliary Resonant Snubber (NPC-ARS) circuit, which is implemented by using PI controller, fuzzy logic controller and artificial neural network (ANN) controller, is presented in this paper for the switching mode power supply applications. Its circuit operation in closed loop controlled model and the performance of the modified forward converter is described and the simulation results are presented

**Keywords:** Steady state analysis, time-domain specifications, transient response and controllers and ANN controller

## INTRODUCTION

In recent years, the switching mode power supply (SMPS) system has been achieved with high power density and high performances by using power semiconductor devices such as IGBT, MOS-FET and SiC. However, using the switching power semiconductor in the SMPS system, the problem of the switching loss and EMI/RFI noises has been closed up. This course produced the EMC limitation like the International Special Committee on Radio Interference (CISPR) and the limitation of harmonics for the International standard is Electro technical Commission (IEC). For keeping up with the limitation, the SMPS system must add its system to the noise filter and the metal and magnetic component shield for the EMI/RFI noises and to the PFC converter circuit and the large input filter for the input harmonic current. On the other hand, the power semiconductor device technology development can achieve the high frequency switching operation in the SMPS system. The increases of the switching losses have occurred by this high frequency switching operation. The inductor and transformer size has been reduced by the high frequency switching, while the size of cooling fan could be huge because of the increase of the switching losses.

Our research target is to reduce the ripple and the switching losses in the SMPS system. One method is the soft switching technique and the other method is by proper choosing of filter circuit. This technique can minimize the switching power losses of the power semiconductor devices, and reduce their electrical dynamic and peak stresses, voltage and current surge-related EMI/RFI noises under high frequency switching strategy. Thus, a new conceptual circuit configuration of the double forward type DC - DC converter circuit is presented in this paper with its operating principle. In addition, it's fundamental operation and its performance characteristics of the proposed forward type DC-DC double forward converter treated here are evaluated on the basis of experimental results. A New Controller scheme for Photo voltaics power generation system is presented in [1]. The design and implementation of an adaptive tuning system based on desired phase margin for digitally controlled DC to DC Converters is given in [2]. Integration of frequency response measurement capabilities in digital controllers for DC to DC Converters is given in [3]. A New single stage, single phase, full bridge converter is presented in [4]. The Electronic ballast control IC with digital phase control and lamp current regulation is given in [5]. A New soft-switched PFC Boost rectifier/inverter is presented in [6]. Design of Single-Inductor Multiple-Output DC-DC Buck Converters is presented in [7]. Boost Converter with Improved Performance through RHP Zero Elimination is given by [8]. High-efficiency dc-dc converter with high voltage gain and reduced switch stress is given in [9]. Snubber design for noise reduction is given in [10].Comparison of active clamp ZVT techniques applied to tapped inductor DC-DC converter is given in [11].The multiple output AC/DC Converter with an internal DC UPS is given in [12].The Bi-directional isolated DC-DC Converter for next generation power distribution –comparison of converters using Si and Sic devices is given in [13]. The simulation and the experimental method of analysis are done for the low noise SMPS system which is demonstrated in [14]. Investigations on forward converter using different types of filters and experimental method of analysis for the forward converters are done, which is to compare it with the conventional circuit are clearly mentioned in [15]. Different types of filters which are utilized in the forward converters and its performance are given in [16]. Forward converter with RCD snubber using the PI controller, fuzzy controller and artificial neural network (ANN) controller are analyzed and compared to get the better performance in [17]. Analysis and reduction of voltage ripple in forward converter using a three different filters and based on the comparison, the Bi-quad high frequency filter gives better performance is illustrated in [18]. The above literature does not deal with the comparison of forward converter using the PI, Fuzzy and ANN controllers. The above cited papers do not deal with the comparison of

FFT analysis, voltage stress and ripple factor and do not identify a converter suitable for SMPS system.

The above literature does not deal with the comparison of modified controlled forward converter using the PI controller, fuzzy controller and artificial neural network (ANN) controller. The above cited papers do not deal also with the modeling of closed loop SMPS system and do not identify a converter suitable for SMPS system. This work aims to develop simulink models for the above closed loop forward converter system using the three controllers. A comparison is also done to find the circuit suitable for the SMPS system.

## CONFIGURATION OF CLOSED LOOP SYSTEM

Figure 1 shows a closed loop circuit model of the SMPS, which is used to implement with fuzzy controller and artificial neural network (ANN) controller. In this closed loop configuration, a 230 V AC supply is connected to the bridge rectifier circuit. The output of this circuit is DC. The output voltage of the rectifier is converted into a variable DC voltage by the boost converter with frequency circuit. When the chopper is OFF, the inductor voltage add to the source voltage and current in the inductor ($i_L$) is forced to flow through the diode and the load ($R_L$). The output of the boost chopper circuit with lesser ripple is filtered by the capacitor. Conversion of DC voltage into AC is done by the high frequency switching. In high frequency switching scaled up AC voltage is induced in the transformer primary and the scaled down voltage appears across the transformer secondary. The AC voltage obtained from the secondary of the transformer is converted into DC by the half – bridge rectifier circuit, and the noise is filtered by the LC-filter, and transferred to the load. The output DC voltage is taken as feedback, to compare. The difference of error signal is amplified and it is applied to the microcontroller. The microcontroller generates switching pulses, and it is amplified by the amplifier circuit. The amplified pulses are used to turn on the circuit.
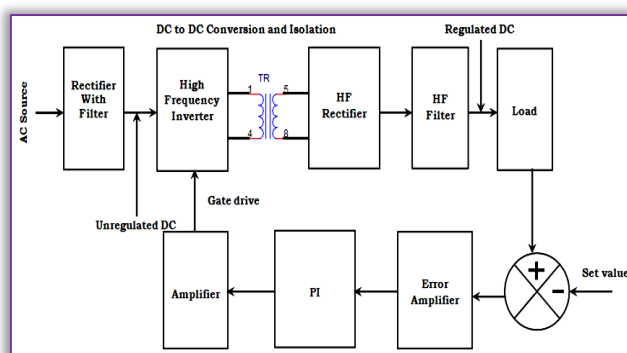


Figure 1. Circuit diagram of a closed loop model SMPS system

## DESIGN OF THE MODIFIED CONVERTER

Figure 2 shows the NPC-ARS auxiliary switch in the forward converter, which is utilized in closed loop model to reduce the noise and to improve the efficiency. The necessary specifications assumed for the NPC-ARS auxiliary switch in the forward converter are frequency f = 100 kHz, Δl = 2.5 A, and R = 100 Ω. By using the relation, 1- δ = $V_i$ / $V_o$, δ = 0.5; By using the formula, L = $V_i$ δ / f Δl, L=200 MH; By the relationship, C =

δ / 2 $f_r$, ;C = 250 µF; The transformer voltage ratio $V_o$ / $V_i$ = K, and by using this relationship the value of K=0.21 is obtained. The transformer primary voltage $E_1$ = 4.44 * $N_1$*Φ* f. By substituting in the equation, the value of $E_1$, Φ, and f in the above equation, the value of $N_1$ = 4.5. By using the equation $N_2$= ($E2$ / $E_1$) $N_1$ the value of $N_2$ = 9 is obtained. Figure 3 shows the NPC-ARS auxiliary switch in the forward converter, which is to modified in the forward converter. The NPC-ARS auxiliary switch in the forward converter will reduce. The NPC-ARS auxiliary switch in the forward converter will reduce the noise and the energy is recycled to improve the efficiency of the system. By the modified SMPS system the freewheeling current is controlled and thus it reduces the switching losses in power devices.
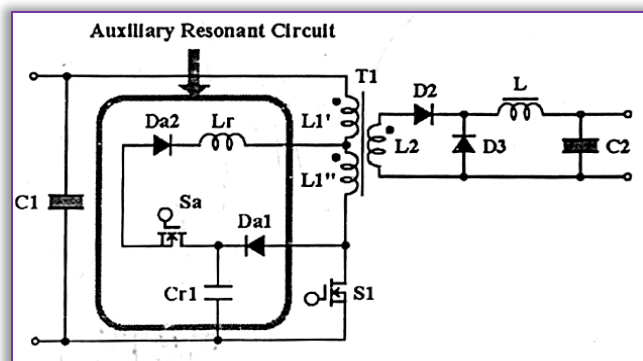


Figure 2. NPC-ARS auxiliary switch

## SIMULATION PARAMETERS

The simulation parameters for the modified forward converter using the NPC-ARS circuit are shown in Table 1. From the given parameters, the system is modeled using MATLAB-Simulink and simulated which is to check the performance of the system.

Table 1. Simulation Parameters for the modified forward converter using the NPC-ARS circuit.

| S.No: | Parameters Unit | Values & Items |
|---|---|---|
| 1 | Input Voltage [V] | 100 |
| 2 | Output Voltage [V] | 42 |
| 3 | Switching Frequency [KHZ] | 20 |
| 4 | Smoothing Capacitor [µf]/V | 2200/63,100/63 |
| 5 | Smoothing Inductor [mH] | 27 |
| 6 | 'L' of NPC-ARS [µH] | 10 |
| 7. | 'C' of NPC-ARS [nf] | 100 |

## PI, FUZZY AND ANN CONTROLLERS

In this work develop the Simulink models for the closed loop forward converter system using PI, fuzzy and Ann controller models. A comparison is also done from the simulation results to stumble on the circuit appropriate for the SMPS system. In the closed loop PI controller, the tuning is done by using a Ziegler-Nicholas method which is defined as the ratio between the rise-time and delay-time and the integral constant is define as 1.6 with delay-time. After tuning is done as by the given method, the fixed saw-tooth pulses using PWM and the sources are compared to get the steady state. In the closed loop fuzzy logic controller, tuning is done by using the number of variables which are five and it is stated as small, medium, large, very large and very small. Between

the widths of the variables, which are lies from zero and one to be stated as manual, we used a fuzzy logic controller. Fuzzy logic means a fuzzification is the process of by which the crisp quantities are converted to fuzzy logic ones. By identifying several suspicions are present in the crunchy values, the fuzzy logic values such as zero and one's are formed. The conversion of fuzzy set values is represented by (MA)-membership functions. This MA function which is a graphical illustration of the scale of contribution of each input value in a given set. The set value could be of any type, which is illustrated as Gaussian (GW), Triangular (TW), Trapezoidal (TRW), and Singleton (SW) etc... The fuzzification progression may absorb assigning (MA) membership function values for various levels of sets to the given quantities.

Fuzzy system which implements by using the rule-based reasoning such as if-then reasoning rules to determine an output response. The inference (IF) engine evaluates all the rules to perform the, if then rule-based reasoning process. Continuity, Consistency, Completeness and Interaction are the four types of properties, which has been considered by the rules based. The operators used mainly in the fuzzy set logic to erect compound based rules. AND, OR and NOT are the Rules considered have to satisfy the following. De-fuzzification is the progression of convert fuzzy to brittle values for further processing. There are some of the famous methods which are used for defuzzification such as Centroid, Weighted Average and Maximum membership method.

In the closed loop artificial neural network controller, tuning is done by using the state variables are: a (w) +b, where, 'a' is the constant, w are the change of weights and b is the bias. As by the change of weighted variables which is given in the state model an auto-tuning is done after compared with the fixed saw-tooth pulses using PWM and the sources are compared to get the steady state. In the closed loop simulink model forward converter system using PI, fuzzy and Ann controller, it operates at high frequency. The switching loss which is directly proportional to the frequency, when the switching frequency increases, the losses in the switching is decreased. In the closed loop simulink model double forward converter system DC supply of 100 V and the circuit breaker $T_2$ [0 2] with the switching time sequence of [0 0.5] sec are used. The step change is introduced in the input DC supply of 12 V and the circuit breaker $T_3$ [2 0] with the switching time sequence of [0 0.5] sec are used. The error in the output is reduced to get the steady state value. From the comparison of responses, it is seen that the closed loop system has reduced steady state error, which is maintain the voltage as constant.

## SIMULATION RESULTS

The circuit diagram with the modes of modified SMPS system with an NPC-ARS switch is shown in Figure 2. The modified system consists of active power switch 'M₂', auxiliary switch 'M₁', resonant capacitor 'C₂', and the two power diodes 'D₁' and 'D₂'. The complete soft switching transition can be achieved in active power devices of the forward converter with the combine of switches 'M₁', 'C₂', and diodes 'D₁' and 'D₂' to recycle. To reduce the switching losses in each power semiconductor device, the active power switch M₂ is turned on with zero current condition and turned off at zero voltage condition. The auxiliary switch M₂ is turned on and turned off with zero current condition. In the forward type proposed soft transition in switching DC to DC conversion is described in four modes, which are: 1.Steady State Mode on, 2.Commutation Mode-1, 3.Steady State Mode off and 4.Commutation Mode 2 and they are shown in Figure 2. The modes of operation, which is already presented in the reference of 7. The open loop controlled modified forward converter is shown in Figure 3.1. DC input voltage with disturbance and DC output voltage with disturbance are shown in Figure 3.2 and Figure 3.3.
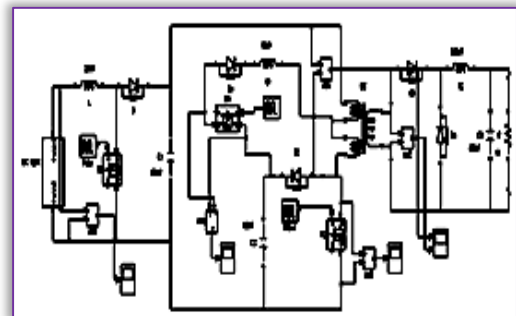


Figure 3.1 Open loop modified forward converter
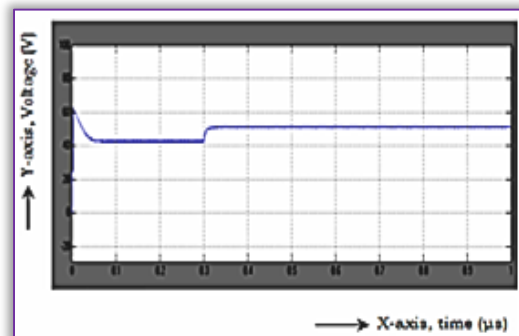


Figure 3.3. DC output voltage with disturbance
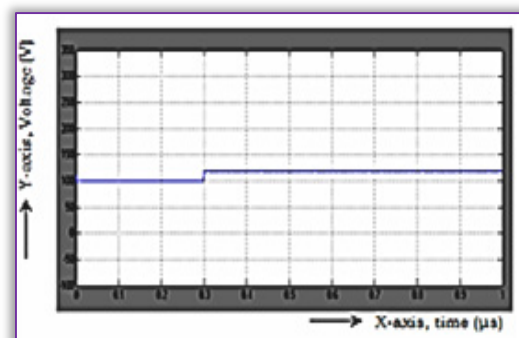


Figure 3.2. DC input voltage with disturbance

Closed loop controlled modified forward converter is shown in Figure 3.4. DC input voltage with disturbance and DC output voltage with disturbance are shown in Figure 3.5 and Figure 3.6. Modified forward converter using fuzzy logic is shown in Figure 3.7. DC input voltage with disturbance and DC output voltage with reduced error are shown in Figure 3.8

and Figure 3.9. Modified forward converter using artificial neural network controller is shown in Figure 3.10. DC input voltage with disturbance and DC output voltage with reduced error are shown in Figure 3.11 and Figure 3.12. Summary of steady state error in open loop and closed loop modified forward converter is shown in Table 2. Summary of time-domain specifications and steady state error is sown in Table 3. Summary of transient response is shown in Table.4.
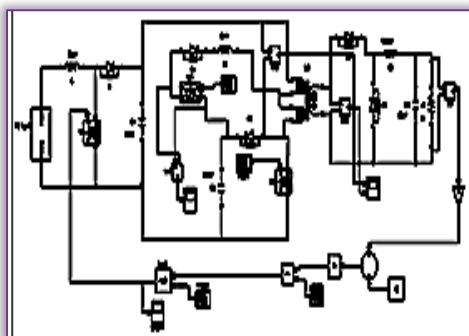


Figure 3.4. Closed loop modified converter
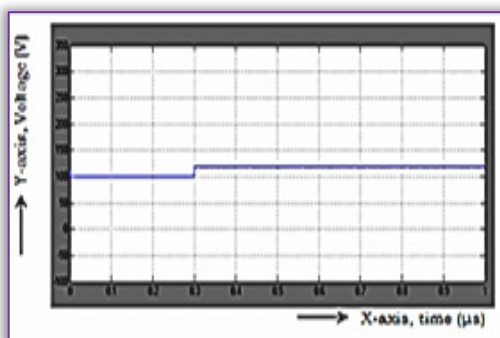


Figure 3.5. DC input voltage with disturbance
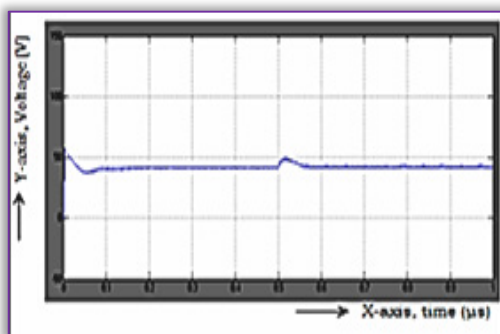


Figure 3.6. DC output voltage
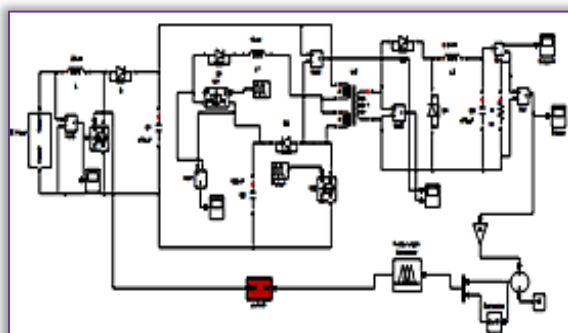


Figure 3.7. Modified converter using fuzzy logic

Table 2: Summary of steady state error

| Parameter | Open loop system | Closed loop system |
|---|---|---|
| Steady state error | 8 V | 2 V |

The summary of steady state error given in Table 2, which represents from the Figure 6.1 to Figure 6.5.
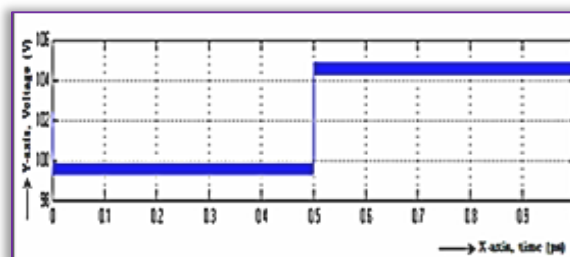


Figure 3.8. DC input voltage with disturbance
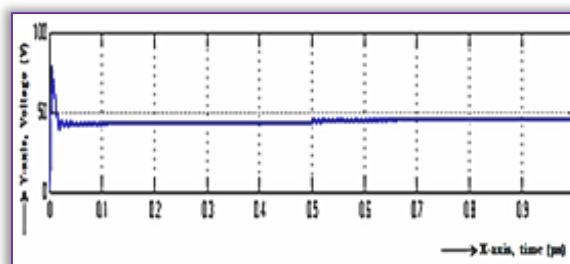


Figure 3.9. DC output voltage
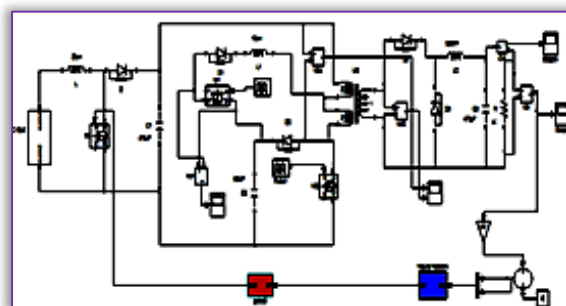


Figure 3.10. Modified converter with ANN logic
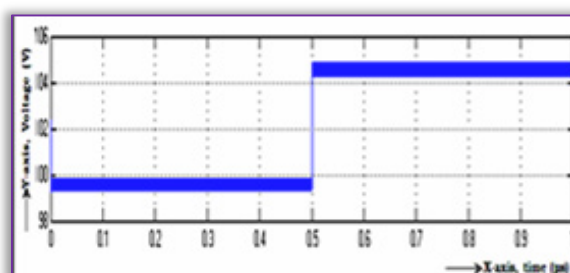


Figure 3.11. DC input voltage with disturbance
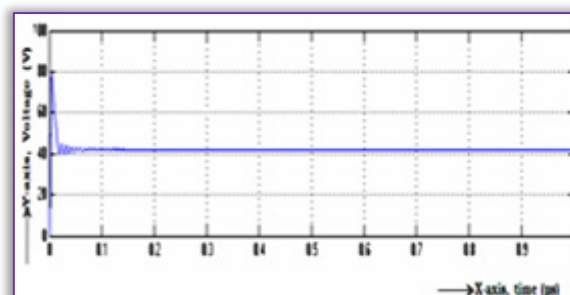


Figure 3.12. DC output voltage

Table 3: Summary of time-domain specifications
and steady state error

| Modified converter | Tr | Ts | Tp | Vp | Ess |
|---|---|---|---|---|---|
| PI controller | 0.036 | 0.56 | 0.53 | 2.7 | 0.5 |
| FUZZY controller | 0.024 | 0.32 | 0.29 | 0.02 | 0.2 |
| ANN controller | 0.022 | 0.13 | 0.11 | 0.01 | 0.1 |

Table 4: Summary of transient response

| Transient Response | | | |
|---|---|---|---|
| $t_d$(ms) | $t_r$(ms) | $t_p$(ms) | $t_s$(ms) |
| 0.01 | 0.02 | 0.03 | 0.2 |
| Transient and range of Steady state | | | |
| Transient State (ms) | | Steady State (ms) | |
| 0 – 0.2 | | 0.2 onwards | |
| Peak over shoot $M_p$ (A) = 13.9 volts | | | |

From the Table 3, the comparison has been done from the PI controller, fuzzy logic controller and also with the artificial neural network (ANN) controller. The steady state response, range of transient and steady state and peak over shoot are described in Table 4. The comparison has done to determine the steady state performance of the modified forward converter which is utilized in the SMPS system.

## CONCLUSIONS

Closed loop controlled modified forward converter is simulated using the blocks of mat lab-Simulink. To determine the steady state, the closed loop controlled model is implemented as with PI controller, fuzzy logic controller and artificial neural network controller (ANN) controller and it is simulated using the Simulink model. The comparison has been done from the three controllers, to determine the steady state analysis. From the comparison of the three controllers, the steady state error (Ess) is reduced in the artificial neural network controller. By using the ANN controller, the error is reduced as high and it is suitable for the forward converter system.

## References

[1] Tamer T.N. Khabib, Azah Mohamed, Nowshad Admin, "A New Controller Scheme for Photo voltaics power generation system, "European journal of scientific research ISSN 1450-216X vol.33 No.3 (2009), pp.515-524.

[2] J. Morroni, R. Zane, D. Maksimovic, "Design and Implementation of an adaptive tuning system based on desired phase margin for digitally controlled DC-DC Converters", IEEETrans. Power Electron., vol.24, no.2, pp.559-564, 2009.

[3] M. Shirazi, J. Morroni, A. Dolgov, R. Zane, D. Maksimovic, "Integration of frequency response measurement capabilities in digital controllers for DC-DC Converters, "IEEE Trans. Power Electron.,vol.23, no.5,pp.2524-2535, 2008.

[4] Hugo Ribeiro, Beatriz V. Borges, "New single stage, single phase, full Bridge Converter, "submitted for appreciation to the Technical committee of IEEE ECCE-Energy conversion congress and exhibition, 2009.

[5] Y. Yin, M. Shirazi, R. Zane, "Electronic Ballast control IC with digital phase control and lamp current regulation, "IEEE Trans. Power Electron., vol. 23, no.1, pp.11-18, 2008.

[6] Yungtaek Jang,David L.Dillman and Milan M.Javanovie, "A New soft-switched PFC Boost Rectifier with Integrated Flyback Converter for stand –by Power, "IEEE Trans.on Power Electronics, pp.66-72, No.1, 2006.

[7] M. Belloni, E. Bonizzoni, and F. Maloberti, "On the Design of Single-Inductor Multiple-Output DC-DC Buck Converters", Proc. of 2008 International Symposium on Circuit and Systems (ISCAS), pp. 3049-3052, 2008.

[8] S.Kapat, A. Patra, and S. Banerjee, "A Current Controlled Tri-State Boost Converter with Improved Performance through RHP Zero Elimination", IEEE Transactions on Power Electronics, Vol. 24, No.3, pp. 776-786, 2009.

[9] R.J. Wai, C. Lin and Y. Chang, "High-efficiency dc-dc converter with high voltage gain and reduced switch stress, " IEEE Transactions on Power Electronics, vol. 54, no.1, 2007.

[10] S.Havanur, "Snubber design for noise reduction in switching circuits, "Alpha & Omega Semiconductor, Tech. Rep., 2007.

[11] S.Abe, T. Ninomiya, Comparison of Active-Clamp and ZVT Techniques Applied to Tapped-Inductor DC-DC Converter with Low Voltage and High Current, Journal of Power Electronics, Vol.2, No.3, pp.199-205, 2002.

[12] Arturo Fernandez, Javier Sebastin, Maria Hernando, "Multiple output AC/DC Converter with an Internal DCUPS,"IEEE Trans on Industrial Electronics, vol.53, no.1., 2006.

[13] Aggeler,D, Inove,S, Akagi,H, Kolar,J.W, "Bi directional isolated DC to DC Converter for next generation power distribution-comparison of converters using Si and Sic devices" Power conversion conference-agoya, 2007, PCC apos; 07, volume, Issue, 2-5 April 2007 Page(s):510-517.

[14] Vijayakumar.P and Rama Reddy.S "Simulation and Experimental Results of Low Noise SMPS system using forward converter" in the Asian Power Electronics Journals (APEJ), Vol.9, No.1, 2015, Page: 1-7.

[15] Palamalai Vijayakumar.A and Ramakrishnan Devi, "Simulation and experimental analysis of forward converters" LAP-Lambert Academic Publishing, Germany. Pages:121, 2016

[16] Palamalai VijayaKumar.A and Ramakrishnan Devi, "Investigations on forward converters using LC, PI and Bi-quad High Frequency filters" in the LAP-Lambert Academic Publishing, Germany. Pages:149, 2016

[17] Vijayakumar.P and Devi.R., "Closed loop controlled forward converter with RCD Snubber using PI, fuzzy logic and artificial neural network controller" in the Annals of "DUNAREA DE JOS" University of Galati, Fascicle III, 2016, Vol.39, No.2, ISSN: 2344-4738. ISSN-L1221-454X, Electrotechnics, Electronics, Automatic Control and Informatics.

[18] P.Vijayakumar and Ramakrishnan Devi, "Analysis and reduction of voltage ripple in forward converter using a bi-quad HF filter" in the ANNALS of Faculty Engineering Hunedoara– International Journal of Engineering, Tome XV [2017] – Fascicule 1 [February], ISSN: 1584-2665, Pages: 97-102.

# Fascicule 3
## [ July - September ]
## t o m e
## [2018] XI

ACTA Technica CORVINIENSIS
BULLETIN OF ENGINEERING

ACTA TECHNICA CORVINIENSIS BULLETIN OF ENGINEERING

## ISSN: 2067-3809

[1.]Abdelnaser OMRAN, [2.]Lai BOON HOOI

# DETERMINING THE CRITICAL FACTORS IN ENSURING THE ACCURACY OF COST ESTIMATE IN OBTAINING A TENDER

[1.]Department of Risk Management, School of Economics, Finance and Banking, College of Banking, Universiti Utara Malaysia, Sintok, 06010, Kedah State, MALAYSIA
[2.] Department of Engineering and Built Environment, Penang Branch Campus, Tunku Abdul Rahman University College, 11200 Tanjung Bungah, Pulau Pinang, MALAYSIA

**Abstract:** In construction industry, cost plays an important role in determining the feasibility of a project and ensuring its continuity from conceptual to reality. Different types of cost estimates are used in different stages of construction, from design stage to tender stage and throughout the whole construction stage at the site. Thus, this study was conducted with the intention to identify the critical factors that are significant in ensuring the accuracy of estimation for the purpose of obtaining a tender and delivering it at the completion date.   A quantitative approach was used to collect the data. The results indicated that "understanding the scope of works" shall be treated as the most important factor, followed by "correct material price and forecasting fluctuation", "read and check all tender drawings, compare the drawings with specification, check for discrepancy", "site visit to be acquainted with the accessibility, topography, constraints, etc.", "reviewing quotations from subcontractors and suppliers" and "experience and competency of estimator". Apparently, these six critical factors identified, have much higher relative importance index and it implies that these six factors have been given appropriate consideration accuracy cost estimating in successfully obtaining a tender and ensuring the work tasks can be delivered after being awarded with the tender.
**Keywords:** construction industry, cost estimation, critical factors, accuracy, tenders, Malaysia

## INTRODUCTION

In construction industry, cost plays an important role in determining the feasibility of a project and ensuring its continuity from conceptual to reality.  Gilson and Vanreyk (2014) stated in their study that cost estimation is a key factor in the construction industry and the success and quality of a project depend on the accurate estimation. Akintoye (2000) described estimating as a process of predicting costs that are required for the completion of the work.  These 2 positive descriptions are supported by Enshassi et al. (2007) who explain that estimating is an important step in the construction process as the reliability of its estimate accuracy from conceptual to detailed stages determines the success or failure of a project. In other words, estimating is one of the most important functions of a successful project (Barzandeh, 2011). He further stated that accurate estimates optimise good contracting as well as the process of calculating and analysing all the costs that will enter into a particular job to arrive at a set total.  The purpose of estimating is to determine the forecast costs required to complete a project in accordance with the contract plans and specifications (Peurifoy and Oberlender, 2002).  They stated that for every given project, the estimator can determine with reasonable accuracy the direct costs for materials, labour and equipment. The tender/bid price can then be determined by adding to the direct cost the costs of overhead and profit.  According to Ashworth (2004), the purpose of estimating is to indicate probable construction costs. This is an important factor that clients consider when deciding to build; it determines the feasibility of a project or even provides the basis for budget control during tendering and construction. Hendrickson (2000) stated that a detailed estimate is created when the scope of work is clearly stated and a more detailed design are in progress so that the essential features of the building are visible.  Ashworth (2004), cost planning process consists of 3 (three) phases include phase one, involving the determination of realistic. The second phase, how to plan estimates on the various parts of the work of a project. The third phase, a checking process to ensure that the actual design detail to the parts of this work can be carried out within the limits of the cost plan.  There are in fact several types of cost estimates which used in different stages of construction, from the design stage to tender stage and throughout the whole construction stage at the site. In during different stages of work in the construction process, the client would require different types of costing information.  Due to the varying requirements, a different type of cost estimates has evolved to enable the estimator or quantity surveyor to produce a cost advice that best fits the needs of the client. Peurifoy and Oberlender (2002) mentioned that there are different types of cost estimates used at different stages of a project. These estimates are performed throughout the life of a project, beginning with the first estimate and extending through the various phases of design and into construction is shown in Figure (1). Although each project is unique, generally three parties are involved: the owner, the designer and the contractor.  Each has responsibility for estimating costs during various phases of the project. In a simple manner,  cost estimates can be classified into three major categories according to their functions.  A construction cost

estimate serves one of the three basic functions (design, tender and control (Peurifoy and Oberlender, 2002). In Malaysia, there are various project procurement methods used for building works, such as traditional, design and build, management contracting, public and private partnerships. Amongst these, the traditional method is the most popular.
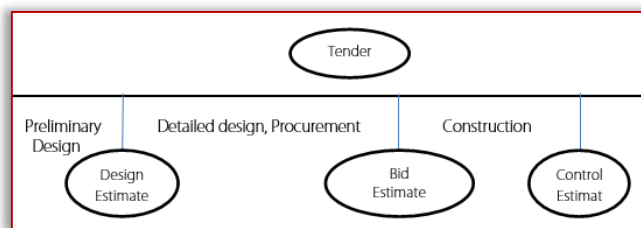


Figure 1. Estimates and Re-estimates through phases of project development
Source: Peurifoy and Oberlender (2002)

Cost estimations for accuracy estimating for a tender are influenced by many factors and there are many empirical studies had looked at these factors. For instance, Dysert (2006) mentioned that there are many factors which influence the estimate accuracy; i.e. the level of project scope, quality of the data, quality of the assumptions, the experience and expertise of the estimator, techniques used, effort put into the preparation of the estimate, and the market conditions. Akintoye (2000) in his research indicated that the biggest factor that influences project cost estimating practice is complexity of design followed closely by the scale and scope of construction. Liu and Zhu (2007) categorised the factors that influence the cost of a project as control factors and idiosyncratic. Control factors are those that can be determined by the estimators to increase the performance of the estimation. Idiosyncratic factors are factors that affect estimation but are outside the control of the estimator; this includes (market conditions, project complexity, weather, size of contract, type of client, site constraints, resource availability, etc). Odusami and Onukwube (2008) identified and studied the influences that affect the accuracy of pre-tender cost estimation. These included (expertise of the estimator, quality of information, project teams experience, tender period, market conditions, design detail, complexity of design, and availability of labour and materials). Oberlender (2000) stated in his published book that a range of accuracy, usually a plus or minus percentage, should be assigned to any estimating by the estimator based on his or her best assessment of the project's true cost. He further mentioned that there is no industry standard that has been agreed on regarding the amount of plus or minus percentage that should be applied to an estimate. In estimating the cost, there are common errors that could affect the accuracy of estimation for a tender where it is impossible for construction cost estimates to be perfect and with no error. Getting too many errors on the plus side or over estimating will make the tender not being competitive. While getting too many errors on the minus side or under estimating can cause the tenderer or eventually the successful contractor to lose money if the contract is being awarded to him. A study by Lim (2011) mentioned that there are some factors which may affect the accuracy of cost estimate during tender stage. These include (political climate, facilities and machineries available in the firm, location of the project, type of project or developer, size of project and site conditions, quality accredited, green building certification, payment terms and financial conditions, differences in standard, types of contract, financing). In this study, the researchers looked at the main problem by establishing a general hypothesis that when there is a tender, definitely there will be only a winner and many losers.

Tenderers spent much money in participating in a tender exercise. They have to pay for tender documentation charges, tender deposit, earnest money (tender bond) and also to hire taker off to carry out measurement if the tender documents are only based on schedule of rates, specifications and drawings without bills of quantities. If they lose the tender, the documentation charges will not be refundable and also the wages paid for the taker off and estimator will be void. Hence, for a contractor to obtain a tender during tendering stage, he or she has to be extra careful in pricing the tender. In another word, a contractor's cost estimate is crucial in determining the success of the tender. When a contractor obtains a tender, there is a possibility that this is the lowest tender among other tenderers and underlying with the issues of under-estimating in his tender without his knowing. Problems exist when construction works carry out at site. Thus, the main purpose of this paper is to study the importance of the cost estimates and determine the critical factors in ensuring the accuracy of the estimation by finding answers to these 2 on why is it important to study the cost estimate? and what are the critical factors in ensuring the accuracy of the estimation?

RESEARCH METHOD

The study was carried out in Penang Island. Essential steps and measures were taken during data collection and process to analysis the findings in which to ensure those findings are sufficient to complete the outlined research questions. A set of questionnaire was used to identify the crucial of accuracy in cost estimation and identifying critical factors in ensuring the accuracy of cost estimations. The respondents were included project managers, contractor estimators, consultant quantity surveyors and others like architects, engineers, site supervisors, and postgraduates. The survey was designed and structured in two main groups as (a) factors related to cost estimates, and (b)factors related to the knowledge and experience of quantity surveyor who does the cost estimate. The respondents were asked to rank some variables in respect of the research questions using a five-point Likert scale (1= strongly disagree to 5= strongly agree). The Statistical Package for the Social Science (SPSS), Version (21.0), was used to calculate the valid percentage ratings of research variables. Finally, Relative Importance Index (RII) was used to determine the underlying relationships among the critical factors into a

fewer number of variables or grouping the factors into lesser dimensions.

$$\text{Relative Importance Index (RII)} = \frac{4n1 + 3n2 + 2n3 + 1n4 + 0n5}{4N}$$

$$(0 \le \text{RII} \le 1)$$

where: N = Total number of respondent, 4, 3, 2, 1, 0 = weighted score on a scale of agreement, n1 = number of respondents who strongly agree, n2= respondents who agree, n3=respondents who are neither agree or disagree, n4=respondents who disagree, n5 = respondents who strongly disagree

The RII value was a ranged from 0 to 1, and the 0 is not inclusive. The higher the RII value the more significant was the critical factors in accuracy estimating in obtaining a tender and ensuring the work task can be delivered.

## RESULTS AND ANALYSIS

### ⊞ Respondents' background

The respondents were classified into four groups, namely project manager, contractor estimator, consultant quantity surveyor and other professions not directly involved in cost estimating in the industry. Detailed information on the socio-demographic variables included in the survey regressions in Table (1).

Table 1. Overall Descriptive Statistics of Respondent's Demographic Data

| Variable | | Number of Respondents | Percentage (%) |
|---|---|---|---|
| Gender | Male | 20 | 62.5% |
| | Female | 12 | 37.5% |
| | Total | 32 | 100% |
| Age | 21 – 30 years old | 10 | 31.3% |
| | 31 - 40 | 8 | 25% |
| | 41 - 50 | 13 | 40.6% |
| | 51 - 60 | 1 | 3.1% |
| | Total | 32 | 100% |
| Profession | Project manager | 6 | 18.8% |
| | Contractor estimator | 8 | 25% |
| | Consultant QS | 11 | 34.4% |
| | Others | 7 | 21.9% |
| | Total | 32 | 100% |
| Working experience | 1 - 5 years | 7 | 21.9% |
| | 6 - 10 years | 6 | 18.8% |
| | 11 - 20 years | 16 | 50.0% |
| | > 20 years | 3 | 9.4% |
| | Total | 32 | 100.0% |
| Education background | Diploma | 9 | 28.1% |
| | Degree | 16 | 50 % |
| | Master & above | 2 | 6.3% |
| | Professional | 5 | 15.6% |
| | Total | 32 | 100.0% |

The table shows that the most of the respondents were males (62.5%) and the age of those surveyed was ranged between 41-40 years old (41.6%) and between 21-30 years old (31.3%). It can be seen from Table (1) that 34.4% of the respondents were consultant quantity surveyors and 25% of them were contractor estimators. Regarding the working experiences of the participants, it was found that 50% of them had working experiences from 11-20 years followed by nearly 22% of them with working experiences between 1-5 years. Concerning the educational background, it can be seen from the analysis that 50% of the participants were holding a degree (BSc degrees) and only 3.6% of them were of those holding postgraduate qualifications like (MSc and PhD degrees).

### ⊞ Factors in ensuring the accuracy of cost estimate in obtaining a tender

With reference to the questionnaire survey with 18 applicable critical factors, Table (2) illustrates the breakdown of relative importance index, thus the significance by percentage and degree of importance for the said factors from the tabulation of combined scores of every respondent's way of perceiving. In line with the study's objective, this was used to determine the 5 most important critical factors perceived by the estimators in the construction industry in Malaysia. The result shows that the most important factor that governs the accuracy in cost estimating "understanding the scope of works of the project" was ranked the first significant factors (RII=0.929) in ensuring the accuracy of estimation for the purpose of obtaining a tender and delivering it at the completion date. The obtained results in this study were also revealed that "correct material price and forecasting fluctuation" as the second highest (RII=0.921) as it is the major percentage in the pricing of the cost estimate. It is generally known that in today's market, the material prices are unstable and they are fluctuating up and down. Therefore, there is a need for the estimator to be clearly understood the frequency and extent of the price variations as well as the timing of the buying cycle with precise anticipating.

The critical factor of "Read and check all tender drawings, compare the drawings with specification, check for discrepancy" was viewed by the respondents as the third highest critical factors (RII=0.9141) and it reveals that the complete set of drawings given by other consultants are relatively important in built-up rates by cost estimators. The fourth factor which is crucial in ensuring the accuracy and ranked by the respondents was "site visit to be acquainted with the accessibility, topography, constraints, etc." with relative important index (RII=0.867).

"Reviewing quotations from sub-contractors and suppliers" and "Experience and competency of estimator" are equally important as both factors are getting the same value of relative importance index, which is (RII=0.875). All the factors that stated in Table (2) are proven to have significant effects in ensuring the accuracy of cost estimates. The RII values of these factors were so close to each other and the difference between the highest and the second lowest is only 0.226.

Table 2. Presents the ranking of Critical Factors in Ensuring the Accuracy of Cost Estimate in Obtaining a Tender

| General | RII | Ranking |
|---|---|---|
| Understanding of the scope of works | 0.929 | 1 |
| Site visit to be acquainted with the accessibility, topography, constraints, etc. | 0.867 | 4 |
| Read and check the tender drawings, compare the drawings with specification, check for discrepancy | 0.914 | 3 |
| Review building codes/ by laws, permits and inspection procedures | 0.609 | 18 |
| Accuracy of measurement if BQ not provided | 0.843 | 7 |
| Adequacy of tender period | 0.703 | 17 |
| Experience and competency of estimator | 0.875 | 5 |
| Ability to collect, classify and evaluate data that would be useful in estimating. | 0.812 | 10 |
| Correct material price and forecasting for fluctuation | 0.921 | 2 |
| Sourcing of materials | 0.812 | 10 |
| Reviewing quotations from sub-contractors and suppliers | 0.875 | 5 |
| Correct wage rates for labour | 0.843 | 7 |
| Standard of workmanship required | 0.757 | 15 |
| Availability of labour (skill or unskilled) | 0.742 | 16 |
| Rates of rental of plant and machineries | 0.812 | 10 |
| Productivity and usage of plant and machineries | 0.812 | 10 |
| Allowance for Preliminaries costs | 0.828 | 9 |
| Allowance for Contingency or unforeseen works by the tenderers | 0.812 | 10 |

## CONCLUSION

This study is conducted with the intention to identify the critical factors that are significant in ensuring the accuracy of estimation for the purpose of obtaining a tender and delivering it at the completion date. This study has managed to come up with 18 critical factors and evaluated their degrees of importance based on the respondents' perceptions.

The results of this study showed that "understanding the scope of works" shall be treated as the most important factor, followed by "correct material price and forecasting fluctuation", "Read and check all tender drawings, compare the drawings with specification, check for discrepancy", "Site visit to be acquainted with the accessibility, topography, constraints, etc.", "Reviewing quotations from subcontractors and suppliers" and "Experience and competency of estimator".

Apparently, these six critical factors identified have much higher relative importance index, and it implies that these six factors have been given appropriate consideration in estimating cost accuracy for obtaining a tender successfully and ensuring the work tasks be delivered after being awarded with the tender.

## References

[1]    Akintoye, A. (2000). Analysis of factors influencing project cost estimating practice. Construction Management & Economics, 18(1), 77–89.

[2]    Ashworth, A. (2004). Cost Studies of Buildings (4 ed.): Harlow, England; New York : Pearson/Prentice Hall.

[3]    Barzandeh, M. (2011). Accuracy of estimating techniques for predicting residential construction costs – a case study of an Auckland residential construction company.  A Bachelor degree Dissertation, Unitec Institute of Technology, Auckland, New Zealand, http://unitec.researchbank.ac.nz/handle/10652/1794.

[4]    Dysert, L.R. (2006). Is "Estimate Accuracy" an Oxymoron? 2006 AACE International Transactions, 1–5.

[5]    Enshassi, A., Mohamed, S., Madi, I. (2007). Cost Estimation Practice in the Gaza Strip: A Case Study. The Islamic University Journal (Series of Natural Studies and Engineering), 15(2), 153–176.

[6]    Gilson, N.N., Vanreyk, A.J. (2016). Review of Cost Estimation Models International Journal of Scientific Engineering and Research, 4(3): 42-44.

[7]    Hendrickson, C. (2000). Organizing for Project Management, Department of Civil and Environmental Engineering, Carnegie Mellon University, Pittsburgh, PA, 2000; sections 2.3 & 2.4.

[8]    Lim, Y.M. (2011). Cost Estimating, A teaching module, Wawasan Open University (WOU), Penang, Malaysia.

[9]    Liu, L., Zhu, K. (2007). Improving Cost Estimates of Construction Projects Using Phased Cost Factors. Journal of Construction Engineering & management, 133(1), 91–95.

[10]    Oberlender, G.D.  (2000). Project Management for Engineering and Construction.  2nd Edition, New York, McGraw –Hill.

[11]    Odusami, K. T., Onukwube, H. N. (2008). Factors Affecting the Accuracy of a Pre-Tender Cost Estimate in Nigeria. Cost Engineering, 50(9), 32–35.

[12]    Peurifoy, R.L., Oberlender, G.D. (2002). Estimating Construction Costs, 6th Edition, New York, McGraw Hill.

[1.]Adekunle Ibrahim MUSA

# MATHEMATICAL APPROACH TO ESTIMATE THE PEAK EXPIRATORY FLOW RATE OF MALE BAKERS IN ABEOKUTA, NIGERIA

[1.]Department of Mechanical Engineering, Moshood Abiola Polytechnic, P.M.B 2210, Abeokuta, NIGERIA

**Abstract:** The study presented the mathematical approach to determine the Peak expiratory flow rate of male bakers in Abeokuta, Ogun State, Nigeria with the relationship of the peak expiratory flow rate and the anthropometrical parameters. A total of One hundred and Eighty (180) individuals were investigated with ninety (90) bakers (study group) who are exposed to flour dust and ninety (90) control subjects. The entire subject both study and control group are male. Peak expiratory flow rate (PEFR) and anthropometrical parameters were measured using mini-Wright peak flow meter (PFM 20, OMRON) and Detecto PD300MDHR (Cardinal Scale manufacturing company USA) column scale respectively. PEFR measured were compared using T-test and regression analysis. A mathematical model was developed to determine the peak expiratory flow rate (PEFR) with four factors of body mass, height, age and year of exposure where applicable. The study showed that PEFR in bakers was 182.67 ± 16.34 L/min as against 287.67 ± 17.03 L/min for control group from the regression analysis. Similarly, the model revealed that baker has 182.69 L/min and 285.77 L/min for control group. The Study concluded that using the developed model will serve as a great importance to workers to determine the level of their health and subsequently prevent untimely death.
**Keywords:** bakery, flour, dust, workers, peak expiratory flow rate, exposure, asthma

## INTRODUCTION

The degree of obstruction of airways in the lung needed to be checked as bakers have being adjudged to have highest incidence rate of occupational heart diseases (Ige and Awoyemi 2002). Different researchers have performed extensive work on the determination of peak expiratory flow rate of individuals to actually prevent the unwanted death among workers (Musa, 2015, Musa et al, 2016). Baatjies et al, (2010) research established the physiological status of bakery workers like allergic conditions, respiratory problems due to the daily exposure to flour dust.

The respiratory effects of exposure to flour dust are influenced by the dose and duration of exposure (Meo, 2006) and these differ from one working environment to other. Rafnsson et al., (1997) presented the peak expiratory flow rate of a healthy adult and non-exposed to dust between 300-600L/min with variation of age, body weight, height and gender. Musa et al., (2016a) investigated the peak expiratory flow rate (PEFR) of female bakers with about One hundred and twenty participant. The results showed that female bakers have 158.17±12.55L/min PEFR but did not consider male bakers as participant in the research. Elebute and Femi Pearse (1971) established values of PEFR in Nigeria with 142 healthy adults participated. The study showed that the mean value of male PEFR was 582±88.3L/min and 385±65.7L/min for female respectively.

Musa et al., (2016b) also investigated the relationship between the PEFR and the anthropometric parameters to determine the model equation for the determination of female bakers PEFR. The result showed that a female baker has 158.07L/min PEFR as against 267.96L/min for the control group. Hence, the aim of this research is to develop a statistical model to predict the peak expiratory flow rate of male bakers and compare it with non-bakers.

## MATERIALS AND METHODS

The study was conducted in Abeokuta with One hundred and Eighty (180) participants. Peak expiratory flow rate and anthropometric parameters of the participant were measured and recorded with ninety (90) adult male bakers and ninety (90) healthy male adult selected as the control group to the bakers. The age of the participated bakers range between 21-28years and they have involved in bakery business between 5month and 8years. The control group was of the same age bracket with the bakers. Both bakers and control group were assumed not to have no earlier reported systematic disease. Similarly, individual with smoking habit or suffering from any respiratory illness were exempted from the study.

The PEFR was measured with mini-Wright peak flow meter, (PFM 20, OMRON) (Figure 1). Three readings were taken from each subject in standing position and the best of the three were considered as Peak Expiratory Flow meter reading for that subject.



Figure 1: mini-Wright peak flow meter

Detecto PD300MDHR (Cardinal Scale manufacturing company, USA) column scale with digital height rod (Figure 2) was used to measure body mass (kg) and height (cm) of the subjects simultaneously.



Figure 2: Detecto (PD300DHR column scale with digital height rod

Questionnaire was also administered to the participant. The data collected from the questionnaire includes the detailed demographic data such as age, marital status, education level, smoking habit, duration of flour dust exposure and working experience. Figure 3 below showed the subjects performing measurement of PEFR.

Reference to the data collected, the relationship between the PEFR and anthropometric parameters existed and this was used to design the multi-linear regression model where PEFR remain the dependant of the anthropometric parameters.

The model follows the trends in equation (1) and (2) respectively (Musa et al, 2016b).

$$Y = a + b_1x_1 + b_2x_2 + b_3x_3 + \dots + b_nx_n \quad (1)$$

$$PEFR = a + b_1(Body\ mass) + b_2(Height) + b_3(Age) + b_4(years\ of\ exposure) \quad (2)$$

where, a is the constant and b is the coefficient of regression. Each coefficient b represent the effect of the independent variable y. $b_4$ is only applicable to bakers only.
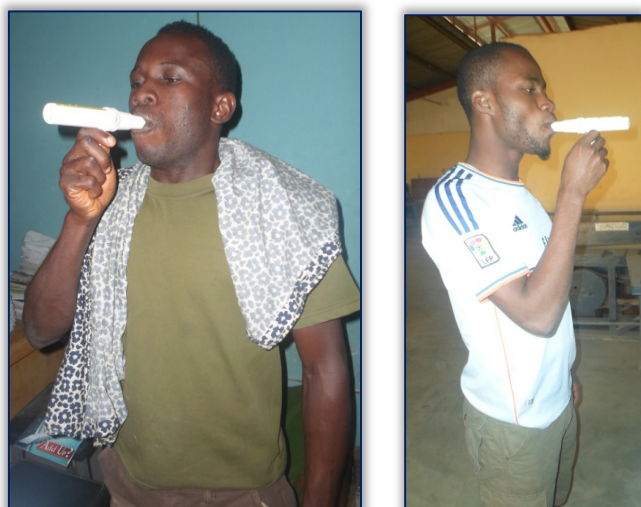


Figure 3: Subjects (Bakers) performing measurement of PEFR

## RESULTS AND DISCUSSION

Table 1 below showed the descriptive statistic and the T-test (one sample test) analysis of the investigated participants.

The results obtained were expressed using mean ± standard deviation, T-test for the two groups' comparisons and regression analysis.

Table 1: Descriptive statistics/ T-test (one sample test) for Male Subjects

|  | MALE (STUDY) | | | | | |
|---|---|---|---|---|---|---|
|  | N | Mean | S. E Mean | Std. Dev | t | df |
| Body mass (kg) | 90 | 61.508 | 0.4201 | 3.9851 | 146.422 | 89 |
| Height (cm) | 90 | 170.184 | 0.3953 | 3.7501 | 430.523 | 89 |
| PEFR (L/min) | 90 | 182.667 | 1.7223 | 16.3391 | 106.060 | 89 |
| Age (yrs) | 90 | 28.04 | 0.260 | 2.467 | 107.829 | 89 |
| Yrs o f Expo | 90 | 2.50 | 0.079 | 0.753 | 31.485 | 89 |
|  | MALE (STUDY) | | | | | |
|  | N | Mean | S. E Mean | Std. Dev | t | df |
| Body mass (kg) | 90 | 65.811 | 0.4837 | 4.5885 | 136.065 | 89 |
| Height (cm) | 90 | 170.904 | 0.4538 | 4.3050 | 376.618 | 89 |
| PEFR (L/min) | 90 | 287.667 | 1.7951 | 17.0294 | 160.255 | 89 |
| Age (yrs) | 90 | 27.97 | 0.327 | 3.107 | 85.405 | 89 |
| Yrs o f Expo | 90 | 2.50 | 0.079 | 0.753 | 31.485 | 89 |

Table 2 and Table 3 below showed the result of multi-linear regression analysis between the peak expiratory flow rate and the anthropometric parameters from the analysis, a model to predict the peak expiratory (PEFR) of the subject was derived.

Table 2: Regression analysis between PEFR and other parameter for Male bakers

| Model | | Unstandardized Coefficients | | Standardized Coefficients | t | Sig. |
|---|---|---|---|---|---|---|
|  |  | B | Std. Error | Beta |  |  |
| 1 | (Constant) | 277.033 | 71.637 |  | 3.867 | 0.000 |
|  | Body mass | -0.480 | 0.477 | -0.117 | -1.007 | 0.317 |
|  | Height | -0.292 | 0.497 | -0.067 | -0.587 | 0.559 |
|  | Age | 0.449 | 0.629 | 0.068 | 0.714 | 0.477 |
|  | Yr of Expo | -11.122 | 2.002 | -0.513 | -5.555 | 0.000 |
| a. Dependent Variable: PEFR | | | | | | |

Table 3: Regression analysis between PEFR and other parameter for Male (control)

| Model | | Unstandardized Coefficients | | Standardized Coefficients | T | Sig. |
|---|---|---|---|---|---|---|
|  |  | B | Std. Error | Beta |  |  |
| 1 | (Constant) | -21.985 | 61.321 |  | -0.359 | 0.721 |
|  | Body mass | 2.035 | 0.359 | 0.548 | 5.669 | 0.000 |
|  | Height | 0.953 | 0.347 | 0.241 | 2.748 | 0.007 |
|  | Age | 0.461 | 0.525 | 0.084 | 0.877 | 0.383 |
| a. Dependent Variable: PEFR | | | | | | |

From Table 2 and the trend in Equation (2), the model for the determination of PEFR for Male baker can be deduced and written as in Equation (3).

$$PEFR_{Male\ baker} = 277.03 - 0.48(Body\ mass) - 0.29(height) + 0.449(Age) - 11.12(yr\ of\ exposure) \quad (3)$$

Similarly, from Table 3 and the trend in Equation (2), the model for the determination of PEFR for the men not exposed to dust (control study) can be deduced and written as in Equation (4).

From table 3 above the model for the determination of PEFR for non-dust exposed Male can be deduced as,

$$PEFR_{Male\ control} = -21.99 + 2.04(Body\ mass) + 0.95(height) + 0.46(Age) \quad (4)$$

Equation 3 and equation 4 showed the regression equations where PEFR remain the dependent variable to determine the mathematical model. The applied anthropometrical parameters such as body mass, height, age and year of exposure played a major role in the determination of this model and they were considered as independent variables.
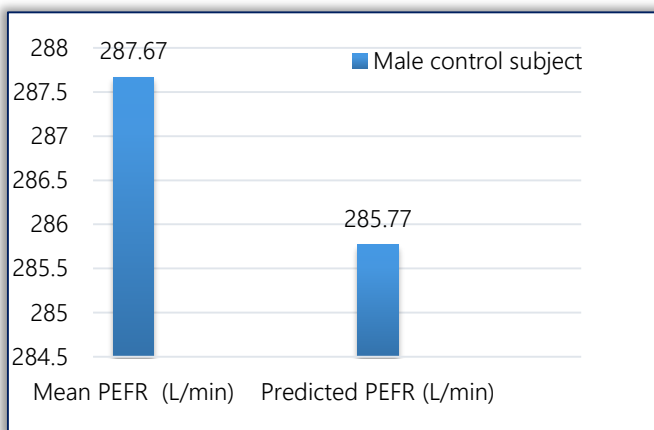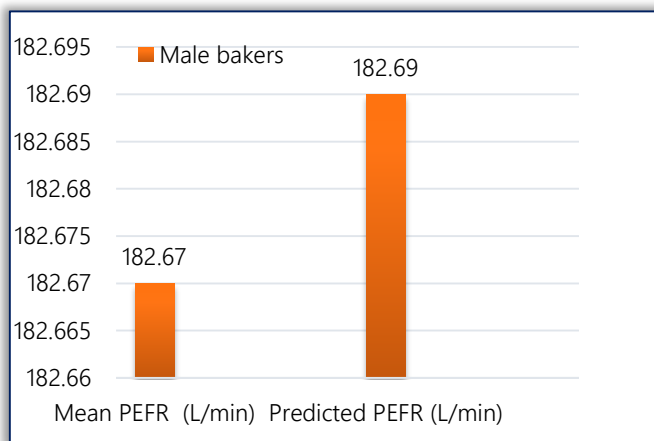




Figure 4: Comparison of Mean
and Predicted PEFR (L/min)

Host et al (1994) and Verma et al (2000) showed that an accuracy of predicted value of PEFR will be higher when age is considered along with height. Figure 4 showed the direct and the calculated measurement of PEFR for comparison. The figure 4 showed that the mean and predicted PEFR were closely similar (±0.02L/min). This little difference may be due to the instrument variations and the physical characteristics of the studied individual. PEFR (L/min) predicted were based on the multi-linear regression equation and this was found very consistent when compared with other study (Benjaponpitak et al 1999).

Musa et al (2016b) determine the female bakers and female flour non-exposed individual model. This model was in variance with the present study but similar trend was adopted. Musa et al (2016b) showed that the predicted PEFR for females both bakers and control study were 158.07L/min and 267.96L/min respectively.

But the present study which were male dominant showed 182.69L/min and 285.77L/min respectively for bakers and the control. This result was compared with Abou Taleb et al (1995), Rafnsson et al (1997) and Vestbo et al (1991) and this revealed that the bakers were not healthy and this might have affected the lung obstruction.

## CONCLUSION

The results obtained in the study can be used as a standard PEFR for any male individual who are exposed or not exposed to the flour dust. These equations can also play a major role in determining the PEFR of any male individual in the absence of the hand-held devices for the measurement.

Further study is also required to develop a model that will be devoid of gender either male or female. This will allow for wide range of determining the PEFR of individual who are exposed or non-exposed to flour dust.

## References

[1] Abou Taleb, A.N.M., Musaniger, A.O. and Abdel Moneim, R B. (1995). Health status of cement workers in the United Arab Emirates. Journal of Royal Social Health; Vol 2:378-383

[2] Baatjies R,Meijster T, Lopata A, Sander I, Raulf-Heimsoth M, Heederik D, Jeebhay M. (2010). Exposure to Flour Dust in South African Supermarket Bakeries: Modeling of Baseline Measurements of an Intervention Study. Annal Occupational Hygiene; 54(3):309–318.

[3] Benjaponpitak S, Direkwattanachai C, Kraisarin C, Sasisakulporn C, (1999). Peak expiratory rate values of students in Bangkok. Journal of Medical Association of Thailand; Nov, 82 (supplementary) 1:S137-143.

[4] Elebute, E.A. and Femi-Pearse, D. (1971). Peak Flow rate in Nigeria: Anthropometric determinants and usefulness in assessment of ventilatory function. Thorax. 26: 597-601.

[5] Host-A, Host A.H and Ibsen. T, (1994). Peak expiratory flow rate in healthy children aged 6-17 years. Acta- Paediatrics; 83(12):1255-1257.

[6] Ige O.M and Awoyemi O.B. (2002). Respiratory symptoms and ventilatory function of the bakery workers in Ibadan Nigeria, West Africa. Journal of Medical Vol 21(4), Pp316-318

[7] Meo S.A. (2006). Dose responses of years of exposure on lung function in flour mill workers. Journal of occupation health; Vol 46:187-91.

[8] Musa, A.I. (2015) "Peak Expiratory Flow Rate model for female Bakers In Abeokuta, Ogun State, Southwest Nigeria" 2nd International Conference on Applied Sciences and Technology (ICAST 2015), October 28-30, 2015 at Technical University (formerly Kumasi Polytechnic), Kumasi, Ghana. www.lcast.kpoly.edu.gh

[9]  Musa A.I., Ishola A.A., & Adeyemi H.O., (2016a), "Investigation of Peak Expiratory Flow Rate of female bakers in Abeokuta, Ogun State, Nigeria". Journal of Scientific and Engineering Research, Volume 3 (3); Pp 67-72, www.jsaer.com

[10] Musa A.I., Adeyemi H.O & Odunlami S.A (2016b), "Modelling the Peak Expiratory Flow Rate for female bakers in Abeokuta, Nigeria". FUTA Journal of Research in Sciences, Volume 12 (1); Pp 46 – 54, www.fjrs.futa.edu.ng

[11] Rafnsson V, Gunnarsdottir H. and Kiilunen M. (1997). Risk of lung cancer among masons in Iceland.  Occup.  Environ. Med; Vol 54: 184-188.

[12] Verma S.S, Sharma Y.K, Arora S, Bandopadhyay P, Selvamurthy W, (2000). Indirect assessment of peak expiratory flow rate in healthy Indian children. Journal of Tropical Paediatric Vol 46:54-55

[13] Vestbo J, Knudsen K.M, Raffn E, Korsgaard B, Rasmussen F.V. (1991).  Exposure to cement dust at a Portland cement factory and the risk of cancer. British Journal of Industrial. Medicine; 48:  803-7.

1.Dominika PALAŠČÁKOVÁ

# COLLECTION OF PRODUCTION INFORMATION INTO THE DATABASE

1.Technical University of Kosice, Faculty of Mechanical Engineering, Department of Production Technology, SLOVAKIA

**Abstract:** The paper focuses on the area software application that helps businesses to significantly increase the production efficiency and the amount of production of products that allows to identify and to quantify the exact causes of production losses caused by inefficient use of their production facilities. The application allows manufacturers to track and analyse the effectiveness of their overall production downtime and machinery, production lines and other equipment in production and obtain as follows detailed information on the efficiency of the production and possible shortcomings with the acquisition in real time directly from the production facilities and production operators. For the evaluation is available, easy to use reports and analytical tools to quickly reveal trouble spots that need to be improved.
**Keywords:** visualization, MES, SCADA

## INTRODUCTION

Timely and accurate production information from the production are in today's competitive market environment, the key to the prosperity of the manufacturing firms. The collection and storage of information of the production is the first necessary step in the production process. Then the following information obtained from the production to different optimal decisions for the improvement of the quality of production to control workers, reducing production costs and increasing production.

Global competition and the need to respond quickly to new business opportunities have raised in recent years the need for new developments in the field of industrial automation and information systems architecture. Production and other industrial companies no longer need to create a comprehensive and indivisible software applications, which require a large amount of time for your design, development and deployment. The requirement is flexible and modular solution, in which it is possible to very quickly create or modify existing applications, keeping in mind that the requirements on them or even to the entire application may change in the future.

## INCREASE OPERATIONAL PERFORMANCE IN THE PRODUCTION PROCESS

The concept and functionality of the software products allow for flexibility in the development of large scale, deployment and updates to applications. Users can flexibly adapt and easily expand their production systems in order to meet not only current, but arbitrarily, practically as well as future needs and continuously improve the management, efficiency and effectiveness of production.

Software architecture for efficient design and operation of the application provides automation and information solutions for:

— Visualization and application of type supervisory HMI (Human-Machine Interface) - visualization and supervisory management/human-machine interface

— Supervisory and visualization applications, SCADA/Geo-SCADA (Supervisory Control and Data Acquisition) - the management and collection of data, including extensive technological units

— Applications for advanced management and analysis of the production operations of the Production and Performance Management category - production management and analysis of the performance of the production, or MES (Manufacturing Execution Systems).

With the help of the software, you create an advanced technological information system, which is closely connected with its own production in the manufacturing process. Software so aptly complements the administrative business information systems, human resources and finance on trade logistics. The necessary information is provided to the workers of various levels of the enterprise, and not only horizontally, but also vertically, i.e. from the production operators to the management of the undertaking. It is broken down by production enterprises in the usual barriers between the world and help to meet the requirements of the various certificates and customer audits.

The most important features include:

— collect data from control systems,

— visualization and supervise solution of technological processes,

— adherence to production processes,

— the actual production history and record all the important technological parameters

— analysis and documentation of the actual course production processes (family tree),

— detailed tracking of production and management (MES)

— static quality management of production processes,

— tracking and analysis of production downtime,

— calculation of the total efficiency of the production facilities,

— access to production information both inside and outside the workplace (Internet).

Software module helps producers improve the operational performance of their operation, the integration of branded products and the ability of the environment to the inner requirements of rapid reaction, [1]. The application of the module ensures consistent operation of machinery or production lines improves the reliability and repeatability of the final settings of the parameters prescribed production equipment and allow for a detailed analysis of all the events in their own production and recording.

Program system allows you to:
— ensure the right parameters for consistent production in order to maintain consistency and quality production manufacturing operations accompanying the branded products,
— improve the reliability and repeatability of production facilities to increase the flexibility of production settings and reducing production scrap,
— a detailed record of all relevant production auto events (actual production history) into an electronic database,
— a detailed analysis and documentation during the production, including the production of pedigrees, bidirectional,
— rapid feedback control of specific products and the identification of the causes of any problems,
— to meet Government or institutional regulations and directives intended to protect public health and safety,
— easy application changes or expansion of the system in case of growing requirements,
— ease of integration of the company's trading system with direct management of production thanks to the standard data structure of the snap-in, in accordance with the norm.

## RELIABILITY AND HOMOGENEITY OF MANUFACTURING OPERATIONS

Software application ensures the homogeneity of the settings and operation of the machinery, consistently production lines and detailed records of all important events, which may be available to the production to the level of each individual product.  Each production order can be assigned to the specified source or device, such as a particular production unit or production line. It automatically selects the necessary parameters of the production processes and associated with the appropriate adjustment points (set-points) production facilities. During the course of production shall be obtained and stored for detailed information about specific materials that have been used in the manufacture of concrete products. The information on which these products were manufactured, who served the machines and other production-related information that can be sorted according to the flow of production, or  the serial numbers of each product. By so called "bloodlines" enabling the tracing back of the complete production history, as shown in figure 1, [2]. Here we can examine the following information:
— used in production processes and adjusting the points assigned to the production,

— the actual consumption of raw materials that were used and the kind of quantity for each manufacturing batch or a batch of the finished product, including the identification of any of the products or waste,
— in the finished products, which was used a feedstock. In the case of additional findings on problems of this raw material so it can instantly and accurately identify all the finished products back,
— the use of specific production equipment for the production of specific products,
— who participated in the production of specific products, operators,
— other events related to a specific part of the manufacturing process, certain equipment or operator,
— comparison of planned and actual values of material consumption, operating cycle times, etc.



Figure 1: A variety of options for the analysis
of production history reports for all products

## RECORDING AND ANALYSIS OF ACTUAL PRODUCTION HISTORY

Client access to stored information is made possible through an online information portal. It's production information portal, which gathers production data from various sources, these data appropriately organizes, secures and provides a large number of candidates eligible customer from the Internet / Intranet. Clients do not need to have any special software installed on your computer.

It turns out that the information is no longer sufficient to provide only the operator and supervisor. Certain information about the status of production in real time, the summary and analysis of the data during the production, and sometimes even the ability to remote control, it is now necessary to make a new category called and everything "casual" users. In the light of to the frequency of access to the data of these users, it is no longer economical to handle their complete system of SCADA/HMI or other special categories of client applications. The system is capable of all of the data and services provided by means of a much simpler interface-a regular browser for the website, figure 2.
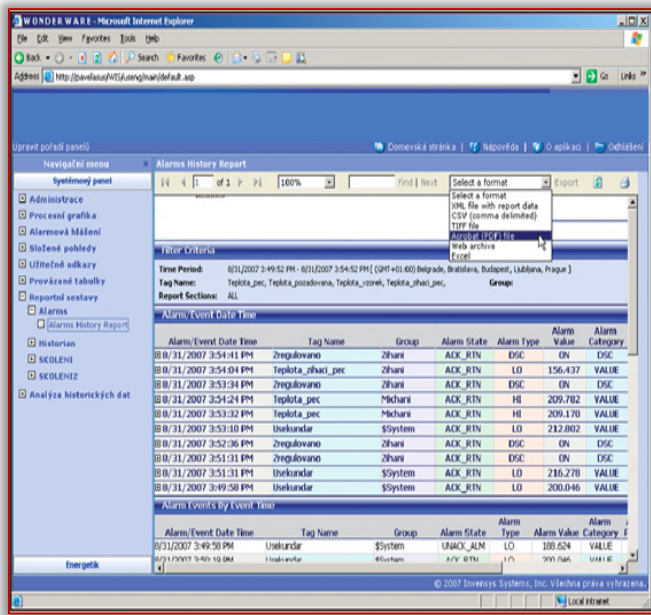
Figure 2: The report data is stored in a database accessible through the Internet

Information server allows clients to access live data and alarm (current and historical), figure 3. The client has the possibility to see the portal "in context", which allows him to quickly get an overview of the State of technology.

Effective protection of published data is further ensured by additional security systems integrated directly in the portal. The panel navigation system allows clients to access only the data that correspond to the declared their vocational focus. The system user role defines the rights of users with respect to the technology (the right entry in the I/O, read-only).
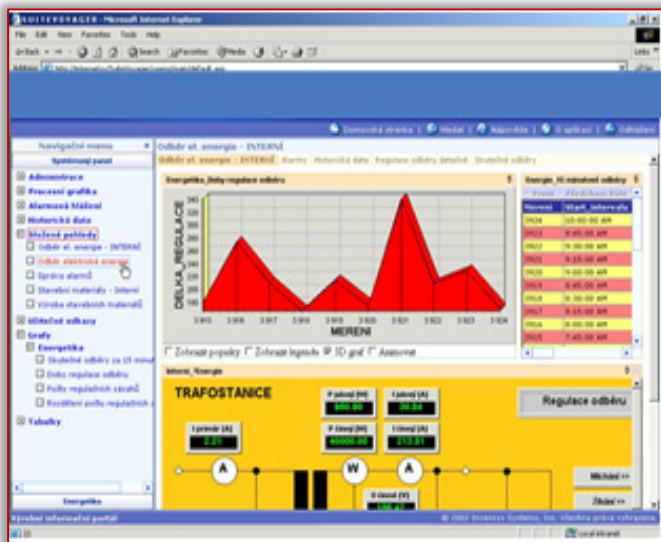


Figure 3: Graphical display technology with current data

The program not only ensure proper production parameters and helps manufacturers system by the quality and homogeneity of production thanks to the automation of production facilities, but also to meet a series of requirements settings, which are given by different governmental regulations, directives and initiatives intended to protect public health and safety. The complete records of the products in the State "as they were actually produced" are stored in the database, and given the system as soon as available. Users module to meet the requirements of accuracy and quick availability of records on the composition and quality of all its products throughout the life-cycle-from raw materials to the final product, as shown in figure 4 [3].
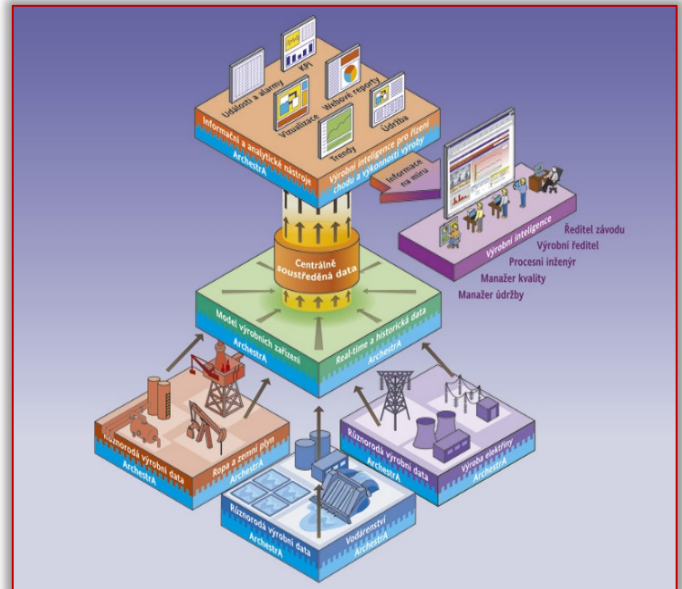


Figure 4: The architecture of the flow of information in the production

You can therefore benefit from all the advantages of the application of a coherent philosophy of the entire system using this technological infrastructure for industrial automation and information applications, [4].

The main benefits include:
— collect data from a variety of management systems (independence from a particular brand of hardware automation),
— a distributed client/server system architecture,
— central deployment, administration and application-wide Diagnostics,
— high repeatability,
— the use of visualization systems for illustrative graphical user environment,
— easy during development and after deployment, applications, accompany,
— unlimited flexibility and scalability for applications of any size.

Thanks to the openness of the architecture can be operated with the new application module and production facilities and control systems from different manufacturers. Thus, there is no loss of previous investments and intellectual knowledge, but rather an extension of the moral life of the developed production systems. The functionality of the solutions can be implemented gradually according to the desired range of functionality and the size of the application. Thanks to the practical system architecture for a solution easily expands to tap the growing demands of the end user.

## WITH HISTORICAL DATA FROM THE PRODUCTION DATABASE

A database management system with historical data is designed for the rapid collection of a large number of technological data from production processes, their effective application and easy provision of different types of client applications, figure 5.

System and related products for the analysis of stored procedures and data access by any interested undertaking to ensure technology exact production information in good time. Data for the first time obtained from production processes are transformed into the information necessary for the correct assessment of the situation and understand what and why going on in a production environment. On the basis of these skilled and quick reference of available information can be efficiently convert smart operational and strategic production decisions.
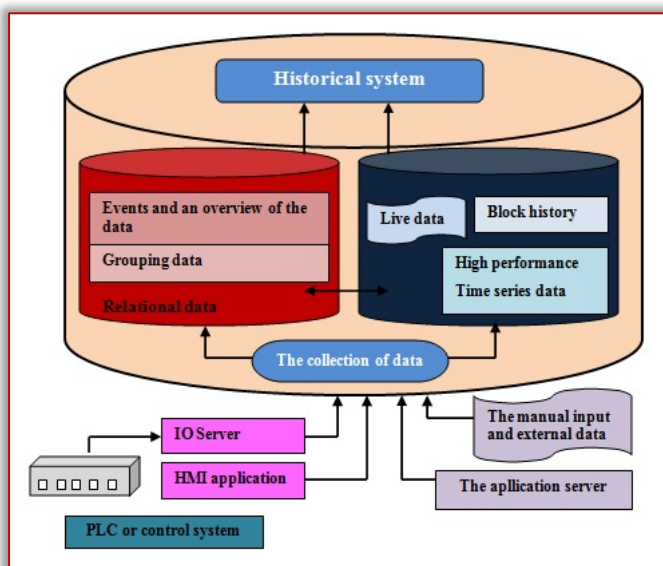


Figure 5: Architecture of the database
with historical data

Obtained "production intelligence" allows the responsible staff at all levels of the company quickly removed the tiny variations in production and technological processes, and the bigger and on an ongoing basis so to ensure a high quality of production.

The main features and benefits:
— the collection of large amounts of data from arbitrary data sources, and production process,
— Real-time performance while maintaining the openness of the system relational database,
— efficient compression algorithm minimizes storage space for data storage,
— integrated database providing universal access not only to the procedural and technological data stored, but also to other related data on production,
— the integration with the portal server Information for convenient delivery of targeted information client users- live process graphics, trends over time, reports, analysis, key performance indicators,
— support of communication and in an environment of slow and unstable networks,
— compliance with safety requirements,
— support to ensure high availability of the critically important applications,
— solution for immediate deployment and easy use of boxed system.

## CONCLUSIONS

Strategic concept the server combines the openness of a relational database by using a database system with special optimizations for high performance and efficient storage of data, which are necessary for the processing of large volumes of data and for the movement in real time. The system receives data and stores it in the necessary place. The data from the various sources of production processes in real time and allows you to keep track of them as well as with manual loading or older data with data stored during a network outage or in distributed systems. All information is available in one place and, thanks to the openness of access to data you can easily analyze a large number of different types of client applications, [5].

The system concentrates all necessary data from the production environment. This is the flexibility of the system, how and where will those obtained the required data is collected and stored. All information, regardless of their place of origin, the manner and time fully integrated in the central data store record.

## Acknowledgment

## References and Notes

[1] Wonderware, Pantek, corporate materials
[2] http://www.pantek.cz/produkty/wonderware-operations-software/
[3] http://www.pantek.cz/produkty.php?id_produktu=8&produkt=wonderware-information-server
[4] http://www.pantek.cz/produkty/wonderware-system-platform/
[5] http://www.pantek.cz/produkty/wonderware-performance-software/

[1.] Victoria Dumebi OBIEKEA, [1.] Israel Olatunde SEKUNOWO,
[2.] Mike Gbeminiyi SOBAMOWO, [1.] Samson Oluropo ADEOSUN

# STUDY OF MACROSEGREGATION EFFECTS ON THERMAL AND ELECTRICAL CHARACTERISTICS OF ALUMINUM-COPPER ALLOY

[1.] Department of Metallurgical and Materials Engineering, University of Lagos, NIGERIA
[2.] Department of Mechanical Engineering, University of Lagos, NIGERIA

**Abstract:** Macrosegregation phenomenon regardless of casting size often induces high partition coefficient (k) impacting adversely the thermal and electrical properties of cast binary alloy. In this study, an experimental investigation of macrosegregation propagation in aluminum-copper alloy solidification is reported. Al6wt. % Cu was produced at varied pouring heights including 100 mm, 200 mm, 300 mm, 400 mm and 500 mm. The combinations of optical, scanning electron and energy dispersive spectrometry were used to evaluate the extent of segregation in the casts while the electrical and thermal conductivity properties were determined using Wiedemann-Franz Law. Results show that the Al-Cu cast at a pouring height of 400 mm demonstrated the highest electrical and thermal conductivity of 55 %IACS and 2.1437 W/mK $10^{-6}$ respectively. This compared well with established standard values in application such as heat exchangers and electronic sensors. The occurrence of minimal macrosegregation at 400 mm pouring height may be attributed to appropriateness of melt-flow regime resulting in desirable microstructure that prevents long-range solute/solvent segregation.
**Keywords:** macrosegregation, Al-Cu alloy, electrical conductivity, thermal conductivity

## INTRODUCTION

Solidification phenomenon involves liquid-to-solid phase transformation along a moving interface, which is often accompanied by the release of latent heat energy (Nastac et al., 2016). Generally, the solidification of castings with columnar structure usually give rise to castings rich in solute at the centre than the skin. This is attributed to solute rejection from the first solidified solid into the liquid just ahead of the solid-liquid interface. For short distance variation in chemical composition, microsegregation occurs but this can be remedied through a simple annealing heat treatment procedure. However, when inhomogeneity in chemical composition occurs over a long range, it produces macrosegregation, which cannot be removed by any heat treatment procedure. The problem of macrosegragation is a common occurrence in aluminium and copper alloys castings (Ahmadein et al., 2015). It is reported that macrosegregation is caused mainly by fluid flow rather than solute diffusion at macroscopic scale (Tveito et al., 2012). The solute diffusion layer is pictured as been much smaller than the actual dimension of the volume element. According to Beckermann, (2008), macrosegregation is more pronounced and problematic in castings with diameters between 20 mm and 40 mm resulting in a relatively high partition coefficient. The solute diffusion and redistribution invariably impacts the mechanical, electrical and thermal properties of the cast.

As-cast structures with macrosegregation of alloying elements also contain impurity elements, gases and shrinkage pores as well as undesirable macroscopic constituents. These constituent have the tendency to affect the overall conductivities of the cast owing to discontinuity created in heat flow. Due to the difficulty of direct and accurate determination of thermal conductivity, it is necessary that another physical property is coupled to thermal conductivity (Clemens, 2000; Volklein et al., 2009). One of such methods is based on Wiedemann-Franz Law for metals. This law stipulates that thermal conductivity approximately tracks electrical conductivity. This is predicated on the fact that freely moving valence electrons transfer not only electric current but also heat energy. However, the general correlation between electrical and thermal conductance does not hold for other materials (Clemens, 2000). Electrical and thermal conductivity being a measure of transport of properties can be subjected to the same physical laws. For this reason, any theoretical predictions and general experimental findings established for the flow of heat in metal alloy or composites are generally applicable to both properties. Theoretical studies (Ahmed et al., 2013) have shown that thermal conductivity of alloys in relation to composites is a function of volume fraction, distribution and thermal conductivity of the constituting elements. The existence of a thermal barrier at the interface owing to inhomogeneity in chemical composition and different intermetallic phases formed can bring about inconsistency in the flow/transport of electrical and thermal properties from one point to another. This assertion is yet to be experimentally verified hence the current study focuses on the effect of macrosegregation on thermal and electrical characteristics of aluminum-copper alloy.

## MATERIALS AND METHODS

Commercial aluminum (1000 series) ingots were obtained from Qualitech, Ojokoro, Lagos, Nigeria and mechanically

sectioned at ambient temperature into smaller sizes suitable for melting. The copper scraps were sourced locally, reconditioned by removing all drib. The materials were then combined and used as alloying element according to the formation presented in Table 1. Melting was done in batches as Copper was charged first into the furnace before aluminum. The molten alloy was continuously stirred in order to ensure a uniform distribution of alloying elements. Casting of samples in sand moulds was carried out for five different pouring heights of 100, 200, 300, 400 and 500 mm. Figure 1 (a and b) show a typical sand mould used and graphic illustration of the internal configuration of the mould. It is to be noted that a thermocouple was inserted in the mould while casting was being carried out to ensure the continuity of temperature profiles measurement. The temperature profile data obtained helps in interpreting the melt- flow behaviour, casting speed, the microstructure and eventually the mechanical properties of the cast. The data was also used to generate the relevant cooling curves.



(a)                                                    (b)
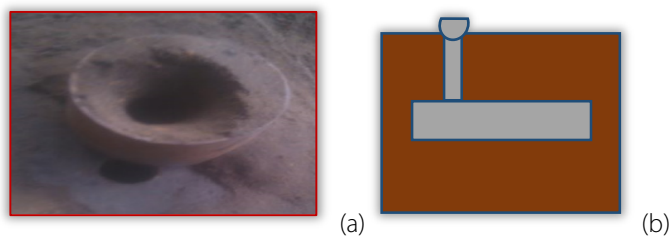
Figure 1. Casting of samples in sand moulds
a) typical sand mould; b) graphic illustration of the internal configuration of the mould

Table 1: Spectrometric Analysis of Aluminum - Copper Alloy

| Sample Designation | Wt.% Composition | | | | |
|---|---|---|---|---|---|
| | Al | Cu | Si | Mg | Fe |
| A1 | 96.01 | 2.000 | 0.951 | 0.667 | 0.372 |
| A2 | 94.80 | 4.000 | 1.063 | 0.039 | 0.098 |
| A3 | 91.98 | 6.000 | 1.010 | 0.050 | 0.960 |
| A4 | 88.66 | 8.000 | 1.832 | 0.131 | 1.377 |

## ⊞ Thermal conductivity & electrical conductivities tests

In these tests, the inverse of conductivity called resistivity was determined for aluminum-copper alloys using a BEKO power AB of TYPE – Rm 0606, 110/240V AC. The input current varied from 10 - 100 and 100 - 600 amperes within the ranges of 10 and 100 amperes respectively. For each sample, ten readings of resistivity were obtained and these data were further used to calculate both electrical and thermal conductivities. The following formula relates resistivity to electrical and thermal conductivity;

$$\sigma = \frac{1}{\rho} \qquad (1)$$

$$k = \sigma LT \qquad (2)$$

Where $\sigma$ is the electrical conductivity in $\Omega^{-1}m^{-1}$, $\rho$ is resistivity in $\Omega$, k is the thermal conductivity in W/mK, T is the absolute temperature in K, and L is the Lorenz number, equal to 2.45 $10^{-8}$ W$\Omega$/K$^2$.

## ⊞ Microstructural analysis

The techniques employed for microstructural study entail Optical, Scanning Electron (SEM) and Energy Dispersive (EDS)

analysis. The specimens for microstructural analysis were sectioned at the edges and middle of cast samples. Grinding and polishing were done using emery papers of different grit sizes ranging from 120, 240, 320, 600 and 1200 until a mirror-like surfaces was achieved. Weck's reagent which is made up of 100 mL water, 4 g $KMnO_4$ and 1 g NaOH was used as etchant at room temperature. The surfaces of the polished samples was swabbed with the etchant for 15 s. The etched specimens were then carefully washed, dried to avoid accidental scratches on their surfaces. The specimens were then mounted on the optical microscope and images were obtained at 200 µm magnification. These same set of samples were used for both SEM and EDS analysis. A Phenon proX SEM machine with model number 80007334 and part number MVE0224651193 was used for this analysis.

## RESULTS AND DISCUSSION

## ⊞ Solidification dynamics of Al-Cu alloy

Figure 3 shows the cooling curves of the alloy casting as measured by the thermocouple. From onset of solidification, the casting temperature drops instantaneously to a range of 670- 650 °C, which is about the melting point of aluminum. This observation remains fairly constant for ~ 160-180 s, thereafter; the cooling rate progressed until the molten metal solidified completely. The stage at which the temperature is fairly constant is due to the release of latent heat of solidification. The temperature decreases rapidly with increasing time once the release of latent heat was completed. It should be noted that all these cooling milestone took place in quick succession and in a matter of minutes the entire Al-Cu casting attained a uniform temperature. This rapidity in solidification process can be attributed to high thermal conductivity of aluminum in the system.
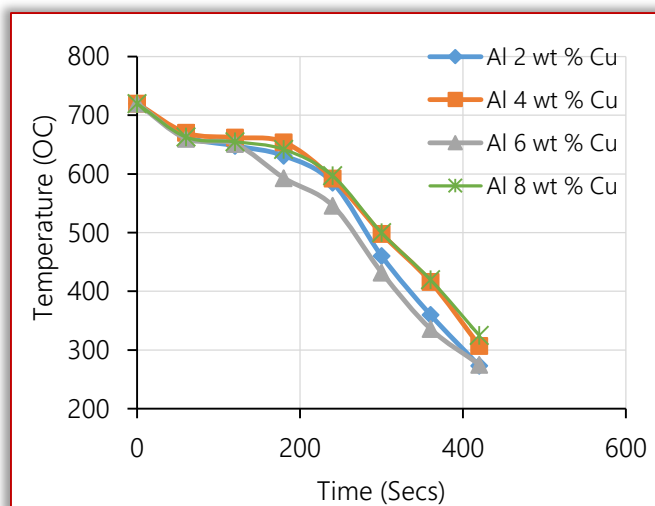


Figure 2: Cooling curves for Al-Cu alloy

## ⊞ Effect of varied pouring height on cast microstructure

The occurrence of solute atom segregation was more pronounced with samples containing 6 wt. % Cu (Figure 3). However, the segregation is observed to be more prominent towards the periphery of the cast while the center of the billet was highly depleted of the solute element. The sample at

400 mm pouring height exhibited a uniform distribution of solute element than at other pouring heights and therefore less segregated. Plate 1 shows respectively the optical scanning electron micrographs and EDS of cast samples. The major impactful phases Al-matrix are predominantly spherodised, $AlSiO_2$ crystals are homogenously distributed while some fringes of $Al_5FeSi$ intermetallic are also observed. Conventionally, Fe appear in Al-Cu alloys as impurity element, and its presence often impairs ductility of castings by the formation of Fe-rich intermetallic compounds, particularly the $Al_5FeSi$ phase (Malakhov et al., 2010; Nowotnik et al., 2007). Plates 2 – 5 revealed the variations that ensued with regards to the volume fraction, dispassion and morphology of the major phases within the matrices at different pouring heights. These varied microstructural features impact significantly the alloys thermal and electrical conductivities.
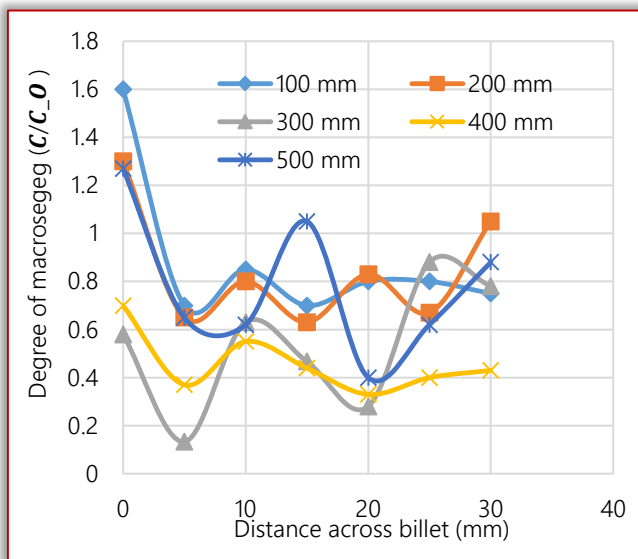


Figure 4: Effect of varied pouring height on relative segregation within Al - 6wt. % Cu Alloy
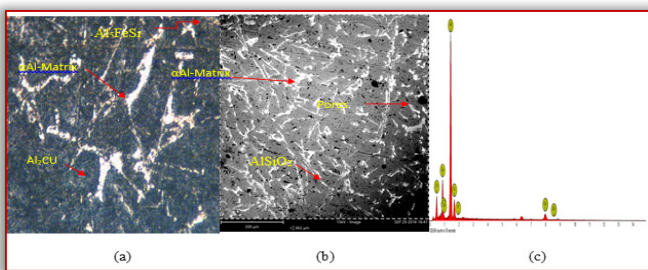


Plate 1: Micrographs of Al -6wt. % Cu 100 mm pouring height (a) optical (b) SEM and (c) EDS
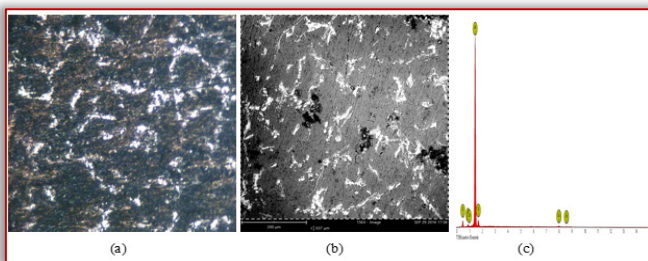


Plate 2: Micrographs of Al -6wt. % Cu 200 mm pouring height (a) optical (b) SEM and (c) EDS
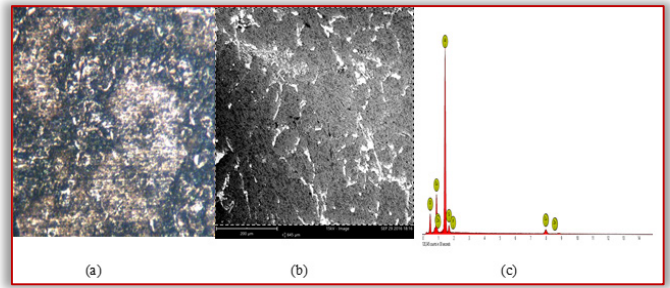


Plate 3: Micrographs of Al -6wt. % Cu 300 mm pouring height (a) optical (b) SEM and (c) EDS
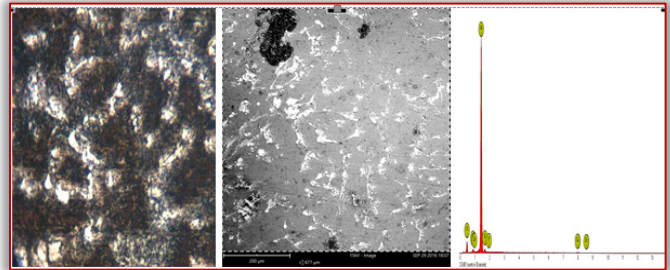


Plate 4: Micrographs of Al -6wt. % Cu 400 mm pouring height (a) optical (b) SEM and (c) EDS
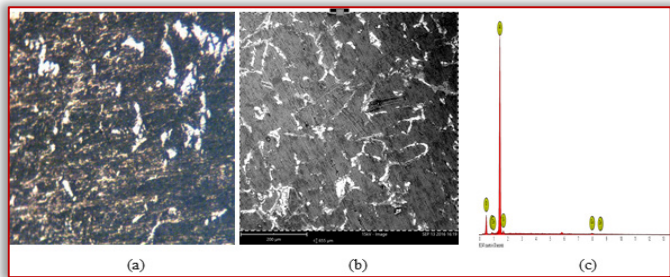


Plate 5: Micrographs of Al -6wt. % Cu 500 mm pouring height (a) optical (b) SEM and (c) EDS

## ⊞ Impact of Macrosegregation on Thermal and Electrical Properties of Al - Cu Alloy

Figures 5 and 6 illustrate the electrical and thermal conductivity characteristics of the Al-Cu alloy at varied pouring heights. From the figures, it is observed that the Al-Cu cast sample at a pouring height of 400 mm has the highest electrical and thermal conductivities of 55.3 IACS and 2.1437 W/mK respectively.
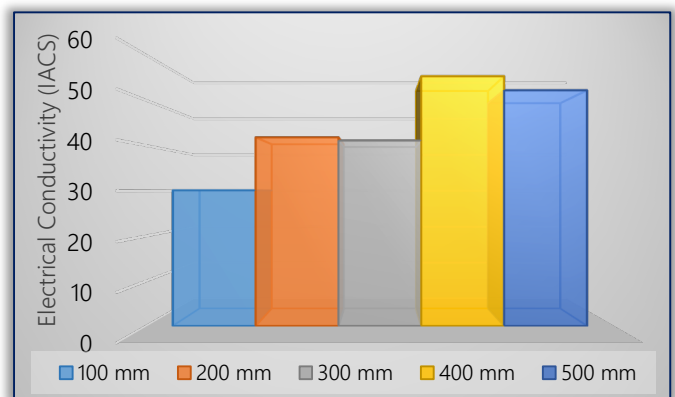


Figure 5: Electrical Conductivity of Al6wt%.Cu Alloy at Varied Pouring Height
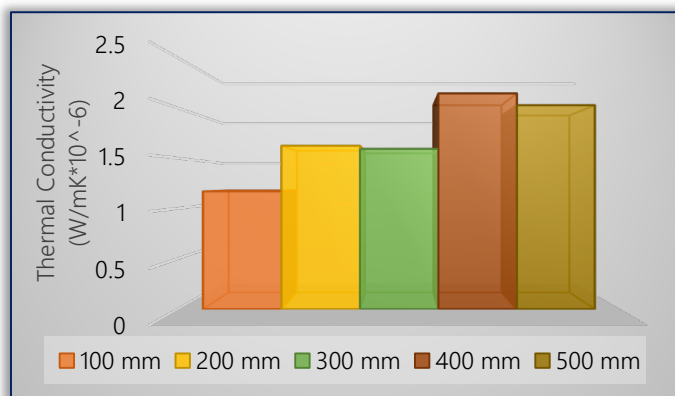
Figure 6: Thermal Conductivity of Al6wt%.Cu Alloy
at Varied Pouring Height

It should be recall that cast alloy at 400 mm pouring height exhibited near-not segregation. Hence, confirms the fact that macrosegregation has great influence on the conductivity of cast samples. Low degree of segregation ensures a more coherent structure that engenders uniformity and consistency in heat flow.

According to Woodcraft (2005) and Zang and Wand (2015) relatively homogenous structure give rise to low thermal barriers, hence increase in thermal barriers are reduced, hence an increase in the thermal and electrical properties.

## CONCLUSIONS

From this study, cast samples produced by pouring from spruce 400 mm height exhibited better and uniform distribution of solute/solvent elements resulting in minimal macrosegregation. The electrical and thermal conductivities at 400 mm pouring height also has the highest value (55.3 IACS and 2.1437 X 10^-6 W/mK) which compares well with standard values (59 IACS and 2.4878 X 10^-6 W/mK). Thus, 400 mm spruce height is deemed the optimum pouring height. It is concluded that the control of molten metal pouring height is critical in reducing the incidence of macrosegregation during solidification of molten binary alloy. The effect of this defect reduction translates into significant improvement in thermal and electrical properties of the cast alloy making it suitable for applications in thermal plants (cooling fins) and industrial refrigerating units.

## References

[1] Ahmadein, M; Wu, M and Ludwig, A: Analysis of macrosegregation formation and columnar to equiaxed transition during solidification of Al-4wt.%Cu ingot using a 5-phase model, Journal of Crystal Growth, 417, 65-74, 2015.

[2] Beckermann, C: Macrosegregation, ASM Handbook Casting, 15, 348-352, 2008.

[3] Clemens, J.M.; Lasance: How thermal conductivity relates to electrical conductivity, Technical Data, Test & Measurement, 6, 2, 1, 2000.

[4] Geiger, A. L; Hasselan, D. P. H, and Welch, P: Electrical and thermal conductivity of discontinuously reinforced aluminum composites at sub-ambient temperatures, Acta mufer, 45, 9, 391 l-3914, 1997

[5] Malakhov, D.V; Panahi, D and Gallerneault, M: On the formation of intermetallics in rapidly solidifying Al–Fe–Si alloys, Calphad, 34, 2, 159-166, 2010.

[6] Mrówka-Nowotnik, G; Sieniawski, J and Wierzbiñska, M: Intermetallic-phase-particles-6082-aluminium-alloy, Archives of Material Science and Engineering, 2, 28, 69-76, 2007.

[7] Rauber, M and Neumann, R: The experimental investigation of thermal conductivity and the wiedemann–franzlaw for single metallic nanowires, IOP Science, Nanotechnology, 20, 32 4484-5706. 2009.

[8] Woodcraft Adam, L: Predicting the Thermal Conductivity of Aluminium alloys in the Cryogenic to Room Temperature Range, Journal of Engineering and Apply Science, 45, 6, 421–431, 2005.

[9] Yulin, L; Ming, L; Lei, L; Jijie, W and Chunzhong, L: The solidification behavior of 2618 aluminum alloy and the influence of cooling rate, Materials, 7, 12, 7875-7890, 2014.

[10] Zhang, D and Wang, J: Thermal conductivity prediction of closed-cell aluminum alloy considering micropore effect, Advances in Mechanical Engineering, 7,2, 1–8, 2015.

[1.]Mirko SAJIĆ, [2.]Dušanka BUNDALO, [3.]Zlatko BUNDALO, [4.]Dražen PAŠALIĆ

# USING DIGITAL AND MOBILE TECHNOLOGIES FOR INCREASING EFFICIENCY OF FINANCIAL INSTITUTIONS

[1.] Sberbank a.d., Banja Luka, BOSNIA & HERZEGOVINA
[2.] Faculty of Philosophy, University of Banja Luka, BOSNIA & HERZEGOVINA
[3.] Faculty of Electrical Engineering, University of Banja Luka, BOSNIA & HERZEGOVINA
[4.] Sberbank a.d., Banja Luka, BOSNIA & HERZEGOVINA

**Abstract:** Possibilities and methods for increasing efficiency of financial institutions operation using digital and mobile electronic technologies are considered, proposed and presented in the paper. Digital and mobile electronic technologies are used in many areas and many practical solutions and applications. One of very important areas is financial business in many financial institutions. Using computers, computer networks, Internet and smart mobile phones, with appropriate software applications, enable to increase speed and security of all financial transactions and increase financial institutions efficiency. Also, it gives many advantages to users of financial services and institutions. Way to increase efficiency of operation of financial institutions using digital and mobile technologies on the example of the typical commercial bank is proposed and described. As an example of using such technologies for increasing efficiency of the bank was designed, developed, implemented and described one system for facilitating and accelerating issuance of bank loans using smart mobile phones. Implementation, used technologies, possibilities, advantages for bank and user and way of using of the system are described.
**Keywords:** digital electronic technologies; mobile technologies; financial institutions; smart mobile phones, information

## INTRODUCTION

Digital and mobile electronic information and communication technologies are widely used in very many areas and practical solutions and applications. One of very important area is financial business and different financial services in many financial institutions, such as for example banks [1-3]. By using computers, computer networks, Internet, smart mobile phones, with appropriate software applications, it is possible to perform almost all bank activities and operations, to increase speed and security of all financial transactions and to increase financial institutions efficiency. It also gives many advantages to the financial institutions and also for users of financial services and institutions.

This paper proposes and describes possibility and way to increase efficiency of operation of financial institutions using digital and mobile electronic technologies on the example of the commercial bank. The paper presents one practically designed, developed and implemented solution as example of using such technologies for facilitating and accelerating issuance of bank loans using smart mobile phone and such increasing efficiency of the bank operation [4]. The developed and implemented solution can be also used in other financial institutions, for example in different types of micro credit organizations, leasing agencies and similar financial institutions. Modern digital and mobile technologies and smart mobile phones were used for the system implementation.

## DIGITAL AND MOBILE TECHNOLOGIES IN FINANCIAL INSTITUTIONS

Since most of the banking products are virtual in nature they are very suitable for implementation using digital and mobile technologies. Modern computers and mobile devices are now the devices for processing and transfer of much information and for connecting people remotely. Such devices are becoming integral elements of the way of life and communicating of the people. Accordingly, such devices become unavoidable in the banking and financial business and operations [1-3]. Very soon using such devices will become one of the primary ways in providing banking business and services, as in some other spheres they already have used.

Modern digital and mobile electronic technologies influence on the way of organization, operation and implementation and on used applications in the financial and banking business. Such technologies also significantly change all that in the financial and banking sector. Under the influence of digital and mobile technologies financial and banking services, applications and Core banking systems (CBS) will be changed and adopted to new needs according to listed possibilities, principles and methods:

— All banking services and products will be supported, sooner or later, on mobile devices (mobile phones and mobile computers).

— The tendency will be that mobile applications will be with as less as possible differences from one to other operation system (OS) platform. It will be possible to start a service on one type of mobile device (for example on mobile computer) and end it on a different mobile device type (for example on mobile phone) with quite different OS. This will enable simple and quick training of the clients. The ultimate goal is that client does not consider how to

perform banking service from a technology perspective but to concentrate on service itself.

— The biggest transformation will not happen either in the interface or in the special technology but in the approach. The approach will have to enable easier anticipation of the client needs, habits and customs and adaptation of the banks to it.

— The emphasis will be on building application programming interface (API) functions and the modular principle of building individual modules and functionality. The concept of centralization at all costs is abandoned in favour of modularity and flexibility.

— Deconstruction of the information system (IS) into components, i.e. products. On that basis banks will be more profiled and will perform only some types of banking operations for what the bank looks that are profitable. Only the members of large bank groups maybe will remain to deal with complete banking operations, as it is now.

— Using services of the financial technology (Fintech) firms to complement and complete banking services and products, rather than spending time in the bank own often late and overdue design and development.

— Implementation of modern Customer Relationship Management (CRM) solutions because of as much as possible sophisticated using of data about financial habits of clients. It is needed for better segmentation of clients and creating successful campaigns among clients from the bank side.

— Symbiosis of CRM solution with Core Banking System (CBS) and Document Management System (DMS) solutions of the bank will be important precondition for successful implementation of modern FrontEnd application solutions. Existing solutions have focus on correctness of information input and entrance obtained by clients. The new modern solutions will have the possibility of interactive relation with clients. In such solutions the bank employee will have more time for contact and conversation with client. In that way the bank employee will be able to offer to client products and services that the program itself suggests to client, depending on already formerly collected information about the client.

## PROPOSED AND IMPLEMENTED SOLUTION

An example of application of digital and mobile electronic technologies for the purpose of facilitating the use and acceleration of services to clients is presented here. The designed and developed application enables facilitating and acceleration of bank loan issues. It is one example how the digital and mobile technologies can be used for increasing efficiency of operation of banks and other financial institutions. It is presented and described the prototype of designed, developed and implemented application for loan issue with the name PhotoLoan [4].

PhotoLoan is application developed and implemented mainly on Android platform. But, there is also a customized the Web version that operates on all the platforms. The primary purpose of the PhotoLoan application is to offer and enable fast forwarding client service requests for financial services using mobile devices (smart mobile phones and mobile computers). It also uses photo (picture, photograph, image) of the goods for what client needs loan (for example television set, washing machine, furniture, car, apartment and similar), taken by mobile device and sent to bank application, to facilitate and accelerate issue of the requested loan.

The PhotoLoan application provides the following possibilities:

— All services are freely available and accessible by mobile and desktop devices.

— Fast and efficient online forming a loan claim to banks, micro credit organizations (MCO) and leasing agencies based on the photograph of the goods for which the loan was asked taken by the mobile device.

— An overview of the available banking loan services and products of each individual bank. The option in the application menu is "Loans - Best offer".

— All the exchange rates in one place. Calculation is with included banking charges. The option in the application menu is "Best offer".

— Loan calculator and the annuity report.

— Geographical location of the nearest bank branch office and Automated Teller Machine (ATM), its GPS position.

The proposed application and solution proposes, presents and describes practical way how to connect the individual private person client (loan claimer) with the legal entity client (goods seller) through the bank. Saying simpler, it proposes, presents and shows how to effectively stimulate and organize buying and transfer of the goods that the client needs from the seller to the buyer (client). One of the best ways for performing all this is through the financial institutions by accelerated loan issuance using mobile devices what the application practically performs.

Using the PhotoLoan mobile application and the solution the user is in possibility to send the requests for the loan, to review the exchange rates, to find basic information about all appropriate banking branches, banking agencies and ATMs, shops/stores, touristic organizations. It can also find and see their location on the Google maps using already collected their GPS positions.

Figure 1 shows the main menu of Android version for mobile phones of developed, designed and implemented PhotoLoan application.

Especially interesting is the option of reviewing and searching the catalogue of the bank products in an interactive way. In such way the client can find the best bank product for client purposes and needs. For each listed bank product there are the buttons "Documentation", "Calculator" and the button for starting an appropriate and suitable presentation. Through the presentation and prepared documentation the user can

learn more about the product and find most suitable product for the user.

By starting the financial calculator the client is able to precisely calculate the monthly amount of the loan return, to receive a repayment (annuity) plan, according to the loan amount and selected number of loan return months. During that, the application takes into account all the specified and set criteria. So, there is no problem in specification and setting the necessary criteria. Such criteria can be, for example, the nominal loan interest rates, the desired loan amount, the number of loan repayment months. In addition, user can also send information about net amount of user salary that would cover obtained loan, brief description of additional information and attach the picture (photograph, image) of what user wants to obtain through such loan.



Figure 1 - PhotoLoan application main menu

Figure 2 shows example of loan calculation option (selected Calculator option) on mobile phone for Android version of PhotoLoan application.

Using picture (photograph, image) of goods that the client wants to be obtained through the loan, attached and sent to the bank and the application, facilitates and accelerates the process of approving and issuing of the requested loan. It increases efficiency of bank operation.

It is known that every so called non-purpose loan is just such called. Finally, each loan has its own purpose. By sending an image (picture, photograph) the client emphasizes what client actually wants to buy and chooses an easier way to perform it through the loan. In some way, such is performed conversion of so called non-purpose loan into a dedicated loan. The bank now knows very well what the client wants. It only remains to the bank to examine the loan ability of the client. It can be performed through the obtained information about the client. Then the bank can start the realization of the loan, request additional information from the client itself or refuse issuing of the loan due to poor loan ability of the client. Figure 3 shows the loan request preparation for sending option for Android version of PhotoLoan application after selection of picture (photo, image) of needed goods/product (in this example the car Mercedes Benz, E class) to be obtained by the loan.
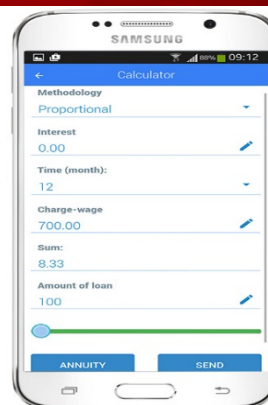


Figure 2 - Loan calculation option of PhotoLoan application
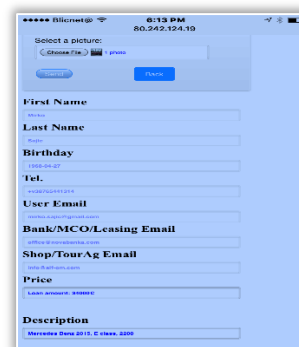


Figure 3 - Loan request preparation for sending option of PhotoLoan application

It also should not forget the third party interest, i.e. interest of appropriate shop or store to sell its products. The bank can use it for facilitating cooperation with sellers for whose products there is the biggest interest of the clients. The bank can find appropriate seller for needed client goods and enable contacts between clients (buyers) and appropriate shops/stores (sellers) such facilitating all process. It also can increase efficiency of the bank operation increasing number of issued loans.

The assumption is that in the future Personal Banker/Account Manager will be more profiled for certain groups of clients, physical persons or legal entities. He/she will be able to use this type of loan application and to use the knowledge of loan purpose (based on sent image, picture or photograph) in order to try to find to client better offer than the client got, by using bank network of contacts with appropriate sellers. In that way the entire circle will be naturally closed to the satisfaction of all parties. The client such gets an even more favourable offer than is the one client has found. That creates a certain kind of gratitude of the client to bank and a stronger connection of the client with the bank (so-called socialization of clients). It is the very same with the seller because bank finds the buyers to seller products or services. In the end, bank is also satisfied that issued more loans that were set on good basis and with good perspective.

In addition to all mentioned, the implemented application has ability to create a list of stores, shops and touristic agencies and their catalogues of products and services that could be purchased by issuing the bank loans. Also, existing stores, shops and travel agencies can be equally interesting

for the banks with which they already have some kind of cooperation as well as making new cooperation with a specific store/tourist agency through this application, expressed by the interest of users of the application.

The application PhotoLoan has a built-in local database that via the network (for example Wi-Fi, Internet) exchanges data with the server (MySQL database). In that way changes are made in the data on the user application. At this moment, the application uses the information available from the Web sites of the banks. But, for the quality of the application operation it would be especially important and recommended that the fresh information, especially information about bank product catalogue with all the relevant data with agreed document formats, be delivered directly from the bank to the application.

Although PhotoLoan application was developed and implemented mainly on Android operating system, there is also Web version that operates on all the operating system platforms. Figure 4 shows look of one example option of the Web version of the PhotoLoan application implemented. The shown example option is taking picture (photo, image) or choosing picture (photo, image) from some library of the goods for what the client wants the loan. The same look of this option is also for the Android version of PhotoLoan.

## CONCLUSION

Based on predicted changes in the information systems of financial institutions and banks and based on the developed and described application example it can be concluded what is the most efficient way to build modern and effective banking and financial institutions information systems. Building of such information systems and mobile applications enable the clients to achieve their own goal in the banks and financial institutions more easily, much faster and much more effectively with much more increased efficiency. It also enables to the banks to be more active and more effective in their operations giving clients better and easier way to access to the bank services and products.



Figure 4 - Example option of Web version
of PhotoLoan application

In the designed, developed and presented example application it is enabled to the client to request a loan from a distance without coming to the bank branch office. The client also can from distance to personally choose the type of offered bank product (loan) that suits to him/her. Client can

also to choose the shop/store and the product that he/she is buying, without being dependent on whether the bank has any relationship with the selected shop/store. The application can be also used in other financial institutions such are for example micro credit organizations, leasing agencies and similar.

For the future of bank relation with customers it would be much better for banks to build a relationship with a clients based on such similar mobile applications and services. It would be better than to offering clients at all costs bank own revolving cards. With revolving cards banks limit number of shops/stores where client can buy desired product, take additional banking fee with higher loan rate, not considering whether or not the client uses the credit card and how much. Some banks sell their products and services to clients on that way although they know in advance that the clients would not use the products/services but only pay the fee. Also, some of banks condition the clients to take bank products only in whole package. Such a short-term strategy applied by some banks already is or will be proved as a bad strategy for the future of the banking sector.

Finding as much as possible information about clients and on the basis of that developing and designing proper bank services and products will also lead to strengthening of connections and mutual trust of clients and the bank. This is often referred as "client socialization" and is one of the most important assumptions and preconditions of strategy and operation of modern digital bank. All this can be achieved and accomplished by applying modern digital and mobile information and communication technologies.

## References

[1] C. Skinner: Digital Bank: Strategies for Launching or Becoming a Digital Bank, Marshall Cavendish Business, 2014.
[2] B. King: BANK 3.0: Why Banking Is No Longer Somewhere You Go But Something You Do. Wiley, 2012.
[3] Being digital: Digital strategy execution drives a new era of banking, Accenture, 2015., available on: https://www.accenture.com/us-en/insight-digital-strategy-new-era-banking
[4] PhotoLoan application, available on: http://www.fotokrediti.com

[1.]Hristo HRISTOV

# ENERGY AND ENVIRONMENTAL EFFICIENCY OF INDUSTRIAL REFRIGERATION INSTALLATIONS

[1.]University of Food Technologies, MAFI – department, Plovdiv, BULGARIA

**Abstract:** Refrigeration installations are one of the biggest electricity consumers in the Food Industry companies. When choosing the refrigerant we have to consider its thermodynamic properties, as well as its impact on the environment. According to Regulation (EU) 517/2014 great part of the currently used refrigerants are going to be limited and put out of use. This article covers the factors that influence the energy efficiency of refrigeration installations. We compare two refrigerating installations – direct and indirect with refrigerant R134a. A comparison of two refrigeration installations, direct and indirect, with refrigerant R134a, has been made. The energy and environmental efficiency have been defined.
**Keywords:** Energy and environmental efficiency, refrigeration installations, global warming potential

## INTRODUCTION

Refrigeration installations are one of the biggest electricity consumers in the Food Industry companies. This consumption may reach up to 85% of the total energy consumption, depending on the industry [5] (Figure1).

On the other hand, the energy consumption of the refrigerating installations is relatively stable as opposed to the processing units, due to the necessity of maintaining stable temperature regimes. That is why the profitability of the final product depends mainly on the energy efficiency of the refrigerating installations.
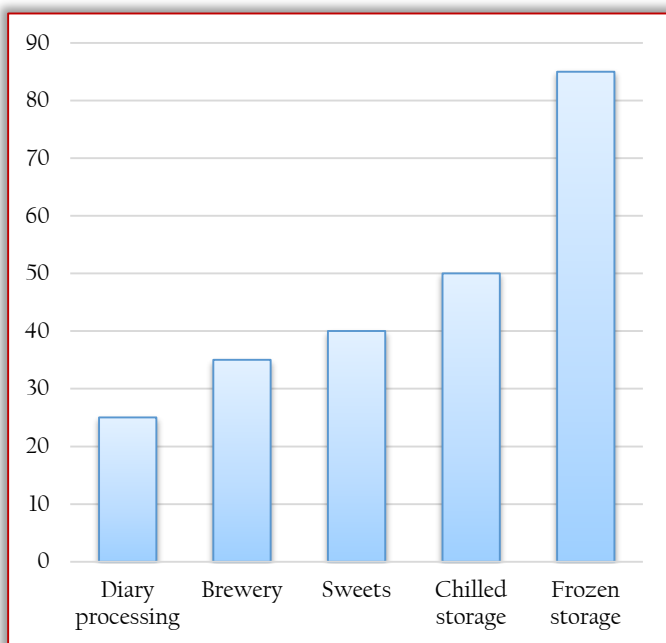


Figure1. Energy consumption during refrigeration processing

The main directions for increasing the energy efficiency of the refrigerating installations are related to:
— Choice of refrigerant.[1 ]
— Choice of refrigeration cycle – thermodynamic analysis.
— Choice of working parameters.
— Optimal thermal insulation of the refrigeration chambers and heat balances.
— Choice of refrigeration equipment.
— Utilization of waste heat.
— Exploitation.

## CHOICE OF REFRIGERANT

When choosing the refrigerant we have to consider its thermodynamic properties, as well as its impact on the environment. According to Regulation (EU) 517/2014 great part of the currently used refrigerants are going to be limited and put out of use. For example, since January 1 2020 the use of fluorine–containing greenhouse gases with potential for global warming 2500 or more – R404A and R507 – for service or maintenance of refrigerating and air–conditioning equipment with charge quantity 40 tons of $CO_2$ equivalent or more.

Since the same date the selling of fresh refrigerants R404A and R507 will be banned. According to the Regulation the impact of the refrigerants is defined by ton(s) $CO_2$ equivalent. European countries, such as Norway, Spain, Poland, Denmark have adopted ecology tax for limitation of high potential global warming refrigerants. This tax is based on the global warming potential (Table 1)

Table 1. Prices in Norway in EU[7]

| Refrigerant | Price tax excluded | Tax | End price |
|---|---|---|---|
| R32 | 46 | 27 | 73 |
| R134a | 25 | 58 | 83 |
| R410a | 28 | 82 | 110 |
| R507 | 32 | 161 | 192 |

## CHOICE OF REFRIGERATION CYCLE

When we have a refrigerant with high global warming potential GWP, one of the ways to reduce the quantity of the refrigerant is the transition from direct to indirect scheme of cooling by means of a cold carrier.

With such scheme the number of compulsory checks according to Regulation (EU) 517/2014 is reduced by half.

## CHOICE OF WORKING PARAMETERS

The energy efficiency of the refrigeration installations mostly depends on the working parameter, which correspond to the normal working regime:

—— evaporation temperature ($t_0$) – depends mainly on the process regime. Its reduction with 1K leads to average decrease of the cold–production $Q_0$ with 4% and the relative energy overconsumption increase with 3, 5%.

—— condensation temperature ($t_к$) – depends on the type of the cooling environment and deviates in great limits during the seasons, as well as during the day and night. The increase of the $t_к$ with 1K leads to an average decrease of $Q_0$ with 2 % and the relative energy overconsumption increases with 3,5%.

## OPTIMAL HEAT INSULATION OF REFRIGERATING CHAMBERS AND HEAT BALANCES

The insulation thickness increase is useful only if after making the heat balances, the heat flows from surrounding constructions are higher percentage from the total heat flows. In order to decrease the quantity of the refrigerant, Regulation (EU) 517/2014 makes transition to autonomous refrigerating installation. They have higher initial investments and installed cooling (electrical) power related to the central refrigeration installations.

The improvement of the technical equipment can lead to energy consumption reduction from 15 to 40%.

Example for such processes is the use of overheated steam after the compressor for heating of water in boilers, as well as use of heat condensation for heating at continuous cooling cycle.

## EXPLOITATION

When evaluating the energy efficiency of a refrigeration installation we have to calculate the expenses for initial purchasing as well as the following exploitation expenses. The energy efficiency at exploitation depends on the following factors:

—— organization of the exploitation;

—— process discipline and personnel training;

—— control and reporting of the refrigerating installation performance;

—— high degree of automation;

—— in time prevention and repair;

—— rebuild and modernization of the refrigeration installations.

The main task of the exploitation is to secure safe and reliable work of the refrigerating units and machines, for maintaining the process regime in the cooling units at minimal cost of the produced artificial cold.

In order to make efficient the exploitation a thorough analysis of the separate elements of the refrigerating installation performance and their impact on the working regimes must be done.

Every refrigerating installation with a global heating potential over 5t equivalent of $CO_2$ must have a file. According to Regulation (EU) 2015/2067 every refrigeration technician must have a certified category for working with refrigeration installations, which is given after taking a theory and practice exam.

## ANALYSIS OF THE REFRIGERATION INSTALLATION EFFICIENCY

We compare two refrigerating installations – direct and indirect with refrigerant R134a. The analysis is made by two way methodology, shown in (Campbell, 2006):

—— Energy efficiency analysis;

—— Environmental impact analysis.

### ⊞ Energy efficiency analysis

The energy efficiency of the refrigerating installations is valued by the total system coefficient of performance ($COP_{total}$), which is calculated by the following equation:

—— For direct system with R134a

$$COP_{total} = \frac{Q_{0,Д}}{P_{k,Д} + P_{f,Д}}$$

—— For indirect system with R134a

$$COP_{total} = \frac{Q_{0,Ин}}{P_{k,134A} + P_{f,134A} + P_p}$$

where:

» $Q_{0,Д}$ and $Q_{0,Ин}$ cool production of the evaporators, kW;

» $P_{k,Д}$ и $P_{k,134A}$ – consumed power of the compressors in the direct and indirect system, kW;

» $P_{f,134A}, P_{f,Д}$ – consumed power by the fans of the condensers and air–cooling units, kW;

» $P_p$ – consumed power of the pump, kW.

The results of the energy analysis are shown in Table 2.

Table 2. Analysis of the energy efficiency

| № | Indicator | Unit | Direct | Indirect |
|---|---|---|---|---|
| I | AVERAGE TEMPERATURE REGIME | | R134a | R134a |
| 1. | Evaporation temperature – $t_0$ | $^0C$ | –7 | –12 |
| 2. | Condensation temperature – $t_k$ | $^0C$ | 50 | 50 |
| 3. | Cold production – R134a | kW | 107 | 113,13 |
| 4. | Compressors power – $P_к$ | kW | 58,2 | 61,2 |
| 5. | Fans power – $P_f$ | kW | 6,03 | 10,2 |
| 6. | Pump power – $P_p$ | kW | – | 0,75 |
| II | COMPARATIVE ANALYSIS | | | |
| 1. | Total cold production– $\sum Q_0$ | kW | 107 | 113,13 |
| 2. | Total power – $\sum P$ | kW | 64,23 | 72,15 |
| | $COP_{total}$ | | 1,67 | 1,57 |

Conclusion: The energy efficiency of the direct refrigerating installation is higher than the indirect one:

$$COP_{total(direct)} = 1{,}67 > COP_{total\ (indirect)} = 1{,}57$$

## ⊞ Analysis of the ecological impact

The ecological impact on the environment is valued by the total equivalent warming impact – TEWI. The methodology of calculating the TEWI is developed by the International Institute of Refrigeration (IIR).

When calculating the TEWI for a defined refrigerating system, we consider the potential of the greenhouse effect from the emissions of the used refrigerant, as well as the indirect potential from the carbon dioxide emissions, caused by the electricity production, consumed during the refrigeration installation exploitation. TEWI is calculated by the following equation:

$$TEWI = (GWP \times L \times N) + (GWP \times M \times (1 - \alpha R) + (N \times P \times \beta)$$

where:

» GWP is the global warming potential of the refrigerant; for $CO_2 = 1{,}00$, for R134a – GWP = 1430;
» L – losses from refrigerant omissions for 1 year, kg;
» N – exploitation lifetime of the refrigeration installation; N = 10 years
» M – system refrigerant mass, kg;
  – in direct refrigeration installation: M R134a = 96 kg;
  – in indirect:    M R134a= 46,4 kg (the quantities in the units and pipelines are calculated);
» αR – coefficient of regeneration of the refrigerant, after the exploitation lifetime; αR = 0,75;
» P– consumed energy of the installation for an year, kWh;
» β – coefficient of the $CO_2$ emissions during production and transportation of energy. β= 0,35.

The yearly losses from omissions are calculated as follows:

$$L = S.M$$

where:

» S – total yearly losses during exploitation, prevention and repairs. During investigating of refrigerating installation it is stated that: S=(7÷27)%.

We accept: for direct S = 20 % and indirect S = 7 %.

Analyzing the equation for calculating the TEWI we can conclude that not always the direct impact of the refrigerant over the global warming is defining. The energy efficiency f the system also has a significant impact.

On the other hand, the equation does not count the ecological impact from the destruction of the refrigerants after the exploitation lifetime (yet there are no true data for the potential when destroying the refrigerants).

When defying the yearly energy consumption we accept:
  —  installation working time: τp = 21h;
  —  number of working days during the year  – 365.

The calculation of the ecological impact over the environment is shown in Table 3.

Table 3 .Ecological impact analysis

| № | Index | Unit | Direct | Indirect |
|---|---|---|---|---|
| I. | OUTPUT DATA | | R134a | R134a |
| 1. | Mass of the refrigerant – M | kg | 96 | 46,4 |
| 2. | Year omissions – L | kg | 19,2 | 3,25 |
| 3. | Total consumed power | kW | 64,23 | 72,15 |
| 4. | Yearly consumed power – P | kWh | 492323 | 553030 |
| I I. | ECOLOGICAL IMPACT: | | | |
| 1. | From omissions | – | 274560 | 46475 |
| 2. | From refrigerant regeneration after the exploit. lifetime | – | 102960 | 49764 |
| 3. | Indirect impact from energy consumption | – | 1723131 | 1935605 |
| * | TEWI – from refrigerant | | 377460 | 96239 |
| * | TEWI$_{total}$ | – | 2100591 | 2031844 |

## CONCLUSIONS

— The ecological impact of the refrigerant in indirect refrigeration installation is 3.9 times lower.
— The total ecological impact of the indirect refrigeration installation decreases by 3.3%.
— The yearly energy consumption in the indirect refrigeration installation is increased by 11%.
— According to Regulation (EU) 517/2014 the checkups number for the direct with 137t equivalent of $CO_2$ is two and for the indirect installation with 66,4t equivalent of $CO_2$ is one.

Main directions for reduction of the ecological impact:

— to use one–component refrigerants or azeotropic ones;
— for reducing the omission the pipeline connections must be soldered;
— in refrigerating installations with high volume branched system pipelines – to use indirect or cascade systems with R744($CO_2$) in the lower cascade.
— In industrial refrigeration installations – use of natural refrigerants such as R717 (ammonia) and cascade machines – R717/R744 ($CO_2$).
— Exploitation discipline – well trained personnel, who can perform the requirements for ecology safety.

Refrigeration is always on, which is why it consumes up to 50% of the energy in a typical Food Industry equipments. Investing in energy-efficient equipment and controls can lower utility bills and keep food fresher longer.

Due to the complex nature of refrigeration, and the current trends towards natural refrigerant options, the refrigerating installations continually invest in engineering and technical training to ensure that provide the customers with expertise that is second to none.

References
[1] REGULATION (EU) №517/2014 of the European Parliament and the Counsil as of 16 April 2014.
[2] REGULATION (EU) 2015/2067 as of 17 November 2015.
[3] Campbell, A., Maidment, G.G. and Missenden, J.F., A Natural Refrigeration System for Supermarkets using $CO_2$ as a Refrigerant., CIBSE National Conference 21–22 March 2006,
[4] Norwegian Regulation on HFCs and Incentives on Alternatives, Presentation at ATMOsphere 2016 "Natural Refrigerants – Solutions for Europe"Torgrim Asphjell, April 19, 2016
[5] Commercial Refrigeration, Energy Smart www.sedo.energy.wa.gov.au/uploads/ comm_refrig_28.pdf

[1.]Alok MUKHERJEE, [2.]Susanta RAY, [3.]Arabinda DAS

# MICROCONTROLLER BASED SPEED CONTROL AND SPEED REGULATION SCHEME FOR BLDC MOTOR UNDER VARIABLE LOADING CONDITIONS

[1-3.] Department of Electrical Engineering, Jadavpur University, Kolkata, INDIA

**Abstract:** Brushless dc (BLDC) motors are gaining immense popularity in recent era due to its major advantages over the more conventional motors, only put behind due to the cost involved in designing its most imperative controller. Hence, the design of a low cost, yet efficient and effective controller is an imperative part of the motor drive system. This paper presents a design and implementation of a microcontroller based low cost drive for a 3-phase, trapezoidal back-emf, permanent magnet BLDC motor. A Pulse Width Modulation (PWM) based modified adaptive two and half step digital on-off control algorithm has been designed to provide a constant operating speed overcoming the effect of variation in load with high load torque, as well as provide faster response during transients to restore speed. Proteus VSM (Virtual System Modeling) software is used as a real-time simulation tool to model the BLDC motor drive. Experimental verification has also been carried out to validate the simulated circuit.
**Keywords:** BLDC motor, PIC18F4331 microcontroller, Proteus VSM software, Pulse Width Modulation (PWM)

## INTRODUCTION

As the recent trend goes Brushless Direct Current (BLDC) motor have achieved huge popularity in recent era due to some remarkable advantages like high efficiency, high torque capability, lesser maintenance etc. over several conventional motors readily available in market. For its ease in control due t the electronic commutation and drive system and lesser maintenance due to the absence of brush-commutator arrangement, hence a higher efficiency, BLDC motor is replacing many conventional motor drives these days, especially in sophisticated drive applications where efficiency and performance plays the major role over its costing. Presence of strong permanent magnet rotor provides it with high power density enabling for high torque supply. The only drawback behind its most popularity as yet is its most essential but high cost controller responsible for the electronic commutation technique [1]-[6].

Microcontroller based embedded drive system, on the other side, are hugely popular these days for designing low cost, yet very much effective and robust controllers for several reasons including wide adaptablity to modern control techniques, especially for systems with variable load applications with high torque demand, simultaneously requiring low speed regulation and of course, providing more flexibility of design etc. [7]-[9].

The proposed work deals with designing of such type of an algorithm using PIC18F4331 microcontroller and hardware implementation of the same. Proteus VSM simulation software is used for the purpose as a primary simulation platform. This allows microcontroller programs to be implemented directly to the simulation block, and later in practical microcontroller unit through any suitable programmer, allowing for lesser hardware development time and effort.

Real time change of input data is another advantage of the software making it closer to practical design [10].

In this work, an attempt has been made for designing a low cost variable load constant speed microcontroller based drive for a three phase trapezoidal back-emf permanent magnet BLDC motor. An 8 bit PIC18F4331 microcontroller has been chosen here due to a certain number of driver application modules like High-Speed Motion Feedback Module, 14-bit Power Control PWM Module, interrupt on bit change and 200 Ksps 10-bit A/D Converter modules etc. [7], [8], [11]. The drive scheme along with the BLDC motor has been initially designed in Proteus VSM simulation software [10].

A modified adaptive on-off control scheme has been proposed here for variable load constant speed applications. Pulse Width Modulation (PWM) technique has been adopted here for developing a modified adaptive digital on-off control algorithm with 120-degree six-step commutation. Motor operation is restricted primarily between two discrete levels, operating between which the motor rotates with an average operating speed. An additional wider speed band is also incorporated in order to achieve faster response in restoration of speed about the reference speed in case of sudden and massive load change causing lesser overshoot. The algorithm is designed to overcome the effect of variation in load and rotate at a constant speed ensuring a good (low) speed regulation with high torque supply. A simulation based study of the proposed controller has been first carried out in software. A prototype has been designed and implemented in laboratory to validate the control scheme.

## BLDC MOTOR DRIVE DESIGN

The block diagram of the close loop control scheme is presented in Figure 1. BLDC motor is the controlled block of the drive scheme. In our work, it is a four pole, star type, trapezoidal back-emf 3-phase BLDC motor. Three electrically equally (120° apart) spaced Hall sensors located over the

three stator phases provide this information to the controller. The tacho-generator voltage output is scaled in compatibility with the microcontroller inbuilt 10-bit high speed ADC hardware module. PIC18F4331 microcontroller has been used as the basic control block which performs the following two basic purposes:

— Maintaining the switching sequence of the six PWM channels in synchronism with the Hall position signals to perform phase commutation.

— Adjust the PWM duty ratio to control the input voltage to the motor in synchronism with the speed feedback signal.

IRFZ44N n-channel MOSFET has been chosen here primarily for its high switching frequency, thus causing lesser switching loss yielding higher efficiency of the drive, high current carrying capability for designing high power drives and low gate drive current requirements. MOSFET driver has been used here primarily to pull up the microcontroller generated PWM logic "High" signal of +5V to +12 to +20V for the successful turn on of the MOSFETs, as well as for the electrical isolation between the control and power circuit. IC IR2101 has been used to design the motor drive for advantages. Besides, an inner current loop is also implemented to estimate the equivalent load as well as to limit load current within the rated value governed by the motor.
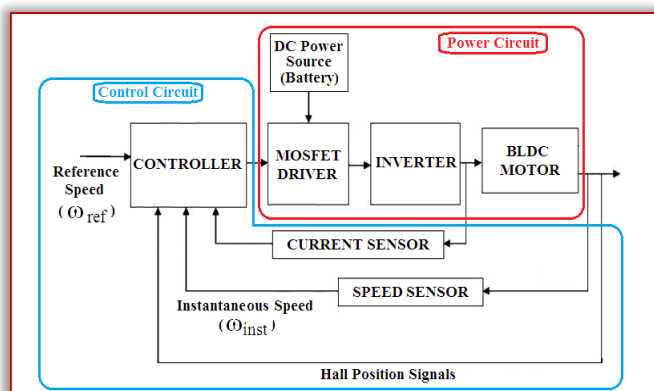


Figure 1. Schematic diagram
of the proposed BLDC motor drive

## SPEED CONTROL OF BLDC MOTOR AND CALIBRATION OF SOFTWARE MOTOR MODEL
— Simple Voltage Control Method:

The Speed Torque Characteristics of an ideal BLDC Motor is shown in Figure2. The Speed Torque Characteristics is drooping in nature providing a high torque at starting. Point C denotes the point of intersection of any load torque $T_L$ with the electromagnetic torque line AB. Thus for a specific load $T_L$, C becomes the stable operating point. Knowledge of the motor speed-torque characteristics enables its easier mathematical modeling, and hence easier design of the constant speed drive under variable loading conditions. Easy speed control is possible due to the almost linear speed voltage characteristics as shown.

The simple PWM voltage control scheme is described by:

Output Voltage ($V_o$) = Duty Ratio (D) × Input Voltage ($V_{in}$)

Which shows the linear speed control can be achieved by the simple control of duty ratio which is controlled only by entering proper duty ratios in the duty cycle registers of each channel; thus implementing a simple linear voltage control of BLDC motor [13].
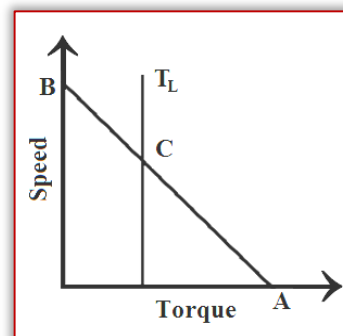


Figure 2. Speed-torque characteristic of BLDC motor

— Calibration of Motor model in Proteus Software and Implementation of Voltage Control Method:

The practical speed torque characteristic of BLDC Motor is somewhat nonlinear and the degree of non-linearity is modeled by knowing the mathematical model of the motor, especially for loading the motor model fully or partially. Calibrate the motor model has been achieved by loading the motor with variable loads in steps and the noting the corresponding speeds, thus the practical characteristics was plotted noting the points A and B initially which are the boundary points, and late the intermediate points by several experiments as shown in fig 3 [13].
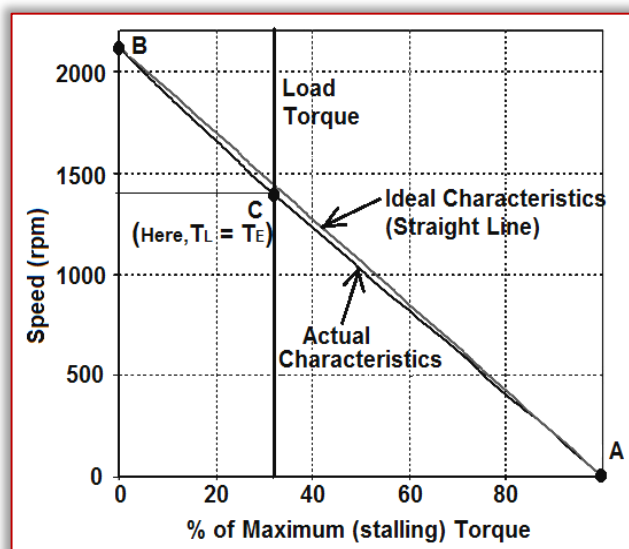


Figure 3. Simulated speed-torque characteristics
of BLDC motor

## PROPOSED CONTROLLER ALGORITHM
— Close Loop Speed Control of BLDC Motor

The simple voltage controlled speed control scheme is described in fig 4. Considering a load torque $T_L$, applied voltage $V_1$ and the ideal motor characteristics the motor, the open loop operating point reduces to the intersection of the load line and he electromagnetic torque line as defined by point C on the speed-torque characteristic and runs with the speed OG. It can be assumed that on gradual increment of

voltage, the motor starts from point A and reaches the stable operating point C following the electromagnetic torque line AB.

The close loop control scheme at any other desired speed less than the speed corresponding to the applied load torque can be achieved by simple voltage adjustment by PWM control. If the motor is to be operated with the load torque $T_L$ and with a different reference speed indicated by OS which is less than OG (the open loop speed) as shown in Figure 4, the motor starts at point A and traverses through the path AB and reaches the point E at which the speed OS' is very close to the reference speed OS, but the electromagnetic torque $T_E$ at this point E is still greater than $T_L$. Hence, the controller reduces the PWM duty ratio to reduce voltage level from $V_1$ to a new reduced voltage $V_2$ at point E in order that motor traverses the path ED and reaches the operating point D and runs with the reference speed (OS) with the same load torque $T_L$ [13].
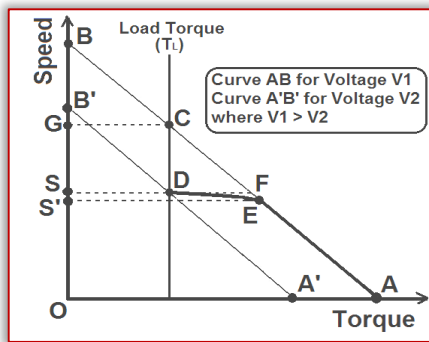


Figure 4. Simple voltage control technique for closed loop control strategy

— Proposed Control Algorithm

The proposed controller is primarily an on off or hysteresis band controller with some modification [1]-[5]. The control technique is very simple in nature and can be implemented very easily in hardware. The controller only switches the voltage level primarily in between two discrete levels at primary higher duty ($D_{H1}$) and primary lower duty ($D_{L1}$) about the reference voltage (i.e. the voltage corresponding to the reference speed) by adjusting the duty ratio of the PWM output. This is shown by the controller characteristics in Figure 5. The flowchart of the proposed controller, as shown in Figure 6 explains the basic topology of the proposed controller. Thus the controller basically restricts the motor motion in between a certain speed band defined as primary upper speed band ($\omega_H$) and primary lower speed band ($\omega_L$) as shown in the predicted speed response by the proposed controller in Figure 7.

Hence the motor rotates with an average speed ($\omega^*$ or $\omega_r$) in between these two speed levels, i.e., within a particular speed band ($\Delta\omega = \omega_H - \omega_L$). Although $D_{H1}$ and $D_{L1}$ are the main governing duties which restrict the motor within a certain speed band, in any case by some accidental reasons, sudden load throw off or change of reference speed itself etc. if the motor instantaneous speed exceeds this speed band from either side, the controller is designed with an additional wider

band with duty ratios $D_{H2}$ and $D_{L2}$. These duties are so designed in order to produce lesser overshoot and bring the motor back towards reference speed at an appreciably faster rate, but without causing much vibration of motor or abrupt torque ripple and sudden current rise. The controller is made adaptive in nature in order to maintain a constant speed profile even on application of varying load.
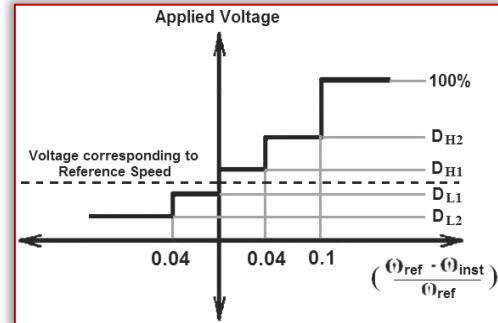


Figure 5. Proposed Controller Characteristics
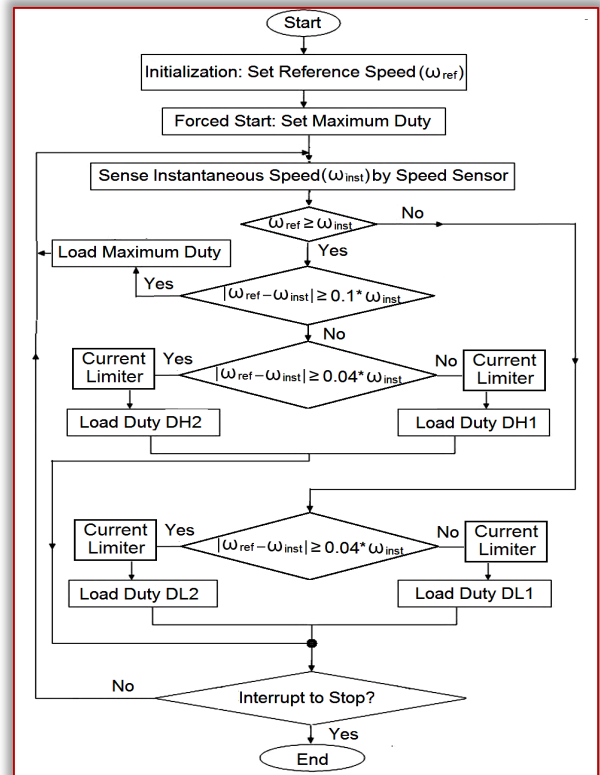


Figure 6. Flowchart of the proposed controller
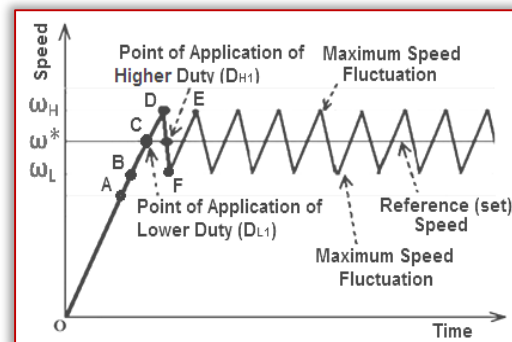


Figure 7. Predicted response of the proposed controller

The motor is forcefully started at first (point O) depending on the initial rotor position in any direction with full voltage applied (100% duty) when it starts rotating and the Hall signals starts changing its bit pattern. On any bit change of any one of the three Hall signals, the program sequence enters the interrupt subroutine where the duty ratio is adjusted properly by the proposed control algorithm. In each loop, the actual speed (ADC instantaneous value) is measured and compared with the reference speed (ADC set value) and the error is defined as follows:

Speed Error (ADC Error) = Speed Set (ADC reference value) - Actual Speed (ADC instantaneous value)

When error is positive and very large (say more than the wider tolerance limit) indicating that the motor instantaneous speed ($\omega_{inst}$) is far away from the reference speed ($\omega_r$), the controller assigns the maximum duty (100%), i,e., full voltage is applied in order to achieve highest acceleration, restrained only by the motor inertia and the load connected to the shaft. Thus rise time reduces considerably. When $\omega_{inst}$ reaches the wider lower speed band at point A (say 10% lesser than the reference rpm), the controller reduces the duty ratio to $D_{H2}$. The purpose of keeping this additional lower band is to slow down the motor in advance, even before crossing $\omega_r$, thus preparing for a reduced overshoot beforehand and yielding a better transient response, although sacrificing for a slightly higher rise time. The above two steps optimize between faster response during starting (i.e. providing faster acceleration) and lesser overshoot near reference speed.

Even on application of this reduced voltage, the motor accelerates and enters the lower speed band at point B when error is still positive but say less than 4% of $\omega_r$, i.e., the $\omega_{inst}$ is in between 96% to 100% of $\omega_r$, the controller imposes a further lower duty $D_{H1}$ (which is slightly higher than the reference voltage corresponding to $\omega_r$) to reduce acceleration faster near the reference speed. These duty ratios are governed by the following factors:

— Part contribution depending on the reference speed;
— Part contribution depending on load connected, i.e., in effect, depending on the current drawn from supply which is sensed by the installed DC link current sensor to estimate the load connected;
— An additional fixed part (depending on motor mechanical inertia) which is added (or subtracted) from the reference duty ratio to allow for hysteresis band control; and
— A very much negligible part contribution depending on the nonlinearity of speed - torque characteristics.

Even after decelerating, if the motor $\omega_{inst}$ goes beyond $\omega_r$ (at point C) due to its inertia and the applied voltage (overshoot region), i.e., if the error becomes just negative (i.e., say less than 4% of $\omega_r$), the controller loads a further lower value of duty $D_{L1}$ (marginally lower than the reference voltage corresponding to $\omega_r$) to bring down $\omega_{inst}$ below reference.

Now the motor decelerates toward reference performing maximum overshoot upto point D. In case of any accidental reasons or others, if the motor still overshoots and the error crosses the 4% band and enters say, 4-10% band (with negative error, beyond point D), a further lower duty $D_{L2}$ is imposed for faster deceleration of the motor towards $\omega_r$. In any case, the motor slows down and crosses the reference speed from upper side this time at E and enters the lower band where higher duty $D_{H1}$ is imposed again to produce acceleration. But similarly due to its inherent rotor inertia, the deceleration continues upto say point F where it starts to accelerate aging.

All these duties are selected governing the same criteria as discussed previously. The combined effect of the rotor inertia and the applied voltage is explained mathematically in the following section.

## CONTROLLER DESIGN

The mathematical model of the controller can be explained in steps as follows. Starting from the very fundamental motor equation, we derived the value of duty ratio (D) for the upper and lower levels, which are of the most importance in designing the proposed controller. The basic motor equations of the motor are given as:

$$V_C = E + IR \qquad (1)$$

$$I = \frac{(V_C - E)}{R} \qquad (2)$$

where:
» $V_C$ - controlled voltage;
» E - motor back emf;
» I - motor current;
» R - motor armature resistance.

The motor back emf and the PWM controlled output voltage can be written as:

$$E = K_E \omega \qquad (3)$$

$$V_C = D V_S \qquad (4)$$

Thus the motor current equations become as:

$$I = \frac{(D V_S - K_E \omega)}{R} \qquad (5)$$

where:
» $K_E$ - back emf constant;
» $\omega$ - speed of motor in rad/sec;
» $V_S$ - supply voltage

Since BLDC motor has permanent magnets in its poles, hence flux can be assumed as constant for further analysis. Hence, the electromagnetic torque produced by the motor can be assumed as directly proportional to the current as:

$$T_E = K_T I \qquad (6)$$

where:
» $T_E$ - electromagnetic torque produced by the motor;
» $K_T$ - torque constant;

Thus putting the value of motor current from (5) into (6) yields (7) as follows:

$$T_E = \frac{K_T V_S}{R} D - \frac{K_T K_E}{R} \omega \qquad (7)$$

Thus, it can be inferred from the above equation that the input voltage produces some toque at some speed depending on the motor constants, both electrical as well as mechanical. But the most important part that needs to be considered is the mechanical transient equation, based on which, all further modeling has been adopted to define the controller characteristics. Transient torque equations can be obtained for the motor from the mechanical side as:

$$T_E = J\frac{d\omega}{dt} + B\omega + T_L \qquad (8)$$

$$K_T I = J\frac{d\omega}{dt} + B\omega + T_L \qquad (9)$$

where:
» $J$ - polar moment of inertia the motor;
» $B$ - viscous friction coefficient;
» $T_L$ - load torque;

— Steady State Analysis

Before going to the transient analysis straight way, steady state operating point must be examined first for building the control logic in a simple way. It is defined at a point where the motor speed settles to almost a fixed value, i.e., the rate of change of speed becomes almost zero. Open loop stated state condition is achieved by applying a voltage on the motor and letting the motor to settle to a fixed speed depending on the load and mechanical parameters. This steady state speed ($\omega_{SS}$) and current ($I_{SS}$) is obtained from (9) as follows:

Since at steady state $\frac{d\omega}{dt} = 0$, thus putting this value in the mechanical transient equation (9) yields:

$$\omega_{SS} = \frac{K_T I_{SS}}{B} - \frac{T_L}{B} \qquad (10)$$

$$I_{SS} = \frac{B}{K_T}\omega_{SS} + \frac{1}{K_T}T_L \qquad (11)$$

The above equation states that the amount of current taken by the motor is partly utilized in driving the load and the other part produces steady state motion depending on the rotor mechanical parameters. Thus equating the electromagnetic torque obtained from the electrical and mechanical equations, i.e., clubbing (7) and (8) gives:

$$J\frac{d\omega}{dt} + B\omega + T_L = \frac{K_T V_S}{R}D - \frac{K_T K_E}{R}\omega \qquad (12)$$

The steady state condition of the above equation can be obtained by considering the same constraints as before:

$$B\omega_{SS} + T_L = \frac{K_T V_S}{r}D_{SS} - \frac{K_T K_E}{r}\omega_{SS} \qquad (13)$$

The steady state speed and the corresponding duty ratio can be obtained from (13) as follows:

$$\omega_{SS} = \left[\frac{V_S}{\frac{BR}{K_T} + K_E}\right]D_{SS} - \left[\frac{\frac{R}{K_T}}{\frac{BR}{K_T} + K_E}\right]T_L \qquad (14)$$

$$D_{SS} = \left[\frac{1}{V_S}\left(\frac{BR}{K_T} + K_E\right)\right]\omega_{SS} + \left[\frac{R}{V_S K_T}\right]T_L \qquad (15)$$

$$D_{SS} = \alpha\omega_{SS} + \beta T_L \qquad (15a)$$

where:
» $\alpha = \left[\frac{1}{V_S}\left(\frac{BR}{K_T} + K_E\right)\right]$;
» $\beta = \left[\frac{R}{V_S K_T}\right]$.

— Transient State Analysis

Equation (15) is vitally important in determining primary higher duty ($D_{H1}$) and primary lower duty ($D_{L1}$). It is apparent from above that PWM duty ratio (D) must be set at a certain value $D_{SS}$ depending on $\omega_{SS}$ and the load $T_L$ on the motor, governed by the motor parameters. In other words, the steady state duty ratio, for steady state speed, must comprise of two parts:

— one ($\alpha\omega_{SS}$) depending on the open loop steady state speed,
— other ($\beta T_L$) depending on load;

$\alpha$ and $\beta$ being constants, only depending on the motor electrical and mechanical parameters. Thus, as discussed in the previous section, these are the two primary components in the determination of steady state duty $D_{SS}$, which in turn helps in determining the values of $D_{H1}$ and $D_{L1}$. The third component which is added to or subtracted from $D_{SS}$ to obtain the upper and lower duties ($\omega_H$ and $\omega_L$ respectively) which in turn governs the speed fluctuation band ($\Delta\omega$), is obtained by solving differential equation (8). The time domain solution of instantaneous rotational speed is obtained as:

$$\omega(t) = \frac{(T_E - T_L)}{B} + [\omega(0) - \frac{(T_E - T_L)}{B}].e^{-\frac{B}{J}t} \qquad (16)$$

where $\omega(0)$ is the initial condition of speed. The transient dynamics is explained in Figure 8. As stated in the previous section that whenever instantaneous speed exceeds the reference speed from below (due to the applied duty $D_{H1}$) at point B, a lower duty $D_{L1}$ is applied immediately on the motor in order to decelerate.

Due to the mechanical inertia, the motor still crosses the reference speed, but the acceleration decelerates and it follows the curve BC to reach the upper speed limit instead of reaching a higher speed corresponding to point D. From (7), it is obvious that $T_E$ can be changed in proportion by changing D, i.e., by changing the input voltage. The solution (16) obtained by solving the transient torque equation shows that it has two components, one steady state component and the other is the transient component, an exponential function which involves the initial speed and the accelerating torque.

Thus, on application of a slightly higher (or lower) duty than that corresponding to the reference speed obtained from (15) will produce a higher (or lower) electromagnetic torque $T_{EH}$ which in turn will accelerate (or decelerate) the motor to a higher (or lower) speed $\omega_H$ governed by the following equations:

$$\omega_H(t) = \frac{(T_{EH} - T_L)}{B} + [\omega(0) - \frac{(T_{EH} - T_L)}{B}].e^{-\frac{B}{J}t}$$

$$\omega_L(t) = \frac{(T_{EL} - T_L)}{B} - [\omega(0) - \frac{(T_{EL} - T_L)}{B}].e^{-\frac{B}{J}t}$$

(17)
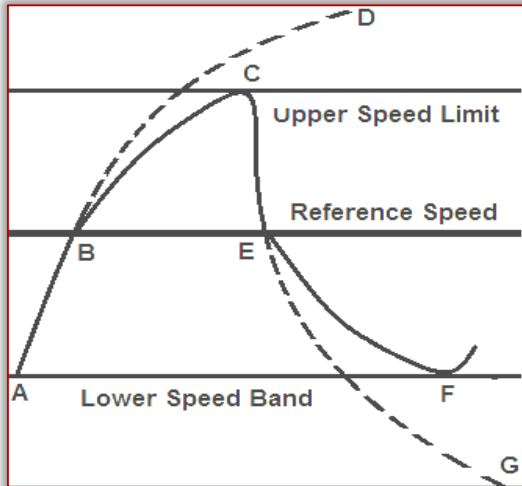


Figure 8. Transient speed response
by the proposed controller

The speed ripple thus can be found as:

$$\Delta\omega = \omega_H(t) - \omega_L(t) \qquad (18)$$

Thus from (18), for any speed ripple Δω depending on the tolerance level, corresponding electromagnetic torques can be found out from (17), which can be used to find the corresponding excess higher and lower duties (ΔD$_{H1}$ and ΔD$_{L1}$ respectively which comes out to be almost equal, say ΔD, if speed fluctuation is assumed to be symmetric about reference speed) from (15) where ω$_{SS}$ will have to be replaced by ω$_H$ and respectively ω$_L$ and ω(0) by reference speed. The additional duties ΔD thus obtained is added to D$_{SS}$ as obtained from (15) or (15a). Thus the final expression for duty ratios become as:

$$D_{H1} = D_{SS} + \Delta D \quad \text{or} \quad D_{H1} = \alpha\omega_{SS} + \beta T_L + \Delta D \qquad (19a)$$

$$D_{L1} = D_{SS} + \Delta D \quad \text{or} \quad D_{L1} = \alpha\omega_{SS} + \beta T_L - \Delta D \qquad (19b)$$

Simulations are carried out for a maximum variation from the reference speed of about 10 rpm. From measurements, this duty ratio resulted in a speed ripple of about 3-8 rpm depending on the reference speed level and the load torque.

## ─ Steady State Motor Model in Frequency Domain

For the purpose of analysis, the proposed digital controller is considered to be equivalent to a proportional controller. This analysis is made in order to observe if the actual motor speed reaches the reference speed at steady state with the proposed controller. The transfer function for a BLDC motor is shown as:

$$\frac{\omega(s)}{V_C(s)} = \frac{\dfrac{K_T}{JL}}{s^2 + \dfrac{(JR + BL)}{JL}s + \dfrac{(BR + K_T K_E)}{JL}} \qquad (20)$$

where *L* - inductance of the motor;
Other symbols bear the same meanings as before.

## SIMULATION RESULTS

The drive scheme has been simulated in Proteus VSM and is shown in figure 9. The proposed on-off control algorithm was compiled using MikroC Pro assembler. PWM signals have been generated by PIC18F4331 microcontroller and the duty ratio is adjusted according to the requirement for close loop control to reach the predefined desired speed at any load (within rated value). Figure 10 shows the three phase back emf of BLDC motor model monitored by using digital oscilloscope.
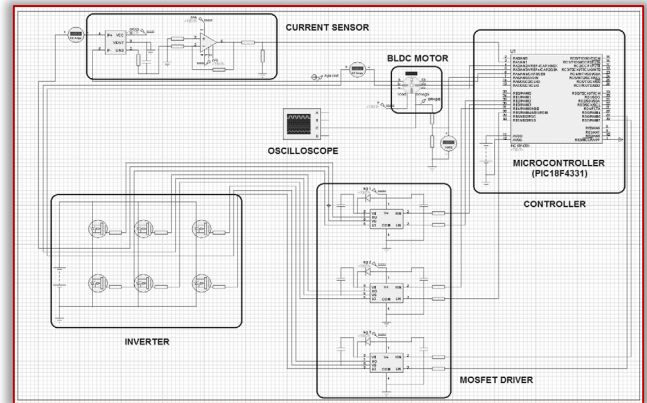


Figure 9. Simulated BLDC motor drive scheme in Proteus VSM.
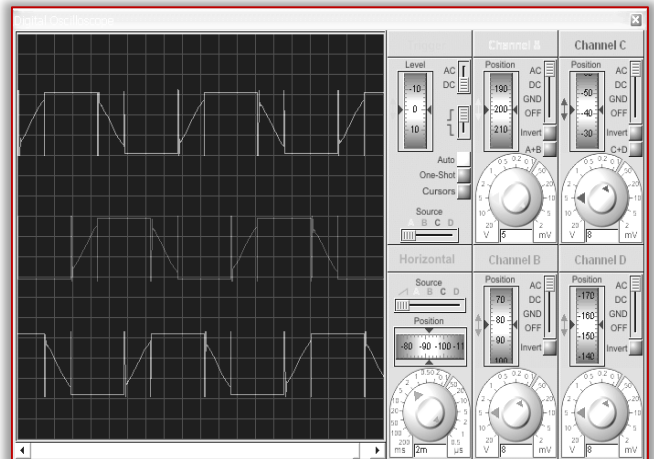


Figure 10. Simulated output of three phase back emf
for the trapezoidal BLDC motor
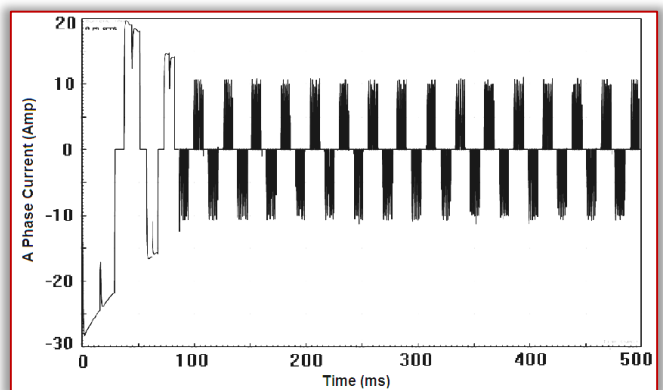


Figure 11. Simulated output of phase current waveform of the three phase BLDC motor employing the proposed on off controller on 30% of full load at 1153 rpm

Figure 11 shows the phase current waveform obtained by using the Proteus inbuilt analog analyzer and Figure 11(a) is a magnified view of the same.

Figure 12 shows the step response of speed. The detailed simulation results are given in tabular form in Table I and II.
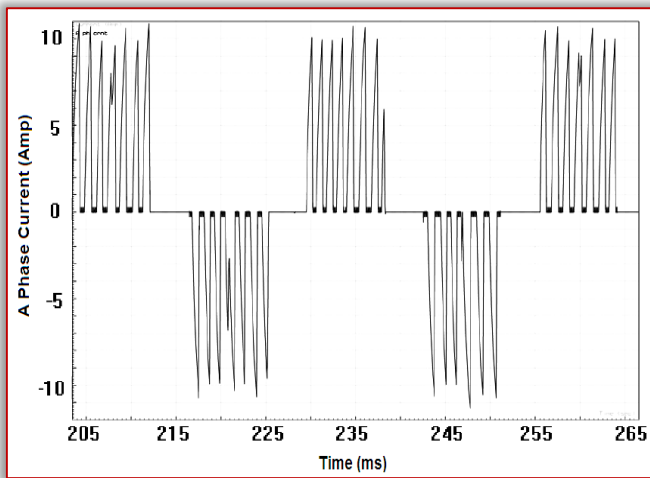


Figure 11(a). Magnified view of simulated output of phase current waveform of the three phase BLDC motor employing the proposed on off controller on 30% of full load at 1153 rpm
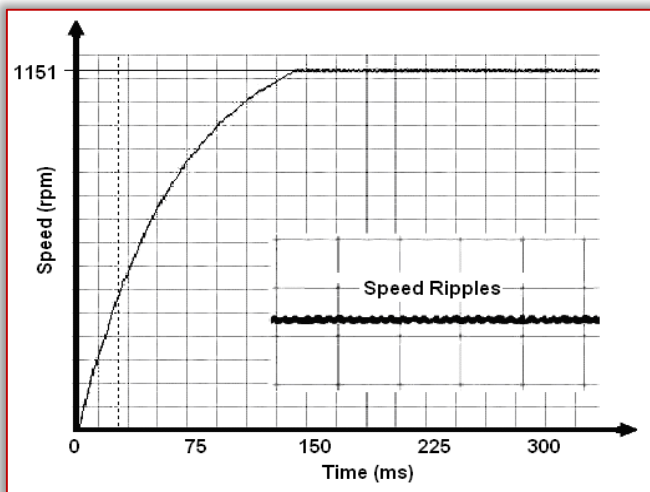


Figure 12. Simulated output of step response of speed by the proposed controller

TABLE I. Summary of simulation results (Higher Speed Reference at 1155 rpm)

| % Of Rated Load | Steady State Speed (rpm) | Maximum Speed Ripple about Steady State Speed (rpm) | Speed Regulation about Steady State Speed (%) | Steady State Error (%) |
|---|---|---|---|---|
| 100 | 1151 | 3.8 | 0.33 | 0.35 |
| 30 | 1153 | 5.6 | 0.49 | 0.17 |
| No Load | 1153.5 | 8.2 | 0.71 | 0.13 |

TABLE II. Summary of simulation results (Lower Speed Reference at 582 rpm)

| % Of Rated Load | Steady State Speed (rpm) | Maximum Speed Ripple about Steady State Speed (rpm) | Speed Regulation about Steady State Speed (%) | Steady State Error (%) |
|---|---|---|---|---|
| 100 | 580.4 | 2.9 | 0.50 | 0.22 |
| 30 | 581.3 | 4.7 | 0.81 | 0.12 |
| No Load | 581.7 | 7.6 | 1.31 | 0.05 |

## EXPERIMENTAL VERIFICATION

Experimental verification is very important to validate the simulation. An experimental set-up was constructed in the laboratory in order to implement and further validate the simulation results obtained by implementing the proposed technique. The hardware design is implemented in consistency with the simulated circuit in laboratory and is shown in Figure 13. The driver circuit consists mainly of microcontroller module, MOSFET driver, three-phase inverter and the BLDC Motor. The load arrangement is done by electrically loading the shaft mounted separately excited DC generator by a load box.
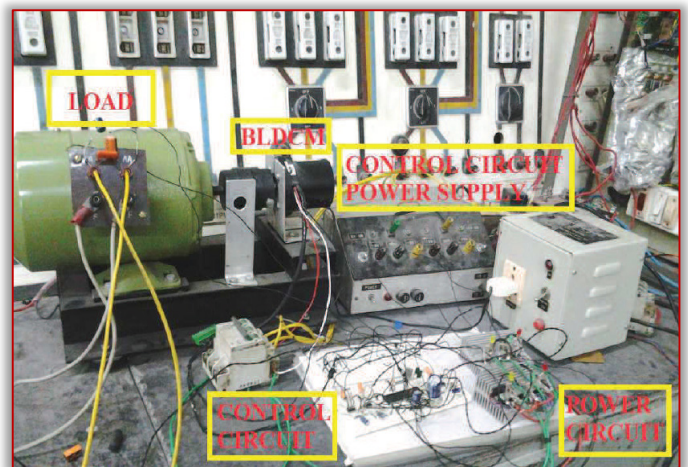


Figure 13. Experimental setup of BLDC motor drive scheme in laboratory

Experimental results are collected using Digital Storage Oscilloscope (DSO). The oscilloscope is used to view and record the speed response (tacho-generator output), PWM signals, Hall sensor signals and back emf signal.

Figure 14 shows the oscillogram of back emf between phases A-B for the trapezoidal BLDC motor on 30% of full load and 1130 rpm and Figure 15 shows the oscillogram of experimental result for close loop step response of speed BLDC Motor under the same condition with the proposed two step on-off control scheme.

Figure 16 and Figure 16(a) show the magnified view of the close loop speed response corresponding to the same conditions.
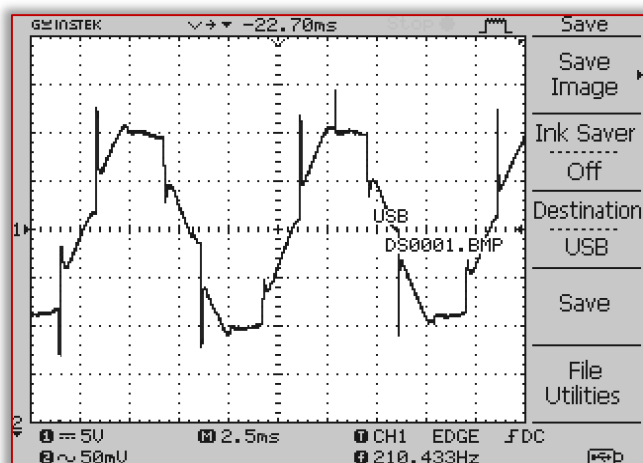
Figure 14. Oscillogram of experimental results
for back emf for the trapezoidal BLDC motor
on 30% of full load and 1130 rpm
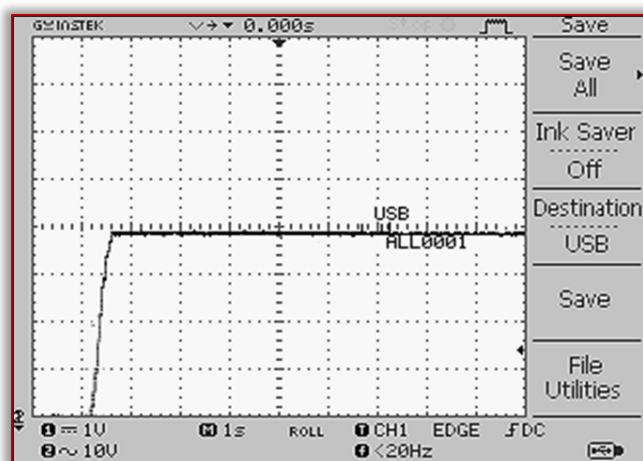


Figure 15. Oscillogram of experimental result
for close loop step response of speed BLDC Motor
on 30% full load and 1130 rpm
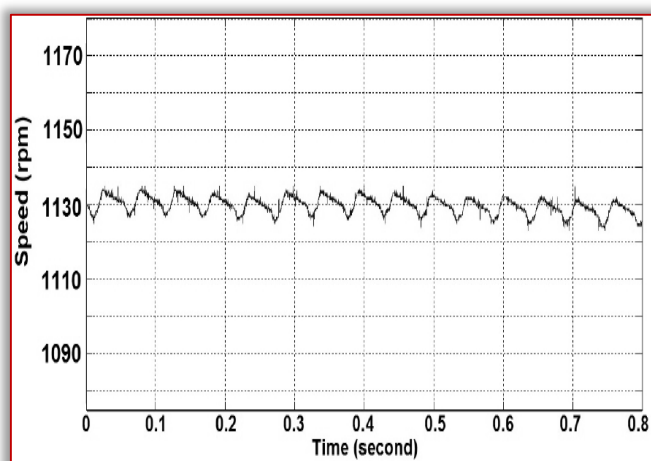


Figure 16. Experimental Result for Step Response
of Speed of BLDC Motor for a reference speed
of 1130 rpm under 30% Full Load
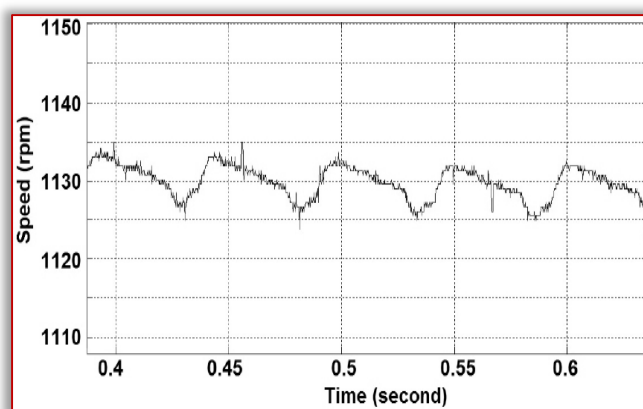


Figure 16(a). Experimental Result for Step Response
of Speed of BLDC Motor for a reference speed
of 1130 rpm under 30% Full Load (Magnified)

The experiment has been carried on by varying the reference speed under different loading conditions and results have been shown in tabular for in Table III and IV, followed by the magnified view of the close loop step response of speed using the proposed algorithm at a reference speed of 785 rpm under 30%, 50% and 100% of full load condition and shown in Figure 17 to 19 respectively.

TABLE III. Summary of Experimental Results
(Higher Speed Reference at 1130 rpm)

| % Of Rated Load | Steady State Speed (rpm) | Maximum Speed Ripple about Steady State Speed (rpm) | Speed Regulation about Steady State Speed (%) | Steady State Error (%) |
|---|---|---|---|---|
| 100 | 1120 | 14 | 1.25 | 0.885 |
| 50 | 1125 | 16 | 1.42 | 0.442 |
| 30 | 1127 | 18 | 1.59 | 0.265 |
| No Load | 1128 | 20 | 1.77 | 0.177 |

TABLE IV. Summary of Experimental Results
(Lower Speed Reference at 785 rpm)

| % Of Rated Load | Steady State Speed (rpm) | Maximum Speed Ripple about Steady State Speed (rpm) | Speed Regulation about Steady State Speed (%) | Steady State Error (%) |
|---|---|---|---|---|
| 100 | 778 | 11 | 1.41 | 0.892 |
| 50 | 781 | 14 | 1.79 | 0.509 |
| 30 | 783 | 24 | 3.06 | 0.225 |
| No Load | 784 | 26 | 3.31 | 0.127 |
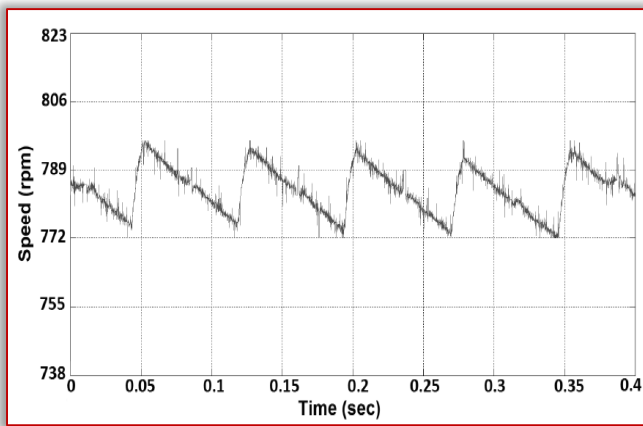
Figure 17. Experimental Result for Step Response
of Speed of BLDC Motor for a reference speed of 785 rpm
under 30% of Full Load
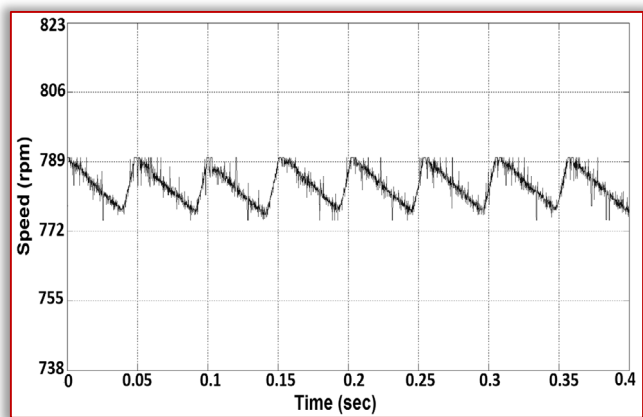


Figure 18. Experimental Result for Step Response
of Speed of BLDC Motor for a reference speed of 785 rpm
under 50% of Full Load
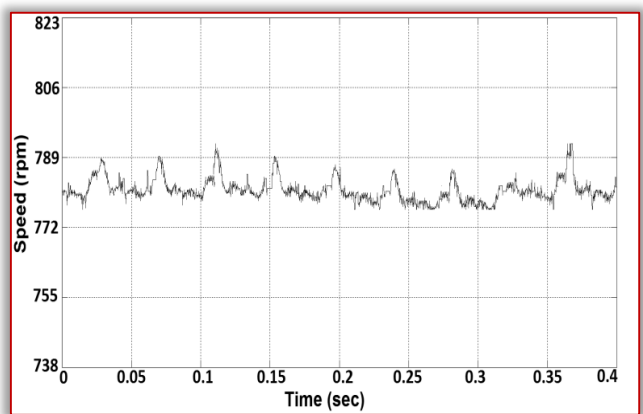


Figure 19. Experimental Result for Step Response
of Speed of BLDC Motor for a reference speed
of 785 rpm under Full Load

## CONCLUSION

An effective BLDC motor drive model has been developed here using low cost PIC18F4331 microcontroller especially for low-power applications. This research investigates the motor drive performance for 120-degree commutation switching technique by an adaptive On-Off control algorithm for variable torque-constant speed applications. The controller restricts the motor operation within a narrow speed band governed by set parameters, motor inertia and load. The controller has been designed to produce minimum speed regulation which is also verified form the experimental results. The controller is also equipped with another wider speed band which produces prompt and faster deceleration or acceleration whenever, by any accidental reasons or very sudden and heavy load change, the motor speed goes beyond the narrow speed band around the base speed. Here lies the novelty and usefulness of the proposed scheme. The introduction of Proteus VSM shows its capability and usefulness in designing virtual model requiring a shorter product development time. Experimental verification has also been carried out. And of course, the cost effectiveness of this low cost controller possesses good commercial appeal for low power applications.

## Appendix

| MOTOR SPECIFICATIONS | | |
|---|---|---|
| Parameter | Unit | Value |
| Terminal Voltage | Volt (dc) | 24 |
| Rated Speed | rpm | 3000 |
| Rated Torque | Nm | 0.573 |
| Rated Current | Amp | 8.0 |
| Rated Power | Watt | 180 |
| Back emf constant | Volt/krpm | 7.73 |
| Terminal Resistance | Ohm | 0.27 |
| Terminal Inductance | milli-Henry (mH) | 0.47 |

## References

[1] Ali Emadi, Anand Sathyan, Nikola Milivojevic, Young-Joo Lee and Mahesh Krishnamurthy, "An FPGA-Based Novel Digital PWM Control Scheme for BLDC Motor Drives", IEEE Transactions on Industrial Electronics, Vol. 56, No. 8, August 2009.
[2] Ali Emadi and Fernando Rodriguez, "A Novel Digital Control Technique for Brushless DC Motor Drives", IEEE Transactions on Industrial Electronics, Vol. 54, No. 5, October 2007.
[3] F. Rodriguez, P. Desai, and A. Emadi, "A novel digital control technique for trapezoidal brush-less DC motor drive", Proc. Power Electron. Technol. Conf., Chicago, IL, Nov. 2004.
[4] F. Rodriguez and A. Emadi, "A novel digital control technique for brushless DC motor drives: Steady state and dynamics," Proc. IEEE Ind. Electron. Conf., Nov. 2006, Pp. 1545–1550.
[5] F. Rodriguez and A. Emadi, "A novel digital control technique for brushless DC motor drives: Conduction-angle control", Proc. IEEE Int. Elect. Mach. Drives Conf., May 2005, Pp. 308–314.
[6] Mary George and Alphonsa Roslin Paul, "Brushless DC Motor Control Using Digital PWM Techniques", Proceedings of International Conference on Signal Processing, Communication, Computing and Networking Technologies (ICSCCN 2011), 2011.

[7] Padmaraja Yedamale, Brushless DC (BLDC) Motor Fundamentals, AN885 (Microchip Technology Inc.) 2003.

[8] Padmaraja Yedamale, Brushless DC Motor Control Using PIC18FXX31 MCUs, AN899 (Microchip Technology Inc.) 2004.

[9] Ward Brown, Brushless DC Motor Control Made Easy, AN857 (Microchip Technology Inc.) 2002.

[10] Mohamad Nasrul, Abdul Satar and Dahaman Ishak, "Application of Proteus VSM in Modelling Brushless DC Motor Drives", 2011 4th International Conference on Mechatronics (ICOM), Kuala Lumpur, Malaysia, 17-19 May 2011.

[11] Microchip PIC18F4331 Data Sheet, Microcontrollers.

[12] T. Kennjo and S. Nagamori, "Permanent Magnet Brushless DC Motors", Oxford, U.K.: Clarendon, 1985.

[13] Alok Mukherjee, Susanta Ray, and Arabinda Das, " Development of Microcontroller Based Speed Control Scheme of BLDC Motor Using Proteus VSM Software", International Journal of Electronics and Electrical Engineering Vol. 2, No. 1, March, 2014

[1.]I.O. SEKUNOWO, [2.]O.B. OGUNSINA

# MECHANICAL CHARACTERISATION OF CARBON-SILICA REINFORCED COMPOSITE FOR TURBINE APPLICATIONS

[1.]Metallurgical and Materials Engineering Department, University of Lagos, NIGERIA
[2.]Metallurgical and Materials Engineering Department, Federal University of Technology, Akure, NIGERIA

**Abstract:** Materials selection and development for applications in advanced systems is becoming highly complex involving the need for lower cost alternatives without compromising service performance. This paper investigated selected critical mechanical properties of ceramic composites synthesized from coconut shell carbon (CSC) reinforced with silica particles (SP). Coconut shells (CCS) and silica sand (SS) were pulverized separately in a plate mill and a ball mill respectively to obtain a particle size of $250\mu m$. The CCS powders were calcined at $500^0C$ in an oven to obtain coconut shell ash (CSA) which was carbonized in a furnace from $500^0C$-$1000^0C$ under argon gas controlled environment. The materials were mechanically blended while the SP additions varied from 10-40 wt.% and compacted using hydraulic press. The compacted mixture was sintered at $500^0C$-$1200^0C$, held for 2 hours and the composite characterized for mechanical properties while the microstructural integrity was analyzed using scanning electron microscope/energy dispersive x-ray spectroscopy (SEM/EDS). Results show that after sintering, coconut shell carbon developed strong cohesion with the silica particles which gave rise to effective load transfer. The mechanical properties that ensued demonstrated on the average, 52.8% comparability with conventional power plant structural materials in terms of hardness, compressive strength and impact energy.
**Keywords:** Ceramic matrix composite, power plant turbine, silica particles, coconut shell, mechanical properties

## INTRODUCTION
One of the factors that impact the efficiency of a power plant is the thermal and mechanical characteristics of critical components of its turbine. Ceramic composites are known to exhibit high thermal characteristics; however, their brittle nature under impact load has been a major concern in application environments where stress is combined with elevated temperature (Nadejda, et al., 2010, Amirtan, et al., 2011, Lewis, et al., 2009 and Xia and Curtin, 2000). Hence, the imperative to develop ceramic composite with a unique structure capable of significantly reducing intrinsic brittleness. Both the choice of reinforcing material suitable for such structure modification and the form in which such material is to be employed, demand scientific investigation. It is reasonably conjectured that certain agro-wastes if properly processed can be utilized for this purpose.

Generation of agro-waste in most developing countries has grossly increased over the years as a result of increase both in population and agricultural activities (Sonmez and Mustafa, 2011). According to Obi et al., 2016, the most widely used method of managing these agro-wastes is open air burning. Due to the adverse effect associated with open air burning, there is a need to explore other disposal options where agro-wastes can be productively utilized with little or no harmful environmental effects. However, apart from the seemingly pioneering work of Madakson, et al., (2012) which reported that the carbon in coconut shell ash has the potential utilization as reinforcement in ceramics composites, there is a huge information gap with regard to using agro-waste in ceramic based composites. This has placed a huge limitation on the scientific basis for processing and utilising carbon particles obtained from agro-waste to produce high performance advanced materials with characteristics light weight. The aim of this work is to develop and evaluate the functional mechanical characteristics of coconut shell carbon reinforced ceramic composites for applications as power plant turbine blades and steam buckets. As an organic contaminant, the productive use of coconut shells will help to mitigate the adverse effect on the environment arising from its improper disposal.

## MATERIALS AND METHOD
The major materials employed for the study consist of coconut shell (CS), silica sand (SS), sodium bentonite and distilled water. Sufficient quantities of coconuts were obtained from a coconut farm and the shafts removed to isolate the nuts. Then, the edible portion of the nuts was removed with a sharp knife while the CS left was first oven dried and then ground into powder in a ball mill (Figures 1a and 1b) and calcined into ash at $500^0C$ in an oven. The coconut shell ash (CSA) was then carbonized in a furnace at $500^0C$-$1000^0C$ under argon gas controlled environment. Figure 2 shows a typical X-ray Diffractogram (XRD) of carbonized coconut shells obtained under the same conditions employed in this study. The silica sand was first oven dried and then pulverized in a ball mill and sieved to $250\mu m$ particle size. Both carbon and silica powders fractions with addition of sufficient amount of distilled water were mechanically mixed with sodium bentonite according to the mix design shown in Table 1. The various mixes were compacted in a cylindrical metal mould using hydraulic press

at 30kgf. Prior to a full scale sintering in a furnace, the green compacts were oven dried between 200⁰C and 300⁰C to avoid crack during sintering. The composites were then sintered (see Figures 2a and 2b) by subjecting them to a gradual heating from 500⁰C-1200⁰C, held for 2 hours and allowed to cool in the furnace.



a)



b)

Figure.1: (a) Pulverizer (b) Ball mill

The sintered composite samples were characterised for microstructural integrity and mechanical properties using JEOL JSM-5900LV scanning electron microscope (SEM) equipped with an energy dispersive X-ray spectrometer (EDS) facility, Instron universal testing machine, Avery impact tester and Brinell hardness testing machine respectively.
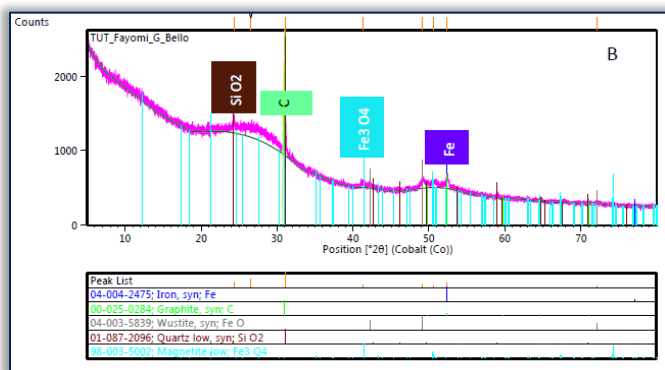


Figure 2. XRD image of coconut shells (Bello, et al., 2016)

Table 1. Samples formulation

| Sample | Materials (wt. %) | | |
|---|---|---|---|
| | Carbon | Silica | Bentonite |
| A | 80 | 0 | 20 |
| B | 70 | 10 | 20 |
| C | 60 | 20 | 20 |
| D | 50 | 30 | 20 |
| E | 40 | 40 | 20 |



a)



b)

Figure 3. Compacted silica reinforced carbon matrix composites (a) Green compacts (b) Sintered samples

## RESULTS AND DISCUSSION

### ⊞ Compressive strength

The maximum load bearing capacity of the composite was determined in a compressive strength test and the results are illustrated in Figure 4. It is observed that the sample without silica particles (SP) addition has the lowest compressive strength of 115.3MPa compared with other samples reinforced with varied additions of SP showing compressive strength ranging between 138.3MPa and 187.8MPa which compare well with that of conventional martensitic steels used in power plant structural components. The sample with 20 wt. % SP demonstrated the highest compressive strength of 187.8 MPa. This behaviour can be explained in term of the extent of wettability provided by the carbon matrix on the SP resulting in effective load transfer. It thus appears that the absence of SP in the control sample invariably gave rise to carbon-carbon interactions that resulted in a relatively low compressive strength. As observed in the current study however, the effectiveness of carbon as a wetting agent in a ceramic system appears to be on the average, in the ratio 8:1 for carbon/silica. This assertion is corroborated by the fact that a decrease in carbon/silica ratio to 4:1 gave rise to corresponding decrease of about 15 percent in compressive strength from 162.5 MPa to 138.3 MPa.
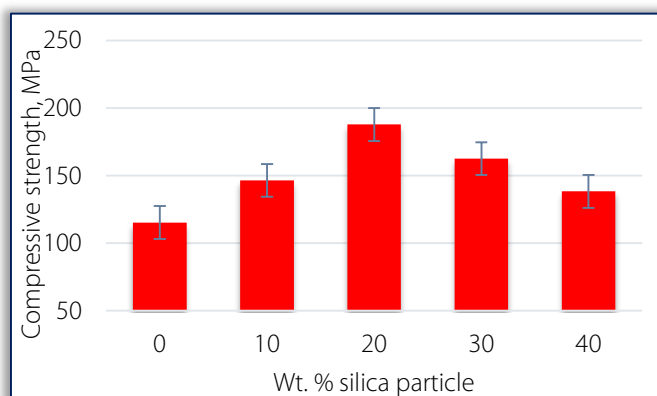


Figure 4. Variation of compressive strength with silica particle additions

## ⌺ Hardness

The results of hardness property analysis conducted on the carbon composite samples are as presented in Figure 5. The composites hardness values range from 106.5-178.4 Brinell hardness number (BHN) with the unreinforced sample having the lowest value while the peak is exhibited by the sample with 20 wt.% SP addition. The contribution to a relative high hardness of the reinforced samples may have stemmed from strong cohesion between the carbon matrix and the reinforcement phase that provide effective barrier to dislocation motion.

Although, on its own, silica is reported (Hassan and Aigbodion, (2010), Alaneme et al., 2013) to be one of the hardest materials however, the low hardness exhibited by the sample with 0 wt.% SP additions can be attributed to the monolithic and relatively soft carbon matrix. Again, the composite hardness reduces on further SP addition probably due to porosity suggesting that 20 wt. % SP is the optimum required for enhanced hardness characteristic of the carbon composite. However, the composites hardness value being in the range 131.8-178.4 BHN is 54.4% of the standard hardness put at 270-300 BHN for most power plant turbine blades (Ziegler et al., 2013, Bouwlte et al., 2015).
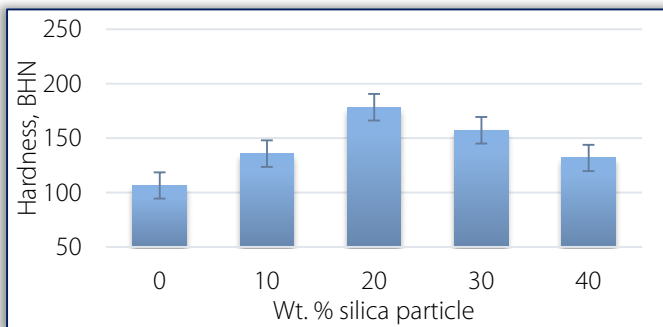


Figure 5. Variation of hardness with silica particle additions

## ⌺ Impact energy

Figure 6 illustrates the amount of energy required to fracture the composites at varied SP additions which is observed to increase progressively from 17.8 Js, peaked at 28.7 Js and then dropped monotonously to 19.6 Js. The unreinforced sample demonstrated the lowest impact energy which is 17.8 Js while the sample with low carbon/silica particle ratio of 4:1 also has relatively low impact energy, 19.6 Js. Given these observations, it appears that variations in the level of cohesion between the carbon particles and SP additions influence significantly the impact energy of the composites as an indication of the tough-to-brittle transition behaviour of the composites (Xia and Curtin (2000), Witold and Haley (2010). This is because, within ratios 8:1 and 5:1 of carbon/silica particle-matching within the system, the composites are conferred with the requisite ability to undergo substantial level of plastic deformation giving rise to impact energy values comparable with standard values of 20 Js (minimum) for steam turbine blades (Dowson et al., 2008).
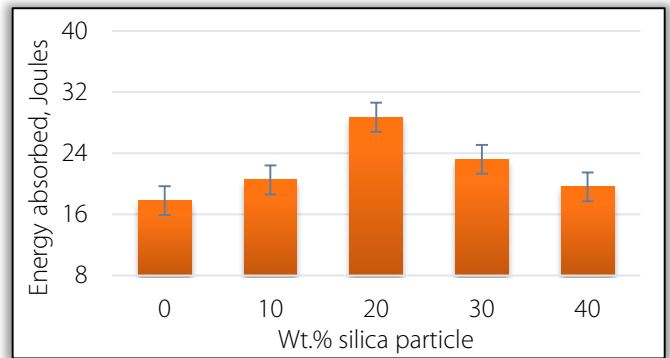


Figure 6. Variation of impact energy with silica particle additions

## ⌺ Microstructure

The SEM/EDS micrographs of the 20 wt.% SP reinforced carbon composite sample, being the composite that demonstrated the best mechanical characteristics is shown in Figure 7a.
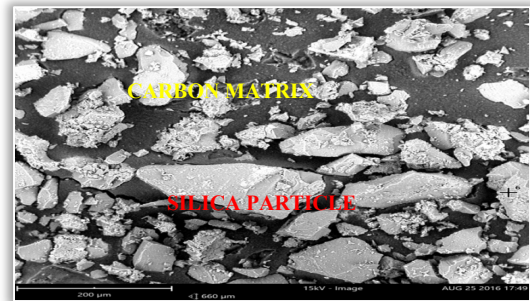


Figure 7a. SEM micrograph of 20 wt. % SP reinforced carbon composite
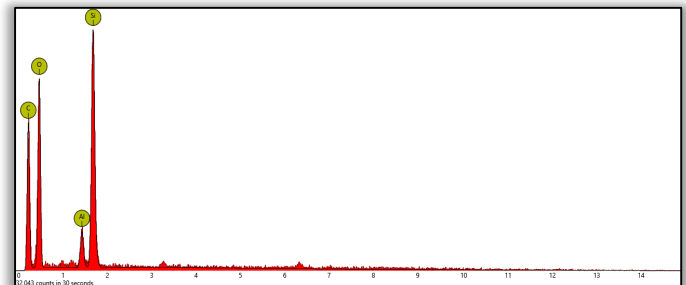


| Elements | Oxygen (O) | Silicon (Si) | Aluminium (Al) | Carbon (C) |
|---|---|---|---|---|
| Concentrations | 11.3 | 20.8 | 4.1 | 63.8 |

Figure 7b. EDS of 20 wt. % SP reinforced carbon composite

It is observed that the silica particles reinforcement phase disperse homogeneously within the carbon matrix. This actually provided the particles sufficient contact area with the carbon matrix which is relatively soft (graphite formed at the fairly low carbonization temperature of $1200^0$C). However, because of the traditional strong and directional bonding between carbon atoms and silica particles, limited plasticity is conferred on the composite confirming the report by Ritchie, (2011), hence the relatively low impact toughness exhibited by the composites. Varied elemental concentrations retained within the composites phases after sintering are presented as obtained by EDS analysis in the accompany Tables under Figures 7b and 8b at 20wt.% and

40wt.% respectively. The structure developed at 40wt.%SP addition (Figure 8a) revealed two features namely: inhomogeneous particles dispersion and an extensive particle coarsening resulting in a relatively large particle size. This type of microstructural feature is known to impair desirable mechanical properties such as toughness (impact energy), modulus and shear strength because it promotes weak cohesion between the particles and the matrix. Thus, the low mechanical properties exhibited by the composite at 40wt.% SP addition is attributable to its poor microstructural integrity.



Figure 8a. SEM micrograph of 40 wt. % SP reinforced carbon composite
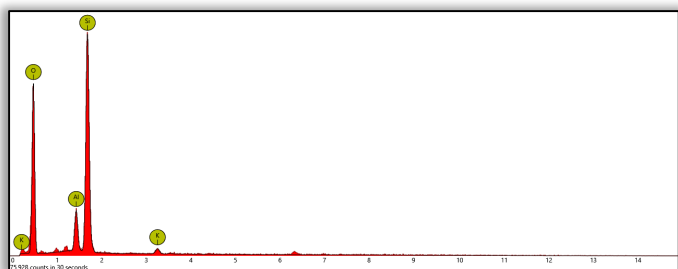


| Elements | Potassium (K) | Silicon (Si) | Oxygen (O) | Carbon (C) | Aluminium (Al) |
|---|---|---|---|---|---|
| Concentrations | 1.6 | 42.3 | 13.5 | 38.7 | 4.9 |

Figure 8b. EDS of 40 wt. % SP reinforced carbon composite

## CONCLUSION

The mechanical characteristics of silica particles reinforced carbon matrix composite have been investigated. From the results and their analyses the following conclusions can be drawn:

— The composites best mechanical properties namely; hardness, compressive strength and impact energy are obtained at 20 wt.% silica particles (SP) addition.

— Hardness of 178.4 BHN exhibited by the composite at 20 wt.% SP addition is adjudged sufficient to prevent any surface dysfunction in service.

— Under compressive loading, the composites ultimate strength performance of 187.8 MPa influenced significantly by matrix-reinforcement ratio are within the values recommended for ceramic composites.

— At an average of 7:1 of matrix/reinforcement ratio, the composite is conferred with the requisite ability to undergo substantial level of plastic deformation culminating in 28.7 Joules impact energy.

— The carbon matrix also serve as an effective wetting agent which significantly reduces the inherent brittleness of the ceramic composites,

In view of the above mechanical performance indices, the ceramic composite produced has a huge potential for application as power plant turbine blade and steam plant bucket.

## References

[1] Alaneme, K. K., Ademilua, A. O. and Bodunrin, M. O. Mechanical Properties and Corrosion Behaviour of Aluminium Hybrid Composites Reinforced with Silicon Carbide and Bamboo Leaf Ash. Tribology in Industry, 35(1), 25-35, 2013.
[2] Amirtan, G., Kumar, A., and Balasubramanian, M. Thermal Conductivity Studies on Si/SiC Ceramic Composites. Ceramics International, Vol. 37, Issue 1, pp. 423-426, 2011.
[3] Bello, S. A., Agunsoye, J. O., Adebisi, J. A., Kolawole, F. O., Hassan, S. B. Physical Properties of Coconut Shell Nanoparticles. Kathmandu University Journal of Science, Engineering and Technology, Vol. 12, No. 1, pp. 63-79, 2016.
[4] Bouwlte Florian, Marie Eric, Stevenson Adam: Strong, Tough and Stiff Bioinspired Ceramics from Brittle Constituents. www.nature.com, 2015.
[5] Dowson Philip, Bauer Derrick and Lanney Scot. Selection of Materials and Materials Related Processes for Centrifugal Compressors and Steam Turbines in the Oil and Petrochemical Industry. Proceedings of the Thirty-seventh Turbomachinery Symposium, pp. 189-209, 2008.
[6] Hassan, S. B. and Aigbodion, V. S. Microstructure and Interfacial Reaction of Al-Cu-Mg/Baggase Ash Particulate Composite. Journal of Alloys and Compounds, 491:571-574, 2010.
[7] Lewis, P., Ingel, R., McDonughs, W. and Rice, R. Microstructure and Thermo-mechanical Properties in Alumina and Mullite-Boron Nitride Particulate Ceramic-Ceramic Composites." Proceedings of the 5th Annual Conference on Composites and Advanced Ceramic Materials, pp. 719-721, 2009.
[8] Madakson P. B., Yawas, D. S. and Apasi, A. Coconut Shell Ash Characterisation for Potential Utilisation in Metal Matrix Composite for Automotive Applications, International Journal of Engineering Science and Technology, Vol. 4, No. 3, pp. 1190 – 1198, 2012.
[9] Nadejda Popoviska, Emad Alkhateeb, Andreas Paul and Alfred Leipertz Thermal Conductivity of Porous SiC Composite Ceramics Derived from Paper Precursor. Ceramics International, Vol. 36, Issue 7, pp. 2203-2207, 2010.
[10] Obi, F. O., Ugwishiwu, B. O., and Nwakaire, J. N. Agricultural Waste Concept, Generation and Utilisation and Management. Nigerian Journal of Technology, University of Nigeria, Nsukka, Vol. 35. No. 4, pp. 957-964, 2016.
[11] Ritchie, R. O. The Conflicts between Materials. Natural Materials, Vol. 10, pp. 817-822, 2011.
[12] Sonmez Liker and Mustafa Kaplan. The Effects of Some Agricultural Wastes Composite Carnation Cultivation. African Journal of Agricultural Research, Vol. 6(10), pp. 3936-3942, 2011.
[13] Witold and Haley. Brittleness of Materials; Implications for Composites in Relation to Impact Strength. Journal of Materials Science, Vol. 45, pp. 242-250, 2010.
[14] Xia, Z. and Curtin. Tough-to-Brittle Transition in Ceramics Matrix Composite with Increasing Interfacial Shear Stress. Acta Materialia, Vol. 48, Issue 20, pp. 4879-4892, 2000.
[15] Ziegler, D., Puccinelli, M., Bergallo, B. and Picasso, A. Investigation of Turbine Blade Failure in Thermal Power Plant. Case Studies in in Engineering Failure Analysis, Vol. 8, pp. 192-199, 2013.

[1.]Beata HRICOVÁ, [2.]Ervin LUMNITZER, [3.]Miriama PIŇOSOVÁ

# THERMOGRAPHY – TOOL FOR ASSESSING LIFE OF PRODUCTS

[1-3.]Technical University in Kosice, Faculty of Mechanical Engineering,
Department of Process & Environmental Engineering, Kosice, SLOVAKIA

**Abstract:** The paper is focused on the usage of thermography to assess the life of products and their failure rate. Thermography was used during routine vehicle technical inspections at the MOT station and focused on exhaust systems of 6 vehicles. For each vehicle tested, thermography identified critical places which, however, did not reduce the effectiveness of the product. The paper details the critical places of 2 cars. Potential damage has been identified in the 2 vehicles, as evidenced by increased values of emitted heat. As the results show, thermography is a suitable tool for identifying the quality reduction in the materials used, thus prolonging the life of the product thanks to early detection of problems.
**Keywords:** thermography, technical inspection, vehicle, lifetime, product

## INTRODUCTION

Thermography is a method of thermal imaging of objects and their temperature field. The infrared radiation is emitted towards the investigated objects and the image is visible thanks to a semiconductor detector that converts the radiation to an electrical signal. Thermography allows a person to observe the distribution of thermal fields that are invisible to the human eye. Depending on the temperature, it is possible to determine critical points as well as to detect mechanical damage. Infrared radiation is located between visible microwave particles of the electromagnetic spectrum. Its primary source is heat or heat radiation. Any object that has a temperature above absolute zero (-273.15 ° C or 0 Kelvin) radiates infrared radiation.

Infrared temperature measurement depends on the infrared radiation emitted by the object. The system's measurement circuit converts the radiation into an electrical signal that conveys information on object's temperature. The thermometric diagram used in the device memory is used to determine the area that emits the heat and heat value. [3]
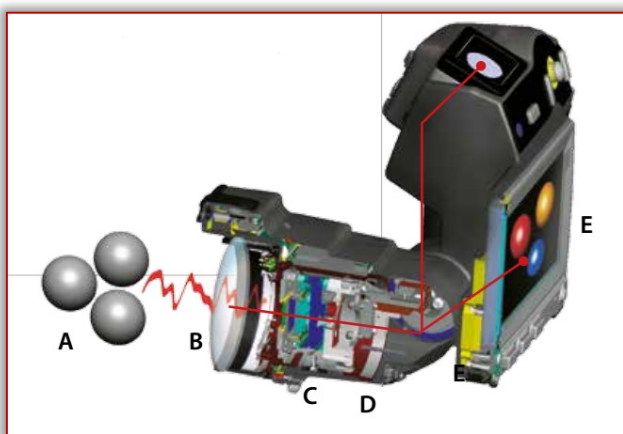


Figure 1. How thermographic camera works [4]

Thermographic works as follows: Infrared energy (A) coming from the object is recorded using the detector (C) of the optics (B), the detector then sends the information to the electronic image sensor (D) for processing. The electronics transform the data from the detector into the image (E), which can be displayed in the viewfinder, on video monitor or LCD screen. [4]

Thermographic solutions for various fields of the automotive industry
— Reconcile thermal behaviour of components with their standard behaviour
— Non-destructive testing allows precise and efficient quality control
— Integration into complex text solutions through interfaces to LabVIEW and MATLAB
— Analysis instruments for fast-rotating objects, such as tires or brakes.

Thermography helps to make defects visible without damaging the device under test on its testing. Therefore, functions of catalysts as well as electric systems of cars and motor assemblies can also be tested with the help of infrared camera systems.

Moreover, defects and deficiencies of multiple products for the automotive industry are only to be detected through temperature changes. Thus, heated seats and window heating can be tried and tested for their functionality by applying infrared camera systems.

## THERMOGRAPHY IN PRACTICE

For the purpose of this paper, we used the thermographic camera during regular vehicle technical inspection at MOT stations. The thermographic camera monitored the horizontal exhaust system of selected vehicles. Vehicles were monitored regardless of their production year, mileage, engine power or fuel type. Diagnostics was performed on 6 passenger cars. The individual characteristics of the diagnosed vehicles are to be found in Tables 1-6.

Methodology:
— The motor vehicle was heated to the operating temperature.
— Visual inspection of the exhaust system.

— Exhaust system diagnostics using a thermographic camera.

— Making thermographic records of the evaluated object.

— Evaluation of thermograms using software.

— Specification of critical places.

The diagnostics took approximately 10-15 minutes depending on the exhaust system of the vehicle.

## RESULTS OF THERMOGRAPHIC ANALYSIS OF EXHAUST SYSTEMS OF PASSENGER VEHICLES

We evaluated 6 vehicles using thermography. Data on vehicles is outlined in Tables 1-6.

Table 1. Data on vehicles (CITROËN)

| Brand | CITROËN | Engine vol. | 1868 cm |
|---|---|---|---|
| Model | Berlingo | Torque | 125 Nm |
| Year of production | 2002 | Power | 51 kW |
| Fuel | Diesel | Acceleration (0-100 km/h) | 15,6 s |
| Engine | 1,9 | Weight | 1125 kg |
| No. of cylinders | 4 | Consumption (average) | 6,90 l |

Table 2. Data on vehicles (SUZUKI)

| Brand | SUZUKI | Engine vol. | 1242 cm |
|---|---|---|---|
| Model | Swift | Torque | 118 Nm |
| Year of production | 2009 | Power | 69 kW |
| Fuel | Diesel | Acceleration (0-100 km/h) | 12,3 s |
| Engine | 1,2 | Weight | 1020 kg |
| No. of cylinders | 4 | Consumption (average) | 5,00 l |

Table 3. Data on vehicles (DACIA)

| brand | DACIA | Engine vol. | 1390 cm |
|---|---|---|---|
| Model | Logan | Torque | 112 Nm |
| Year of production | 2007 | Power | 55 kW |
| Fuel | Petrol | Acceleration (0-100 km/h) | 13,0 s |
| Engine | 1,4 | Weight | 1050 kg |
| No. of cylinders | 4 | Consumption (average) | 6,90 l |

Table 4. Data on vehicles (VOLKSWAGEN)

| Brand | VOLKSWAGEN | Engine vol. | 1390 cm |
|---|---|---|---|
| Model | Polo Classic | Torque | 110 Nm |
| Year of production | 1997 | Power | 44 kW |
| Fuel | Petrol | Acceleration (0-100 km/h) | 15,6 s |
| Engine | 1,4 | Weight | 945 kg |
| No. of cylinders | 4 | Consumption (average) | 6,70 l |

Table 5. Data on vehicles (KIA)

| Brand | KIA | Engine vol. | 998 cm |
|---|---|---|---|
| Model | Picanto | Torque | 95 Nm |
| Year of production | 2013 | Power | 51 kW |
| Fuel | Petrol | Acceleration (0-100 km/h) | 14,4 s |
| Engine | 1,0 | Weight | 905 kg |
| No. of cylinders | 4 | Consumption (average) | 4,20 l |

Table 6. Data on vehicles (CITROËN)

| Brand | CITROËN | Engine vol. | 1360 cm |
|---|---|---|---|
| Model | Berlingo | Torque | 120 Nm |
| Year of production | 2007 | Power | 55 kW |
| Fuel | Petrol | Acceleration (0-100 km/h) | 14,2 s |
| Engine | 1,4 | Weight | 1180 kg |
| No. of cylinders | 4 | Consumption (average) | 6,20 l |

Of the listed and evaluated vehicles we focus only on 2 which thanks to thermographics showed thermal loss points caused by the extended corrosion of the exhaust system. The first of these was DACIA Logan. The thermogram showing the critical places is shown in Figure 2 and thermal limits of the marked places are shown in Table 7.
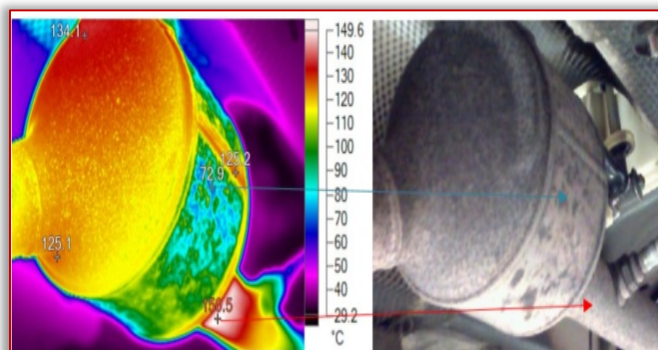


Figure 2. Infrared image of the exhaust system and real shot of the exhaust system

Table 7. Limitations of the marked places

| Title | Temperature | Emissions | Environment |
|---|---|---|---|
| Warm | 150,5°C | 0,92 | 18,0°C |
| P0 | 72,9°C | 0,92 | 18,0°C |
| P1 | 134,1°C | 0,92 | 18,0°C |
| P2 | 125,1°C | 0,92 | 18,0°C |
| P3 | 125,2°C | 0,92 | 18,0°C |

This exhaust system shows that corrosion has disturbed the original properties of the material to such an extent that its quality is already reduced. This is manifested by large temperature differences between the individual parts of the exhaust system. Temperatures on the thermogram range from 45 °C to 160 °C. Figure 2 shows the difference between

the highest and lowest temperature of the evaluated surface - up to about 90 ° C.

The second assessed vehicle was VOLKSWAGEN Polo Classic. The thermogram showing the critical places is shown in Figure 3 and the thermal limits of the marked places are shown in Table 8.
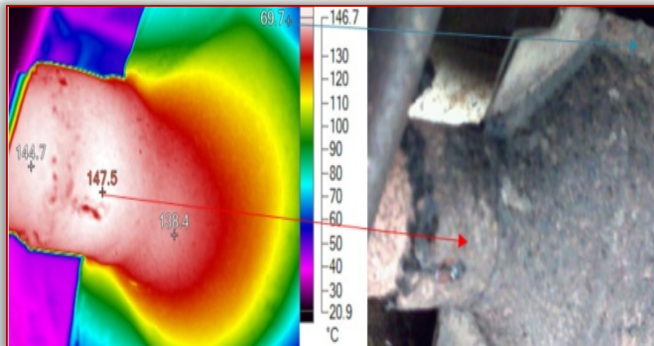


Figure 3. Infrared image of the exhaust system and real shot of the exhaust system

Tab. 8 Limitations of the marked places

| Title | Temperature | Emissions | Environment |
|---|---|---|---|
| Warm | 147.5°C | 0.92 | 18.0°C |
| P0 | 69.7°C | 0.92 | 18.0°C |
| P1 | 144.7°C | 0.92 | 18.0°C |
| P2 | 138.4°C | 0.92 | 18.0°C |

Since the car is 20 years old, it was evident that the individual parts of the exhaust system had been replaced. The replaced parts showed the average temperature of about 48-55 °C. The critical place, which is an original part, is shown in Figure 3, (the part has not been changed since the vehicle left the production). These places showed temperatures up to 177 °C. The reason is advanced corrosion and the evident reduction in the quality of the material due to its aging.

## CONCLUSION

The main objective of the paper was to find out if the thermographics is a suitable tool for diagnostics of exhaust systems during vehicle technical inspection, and whether it can be used to estimate the time need for replacement of the exhaust system of vehicles. The time required to replace the exhaust system of a vehicle varies. It may happen that at the time of the vehicle technical inspection, the exhaust system was in a good shape but got damaged after a few days/ months following the inspection. Such a vehicle then does not comply with MOT regulations. The measurements showed that the average temperature of the exhaust system of the assessed vehicles at the operating temperature was about 50 ° C.

Results showed that some parts of the exhaust systems reached temperatures of 150-170 °C. The analysis showed that these values are caused by advanced material aging and visible corrosion. Corrosion was visible by the naked eye, and the thermogram showed that the thickness of the material had diminished so much that the emitted heat reached critical values.

With regard to the results we note that thermodynamic would be an appropriate way to determine products' life cycle stage - in this case the vehicle's exhaust system. Thanks to a timely intervention it is possible to extend the useful life of the vehicle.

## Acknowledgement

## Bibliography

[1] NOWACKI,J., WYPYCH,A., : Application of thermovision method In.: Journal of Achievements in materials and Manufacturing engineering, ISSUE 2, 2010

[2] BOERNER,E et al.: Application of thermovision In.: Journal of Thermal Analysis, 2014,pp1-8, ISSN 10973-014-4026-6

[3] Thermal imaging guidebook for building and renewable energy applications. [online]. [citované 7.2.2017]. Dostupné na internete:

[4] Thermal imaging cameras for electrical and mechanical applications. [online]. [citované 22.2.2017]. Dostupné na internete:

# Fascicule 3

## [ July - September ]

## t o m e
## [2018] XI

**ACTA Technica CORVINIENSIS**
**BULLETIN OF ENGINEERING**

**ISSN: 2067-3809**

[1.]Cristina Carmen MIKLOS, [2.]Carmen Inge ALIC, [3.]Imre Zsolt MIKLOS

# ASIMETRIC PANTOGRAPH MECHANISM STATIC ANALYSIS BY FINITE ELEMENT METHOD

[1-3.]University Politehnica Timisoara, Faculty of Engineering Hunedoara, ROMANIA

**Abstract:** The paper deals with the static analysis of the asymmetric pantograph mechanism used in the railway electric traction. In order to model the asymmetric pantograph mechanism subject study through the finite element analysis, was used Autodesk Inventor Professional program, a software package that is part of the Computer Aided Design (CAD) family, enables 3D product modeling and assembly of parts, thus representing an integrated and intelligent solution for 2D/3D design dedicated to mechanical and electromechanical engineers. 3D modeling in Autodesk Inventor of the pantograph mechanism was accomplished using the principles of parameterized modeling and adaptability for Stable Part (Part) and 3D constraints: insertion, overlap, angular constraint, insertion (Insert, Mate, Angular, and Flush). After assembly of the component elements and after the introduction of 3D constraints, the pantograph mechanism kinematic verification was performed by simulating the movement. The conclusions and results obtained are useful in the design and operation of these types of mechanisms from the railway electric traction.
**Keywords:** railway electric traction, asymmetric pantograph, 3D modeling, static analysis, finite element method

## INTRODUCTION

Rail transport is an important part of the general freight and passenger transport, which is steadily increasing, mainly due to the increase of the commercial speed by increasing the speed of the traffic and the automation of the related installations [1]. In electric traction, a modern and rational traction system that offers increased safety in trains circulation and technical-economic advantages in the railway transport, the vehicle movement on the rail road occurs as a result of the use of a propulsion system - made with rotary or linear electric motors - of the traction force that develops as a consequence of some pondero-motor actions in the electromagnetic field [2].

The electric locomotive, as an electric motor, captures energy from the contact line, and the mono, bi or trifilar contact captures can be made either from a classical line or from a rigid rail. With all the inconveniences generated by the amount of investment and construction required, in this moment, the power supply solution from an elastic contact line remains the most economical in the event of intense traffic and significant declines.

The electricity from the contact line is transferred to the locomotive via the pantograph mechanical arm supporting the current collector [3]. Since the supply of the locomotive must be continuous, the pantograph must exert a stable and constant force at the current collector shoe.

The contact force must be large enough to ensure continuity of current collection, but also small enough to prevent overturned vertical movements by forced lifting of the catenary, especially in the middle areas between the supporting posts, which would accentuate the dynamic character of phenomena in the behavior of the ensemble [4].

The problem of ensuring continuous current collection depends on kineto-static characteristics of pantograph and flexibility characteristics of the catenary: the pantograph geometry in motion should allow easy tracking of the catenary route to ensure continuous electric contact, but not to displace the catenary in an appreciable manner; the catenary suspension should be as rigid as possible, but with the most uniform stiffness of the assembly, to ensure minimum displacements in the wire [5].

Ideally, the pantograph must touch the wire fairly firmly to ensure a good electrical contact, but easy enough not to move the catenary significantly [6].

## MODELING ASYMMETRIC PANTOGRAPH MECHANISM

Pantograph mechanism in Autodesk Inventor [7] 3D modeling was made using parametric modeling principles and adaptability for independent benchmarks (Part) and 3D constraints: insert, overlay, and angle constraint, restraint (Insert, Mate, Angular and Flush).

Thus modeled, the components of the asymmetrical pantograph mechanism studied are shown in Figures 1-5.



Figure 1. Support subassembly

Figure 2. Pantograph mechanism connecting rod



Figure 3. Pantograph mechanism rocker
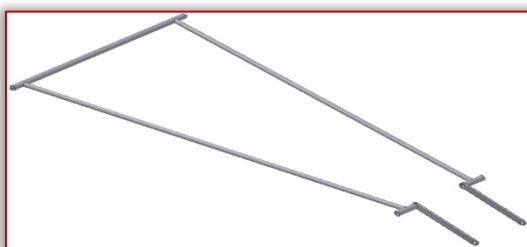


Figure 4. Upper arm subassembly



Figure 5. Pantograph sleigh

## PANTOGRAPH MECHANISM FUNCTIONING SIMULATION

As a result of the assembly of the component elements presented in the previous figures and after the introduction of the 3D constraints (Angular, Mate), the pantograph mechanism kinematic verification was performed by simulating the movement. It was found that between its extreme positions (Figures 6 and 7) given by the angular constraint of the driving element (rod) - min.$5^0$ and max.$54^0$ - the maximum travel of the sleigh is related to a vertical direction displacement of approx. 2600mm, which demonstrates that the modeled mechanism works correctly.
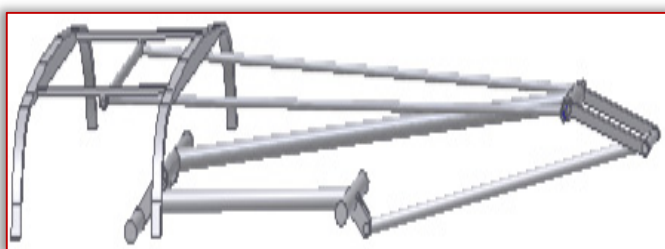


Figure 6. Minimum angular position for opening the pantograph mechanism (pantograph lowered position)
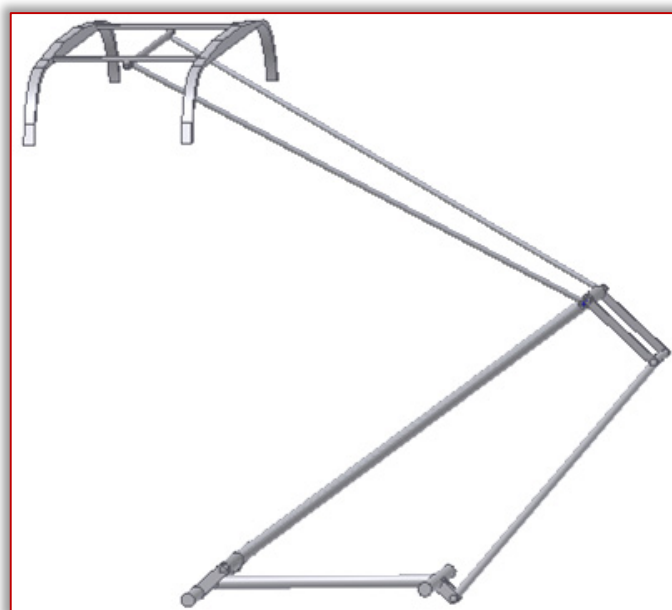


Figure 7. Maximum angular position for opening the pantograph mechanism (pantograph higher position)

## PANTOGRAPH MECHANISM ELEMENTS STATIC ANALYSIS

Pantograph mechanism elements static analysis was done using the finite element method in Autodesk Inventor Professional [7]. Parametric 3D models, which have the property to change automatically with size changes, are obtained by geometric generation using the specific operations of: extrusion, rotation around an axis of the profiles, etc.

Therefore, in a first phase is being drawn contours open or closed mostly made up of a series of lines and arcs called sketch, which follows a series of geometric and dimensional constraints, and the sketch after applying constraints becomes profile. A sketch needs geometric and dimensional constraints to be defined as shape and size, and constraints reduce degrees of freedom between sketch elements and control how it behaves when a dimension is changed.

In order to realize a profile, do the following steps:

— Making the sketch;

— Validate and obtained the profile;

— Applying geometric constraints.

For the static analysis of the pantograph mechanism, it was considered that on the mechanism structure a contact force acts at the level of the skate $F_c$=90N, and the efforts are taken over by the upper frame elements and the support subassembly, assumed as a fixed element.

For the analysis by the finite element method, we have to make the following steps:

— Launching the FEA module;

— Defining the piece's material;

— Determining the static and loading scheme for each element-part by declaring the forces and the supporting mode (figures 8-10);
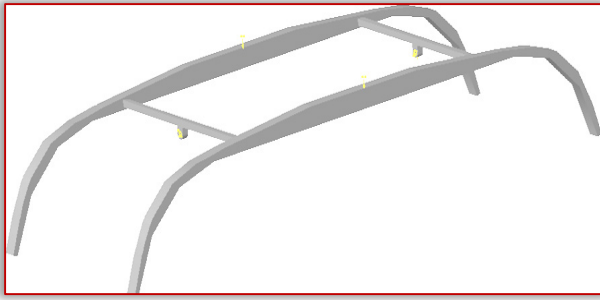
Figure 8. The static and loading scheme of the frame
substructure of the pantograph sleigh
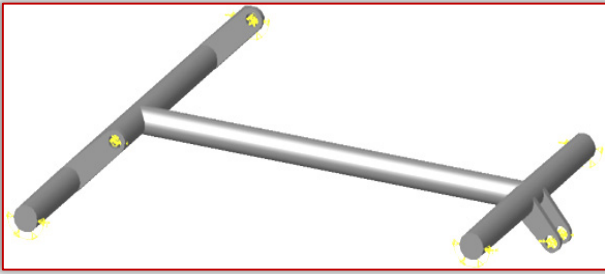


Figure 9. Static and load scheme
of the support subassembly



Figure 10. Static and load scheme
of the connecting rod element

⊡ Component parts and pantograph subassemblies
meshing (figures 11–13);
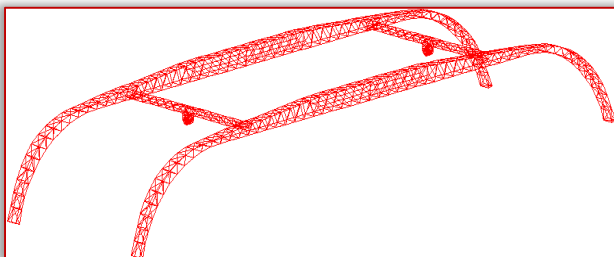


Figure 11. Frame substructure
of the pantograph sleigh meshing
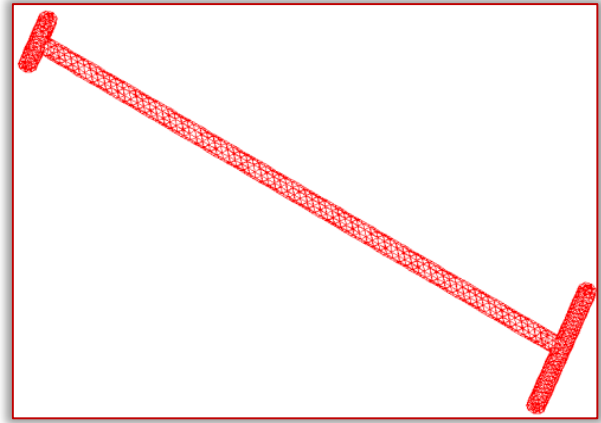


Figure 12. Structure rod element meshing
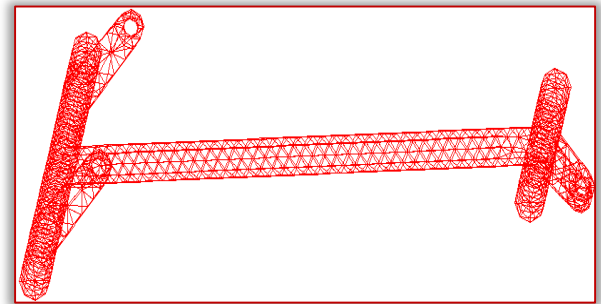


Figure 13. Support part structure meshing

⊡ Running the program for finite element analysis and
displaying the results of the unit efforts and deformations
distribution (example in figures 14–16) determined for each
assembly components based on VonMises theory.
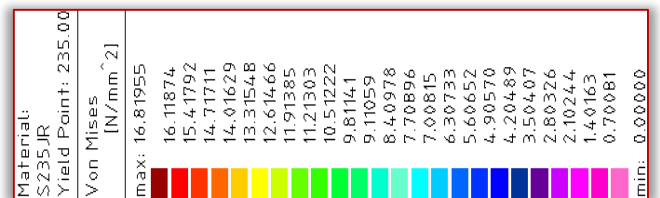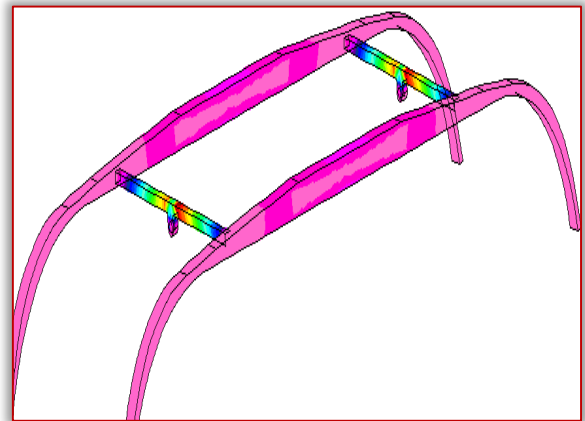


Figure 14. Stress distribution in the frame type substructure
of the pantograph sleigh
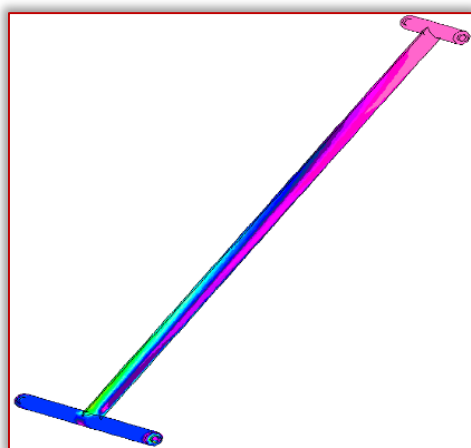
Figure 15. Stress distribution in rod element
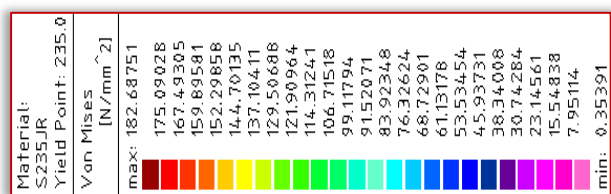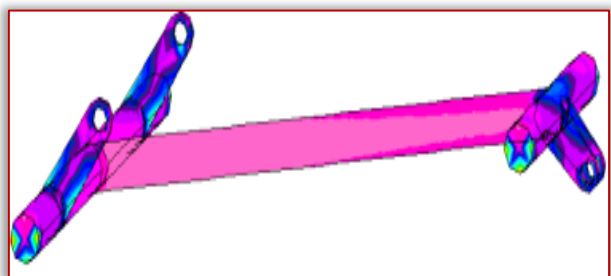


Figure 16. Unitary efforts distribution in the support subassembly

## CONCLUSIONS

The results obtained from the calculation show that both the values of the unitary stresses and the deformations produced in the structural elements of the pantograph mechanism, fit within the limits imposed by the available norms. It was found that between its extreme positions (Figures 6 and 7) given by the angular constraint of the driving element (rod) - min.$5^0$ and max.$54^0$ - the maximum travel of the sleigh is related to a vertical direction displacement of approx. 2600mm, which demonstrates that the modeled mechanism works correctly.

## Bibliography

[1] Alic (Miklos) Cristina, Studiul ansamblului suspensie catenară-pantograf în tracţiunea electrică feroviară, în vederea îmbunătăţirii transferului de energie, teză de doctorat, 2011

[2] Bandi Punit, High Speed Rail Pantograph Control System design, University of Notre Dame, USA, May 1, 2009

[3] Belongie, S., Malik, J., et Puzicha, J., Shape matching and object recognition using shape contexts. IEEE Transactions on pattern analyses and machine intelligence, 24: 509-522, 2002

[4] Benet J., Cuartero F., Rojo T., A tool to calculate mechanical forces on railway catenary, Escuela Politecnica Superior, Univ. de Castilla-La Mancha, Campus, 02071 Albacete, Spain

[5] Bocciolone, M., Resta, F., Rocchi, D., Tosi, A., et Collina, A., Pantograph aerodynamic effects on the pantograph-catenary interaction. Vehicle System Dynamics, 44 Supplement: 560-570, 2006

[6] Nordborg, A., Vertical rail vibrations: noise and structure-borne sound generation. Thèse de doctorat, Kungl Tekniska Hogskolan, 1995

[7] ***, Autodesk Inventor Professional 2011 – User guide, 2011

[1.]Vasil VLASEV

# DETERMINATING THE CUTTING FORCES IN CIRCULAR CUTTING MACHINES WITH REGARD TO THE EFFECT IN THE RADIAL RUN-OUT OF THE CUTTING MECHANISM

[1.]University of Forestry, Faculty of Forest Industry, Department Woodworking Machines, BULGARIA

**Abstract:** The cutting forces in circular cutting machines have been determined by calculating the cumulative radial run-out, according to known normative documents about the cutting mechanism. The radial run-out in this mechanism is seen as a periodic movement, towards and away of the cutting body to the workpiece. As a result, the velocity of this movement is summed with the feed rate. It is found, that its velocity is comparable to the feed rate, and it is approximately 25% of its size. The cutting forces are also equally greater than the traditionally calculated ones and within one full rotation of the cutting tool, they are changed in an asymmetric cycle. For a better perception, this approach and offset can be represented as a periodic shift of the cutting body in the direction and against the direction of feed. For strength calculations, it is sufficient to calculate the feed rate only with its increase. Research in this regard has not been found in any literature known to the author. Therefore, the purpose of the present work is to determine the movement velocity of the tooth line of the circular saw to the workpiece as a result of the radial run-out, and whether it is comparable to the feed rate. This would, consequently, determine how this affects the cutting forces.

**Keywords:** circular cutting machines, cutting forces, radial run-out

## INTRODUCTION

The cutting forces, for circular as well as other woodworking machines, are the basis for the strength dimensioning of the elements of their cutting mechanisms as well as other machine elements. These forces need to be known for the proper operation of the machines.

The cutting forces are tangential and radial [3], [4], [8]. According to A. L. Bershadskiy's [3] famous theory the tangential force of cutting is determined by the formula /the radial force of cutting is calculated by means of the tangential force.

$$P = \frac{KbhU}{V}, N, \qquad (1)$$

where:

— P is the tangential force of cutting,
— N; b – width of the slot,
— m; h – height of the slot,
— m; U – feed rate, m.s$^{-1}$;
— V – cutting velocity, m.s$^{-1}$.

As it can be seen from formula (1), the tangential force of cutting is in direct proportion to the feed rate, which, according to known literary sources [3], [4], [8] is assumed to be uniform within a complete rotation of the cutting tool /figure 2a/.

In these machines, as well as in many others, the geometric accuracy of some of the cutting mechanism's elements is essential to their operation. One of the geometrical inaccuracies of this mechanism is the radial run-out [5]. Such run-out can occur on the shaft of this mechanism [2], as well as on the circular saw [7].

The specified geometrical inaccuracies in practice can occur in any probable situation, but for certain calculations they are summed up unambiguously and with their maximum values [6]. Therefore, it is possible to have a maximum radial run-out equal to the sum of the radial run-out of the shaft and circular saw. As a result of this radial run-out, a part of the circular saw's teeth are periodically moving away and towards the processed material, thereby the speed of the approach is summed with the feed rate and the offset speed is subtracted from it.

For a better perception, this approach and offset can be represented as a periodic shift of the cutting body in the direction and against the direction of feed. The latter means that the feed rate by which the cutting force in formula (1) is to be calculated, needs to be increased or decreased in accordance with the rate of the periodic approach or offset of the circular saw to the processed material. For strength calculations, it is sufficient to calculate the feed rate only with its increase. For the convenience of expression, the term "tooth line" will be used in the article since it does not coincide with the circumference of a geometrically accurate circular saw.

Considering the explanation given above, the cutting forces in circular machines would be different in size compared to those in the formula (1), if the radial run-out is taken into account. Research in this regard has not been found in any literature known to the author.

Therefore, the purpose of the present work is to determine the movement velocity of the tooth line of the circular saw to the workpiece as a result of the radial run-out, and whether it is comparable to the feed rate. This would, consequently, determine how this affects the cutting forces.

THEORETICAL FORMULATION

In order to achieve this goal, it is necessary to determine the two velocities defined above. The first is the movement velocity of the tooth line of the circular saw in the direction of feed. The method of determining this velocity is illustrated in Figure 1.

Position 1 shows the workpiece that moves in the direction indicated by U. Position 2 is the circular saw. The total radial run-out is shown along the η axis, which passes through the circular saw's tooth line and through the middle of the workpiece. For axis η this space is determined, as the power calculations are made for it [3].

The magnitude of the cumulative radial run-out of the figure corresponds to the distance $A_1B$ where the workpiece is, and on the opposite side (at $180^0$) - $AB_1$. The center of rotation is point O around which the circular saw rotates eccentrically. Its center of rotation is displaced by the geometry at a distance equal to half of the total radial run-out, which in the figure corresponds to the distance $AA_1$.
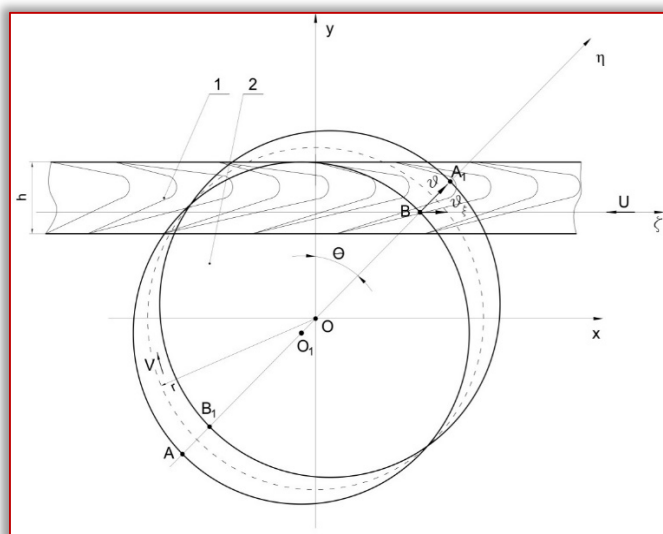


Figure 1: Scheme for determining the speed of movement of the circular saw in direction of the feed rate

In figure 1, points A and B show two end positions of the radial run-out of the tooth line along the axis η when the circular saw circles around point O. Point A is the most convex part, and point B is the most concave part. When rotating the circular saw by $180^0$, point A moves to point $A_1$ and point B to point $B_1$. From this it is seen how the tooth line moves along the axis η from point B to point $A_1$, i.e., the circular saw is periodically moving towards and away from the workpiece within a complete rotation. The latter means that the feed of the tooth will also change within one turn and hence the cutting power.

Once the tooth line moves along the axis n, it does that at some velocity $\vartheta$. The law associated with the changes in this velocity cannot be accurately determined. The reason for this is that the shape of the geometrical inaccuracies of individual elements and their surfaces are of a random nature, as well as their summing. Therefore, assuming that the circular saw after mounting and tightening it to the shaft, with its geometrical inaccuracies is rotating around a displaced geometric center of rotation, it can be assumed that the movement of the tooth line is harmonious and thus this velocity changes by a harmonious law. The projection on the axis η is determined by the formula [1], [9]

$$\vartheta = A\omega\cos(\omega t+\varphi), \text{m.s}^{-1}, \qquad (2)$$

where:
— $\vartheta$ is the movement speed of the tooth line to the workpiece, m.s$^{-1}$;
— A – the amplitude of vibration of the tooth line, m;
— ω – angular velocity, rad.s$^{-1}$;
— t - time, s;
— $\varphi$ - initial phase of motion, rad.s$^{-1}$.

As it can be seen from the formula above, the tooth line's movement velocity is variable and it is determined by the angle of rotation of the circular saw.

To calculate the cutting forces in strength dimensioning it is necessary to know the maximum velocity, which is determined by the formula [1], [9]

$$\vartheta_{max}= A\omega, \text{m.s}^{-1}, \qquad (3)$$

where: $\vartheta_{max}$ is the maximum speed of movement of the tooth line on the axis η, m.s$^{-1}$;

In order to determine the magnitude of this velocity, it is necessary to know the magnitude of the amplitude, which is determined by the sum of the radial run-out of the shaft and the radial run-out of the circular saw.

The radial run-out of the shaft according to BDS 4297 [2] is 0,04 mm for machines with normal precision and 0.02 mm for machines with higher precision and according to Obreshkov [7] the radial run-out of the teeth of the circular saw is 0,06 mm to 0,1 mm after sharpening. The magnitude of the amplitude, considering the measurement method of the radial run-out [6], [2], is half of the total radial run-out and is determined by the formula:

$$A = \frac{\delta}{2}, \text{m}, \qquad (4)$$

where: δ is the total radial run-out of the tooth line, m.

In order to determine whether the magnitude of the movement speed of the tooth line is comparable to the feed rate, it is necessary to determine the rate at which the tooth line moves in the direction of feed, i. e. along the axis ζ (Figure 1).

Thus far, the maximum velocity along the axis η is determined, and the velocity along the axis ζ, according to Figure 1 is determined by the formula.

$$\vartheta_{\zeta max} = \vartheta_{max}\cos(90-\theta), \text{ m.s}^{-1} \qquad (5)$$

where:
— $\vartheta_{\zeta max}$ is the maximum speed at which the tooth line moves at the direction of feed, m.s$^{-1}$;
— θ - cinematic angle of encounter, $^0$.

By replacing equations (3) and (4) in (5) it is obtained:

$$\vartheta_{\zeta max} = \frac{\delta}{2}\omega\cos(90-\theta), \text{ m.s}^{-1} \qquad (6)$$

## RESULTS AND DISCUSSION

In order to determine whether the speed of movement of the tooth line $\vartheta_{\zeta max}$ is comparable to the feed rate U, it is necessary to make specific calculations for both speeds. The calculations to be made for the feed rate are for a case in which the circular shaft is heavily loaded at a low feed rate /to be comparable to the movement speed of the tooth line / and with a large slot height.

The aim is to maximize the kinematic angle of encounter as the movement speed of the tooth line in the direction of feed is determined by it. This is one of the possibilities that can be encountered in practice and during which a maximum shaft load is obtained.

The cutting mode selected to determine the feed rate is based on the following parameters:
— Circular Saw Diameter - 400 mm;
— Rotation speed - 75 s$^{-1}$;
— Number of teeth - 48;
— Slot width - 4 mm;
— Slot height – 0,1 m;
— Wood type - beech.

The calculations are based on a methodology developed by Bershadskiy [3]. Since the feed rate is also dependent on the dulling of the cutting edges, it has been found that feed rates of less than 0,096 m.s$^{-1}$ are obtained when dulling of the same above 39 μm.

The maximum movement speed of the tooth line in the direction of feed is calculated by the summed radial run-out δ = 0.14 mm / A = 0.00007 m / and a kinematic angle of encounter θ = 46$^0$. It has been determined that at these values its magnitude is 0.0235 ms$^{-1}$.

From the calculations made, it can be seen that the movement speed of the tooth line in the direction of feed is a quantity which can be comparable to the feed rate. It can have values approximately 4 times lower (24.6%), and as it can be seen from formula (6) it changes approximately within the range of ± 0.25U by a harmonious law, within one complete rotation of the cutting tool.

Considering the above and formula (1) it follows that the cutting force is also changed by a harmonious law, as shown in Figure 2b, i.e by an asymmetric cycle [5].

The analysis made shows that a circular machine which is within its geometric precision can be loaded with cutting forces over the traditionally computed and with a variable sign.

Here, a question can arise regarding the cutting speed in the more protruding and recessed part of the circular saw's tooth. Calculations have been made for these two regions, and it was found that the cutting speed varied by ± 0.033 m.s$^{-1}$. Concerning the cutting speed for case above, this change is 0.035%, which indicates that it would practically not change the results of this study.



a)



b)
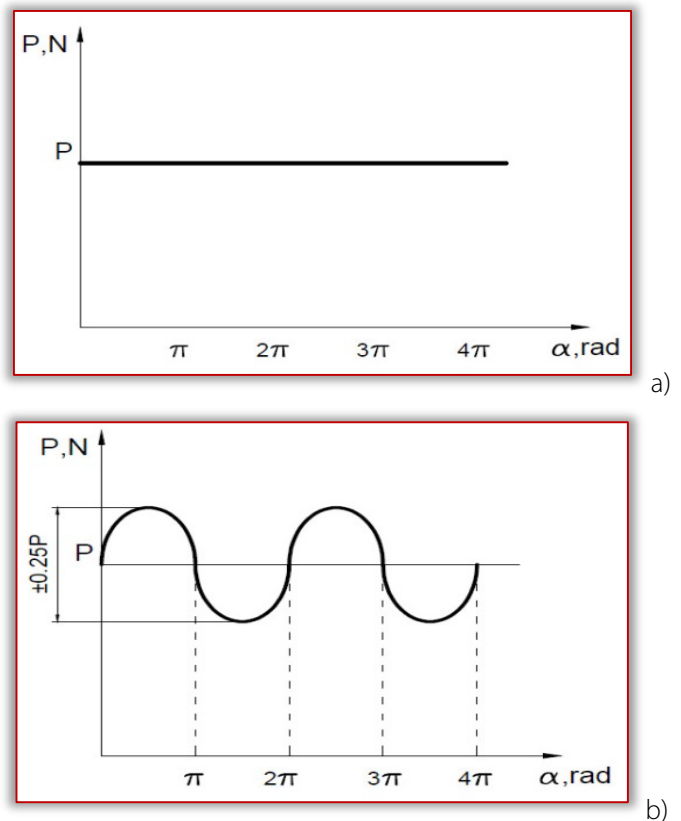
Figure 2. Graphical dependencies for loading of the circular shaft:
a - at constant magnitude of the cutting force;
b- cutting force, with regard to the radial run-out.

## CONCLUSIONS

— The tangential and radial cutting force in strength dimensioning of the shafts in circular machines, taking into account the radial run-out in the cutting mechanism, is approximately 25% greater compared to the traditional calculation method;
— In strength dimensioning of the shafts in circular machines which operate at high loads, the unsymmetrical dynamic load cycle must be considered;
— The analysis made indicates that the radial run-out is the greatest as a result of the inaccuracies when sharpening the circular saw. From the latter it follows, that the

sharpening machines for these saws need to be with high accuracy.

References:

[1]     Artobolevskiy I.I: Mechanisms in modern technology, vol. V. Moscow. Science. 1981. p. 29.
[2]     BDS 4297 - 69. Woodworking machines. Universal circulars. Accuracy standards.
[3]     Bershadskiy A.L., Tsvetkova N.I: Wood cutting. High school. Minsk. 1975. p. 150–163.
[4]     Filippov G: Woodworking machines. Zemizdat. Sofia. 1977. p. 170-171.
[5]     Hristov D., Petkov G. etc: Calculation and Design of Machine Elements. Technical. Sofia. 1980. p. 66.
[6]     Kyuchukov G., Filipov G., Genchev G.: Interchangeability and technical measurements in woodworking. Sofia. Technical. 1976. p. 187 – 206.
[7]     Obreshkov P.: Guide to woodcutting tools. Technical. 1976. Sofia. p. 201.
[8]     Obreshkov P.: Woodcutting Machines, vol. 2. Sofia. IC "VM". 1996. p. 7.
[9]     Pisarev A., Paraskov T., Bachvarov S.: Theoretical Mechanics Course part 1. Technical. Sofia. 1986. p. 293.

1, 2.Fatai Olufemi ARAMIDE, 1.Abel A. BARNABAS, 2.Patricia Abimbola POPOOLA

# PRODUCTION OF INSULATING CERAMIC FROM ISEYIN CLAY

1. Department of Metallurgical & Materials Engineering, Federal University of Technology, P.M.B. 704, Akure, NIGERIA
2. Department of Chemical, Metallurgical & Materials Engineering, Tshwane University of Technology, Staatsartillerie Road, Pretoria West, SOUTH AFRICA

**Abstract:** The effect of adding varied amount of rice husk on thermal and mechanical/refractory properties of Iseyin clay was investigated. The clay obtained from Iseyin in Oyo State was preprocessed to very fine particles and characterized using scanning electron microscope (SEM) equipped with energy dispersive spectroscopy (EDS) and x-ray diffractometry analysis (XRD). Rice husk procured from a large rice plantation in Akure was dried. It was then pulverized into powder. A mixture of this dried rice husk powder with the processed clay was made at various proportions of the rice husk, with a little addition of water. Samples of standard dimensions were produced through uni-axial compaction. The samples were dried and then fired at 1000°C. The sintered samples were characterized for various properties using standard ASTM method. The microstructures of the fired samples were characterized with SEM. It was observed that increase in the rice husk leads to increase in the porosity of the sample. This resulted in the reduction in other properties of the samples. It was concluded that service condition where the ceramic will be in contact with molten metal/slag, sample with 0% admixture is optimum. For insulation, sample with 40% admixture is optimum.
**Keywords:** porous ceramic; sintering temperature; thermal conductivity; insulating brick; clay

## INTRODUCTION

Clays are vital raw materials for the industries. They are used in making ceramics, paper making, paint, petroleum industry, catalysis etc. Their area of applications depends upon their structure, composition, and physical attributes [1, 2].

Insulating ceramics are materials with low thermal conductivity due to their high porosity. They are generally used in the conservation of heat in furnaces where they will not be in contact with molten metal [3]. Because of their high porosity they are inherently lightweight refractories that have very low thermal conductivity and heat capacity than other refractories [4]. They are also used in other industrial areas, such as catalyst supports for heterogeneous chemical reactions, filters, membranes and bioceramics [5]. Porosity is normally incorporated by the addition of combustible materials to the ceramic raw material mixture. These combustible materials are burnt off during firing, which leaves a large fraction of pores within the ceramic body. There are different types of pore formers available today such as sawdust, foam polystyrene, fine coke, binders and organic foams, or granular materials such as hollow microspheres and bubble alumina [4, 6].

Many researchers have worked extensively on clay; production of refractory and insulating ceramics from natural clay. Aramide, [1] reported on the effects of firing temperature on the mechanical properties of masonry bricks produced from Ipetumodu clay. He reported that the optimum mechanical properties of the masonry bricks were obtained at 950°C. The same author in 2015 [2] investigated the effects of sintering temperature on the phase development and mechanical properties of ceramics produced from Ifon clay. He observed that the sintered samples were composed mainly of quartz, microcline and anorthite and only the sample sintered at 800°C contains muscovite. He concluded that the sample which was sintered at 800°C held for 1 hour and cooled in the furnace. Moreover, Hassan et al., (2014) [7] investigated the effects of saw dust and rice husk on the properties of local refractory clay.

Furthermore Aramide, [5] produced and characterized porous insulating fired brick from Ifon clay. In all the references above only the later investigated the thermal conductivity among the properties examined. The aim of the present work is to evaluate the effects of varying porosity (through varied amount of saw dust admixture) on the properties (including thermal conductivity) of the porous ceramic bricks produced from Ipetumodu clay.

## EXPERIMENTAL PROCEDURE

The materials used for this study include; dried saw dust, Ifon clay as mined, water, wooden sieve, beaker, conical flask and thermometer. The equipment used for this study include; a furnace, mounting press, grinding mill, pulverizer, seive shaker and set of sieves, and com- pression strength tester. Dried saw dust from mahogany tree acquired from a saw mill in Akure was sun dried further to remove moisture present. Clay acquired from Ifon, also in Ondo State was soaked in water for three days to dissolve the clay and at the same time to form slurry. The resulting slurry was then sieved to remove dirt and other foreign substances using a sieve. More water was thereafter poured into the clay to form slurry once again. This is then allowed to settle down for seven days. The floating clear liquid was decanted after the seventh day. The settled fine clay was then poured into a P.O.P mould and left undisturbed for three days in other to allow the liquid still present to drain out completely. The resulting clay was then sun dried for two days. This was followed by grinding in a grinding mill to reduce the particle sizes. A pulverizer was

then used to reduce the sizes of the clay particles further into still finer particles. A final sieving of the pulverized sample was then carried out. A sieve analysis of the clay and saw dust used in this project is as stated: Clay; <850 μm, Saw dust; <1700 μm. A mixture of clay and saw dust was made with the saw dust in various proportions of 0%, 5%, 10%, 15%, 20%, 30% and 40%. Each mixture was made thoroughly with a little addition of water to induce some plasticity and homogeneity of both the clay and saw dusts. The resulting mixtures (for each proportions of saw dust), were then compacted in a mounting press to obtain cylindrical shaped samples. These samples were then placed in the furnace and fired at 1000°C (held at the temperature for 1 hour) such that the saw dust burns off leaving some ash and pores. Series of tests were then performed on the fired samples. These tests include; cold crushing strength, bulk density, porosity, thermal shock resistance, permeability and thermal conductivity.

## Apparent Porosity

Test samples from each clay/saw dust blend (for varying proportions) were dried for 12 hours at 110°C. The dry weight of each fired sample was taken and recorded as D. Each sample was immersed in water for 6 hrs to soak and weighed while been suspended in air. The weight was recorded as W. Finally, the specimen was weighed when immersed in water. This was recorded as S. The apparent porosity was then calculated from the expression:

$$p = \frac{(W-D)}{(W-S)} \times 100 \qquad (1)$$

## Cold Compression Strength

Cold compression strength test is to determine the compression strength to failure of each sample, an indication of its probable performance under load. The shaped samples of clay blends with saw dust were dried in an oven at a temperature of 110°C, allowed to cool and then placed between two plates of the compression strength tester. This was followed by the application of a uniform load to it. The load at which a crack appears on the sample was noted and the cold compression strength (CCS) is calculated from the equation:

$$CCS = \frac{\text{Load to Fracture}}{\text{Surface area of sample}} \qquad (2)$$

## Thermal Shock Resistance

Each sample of the clay/saw dust blend was placed in an electrically heated furnace to attain the test temperature of 1000°C for over 3 hours. Each sample was then with- drawn from the furnace and held for 10 minutes. The procedure was repeated until an appearance of a crack was visible. The number of cycles necessary to cause a crack was recorded for each of the samples and taken as a measure of its thermal shock resistance.

## Bulk Density

The test specimens were dried at 110°C for 12 hours to ensure total water loss. Their dry weights were measured and recorded. They were allowed to cool and then immersed in a beaker of water. Bubbles were observed as the pores in the specimens were filled with water. Their soaked weights were measured and recorded. They were then suspended in a beaker one after the other using a sling and their respective suspended weights were measured and recorded. Bulk densities of the samples were calculated using the formula:

$$\text{Bulk density} = \frac{D}{(W-S)} \times 100 \qquad (3)$$

where: D = Weight of dried specimen, S = Weight of dried specimen suspended in water, and W = Weight of soaked specimen suspended in air

## Thermal Conductivity Test (Using Ibrahim's Thermal Conductivity Apparatus; the Steam Method)

Test specimens of area 0.002 m$^2$ and thickness of 0.01 m were cut from their respective mother bricks. The test specimens were tested one after the other. Each specimen was fixed between two copper discs provided within the equipment. A conical flask containing 50 ml of water was placed directly above and in contact with the specimen. A cork having a thermometer passing through it was used to cork the mouth of the conical flask. The thermometer reads the temperature changes of the water in the flask. The test section was then closed and the initial water temperature was noted. A second thermometer with the aid of a cork was inserted into the steam outlet pipe offset to monitor the steam temperature so as to ensure a constant base temperature of 100°C.

The boiler water outlet valve was closed while 5 litres of water was measured and poured into the boiler. The steam inlet valve, outlet valve, and condensate outlet valve were all closed. With the boiler cover remaining opened, the boiler was switched on. Immediately the water started boiling, the boiler cover was closed, while the steam inlet valve was fully opened with all the remaining valves closed. Timing commenced with the aid of a stopwatch immediately the steam inlet valve was opened. The testing was timed in each case for 10 minutes and final temperature of the water in the beaker was noted at the end of time. Each specimen was tested (experimented) twice and a mean temperature value was obtained. At the end of each experiment, the steam outlet valve was opened to release steam. The water in the boiler was refilled to maintain 5 litres and the experiment was repeated as stated above for other specimens. The value of the thermal conductivity, K for each of the specimen was determined using the formula [8, 9];

$$K = \frac{2.303 \frac{MCL}{A}[\log(\frac{\theta_1}{\theta_2})]}{t} \qquad (4)$$

where, K = thermal conductivity of the specimen, $T_l$ = temperature of steam (in Kelvin), $T_i$ = Initial temperature of water in conical flask, $T_4$ = Final temperature of water in conical flask, t = Time (s), A = Specimen area, (m$^2$), M = mass of water in conical flask (kg), C = specific heat capacity of water in conical flask (J/kgK), L = thickness of specimen (m), $\theta_1 = T_1 - T_i$, $\theta_2 = T_1 - T_4$.

## Qualitative and Quantitative XRD

The samples were prepared for XRD analysis using a back loading preparation method [10]. They were analysed using a PANalytical X'Pert Pro powder diffractometer with X'Celerator detector and variable divergence- and receiving slits with Fe

filtered Co-Kα radiation. The phases were identified using X'Pert Highscore plus software. The receiving slit was placed at 0.040°. The counting area was from 5 to 70° on a 2θ scale. The count time was 1.5 s. The temperature-scanned XRD data were obtained using an Anton Paar HTK 16 heating chamber with Pt heating strip. Graphical representations of the qualitative result follow below.

The relative phase amounts (weight %) were estimated using the Rietveld method (Autoquan Program) as reported by Young et al [11]. Amorphous phases, if present were not taken into consideration in the quantification.

## ⊞ Scanning Electron Microscopy

Morphology and microanalysis of raw clay and sintered ceramic composite samples were determined using ultrahigh resolution field emission scanning electron microscope (UHR-FEGSEM) equipped with energy dispersive spectroscopy (EDS). The pulverized clay samples/sintered ceramic composite samples were previously gold coated. The samples were studied using ultra-high resolution field emission scanning electron microscope (UHR-FEGSEM) equipped with energy dispersive spectroscopy (EDS). Particle images were obtained with a secondary electron detector.

## RESULTS AND DISCUSSION

Figures 1 to 5 show the effects of varying the amount of rice husk admixtures on various physical and mechanical properties of the ceramic samples. While Figure 6 (a) to (g) show the SEM images of the various sample revealing their relative pores.

Aramide et al. 2014 [12] characterized and discussed the Iseyin clay sample with some other clay samples from other part of the country. They carried out x-ray diffractometry analysis and scanning electron microscopy of the raw clay sample used in this work. From their report it can be seen that the Iseyin clay contains 39.71% kaolinite and 39.55% quartz (which are refractory materials).

## ⊞ Effect rice husk admixture on the bulk density of the ceramic sample

Figure 1 show the effect of varying the amount of rice husk admixture on the bulk density of the ceramic sample. From the figure it is observed that the bulk density of the sample reduced with increase in the rice husk admixture. It is is observed that the bulk density of the sample was 2.42 g/cm$^3$ when there was no rice husk incorporated into the sample. However, when 5% rice husk was incorporated into the sample, the bulk density reduced to 1.34 g/cm$^3$. Further increase in the rice husk admixture to 10% leads to further reduction in the bulk density to 1.19 g/cm$^3$. As the rice husk admixture was increased to 15% the bulk density is observed to reduce further to 1.076 g/cm$^3$. Furthermore, increasing the rice husk admixture content to 20% leads to the bulk density of the sample being decreased to 1.04 g/cm$^3$. This is because when the sample is fired at the sintering temperature of 1000°C, all the rice husk is burnt off from the matrix of the ceramic leaving empty pores within the ceramic. This can be observed in the Figure 6 (a) to (g); it can be estimated from

the figure that the pore volume in each of the micrographs increased with the least (very little) in Figure 6 (a) and the highest pore volume in Figure 6 (g). The more the rice husk admixture added to the sample, the more the pores that will be left after sintering. This is the reason for the reduction in the bulk density of the sample with increased rice husk admixture [5, 13].
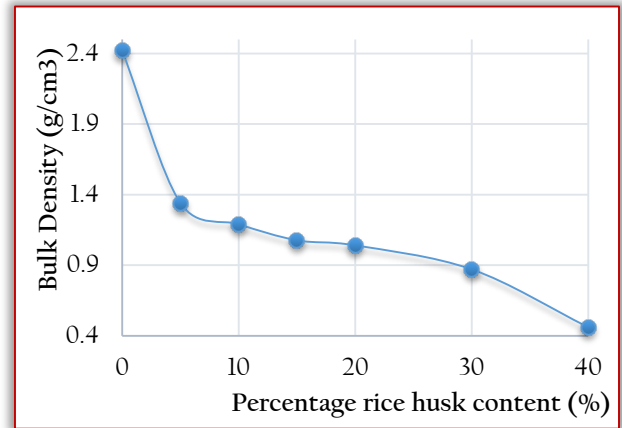


Figure 1. Effects of percentage rice husk content on the bulk density of the samples
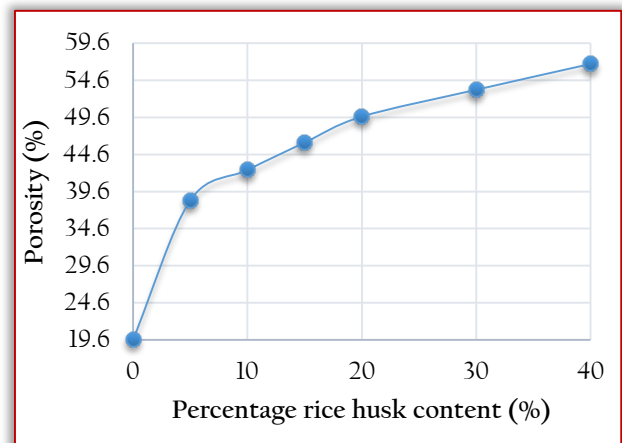


Figure 2. Effects of percentage rice husk content on the porosity of the samples

## ⊞ Effect rice husk admixture on the porosity of the ceramic sample

Figure 2 shows the effects of rice husk admixture on the porosity of the sintered ceramic samples. From the figure, it is observed that the porosity of the ceramic samples increases with increase in the rice husk admixture. The porosity of the sample was 19.65% when it rice husk admixture was 0%; it increased to 38.4% as the rice husk admixture increased to 5%. Moreover, it is observed that the porosity of the sample increased further to 42.5% as the rice husk content was increased to 10%. Further increase in the rice husk admixture to 15% is observed to lead to increase in the porosity of the sample to 46.2%. A porosity of 49.7% is observed for the sample with 20% rice husk admixture, further increase in the rice husk admixture content to 30% is observed to result in the porosity being increased to 53.32%. Lastly, the porosity of the sample is observed to increase further to 56.8% with increase in the rice husk admixture to 40%. This is because

when the samples are sintered at the 1000°C, the combustible rice husk content got burnt off thereby leaving empty pores within the ceramic matrix. As earlier explained, the more the rice husk content, the more the empty pores that would be left after sintering [13, 14, 15].

## ⊡ Effect rice husk admixture on the thermal conductivity of the ceramic sample

Figure 3 shows the effect of the rice husk admixture on the thermal conductivity of the ceramic samples. From the figure, it is observed that the thermal conductivity of the sintered ceramic samples decreases with increase in the rice husk admixture. It could be observed that the thermal conductivity of the sample was 0.24 W/m/K when the rice husk admixture was 0%; it then reduced to 0.19 W/m/K as the rice husk admixture was increased to 5%.
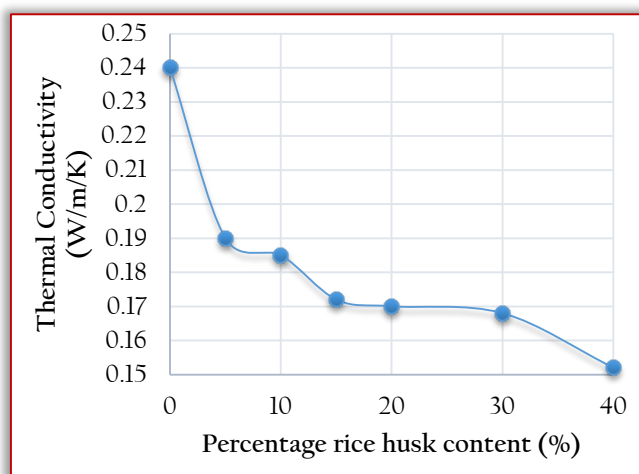


Figure 3. Effects of percentage rice husk content on the thermal conductivity of the samples

Moreover, further increased in the rice husk admixture to 10% is observed to lead to further reduction in the thermal conductivity of the sample to 0.185 W/m/K. When the rice husk admixture was 15% the thermal conductivity is observed to be 0.172 W/m/K, as the rice husk content increased to 20% the thermal conductivity is observed to reduce to 0.17 W/m/K. Moreover, increase in the rice husk admixture to 30% is observed to lead to further reduction in the thermal conductivity of the samples to 0.168 W/m/K. This is majorly because the porosity of the samples increases with the increase in the rice husk admixture.

Increased porosity means increased percentage pores within the ceramic matrix which insulates the flow of heat through conduction from the hotter part to the cold part [5, 13, 15].

## ⊡ Effect rice husk admixture on the thermal shock resistance of the ceramic sample

Figure 4 shows the effect of the percentage rice husk admixture on the thermal shock resistance of the ceramic samples. From the figure it is clearly observed that the thermal shock resistance of the samples reduces with increase in the rice husk admixture. The thermal shock resistance of the sample with 0% rice husk admixture was observed to be 26 cycles. Addition of 5% rice husk admixture lead to the reduction of the thermal shock resistance to 18

cycles. It was also observed that the thermal shock resistance of the sample reduced to 14 cycles as the rice husk admixture was increased to 10%. Furthermore, increase in the rice husk admixture to 15% lead to further reduction in the thermal shock resistance of the sample being reduced to 11 cycles.
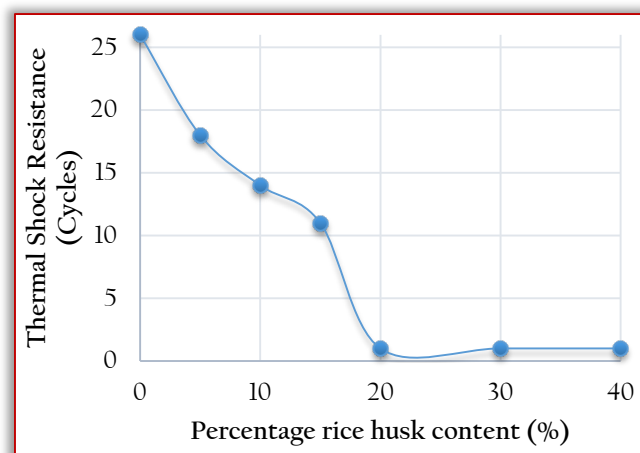


Figure 4. Effects of percentage rice husk content on the thermal shock resistance of the samples

Beyond this point, further increase in the rice husk admixture of the sample lead to the sample possessing the lowest value of thermal shock resistance of 1 cycle. The explanation that could be given to this is that the shapes of the pores have great influence on the mechanical properties of the ceramic. A pointed end pore will aggravate any form of stress within the ceramic body. That is it will have a multiplying effect on the stress (thermal or mechanical), thereby making the ceramic to fail through propagation of intrinsic cracks at much lower stress than it should have failed [16, 17].

## ⊡ Effect rice husk admixture on the cold crushing strength of the ceramic sample

Figure 5 shows the effect of rice husk additive on the cold crushing strength of the ceramic sample. From the figure, it can be observed that the cold crushing strength of the samples decreases with increase in the rice husk admixture. It is observed that the cold crushing strength of the sample with 0% rice husk additive is 14.5 N/mm$^2$, it declined slightly to 13.7 N/mm$^2$ when the rice husk admixture was increased to 5%. Moreover, the cold crushing strength is observed to decline sharply to 9.7 N/mm$^2$ when 10% rice husk was incorporated into the sample. Furthermore, additional increase in the amount of rice husk additive into the sample (to 15%) leads to further reduction in the cold crushing strength of the sample (5.7 N/mm$^2$).

The cold crushing strength of the sample is observed to reduce to 4.9 N/mm$^2$ as the rice husk admixture is increased further to 20%. It was earlier explained that when the samples were fired at the sintering temperature, the rice husk content, being combustible, is burnt off, leaving voids/pore within the ceramic matrix.

The empty voids in the ceramic matrix makes the samples to contain less matter per unit surface area; this implies that increased rice husk admixture means less matter would be available within the sample to bear the applied load. In other

word, less matter per unit surface area means that the samples would (more porous) lighter with increased rice husk admixture. Porous bricks are lighter, hence they cannot carry heavy load [18].
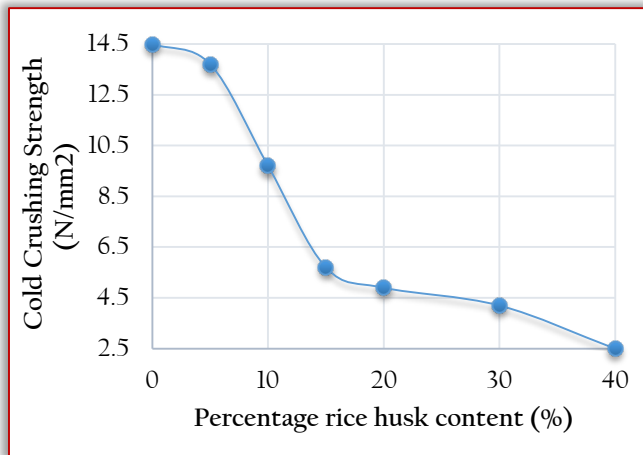


Figure 5. Effects of percentage rice husk content on the cold crushing strength of the samples

From Figure 6, the scanning electron microscope of the various samples is shown.

Figure 6 (a) shows the SEM image of the sample with 0% rice husk admixture, (b) shows the SEM image of the sample with 5% rice husk admixture, (c) shows the SEM image of the sample with 10% rice husk admixture, (d) shows the SEM image of the sample with 15% rice husk admixture, (e) shows the SEM image of the sample with 20% rice husk admixture, (f) shows the SEM image of the sample with 30% rice husk admixture and (g) shows the SEM image of the sample with 40% rice husk admixture. The figure shows relative pores on each of the samples.
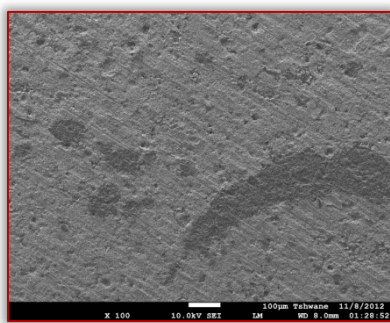


(a)
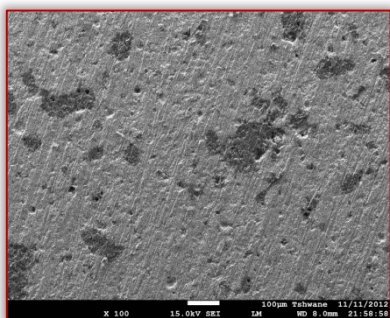


(b)
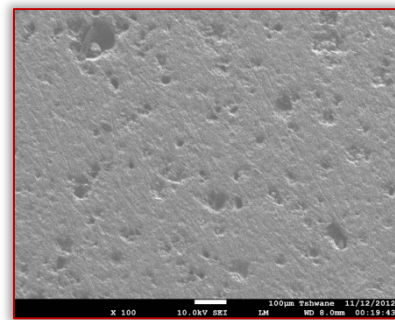


(c)
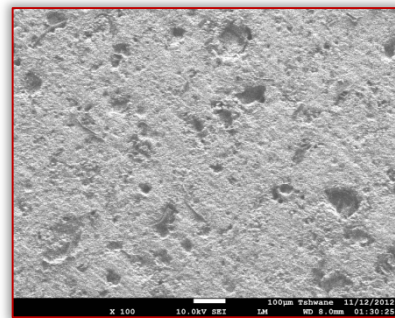


(d)
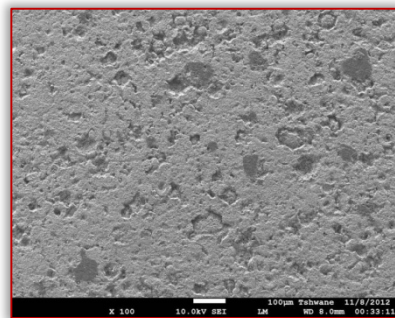


(e)
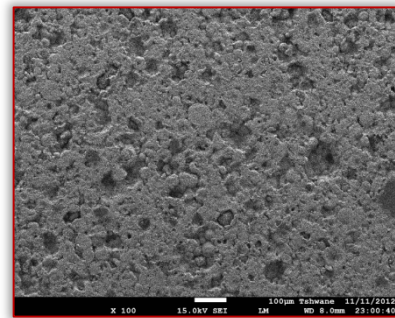


(f)
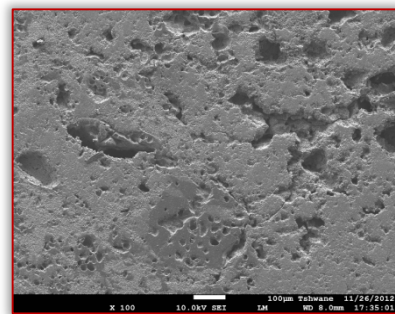


(g)

Figure 6. Scanning electron microscope images of the various sintered ceramic samples: (a) 0% rice husk, (b) 5% rice husk, (c) 10% rice husk, (d) 15% rice husk, (e) 20% rice husk, (f) 30% rice husk, (g) 40% rice husk

## CONCLUSION

Increase in the rice husk admixture in the sample leads to increase in the porosity of the sample. This also resulted in the reduction in the bulk density, cold crushing strength, thermal shock resistance and thermal conductivity of the sintered ceramic samples. The choice of optimum parameter for application of the sintered ceramic sample depends on the service condition the sample will meet in application. For a service condition where the ceramic will be in contact with molten metal or slag, sample with 0% rice husk admixture would be optimum. But for efficient insulation in a heat treatment furnace sample with 40% rice husk admixture would be optimum.

## ACKNOWLEDGEMENT

## REFERENCES

[1] Aramide Fatai Olufemi, Effect of Firing Temperature on Mechanical Properties of Fired Masonry Bricks Produced from Ipetumodu Clay, Leonardo Journal of Sciences, 11, 21 (2012) 70-82.

[2] Aramide Fatai Olufemi, Effects of sintering temperature on the phase developments and mechanical properties ifon clay Leonardo Journal of Sciences, 14, 26 (2015) 67-82.

[3] Chaouki Sadik, Abderrahman Albizane1, Iz-Eddine El Amrani, Production of porous firebrick from mixtures of clay and recycled refractory waste with expanded perlite addition J. Mater Environ. Sci. 4, 6 (2013) 981-986

[4] Sutcu M., Akkurt S., The use of recycled paper processing residues in making porous brick with reduced thermal conductivity, Ceram. Inter. 35, (2009) 2625-2631.

[5] Aramide Fatai Olufemi, Production and Characterization of Porous Insulating Fired Bricks from Ifon Clay with Varied Sawdust Admixture Journal of Minerals and Materials Characterization and Engineering, 11, (2012) 970-975.

[6] M. Sutcu, S. Akkurt, A. Bayram, U. Uluca, Production of anorthite refractory insulating firebrick from mixtures of clay and recycled paper waste with sawdust addition Ceram. Int. 38, (2012) 1033-1041.

[7] M.A. Hassan, A.M. Yami, A. Raji, M.J. Ngala, Enhancement of Refractory Properties of Blended Clay with Groundnut Shell and Rice Husk Additives International Journal of Engineering and Science (IJES), 3, 8 (2014) 40-44.

[8] I. Ibrahim, "Design, Construction and Testing of Thermal Conductivity Equipment," B.Eng. Thesis, Federal University of Technology, Yola (2005).

[9] B. I. Ugheoke, E. O. Onche, O. N. Namessan, G. A. Asikpo, Property Optimization of Kaolin-Rice Husk In- sulating Fire-Bricks Leonardo Electronic Journal of Practices and Technologies, 5, 9 (2006) 167-178.

[10] R. Kleeberg, T. Monecke, S. Hillier, Preferred orientation of mineral grains in sample mounts for quantitative XRD measurements: How random are powder samples? Clays and Clay Minerals, 56, 4 (2008) 404-415.

[11] R. A Young, A. Sakthivel, T. S. Moss, C. O. Paiva-Santos, Rietveld analysis of X-ray and neutron powder diffraction patterns, Georgia institute of technology, Georgia (1994).

[12] F. O. Aramide, K. K. Alaneme, P. A. Olubambi and J. O. Borode, Characterization of some clay deposits in South West Nigeria, Leonardo Electronic Journal of Practices and Technologies, 13, 25 (2014) 46-57.

[13] J. U. Manukaji, Effects of groundnut shell additive on the insulating properties of clay samples from Kogi State Nigeria, American Journal of Engineering Research (AJER), 2, 4 (2013) 12-15.

[14] A. R. Chesti, "Refractories: Manufacture, Properties, and Applications," Prentice-Hall of India Private Limited, Delhi (1986) 70-77.

[15] L. P. Li, Z. G. Wu, Z. Y. Li, Y. L. He and W. Q. Tao, Numerical thermal optimization of the configuration of multi-holed clay bricks used for constructing building walls by the finite volume method, International Journal of Heat and Mass Transfer, 51, 3 (2008) 3669-3682.

[16] W. Schulle and E. Schlegel Ceramic, Monographs-Handbook, Verslag Schmid (1991) 1-6.

[17] A. Jonker, Insulating Refractory Materials from Inorganic Waste Resources, Ph.D. Thesis, Tshwane University of Technology, Pretoria (2006).

[18] F. H. Norton, Refractories, 4th Edition, McGraw-Hill, New York (1968) 92-95.

[1.]Ferenc FARKAS, [2.]József GÁL,[3.]István Tibor TÓTH, [4.]István Péter SZABÓ,
[5.]István BÍRÓ, [6.]Antal VÉHA, [7.]Tamás MOLNÁR

# MONITORING THE SET UP AND USE OF ELECTRIC CARS AND CHARGING POINTS IN SZEGED

[1–7.]University of Szeged, Faculty of Engineering, Szeged, HUNGARY

**Abstract:** In our wider and narrower environment, due to the significant developments in the automotive industry, increasing attention is trending towards electric powered vehicles. Trams and trolley buses have been running in Szeged for many decades, and recent years in self–propelling version. At the same time the population's buying activity of electric powered cars is increasing, which on the one hand causes favorable environmental effects in the city, however it sets out new challenges to promote their decent operation. Does it mean changing or complementing traditional filling points or creating a totally new system of energy supply? With our survey we will measure the population's knowledge of this, we will ask their opinion and we will search answers to the emerging challenge. Our investigation is a part of a project (H2020) run for several years, which is to reveal opportunities for public transport and personal transport to become electric.
**Keywords:** electric cars, electric charging, Szeged, environment protection

## INTRODUCTION

The University of Szeged, Faculty of Engineering (together with the Szeged Transport Company) participate in a HORIZON2020 tender called „ELIPTIC" (Electrification of Public Transport in Cities) research–development project, which started on 1 June 2015 and ends on 31 May 2018.

The tender programme has the object to test the battery–driven trolley buses in battery mode and to extend the trolley bus lines of trolley–wire without configuration, taking advantage of the possibility of self–propelling mode. With the use of self–propelling, namely both trolley–wire and battery–driven trolley buses more districts of Szeged can be covered, where cannot get by public transport at night. (1) For the self–propelling mode in Szeged Transport Company's 13 IKARUS–SKODA type trolley buses 575 kg weight Li–based batteries provide the energy, which charge up on the trolley–wire section, but when braking they are able to save the kinetic energy, so the vehicle's propellant consumption decreases. (2)

The driving and braking of the trolley buses are insured by a 248 kW (337 horsepower) asynchronous electric motor. The modern drive system transforms the 600V direct current trolley–wire voltage for the electric motor into triphase alternating current and it charges the direct current batteries. The self–propelling mode – among others – made the spectacular use of 'overhead connectors' necessary for automatic connection of pantographs (to the trolley–wire), which were applied succesfully and for the first time in the Szeged network.

The driver can control the disconnection of the pneumaticly operated pantographs with the press of a button (at the end of the trolley–wire section), after that the pantograph will be pulled down and fixed in a few seconds.

The batteries need one hour to be fully recharged and the vehicles can go in battery mode more than 7 km at full weight. However, the trolley buses could reach the double of this distance in an optimum case. The average consumption of trolley buses is 200 – 250 kWh/100km, which greatly depends on the demand of heating and air conditioning. This number is significantly more favourable for diesel buses (The diesel fuel costs are 30–40% of the electric cost). The modern trolley buses with lower propellant consumption produce less noise pollution than diesel buses, and they naturally do not encumber the urban air with harmful emissions. The 13 IKARUS–SKODA self–propelling trolley buses will redeem the burning of 400,000 liters of gasoline in the city in one year, so this will significantly contribute to clean air, and through this keeping our health. (3)

One of the main aims of the Eliptic project is to explore what kind of extra services the hybrid trolleybuses can provide in Szeged, and how they can contribute sustainable public transport, thereby shaping and developing the attitude of the population in this area.

Connected to the application's topic,with our survey we measured what the population know about electric vehicles and the filling points, asked their opinion, and searched for an answer to the reveled challges.

In September 2017 University of Szeged, Faculty of Engineering cooperated with university's students and they did the questionnaire survey among the population. The survey's aim was to explore the travel habits, as well as the general awareness and expectations about electric cars and filling points, furthermore the experiences, and the public support of electric transport.

To sum up, the most important influential factors in the use of electric vehicles according to theoretical research:

» Demographic attributes: (4), (5)
  — sex,
  — age,
  — place of residence.
  — number of vehicles per haushold.
» Traffic attributes:
  — number of vehicles per haushold,
  — average daily distance,
  — proportion of long distance travel,
  — parking attributes.
» Service attributes:
  — range of available services,
  — wait–in–line time.

## QUESTIONNAIRE SURVEY METHOD

We did a personal questionnaire survey during our research to explore the habits of current and potential, in the future electric car users in connection with traffic and charging, demands and preferences related to electro–mobility.

The current vehicles users and the potential electric car customers belong to the questionnaire's focus group.

Questions of the questionnaire covered the following topics (7):

  — Personal data (sex, age, place of residence).
  — Current vehicle traffic customs.
  — Willingness to buy electric cars.
  — Charging requirements (e.g.: services, charging time).

The designation of the topics was made based on the international and national professional literature and the own experience. We asked 20 questions in the questionnaire, because the reliability of the answers probably deteriorates over 25 questions [6]. 311 people (182 men and 129 women) participated in the questionnaire survey, and the survey was done in a shopping mall in Szeged. The questions included simple choice questions with two or multiple possibilities and the respondents could give answers evaluable on a scale. Apart from closed questions, open questions assured additional useful rematch.

## DATA PROCESSING BASED ON QUESTIONNAIRE

The great majority of responders are middle–aged, graduated (48%) living in shire–towns.

Among vehicle usage habits the first to be asked in the survey was a car usage (Diagram 1).

Predominantly (72%) of the responders used car for daily commuting (at most 10 km) while (26%) used it for commuting (at most 100 km ) and only a few times yearly they cover more than 600 km daily .

Following this we wanted to know how much kilometers do the motorists cover on daily basis.

Based on this survey 31% of the responders cover only a few times more than 150 kilometers daily on yearly bases, 29% of them cover this range only a few times monthly respectively while 2% of them cover this range daily.
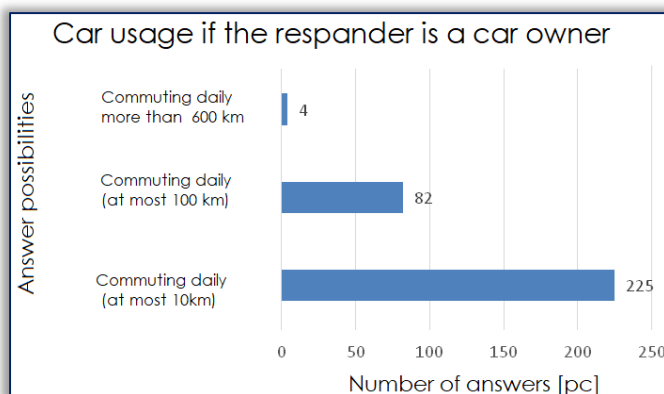


Diagram 1: Car usage habits
Source: Eliptic according to survey, 2017
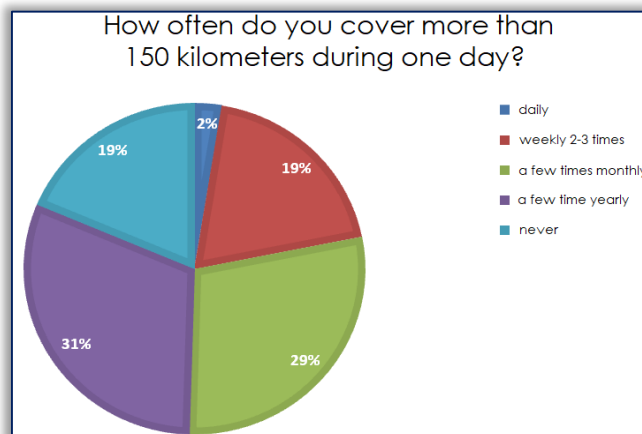


Diagram 2: Daily covered ranges
Source: Eliptic according to survey, 2017

In diagram 3 we were interested in consumer awareness of different engine propellants.

A bit unexpectedly the responders are better informed of electric propellant (90%) than biodiesel (73%), bioethanol (50%) respectively, or the LPG (63%), CNG (42%) respectively.
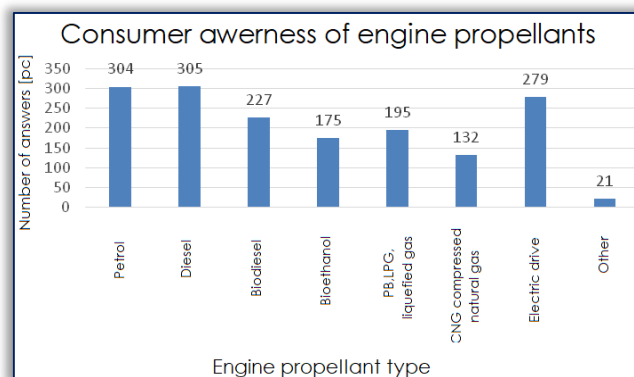


Diagram 3: Consumer awerness of certain engine propellants
Source: Eliptic according to survey, 2017

Following this in our survey in diagram 4 we were curious about consumer awareness of certain electric car brands. It is not a mere coincidence that the most well–known electric car brand is Tesla (34%), followed by Japanese brands such as Nissan (20%), Toyota (17%), Lexus (8%) and then the German brands BMW (28%), VW (9%), Mercedes Benz (4%) according to our survey.
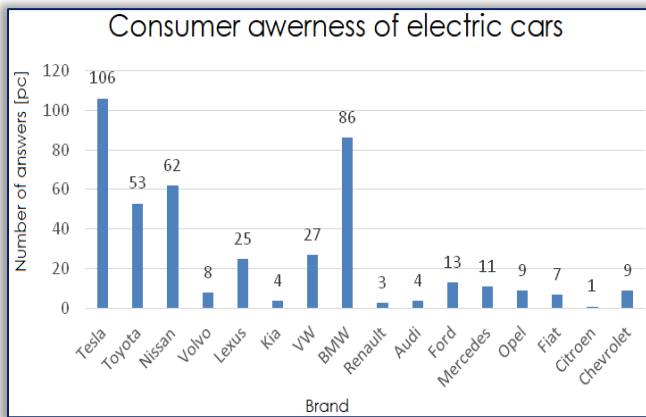
Diagram 4: Consumer awerness of electric car brands
Source: Eliptic according to survey, 2017

In diagram 5 you can see the driving possibilities of electric cars. The great majority of people taking part of in our survey (63%) have never driven an electric car, however, the participants would be glad to do so, while (18%) rules out such a possibilities. Among those who have already driven an electric car (20%) there are four times more participants who liked it than those who did not.
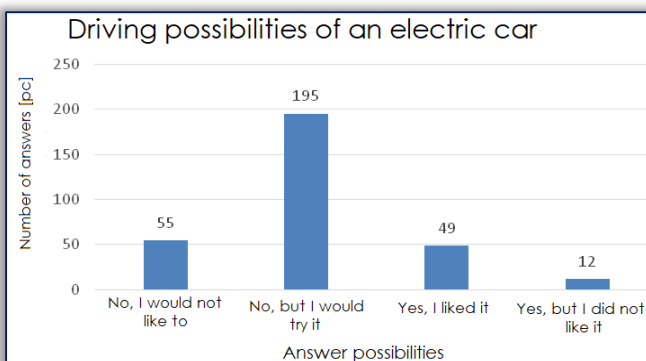


Diagram 5: Driving possibilities of an electric car
Source: Eliptic according to survey, 2017

In our survey we asked the participants of their willingness to buy an electric car. Predominantly the participants do not intend to buy an electric car within three years and majority of them (47%) is willing to pay for an electric car at most 4 million Forints. (Diagram 6) According to this they would rather buy an used electric car than buy a new one. In connection with this, a question may come up if the potential buyers are aware of the necessary service cost that can be rather high. It is to be noticed that the brand new, purely electric car is some 3 million Forints more expensive than a traditional principal based car, having the same technical parameters.

Nowadays, among electric cars we can find more types that are capable of covering 250 kilometers with a single charge but the range of above 150 kilometers can be regarded as usual. At the same time the range depends on the car load, nature of usage, speed and weather conditions. According to diagram 7 the half of the interviewed people expected an average range of 150–200 that is in consonance with range of today's purely electric cars.
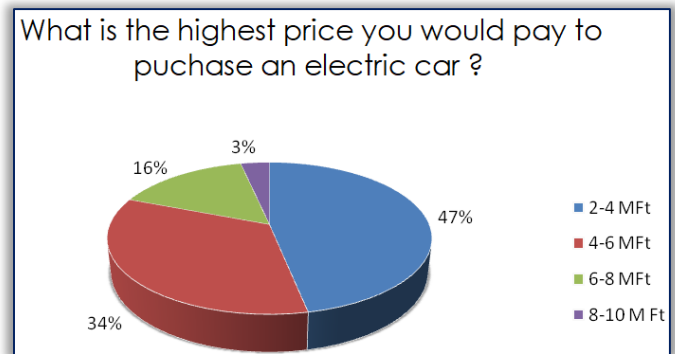


Diagram 6: The willingness of buying an electric car
Source: Eliptic according to survey, 2017
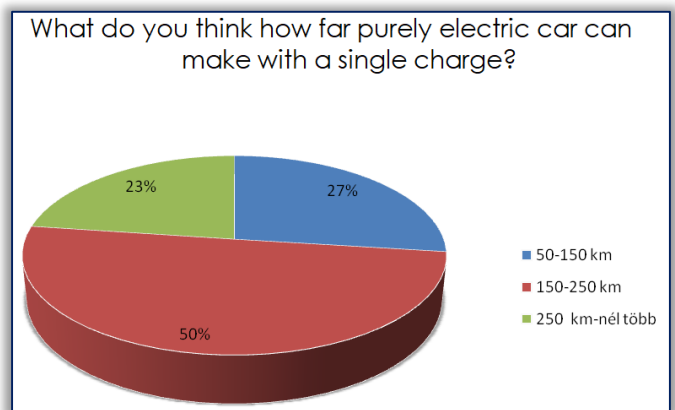


Diagram 7: Range of electric car
Source: Eliptic according to survey, 2017

In our study we regarded as a focal point to ask opinions about installation of electric car recharging pionts, recharging frequency and time.

According to academic literature, users of electric cars predominantely recharge the vehicles at their workplace and park and ride lots and petrol stations. However, recharging points at deparment stores, at public officies and stations' parking lots, as well. (8)(9)

The great majority of interviewed people regards useful installation of the recharging points in the vicinity of the following places: petrol stations ( 31%), deparmtent stroes, farmers market (25%), park and ride lots (13%) and around stations and turistical destinations, respectively.
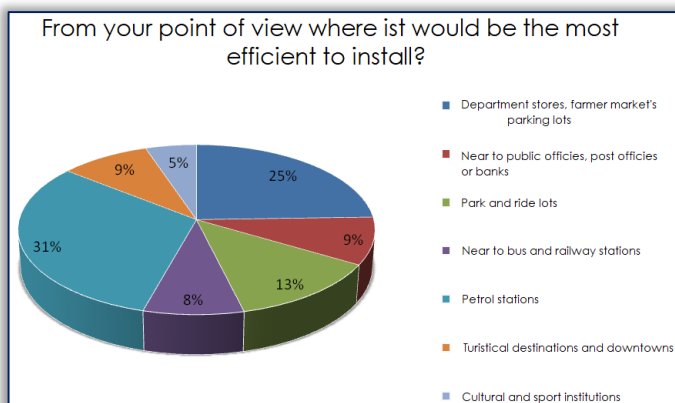


Diagram 8: Possible locations of charge points installment
Source: Eliptic according to survey, 2017

Nowadays the fast charger output is usually 60 kW and in the near future the expected output is 150 kw or even more rapid fast chargers are to be expected. Owing to this fact the recharging time is expected to be reduced, however, this is to be balanced by the even growing capacity of the batteries. It becomes important that the services during recharging time should fit the daily routine activities. In our country an electric vehicle is usually 2.57 times recharged on daily basis. This fits with foreign observations according to which vehicle is being recharged on driver occasions but with shorter intervals. As you can see on diagram 9 according to our survey 51% of the interviewed people use once the charge points while 30% of them used them four times a week.
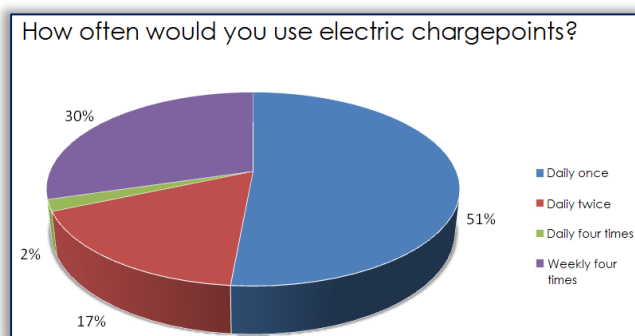


Diagram 9: Usage frequency of charge points
Source: Eliptic according to survey, 2017

We also asked the operators how much time they would spend recharging their electric cars at a petrol station besides a motorway. According to diagram 10, 52% of the interviewed would spend 15 minutes, 27% of them would spend 5 minutes recharging their cars.
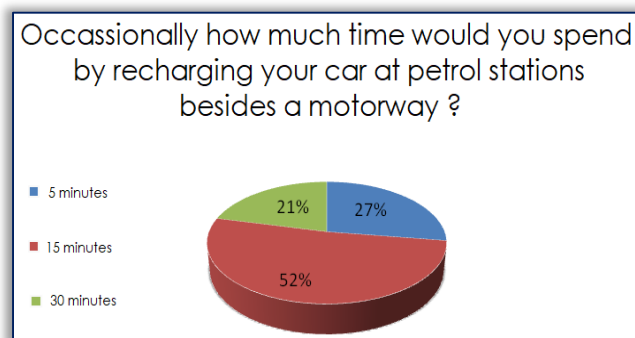


Diagram 10. Charging time willingness
Source: Eliptic according to survey, 2017

In the questionnaire we sought answer to that electric car owners use those for what distance on a daily basis.

As seen on the 11th diagram, the answers state that the users big portion (50%) uses it for a maximum distance of 25 km, 30% of them uses it for 25–50km and only 2% of the respondent uses it for more than 100 km in a day.

Henceforward the respondents could give an answer to that for them, how important is Szeged's air purity? Based on the processing of the 12th diagram, Szeged's population finds it very important (68%) and important (20%) securing the purity of Szeged's air. Naturally we have to place this air pollution issue in a complex social problem circle.
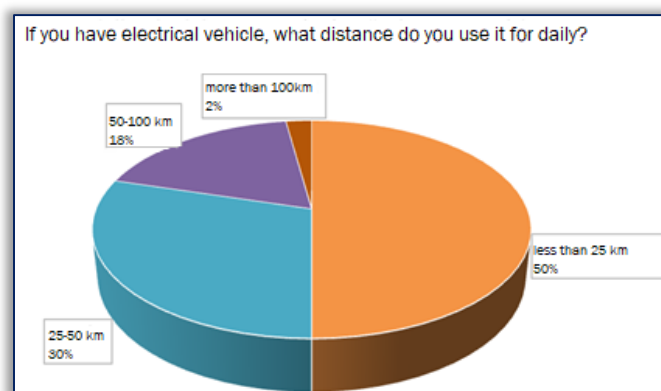


Diagram 11. Electric car daily average range
Source: Based on ELIPTIC survey, 2017
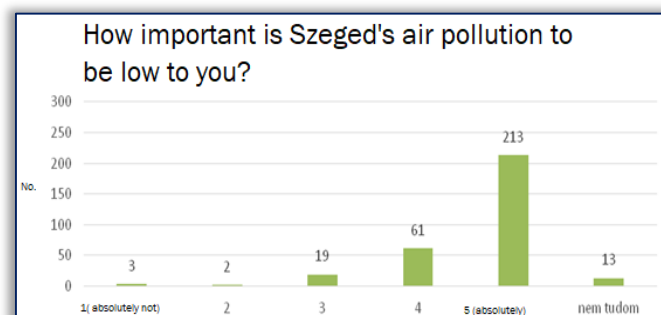


Diagram 12. The importance of air pollution in Szeged
Source: Based on the ELIPTIC questionnaire, 2017

On the apropos of the 13th diagram we asked that the respondents on what degree they agree on planting more charger points. Processing the answers it is clear that comprehensively (87%) they support the expansion of the charger network.
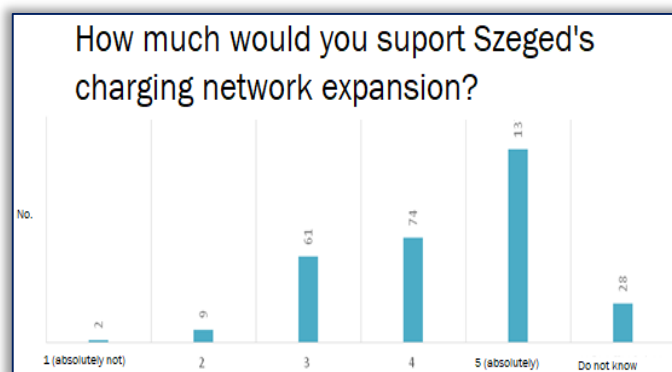


Diagram 13. Charging network expansion support
Source: Based on the ELIPTIC questionnaire, 2017

Nowadays there is a significant number of news and programme attends with the expansion of the electric vehicular instruments and attendant units which enjoy governmental priority. Following this we also asked about that according to the respondents what factors would advance the growth of the number of e–vehicles in our country. (Diagram 14) The answers suggest that they think financially supporting it more (70%), with expanding the charging network significantly (48%) and by expanding the user allowance (31%) the domestic e–driving spreading would be feasible.
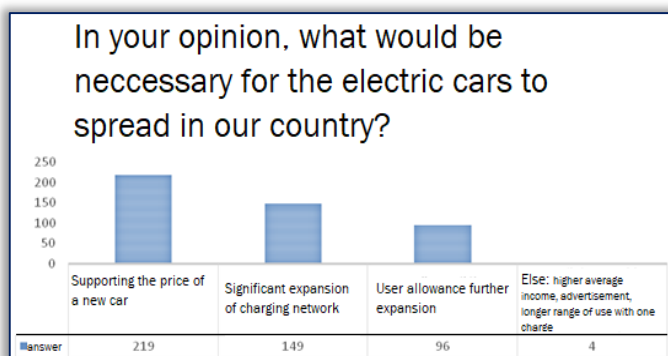
Diagram 14. Electric vehicles spreading conditions
Based on the ELIPTIC questionnaire, 2017

## SUMMARY

Szeged's community traffic's examination in the context of ELIPTIC project comes with several staged questionnaire. During the first stage, in 2015 October 10th, in stations and sometimes in vehicles with a 465 participant sample. After a fast evaluation a targeted passenger group examination was configured, where based on experiences the questions were swapped or modified. From the present questionnaire survey's lessons the question group regarding passenger comfort should be highlighted, which can be interpreted for the whole network. Especially important that how much a modern Ikarus–Skoda trolleybus is a present in the passenger, citizen's minds, common sense that is, with all the externals in consideration of environmental protection. Instructive survey outcomes were achieved, which gives an adequate base for further examinations.

Present questionnaire's goal was investigating the travelling habits as well as the general currency and expectations of electric driving and charging points, the ventilation of incidental experiences, and with the estimation of social support of electric travelling.

Examining the travelling habits it can be established that for most of the surveyed, using the electric vehicles could be a real alternative. However, the majority of the respondents are not considering buying new electric vehicles in the near future because of the relatively low range, the few charging points and the high purchase price.

Because of the significant price differential between the new traditional and electric cars, it is more expected that the demand for used hybrid electric cars will grow first and only after that will the demand for purely electric cars grow, since the problem of short range only affects these.

Based on the expected frequency of charging, the most valuable charging points are the gas stations next to highways, supermarkets, market parking's and the P+R parking.

Based on the processing of the answers Szeged's population finds it very important or important protecting the purity of air, and expansively supports the expansion of the charging network in the city.

The study also highlighted that supporting more the price of a new electric car, the relevant expansion of the charging network and the further growth of user discounts, the number of potential buyers of electric cars.

## Acknowledgement
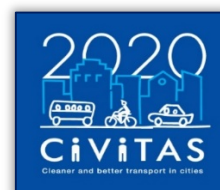
## References:

[1] Gál J. – Tóth I.T. – Véha A. – Keszthelyi–Szabó G.: Hibrid trolikkal a kulturális és szakmai programokra

[2] Gál J. – Tóth I. T.: Közösségi közlekedés színvonalának utas elégedettségi vizsgálata – előfelmérés Szegeden

[3] Náday A.–Újhelyi N.: ] Kiemelt önjárások 2016–ban, Összefoglaló anyag, SZKT

[4] Xi, Xiaomin – Sioshansi, Ramteen – Marano, Vincenzo: Simulation–optimization model for location of a public electric vehicle charging infrastructure, Transportation Research Part D 2013/22 60–69 p.

[5] Philipsen, Ralf – Schmidt, Teresa – Ziefle, Martina: A Charging Place to Be – Users' Evaluation Criteria for the Positioning of Fast–charging Infrastructure for Electro Mobility, Procedia Manufacturing 2015/3 2792 – 2799 p.

[6] Bliemer, Michiel C. J. – Rose, John Matthew: Efficiency And Sample Size Requirements for Stated Choice Experiments, Transportation Research Board 88th Annual Meeting, Washington DC January 11–15, 2009

[7] Csiszár Cs.–Csonka B.: Elektromos járművek töltő-infrastruktúrájának kiépítéséhez a felhasználói elvárások feltárása
https://www.researchgate.net/publication/315767310

[8] De Gennaro, Michele – Paffumi, Elena – Martini, Giorgio: Customer–driven design of the recharge infrastructure and Vehicle–to– Grid in urban areas: A large–scale application for electric vehicles deployment, Energy 2015/82 294–311 p.

[9] Andrenacci, Natascia – Ragona, Roberto – Valenti, Gaetano: A demand–side approach to the optimal deployment of electric vehicle charging stations in metropolitan areas, Applied Energy 2016/182 39–46 p.

[10] Morrissey, P., Weldon, P., O'Mahony, M. (2016) Future standard and fast charging infrastructure planning: An analysis of electric vehicle charging behaviour. Energy Policy 89: 257–270. p.

# Fascicule 3
## [ July - September ]
## t o m e
## [2018]  XI

ACTA Technica CORVINIENSIS
BULLETIN OF ENGINEERING

**ISSN: 2067-3809**

[1.]Vlado MEDAKOVIĆ, [2.]Bogdan MARIĆ

# A MODEL OF MANAGEMENT INFORMATION SYSTEM FOR TECHNICAL SYSTEM MAINTENANCE

[1,2.] University of East Sarajevo, Faculty of Mechanical Engineering East Sarajevo, East Sarajevo, BOSNIA & HERZEGOVINA

**Abstract:** Technical systems for production are increasingly automate, which means that they have to work reliably. Therefore, the rapidly expanding concept of maintenance, where people would say that maintaining a process that allows the management of the technical condition and reliability during the entire life cycle of the system. Traditionally, maintenance has been considered as a support function, non-productive and not a core function adding little value to business. However it has been noticed that many manufacturing industries have used various approaches to improve maintenance effectiveness. An analysis of the problem of machines and industrial systems maintenance as well as maintenance strategies and maintenance management process is presented in this paper. Furthermore, a development process of traditional and modern maintenance management information system is given. The possibility of development maintenance management, applying decision support systems and expert systems, are presented, at the end.
**Keywords:** Maintenance, Information system, Decision Support Systems, Expert systems

## INTRODUCTION

Maintenance of technical systems must ensure that all technical systems fulfill their function with as little downtime as a longer life cycle and with less maintenance costs. Surroundings, in which the maintenance system builds, is certainly a production, business or other process or system (housing facilities, communication etc.).

In the work [9] is benchmarking of real estate performance is a commonly used tool in the efficient and sustainable maintenance management of existing facilities. Performance needs to be measured and monitored to support stakeholders' core business and maintenance strategies. Many of the performance indicators used to measure real estate are based on the area of the maintained property.

Maintenance can be defined as a set of actions which are carried out to replace, repair and service an identifiable set of manufacturing components, so that the plant continuous to operate at a specified level of availability for a specified time. The main objective of Maintenance is to maximize the availability of machinery and equipments for production. Preserve the values of the plant, machinery or equipment by minimizing wear and deterioration. Accomplish the above goals most economically on a long term basis. By systematic maintenance it is possible to achieve substantial savings in money, material and manpower as every effort is directed towards avoiding catastrophic failures [8].

High-speed technological innovation combined with severe competition shortens the equipment life cycle and puts equipment under higher stress. In order to deal with this problem, a company's strategic investments in production equipment should not only consider cost and capacity, but also technology trends, flexibility, etc.

Another important aspect is maintenance. Proper maintenance helps to keep the life cycle cost down and ensures proper operations and smooth internal logistics. The decision on the required maintenance concept and a thorough and easily accessible technical knowledge are crucial here [13].

The growing importance maintenance of technical systems in the last decades of the twentieth and beginning of the twenty-first century is related to the mass automation, computerized and robotization in all areas of industry and requirements for reliable operation of such systems as a prerequisite for the competitive ability of the organization. In some the industry has long been the number of employees in maintenance is greater than the number of employees in production, at the same time and with higher level of professional engineering knowledge.

Furthermore, next to the energy costs, maintenance costs can be the largest part of any operational budget. Yet, the main question faced by the maintenance management, whether its output is produced more effectively, in terms of contribution to company profits and efficiently, in terms of manpower and materials employed, is very difficult to answer [2].

Over time, the role of maintenance in the manufacturing sector has become increasingly important. Globalized markets are forcing organizations to compete not only in quality or price, but also in technology, reduced lead times, innovation, reliability and information technology[4].

In this information age, data has become one of the most important resources to organizations. The effective and efficient management of large quantities of data is a common problem found in many industries.

The study [7] is carried out to design, development and implementation of a computerized maintenance management information system (CMMIS) according to the requirements of a medium scale industry, with an intention

to assist the maintenance and other activities of the industry in an organized manner.

Reviews overall models for maintenance management from the viewpoint of one who believes that improvements can be made by regarding maintenance as a "contributor to profits" rather than "a necessary evil". The reasons why maintenance is such a "Cinderella function" are largely historical and can mostly be overcome by new information technology (IT) and its falling cost [10].

The paper [11] deals with the topic of facility management focusing on maintenance area and its importance for increasing company competitiveness. The importance of functional company facility management has risen dramatically in recent years. The reason for this is the increased pressure on cost reduction and additional value to the core business of the enterprise. The paper introduces a current theoretical literature-based framework for this topic in order to examine and analyze the supporting activities and processes connected with production facilities and maintenance particularly.

Maintenance has gained in importance as a support function for ensuring equipment availability, quality products, on-time deliveries, and plant safety. Cost-effectiveness and accuracy are two basic criteria for good maintenance. Reducing maintenance cost can increase enterprise profit, while accurate maintenance action can sustain continuous and reliable operation of equipment. As instrumentation and information systems become cheaper and more reliable, condition-based maintenance becomes an important tool for running a plant or a factory [5].

The paper [5] presents a novel condition-based maintenance system that uses reliability-centered maintenance mechanism to optimize maintenance cost, and employs data fusion strategy for improving condition monitoring, health assessment, and prognostics.

Forecasts of some analysts are that this activity in the twenty-first century will be one of the most important because of the growing need for rational use of resources.

Maintenance of technical systems is defined as the process of implementing measures the ensuring properly functioning of the system with competitive performance and minimum duration of interruptions because failures and maintenance activities. This is the most general term criterion function (objective function) the maintenance process.

The state of technical system is changed during exploitation and it is stochastic process that describes the probability that the system will be in properly the state over time ("in the work" as opposed to states "in failure" - factual and "In the conditional failure").

Activities of maintenance and management of maintenance are inevitable because failure of the system during operation, as a natural occurrence, as a result of the increase entropy of the system. There are several classifications of maintaining a methodology, and today is considered the most complete one that maintenance is divided into:

— Maintenance by reliability, and
— Total Productive Maintenance.

In the first case, the goal is maximum reliability, and in the second case, the maximum economic efficiency where operators assess the state of the system and undertake action to maintain "when is sufficiently clear" that will reach to failure (Japanese philosophy that is applicable eg. in serial production).

Traditional maintenance methodology is:

— Corrective maintenance,
— Prevention maintenance, and
— Combined maintenance.

In the second and third case, it is particularly important the maintenance by state of the system, with the use of diagnostic methods.

## STRATEGIES OF MAINTENANCE AND MAINTENANCE MANAGEMENT

The type and content of the process within the maintenance of the system identifies selected method of maintenance (selection of the best models of maintenance). Without a good strategy and functioning all elements of the process, the maintenance of the system is not effective. Absence achievement of the objective of the system is expected.

During the last decade, many companies have made large investments in the development and implementation of enterprise resource planning (ERP) systems. However, only a few of these systems developed or installed have actually considered maintenance strategies.

Maintenance is a complex process that is triggered by planned periodic repair (scheduled or planned maintenance), equipment breakdown or deterioration indicated by a monitored parameter (unplanned or emergency maintenance).

This process requires planning, scheduling, monitoring, quality assurance and deployment of necessary resources (workshop, manpower, machines, equipment, tools, spare parts, materials). The proper design and integration of maintenance management into ERP systems enable enterprises to effectively manage their production planning and scheduling, as well as to analyze their maintenance history so as to carry out cost analysis and produce future projections of failure trends [6].

Maintenance management using the maintenance strategies as a set of policies that specify procedures for advance maintenance lick situations based on maintenance planning and implementation of maintenance plans.

These planned maintenance strategies can be applied in the maintenance by state of the system, monitoring changes of the parameters of state of the system and the level of reliability.

Monitoring the state parameters can be carried out continuously or periodically, and for each parameter will determine its value and in that way achieve preventive maintenance that meets the most practical situations and types of technical systems.

Maintenance management, however, is a much broader process. It includes activities:
— Forecasting and prediction,
— Planning,
— The execution and coordination of maintenance actions,
— Control of deadlines and quality performance of maintenance actions,
— Control the output achieved performance of the system and
— Control of maintenance costs and the current maintenance and investment maintenance (The investment maintenance is funded from amortization, while the current maintenance is financed as and production).

Maintenance Planning is the key function of maintenance management here. The maintenance plan must be in accordance with plan to produce, and horizon of planning in most of the system is one to two years.

The maintenance plan contains maintenance actions, and the plan spare parts, plan personnel and other resources, while elaborating preventive maintenance activities as a special program of preventive maintenance.

## INFORMATION SYSTEM FOR MAINTENANCE MANAGEMENT

Management information systems for maintenance are crucial "tool" for maintenance management. Maintenance is one of the most important functions of the total logistic support (integrated logistics) industry organizations.

Information technology (IT) could be an important tool for reaching efficiency and effectiveness within maintenance, provided that correct and relevant IT is applied.

In this paper, a conceptual model for identifying maintenance management IT requirements is developed, with its practical application in a process for the IT requirements identification for maintenance management. The process is exemplified in two real-world cases [3].

The paper [3] suggests that the factors of goals, purpose and use should be considered on organizational and individual level in order to identify the IT demands. Correct level of IT applied, i.e. IT consisting of correct functionality required for planning, conducting and following up maintenance activities according to the state of maintenance and the strategy adapted, will contribute to successful maintenance management. Moreover, paper [3] promotes the use of a structured procedure for the identification of IT requirements for maintenance management.

Information is an essential resource for setting and meeting management objectives. The role it plays within the organization is of vital importance as it helps to build knowledge and measure the overall performance of the organization. As a result, information systems (IS) are no longer used to supply support to the operation of a business, or in the case of maintenance, to collect and analyze data. The IS must contain modules that can provide management with

value added information necessary for decision support and decision making [1].

The main tasks of the information system are:
— Data collection of all relevant events during operation of the technical system and its maintenance,
— Data processing in order to obtain information for diagnosing,
— Forecasting,
— Planning,
— Decision-making,
— Realization and control of corrective and preventive maintenance.

The information is used to manage the supply of spare parts, cost, training workers to increase the reliability of the whole technical system and not just its components.

The functional scheme of flows of data and information in the process of maintenance management is presented in Figure 1.
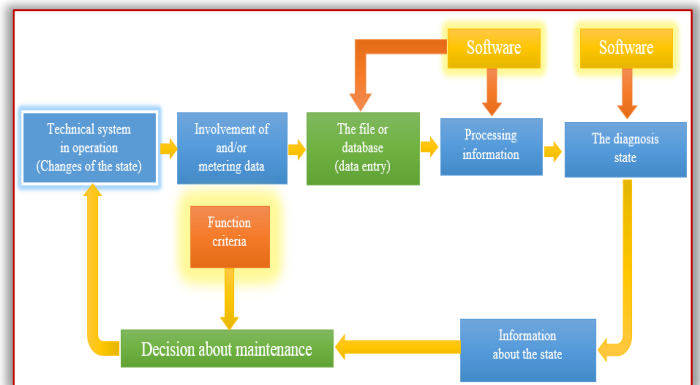


Figure 1. The process of maintenance management using information system for maintenance

The function of goal (function criteria) is determined by the requirements of the owner (user) of a technical system. It can be defined maximum the reliability (eg. In the case of aviation) or maximum economic efficiency, minimal cost maintenance and maximum productivity (eg. In the case of machine tools), and the like.

Data refer to failures, malfunction, parameters of the state of system and the reliability is established inspections and measurements, the maintenance operations maintenance costs, etc.

Holders of the original data are different documents on the forms created for information system on plain paper (but can be and magnetic media) such as map failures, reports of inspections and the like.

For entering data from source documents (which are coded) is used a mask (the software is created corresponding mask for each group of data).

Information system in a logical sense reflects real (technical) system and presents a model of operation and maintenance of technical systems.

Information system architecture consists of the following segments:

— The data model that contains information about the states of the technical system because they are the basis of the information system.

— Model the process describes the physical flows of the data, entering data into a computer as well as generating.

— Model Support, which contains physical support elements (equipment installation) then the manpower, training of workers and the like.

For the analysis and design of information systems important are three tools:

— Vocabulary data wich contains tabular systematic review (inventory) of all data by function (parts) of technical system is maintained.

— Chart of flows data is established vocabulary of data (document workflow).

— The program for processing data including files or databases.

The basic files are those which referee to the failure, orders for maintenance operations, and reports of executed maintenance operations.

The content output information and the database are the most important features of the system in general. The content output information must be adapted to the type of decisions that will be made and are expressed in the form of tables and diagrams etc.

Conventional information system "dramatically" reduces the amount of tedious routine work on the monitoring process and decision-making.

It enables to constantly comparing actual results with the expected and planned results, and to undertake a possible corrective actions.

The life cycle of a project system with delivered outputs of each stage is presented in Figure 2.
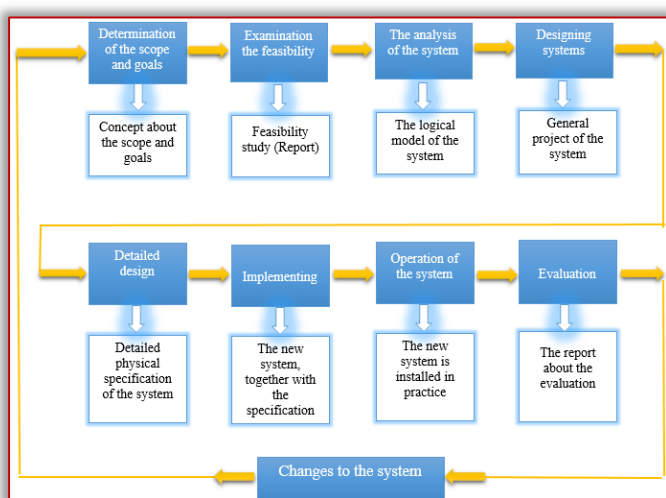


Figure 2. The methodology development of information system

The role of information system as component for interaction with user enables that he formulates your request and immediately receives a response and it is a special important for maintenance management.

The role of components for connecting with important sources of information in the environment that are mostly relevant for tactical and strategic decision making (because these sources of professional are journals and newspapers, followed by industrial statistical surveys, database expert and scientific institutions, etc.).

For the maintenance management is a significantly staff education or for other purposes.

## DEVELOPMENT OF INFORMATION SYSTEMS

Information system should be designed so as to be oriented to user and serves to man, to "thinks" like a man when he solves a problem or when makes decisions in managing the process. These are increased requirements compared with traditional information systems.

They can be filled out by the information system is being developed expanded roles. These roles can be [12]:

— The role of monitors,

— The role of filter information,

— The role of the components for interaction "on line" with the user and

— The role of components for connecting with the environment.

In order served as a monitor, information system should be designed so that it continuously monitors key variables of the maintenance process (eg. The number of machines in failure, the costs of corrective and preventive maintenance, etc.), but some variables can serve as predictors in the planning and predictions. So you can automatically undertake actions of maintenance when the variation of some key variables become significantly.

As a monitor of information system, further, can be used for decision-making that are programmed. Using that information and certain decision rules automatically decision-making (eg. calculate) a specific decision that managers can concentrate on non-programmed decision-making. The largest number of technical and fewer tactical decisions are routine, repetitive decisions that can be programmed.

Un-programmed decision making is presented in most of the strategic problems and in the maintenance management of them is not much, but it can be very significantly.

As a filter of information, information system reduces the amount of information that is distributed to the middle hierarchical level, and more reduced amount of information that is distributed to top management, where this information is synthesized. Thus, a vast quantity of information is distributed rationally, with at the same time, increasing functionality of the system.

The high costs in maintaining today's complex and sophisticated equipment make it necessary to enhance modern maintenance management systems. Conventional condition-based maintenance (CBM) reduces the uncertainty of maintenance according to the needs indicated by the equipment condition. The intelligent predictive decision support system (IPDSS) for condition-based maintenance (CBM) supplements the conventional CBM approach by

adding the capability of intelligent condition-based fault diagnosis and the power of predicting the trend of equipment deterioration. An IPDSS model, based on the recurrent neural network (RNN) approach, was developed and tested and run for the critical equipment of a power plant. The results showed that the IPDSS model provided reliable fault diagnosis and strong predictive power for the trend of equipment deterioration [14].

Decision Support Systems (DSS) and expert systems (ES) are even more powerful tools compared with the information systems, which in the management of the maintenance can find wide application. DSS represent a symbiosis between users (engineers and managers) and information systems in decision-making and solving unstructured problems using information and decision-making models, a special software tools and often specific additional hardware tools.

Expert systems in the maintenance management especially in technical diagnosing have found significant application. They have in addition to the database or file and knowledge base that contains sophisticated models of decision-making, that decision process execute as it seems reasoning man.

This is software that solves a problem that otherwise can only be resolved expert.

In Figure 3 are presented as dominant area of application of electronic data processing (EDP), management information systems, decision support systems and expert systems in the hierarchical structure of industrial organization.
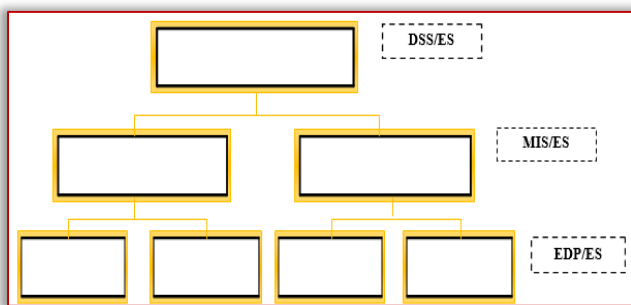


Figure 3. EDP, MIS, DSS, ES in the hierarchical structure of the organization

At the level of top management are relevant DSS (focus on decision-making) in the middle hierarchical level MIS (focus on information) on a basic level EDP (focus on data). Expert systems are relevant to the problems of decision-making at all levels.

## CONCLUSIONS

The expediency of maintenance can be seen only through the effectiveness of the basic production process.

Maintenance management has gained in importance in the last decades of the twentieth century and beginning of the twenty-first century, with a tendency of further growth.

IT tools are important, and in many cases invaluable, for reaching the goals of maintenance. This paper suggests that the factors of goals are expressed in terms of efficiency, effectiveness and cost-effectiveness, purpose and use should be considered on organisational and individual level in order to identify the demands of IT.

Automation, computerization and robotics work processes require sophisticated methods of maintenance management and the increasing internationalization of markets requires greater the reliability of production systems and competitive the ability. Without modern information system with expanded roles compared with traditional, and on these challenges can not be successfully respond. Even greater opportunities lie in the application of decision support systems and expert systems.

In the paper is presented a methodological basis for the approach designing specific information system for the maintenance management.

## References

[1] Fernandez, O., Labib, A. W., Walmsley, R., Petty, J. D., A decision support maintenance management system: Development and implementation, International Journal of Quality & Reliability Management, Vol. 20, No. 8, pp. 965-979., 2003.

[2] Garg, A., Deshmukh, S.G., Maintenance management: literature review and directions, Journal of Quality in Maintenance Engineering, Vol. 12 Iss: 3 pp. 205 – 238., 2006.

[3] Kans, M., An approach for determining the requirements of computerized maintenance management systems Computers in Industry, 59, pp. 32–40, 2008.

[4] Madu, C.N., Competing through maintenance strategies", International Journal of Quality & Reliability Management, Vol. 17, No. 9, pp. 937-949., 2000.

[5] Niu G., Yang B-S., Pecht, M., Development of an optimized condition-based maintenance system by data fusion and reliability-centered maintenance, Reliability Engineering and System Safety, 95, pp. 786-796, 2010.

[6] Nikolopoulos, K., Metaxiotis, K., Lekatis, N., Assimakopoulos, V., Integrating industrial maintenance strategy into ERP, Industrial Management & Data Systems, Vol. 103, Iss 3, pp. 184 – 191, 2003.

[7] Ramachandra, C. G., Srinivas, T. R., Design, Development and Implementation of Computerized Maintenance Management Information System (CMMIS) for a Selected Medium Scale Industry, International Journal of Science, Engineering and Technology Research, Vol. 2, Issue 8, 2013.

[8] Ramachandra, C.G., Srinivas, T.R., Shruthi, T.S., A Study on Development and Implementation of a Computerized Maintenance Management Information System for a Process Industry, International Journal of Engineering and Innovative Technology, Vol. 2, Iss 5, 2012.

[9] Róka-Madarász, L., Performance Measurement for Maintenance Management of Real Estate, Acta Polytechnica Hungarica, Vol. 8, No. 1, pp.161-172, 2011.

[10] Sherwin D., A review of overall models for maintenance management, Journal of Quality in Maintenance Engineering, Vol. 6 No. 3, pp. 138-164, 2000.

[11] Šlaichová E., Maršíková K., The Effect of Implementing a Maintenance Information System on the Efficiency of Production Facilities, Journal of Competitiveness, Vol. 5, Issue 3, pp. 60-75, 2013.

[12] Šibalija LJ., Architecture of on expert system for quality assurance in individual production of complex mechanical products, Proceedings of the Eleventh European Meeting on Cybernetics and Systems Research, University of Viena, 1992.

[13] Waeyenbergh, G., Pintelon, L., A framework for maintenance concept development, Int. J. Production Economics, 77, pp. 299–313., 2002.

[14] Yam, R.C.M., Tse, P.W., Li, L., Tu, P., Intelligent Predictive Decision Support System for Condition-Based Maintenance, Int J Adv Manuf Technol, 17, pp. 383–391, 2001.

[1.]O.A. ADETAYO, [2.]B.I.O. DAHUNSI

# CHARRING RATE CHARACTERISTICS OF SOME SELECTED SOUTHERN NIGERIA STRUCTURAL WOOD SPECIES BASED ON THEIR FIRE RESISTANCE ABILITY

[1.]Department of Civil Engineering, Federal University Oye Ekiti, NIGERIA
[2.]Department of Civil Engineering, University of Ibadan, NIGERIA

**Abstract:** The performance of Nigeria structural wood species under fire exposure to prevent structural collapse have not been adequately researched. This paper explores the charring rate of six identified structural wood species. They are: terminalia superba (Afara), milicia excelsa (Iroko), khaya ivorensis (Mahogany), mansonia altissima (Mansonia), nauclea diderrichii (Opepe), and tectona grandis (Teak). The densities of the wood species were determined at Moisture Contents (MC) of 9.0, 12.0, and 15.0%. Samples from each of the selected species, were exposed to fire at temperature ranges of 20° to 230℃ for 30 minutes; 20° to 300℃ for 60 minutes; 230° to 600° C for 30 minutes. Empirical statistical model was developed for charring rate of the samples. The models were analysed using ANOVA at α0.05. At 60 minutes (20° to 300℃), Opepe of 9.0, 12.0 and 15.0% MC had the lowest charring rates of 0.44±0.03mm/min, 0.46±0.05mm/min and 0.45±0.03mm/min respectively, while Afara exhibited the highest charring rates of 0.74±0.02mm/min, 0.74±0.02mm/min and 0.68±0.02mm/min at the three MC levels. At temperature ranges of 20° to 230℃, and 12% MC, it showed that at r = 0.836, there is a linear positive correlation between the experimental charring rate and predicted charring rate.
**Keywords:** Nigeria woods, structural collapse, moisture content, charring rate, linear correlation

## INTRODUCTION

Wood is an indispensable engineering material that has served man throughout history. People relied on wood for needs varying from farming tools to building materials, fuel, weapons of hunting and warfare [1]. The rain forest zone of Nigeria is blessed with abundant natural forests because the geographical location of the country in the tropics has naturally favored the growth of trees, which is the source of abundant wood in Nigeria [2].

Wood as a perfect material for construction purpose is not easily ignitable but combustible. Wood is composed of a mixture of cellulose, hemicellulose, and lignin bound together in a complex network. Heating wood above 300℃ causes decomposition or pyrolysis converting it to gases, tar and charcoal. At temperatures above 300℃ the gases will flame vigorously but the charcoal requires temperatures of about 500℃ for its consumption.

Wood most important property at elevated temperature is the formation of char after ignition [3]. The charring rate is the linear rate at which wood is converted to char [4]. A build-up of char tends to protect the unburnt wood from rapid pyrolysis. The unburnt timber, being a good insulator, results in the wood close to the char edge being unaffected by the fire. The charring rate is dependent on a number of factors such as: wood species, wood density, wood thickness, moisture content, and chemical composition. Of all the common physical properties of wood, density is one of the most important [5, 6].

Different wood char at varying rates, largely as a function of their density with the higher density woods charring more slowly [7]. The char layer does not usually burn because there is insufficient oxygen in the flames at the surface of the char layer for oxidation to occur. When the wood below the char layer is heated above 100℃, the moisture in the wood evaporates [8]. Some of this moisture travels out to the burning face, but some travels into the wood, resulting in an increase in moisture content of the heated wood a few centimeters below the char [9, 10].

The rate of charring is little affected by the severity of the fire, so for an hour's exposure, the depletions are 40 mm for most structural wood and 30 mm for the denser hardwoods. This enables the fire resistance of simple timber elements to be calculated. The predictive method is published in EN 1995-1-2 Fire resistance of timber structures as shown in Table 1 [11].

Table 1: Notational rate of charring for the calculation of residual section

| Species | Charring in 30 min | Charring in 60 min |
|---|---|---|
| All structural wood species | 20mm depletion | 40mm depletion |
| Hardwoods having a nominal density not less than 650kg/m³ at 18% moisture content | 15mm depletion | 30mm depletion |

Source: EN 1995-1-2 (2004)

Charring rate models use the charring rate concept to calculate the residual section of a wooden cross-section after a certain exposure to fire. It assumes that the charring rate of timber made of solid or glued-laminated hardwood decreases linearly with density, with a limit of 0.5 mm/min for

density larger than 450 kg/m$^3$. For softwood species the standard provides a mean value of 0.7 mm/min for density larger than 290 kg/m$^3$. The fact that the charring rate really changes with wood density has been demonstrated by several authors from several countries [12, 13]. Thermal conductivity of solid wood depends on the moisture content as reported by several authors [14, 15, 16, 17].

The water content of wood has an influence on its thermal behaviour. The effects of changes in conductivity of wood below 300° C on the charring rate are not significant. The evaporation of water consumes energy, changing the apparent specific heat curve of the composite wood-water material. Temperature at any point in wood will remain approximately constant at about 100°C until the water has been evaporated.

The charring rate, β, is an important factor in the fire design of exposed structural timbers, because it determines how quickly the size of the load-bearing section decreases to a critical level. Design procedures for fire-resistant wood members in the U.S. model building codes [18] are based on work done by Lie in the early 1970's [19]. Lie assumed a constant charring rate of 0.6 mm/min, regardless of species and moisture content.

White performed extensive measurements of the charring rate of eight wood species exposed according to ASTM E 119 [20]. He found that the data could be correlated according to the following equation:

$$t = mx_c^{1.23} \qquad (1)$$

with: t = time (min), m = char rate coefficient (min/mm$^{1.23}$), $x_c$ = char depth (mm).

Based on the experimental data, an empirical model was developed that expresses m as a function of density, moisture content, and a char contraction factor. The latter is the ratio of the thickness of the char layer at the end of the fire exposure divided by the original thickness of the wood layer that charred. The char contraction is primarily a function of the lignin content in the wood.

## METHODOLOGY

### — Experimental research into the selected structural woods

In this study, we assumed the charring rate was a function of density, moisture content, and level of heat exposure. Samples of six different wood species out of ten samples mostly used for structural purpose were tested for charring rates.

The six species tested were Afara (Terminalia superba), Iroko (Milicia excelsa), Mahogany (Khaya ivorensis), Mansonia (Mansonia altissima), Opepe (Nauclea diderrichii) and Teak (Tectona grandis).

The samples were taken from the heartwood region of the individual tree. And they were specially ordered from lumber market.

## — Charring Rate Tests

Wood specimens were tested in a big vertical electrical-fired furnace. Fifty-four samples tested were done in three groups. Nine specimens of overall dimension 150mm x150mm x 510mm (0.15m x 0.15m x 0.51m) blocks from one board of the six species.

In the first group of 18 tests, three specimens from one board of each of the six species were tested at moisture content levels of 9, 12, and 15 percent at the furnace exposure period of (0 – 30 minutes) temperature ranges of 20°C to 230°C . The second group of 18 tests, was tested at the furnace exposure period of (0 – 30 minutes) temperature ranges of 230°C to 600°C. The last group of 18 test was at the furnace exposure period of (0 – 60 minutes) temperature ranges of 20°C to 300°C.

At time of test, the following data were recorded for the specimen properties:

- — Species
- — Ring orientation
- — Specimen dimensions
- — Specimen weight
- — Moisture content (percent)
- — Specimen density

The specimens were held horizontally and subjected to the nominated heat flux perpendicular to the wood grain. Traditionally and in the procedure, it would be assumed that the charring front reaches when its temperature indicates 300°C, assuming that ignition starts at this point.

The specimen, as installed in the furnace. The electric furnace was powered, the furnace temperature switched on was 20°C. At time of burner ignition, the following functions were done as simultaneously as possible; Automatic temperature recorder was started; Stop watches started; Furnace temperature controller started.

The first test was terminated at the time when the fire-exposed time reached 30 minutes and temperature stopped climax 230°C.

Second test samples were immediately subjected to higher temperature 230°C to 600° C for 30 minutes.

The third test, for exposure period 0–60 minutes was terminated when the furnace temperature reached 20°C to 300°C.

When testing completed, the charred wood was scrapped away from the samples. The charred specimens were also cut in half to obtain the thickness of the charred slab and the char layer measured millimetres.

The values of density of each species at their corresponding moisture content (MC) 9, 12 and 15% is shown in the column chart of Figure 1. At 9% MC, Mahogany had the lowest density value of 439 ± 10.58 Kg/m$^3$. At 12 and 15% MC, Afara had the lowest density values of 444 ± 4.18 Kg/m$^3$ and 469 ± 7.07 Kg/m$^3$ respectively. At 9, 12 and 15% MC, Opepe had the highest density values of 630 ± 28.85 Kg/m$^3$, 686 ± 22.64 Kg/m$^3$ and 752 ± 17.22 Kg/m$^3$ respectively.
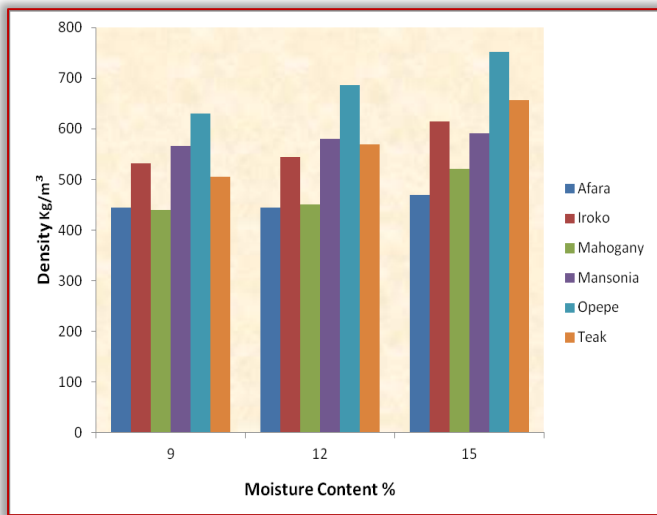
Figure 1: Density of selected Species at their corresponding Moisture Content

## RESULTS AND DISCUSSION

As noted previously, charring rates were determined by dividing char depth with the corresponding fire exposure time.

In a cause and effect relationship, the predicted charring rate (the independent variable) is the cause, and the actual charring rate (the dependent variable) is the effect.

The predicted charring rate could be calculated based on existing linear models of Eurocode EC5 recommendation [ENV 1995] and the Australian standard AS 1720.4 [21].

Eurocode EC5 model is given as:

$$d_{char} = \beta_o t \tag{2}$$

where, $d_{char}$ = charring depth mm, $\beta_o$ = charring rate (mm/min), usually between (0.5 to 0.8) mm/min, t = time in minutes

The Australian standard AS 1720.4 gives the following equation for the notional charring rate β (mm/min) as a function of wood density:

$$\beta = 0.4 + [280/\rho]^2 \tag{3}$$

where, ρ is the wood density at 12% moisture content (kg/m3).

Experimental charring rates were determined by scrapping away the charred timber and measuring the average depth remaining (char depth), to determine the amount lost through charring in millimeters. This was divided by the exposure time (min) and is expressed in (mm/min) were determined using equation (6) as the ratio of the char depth (mm) and the exposure time (min).

The correlation coefficient between the experimental (actual) charring rate and predicted charring were determined from the linear relationship between the actual charring rates and the predicted charring rates for each wood samples moisture content, time of exposure and temperature range. The results

were plotted in Figures 3 to 5. The correlation coefficient 'r' is given as:

$$r = \sqrt{R^2} \tag{4}$$

where $R^2$ = coefficient of determination

From Figure 2, the coefficient of determination, $R^2 = 0.6489$, it implied that at r = 0.806, there is a very strong positive correlation of actual charring rate that can be explained by the relationship to the predicted charring rate.
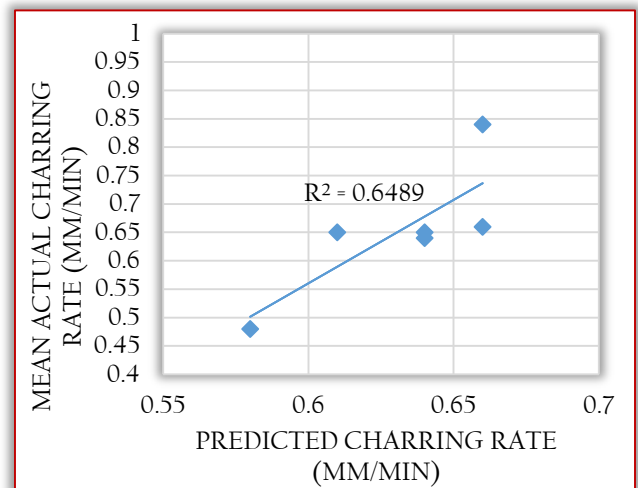


Figure 2: Linear correlation for samples exposed to 20℃ to 230℃ (9% MC, 0-30 minutes)

The coefficient of determination at 12% moisture content is $R^2 = 0.6994$ (Figure 3), it implied that a very strong positive correlation of actual charring rate can be explained by the relationship to the predicted charring rate with the correlation coefficient, r = 0.836.
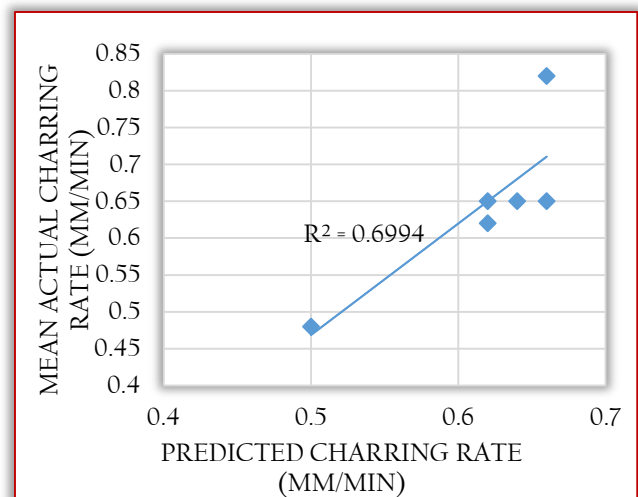


Figure 3: Linear correlation for samples exposed to 20℃ to 230℃ (12% MC, 0-30 minutes)

Figure 4 showed that at correlation coefficient, r = 0.737, there is a very strong positive correlation of actual charring rate that can be explained by the relationship to the predicted charring rate.
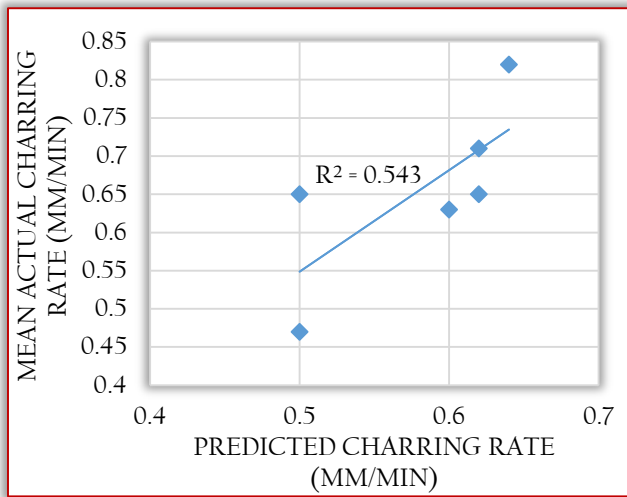
Figure 4: Linear equation for samples exposed
to 20℃ to 230℃ (15% MC, 0-30 minutes)

From figures 5, 6, and 7 , there is negligible correlation of actual charring rate that can be explained by the relationship to the predicted charring rate from Figures 6, 7 and 8 at, r = 0.04, r = 0.1746, and r = 0.01 respectively.



Figure 5: Linear correlation for samples exposed
to 230℃ to 600℃ (9% MC, 30-60 minutes)



Figure 6: Linear correlation for samples exposed
to 230℃ to 600℃ (12% MC, 30-60 minutes)



Figure 7: Linear correlation for samples exposed
to 230℃ to 600℃ (15% MC, 30- 60 minutes)

Figures 8, 9, and 10 showed a strong positive correlation of actual charring rate that can be explained by the relationship to the predicted charring rate at, r = 0.682, r = 0.582, and r = 0.578 respectively.



Figure 8: Linear correlation for samples exposed
to 20℃ to 300℃ (9% MC, 0-60 minutes)
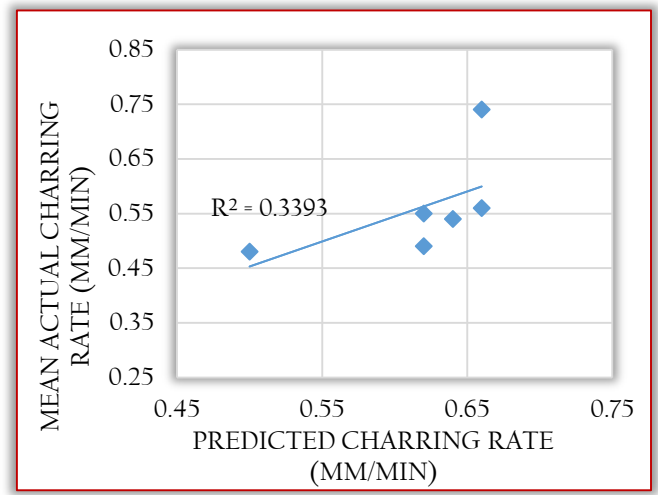


Figure 9: Linear correlation for samples exposed
to 20℃ to 300℃ (12% MC, 0-60 minutes)

Figure 10: Linear correlation for samples exposed
to 20°C to 300°C (15% MC, 0-60 minutes)

## CONCLUSION

The fire resistance of constructional wood members has been studied through laboratory experiments and existing models calculations. Like most wood properties, fire performance and charring properties are affected by density, moisture content, level of heat influx, and chemical composition. In general, woods of higher density and moisture content have better charring rate. The rate of charring of wood is improved by increasing the residual char content.

The fire resistive nature of solid wood walls is a combination of the insulating response of the charred wood at the surface with the slow rate at which flame will spread along the wood surface. Under conditions of severe fires, but not absolute worst-case extreme conditions, heavy wood or similar members will char at similar rates to those found in fire-resistance furnace tests, roughly 0.5 to 0.8 mm/min.

The research showed that the charring rate of wood species was optimum at 12 percent moisture content with Opepe species which had the highest density exhibited the lowest charring rate of 0.48 mm/min.

Based on the results obtained in this study, the following recommendations are made:

— The charring rate of timber presented in this study was limited to only six timber species. There is the need to consider the charring rates of other timber species.
— Determination of the charring rate for different wood species with varying dimensions and checks their variations and similarities.
— Systematic research on how various material properties and external factors influence the charring rate of structural wood.

## References

[1] Fuwape, J.A., 2001. Wood utilization. From cradle to grave. Inaugural lecture delivered at Federal University of Technology, Akure. 1-33pp.
[2] Johnson, D. M. V, Bodede, O. R. and Adesina, F., 2014. 'Wood Processing Industries in Nigeria : Problems and the Way Forward' Innovative Systems Design and Engineering. ISSN 2222-1727 (Paper) ISSN 2222-2871.Vol.5, No.6.
[3] Huntierova, Z., 1995. Analysis of the burning behaviour of wood and timber considering the use of fire protection layers: Graefelfing publishing house, Munich.
[4] Maciulaitis, R., Lipinskas, D., Lukosius, K., 2006. Singularity and importance of determination of wood charring rate in fire investigation. Materials Science. pp. 42-47.
[5] Desch, H.E., Dinwoodie, J.M., 1996. The Strength Properties of Wood (revised edition). London. pp. 177-202.
[6] Bowyer, J., Shmulsky, R., & Haygreen, J.G., (2003). Forest Products and Wood Science: an Introduction. 4th Edition. Iowa City, IA: Iowa State Press. pp. 554.
[7] Dahunsi, B.I.O., Adetayo, O.A., 2015. Burning Characteristics of Some Selected Structural Timbers Species of Southwestern Nigeria. IOSR Journal of Mechanical and Civil Engineering, 12(4) 112-120
[8] Drysdale, D.D., 1998. An Introduction to Fire Dynamics, 2nd Edition. John Wiley & Sons Ltd., Chichester, UK.
[9] Fredlund, B., 1993. Modelling of Heat and Mass Transfer in Wood Structures During Fire. Fire Safety Journal, 20: pp. 39.
[10] White, R. H., Schaffer, E.L. 1981. Transient Moisture Gradient in Fire Exposed Wood slab. Wood and Fiber 13: pp. 17-3
[11] Eurocode 5 EN 1995-1-2., 2004. Design of Timber Structures--Part 1-2: General rules-Structural fire design. European prestandard.
[12] White R.H, Erik V, Nordheim E.V., 1992. Charring rate of wood for ASTM E 119 fire exposure. Fire Technology; 28(l):5-30. DOI
[13] König J, Walleij L., 1999. One-dimensional charring of timber exposed to standard and parametric fires in initially unprotected and post protection situations. Rapport I 9908029. Swedish Institute Wood Technology Research
[14] Gu H, Hunt J.F., 2007. Two-dimensional finite element heat transfer model of softwood. Part III. Effect of moisture content on thermal conductivity. Society of Wood Science and Technology. Wood and Fiber Science; 39:159-166.
[15] Report FPL-9 FPL. 1977. Thermal conductive properties of wood, green or dry, from -40° to +100°C: a literature review. Report FPL-9, Forest Products Laboratory, Madison, Wisconsin, U.S.A.
[16] Parker W.J., 1985. Development of a model for the heat release rate of wood-a status report. Report NBSIR 85-3163, U.S. Department of Commerce
[17] Ragland KW, Aerts D.J. 1991. Properties of wood for combustion analysis. Bioresource Technology; 37:161-168.DOI:10.1016/0960-8524(91)90205-X.
[18] Anon, 2000. "International Building Code," International Code Council, Fairfax, VA.

[19] Lie T., 1977. "A Method for Assessing the Fire Resistance of Laminated Timber Beams and Columns," Canadian Journal of Civil Engineering, Vol. 4, pp. 161-169.

[20] White, R.H., 1988. Charring Rates of Different Wood Species. PhD dissertation, Madison University, off Wisconsin. Madison (WI).

[21] AS 1720.4; 1990. Timber structures Part 4: Fire Resistance of Structural Timber Members. North Sydney, Australia: Standard Australia.

[1.]Ervin LUMNITZER, [2.]Beata HRICOVÁ

# ANALYSIS OF RAILWAY NOISE EMISSIONS AND ITS VISUALIZATION

[1-2.]Technical University, Faculty of Mechanical Engineering,
Department of Process and Environmental Engineering, Košice, SLOVAKIA

**Abstract:** Environmental noise is inherently linked to various forms of transport, as well as other work-related or free-time activities. With the increasing intensity of traffic and the increasing rate of urbanization the impact of traffic noise is becoming even more pronounced, as it influences the quality of life and health of the population. One of the non-negligible partial sources of environmental noise is a rail transport. The paper presents the results of measurements of noise of passing trains, their visualization and evaluation. The paper also identified dominant sources of noise that contribute to the resulting noise emissions from rail transport.
**Keywords:** emissions, environmental noise, rail transport, visualization

## INTRODUCTION

Nowadays, railway traffic noise is acknowledged to negatively impact the wellbeing of the whole community, particularly in urban environments. Unfortunately, the traditional approach to support decision making in noise reduction intervention seems to start only from the compliance to the regulations in place, rather than from the identification of an optimal trade-off between the cost of the annoyance of the community and the cost of the intervention.

The expansion of the existing route system for increasing freight transport and long-distance traffic as well as reactivating routes for communal or privately operated local public transport is moving into the spotlight of transport policy. Noise pollution frequently leads to considerable reservations among the population in this infrastructure plan particularly when freight transport is planned at night. To counter these reservations, ambitious goals were formulated for noise reduction of rail traffic. Innovative sound control measures and quiet vehicles are supposed to help the achievement of these goals. Especially in recent years, many technologies have been developed and tested which can be taken into account due to the introduction of the new calculation methods (Schall 03, CNOSSOS EU).

Rail traffic noise is made of 3 dominant components:
— aerodynamic noise,
— rolling noise,
— traction noise.

**Aerodynamic noise** dominates at speeds above 200 km.h^{-1}. Therefore, this kind of noise is nearly absent in the Slovak Republic. Significant noise sources at high speeds include a pantograph, uncoupled chassis and turbulence due to inappropriate aerodynamic shape of a vehicle. Traction engine noise dominates at speeds of up to 60 km.h-1 and its level does not change with the change of the speed. Significant noise emissions are produced by independent traction, where the drive vehicles are driven mostly by a diesel engine.

In this case, noise emissions depend on the actual engine speed more than it is the case with electric traction. At certain speeds as well as at the start-up, noise emissions of traction vehicles using independent traction are significantly higher than when using electric traction.

In the range of about 60 to 200 km.h^{-1}, that is the medium speed (and in the vast majority of cases considered), **the rolling noise** generated by the interaction of the surface of the wheel and tracks. In extreme cases, the difference between the noise emitted by the rough track and the smooth track may be up to 20 dB. Another key contributor to the rolling noise is the roughness of circular surfaces of wheels. The main cause of wheel roughness is a brake with a classic cast iron brake pad. Carriages with the disc brake have smoother wheels and thus emit lower amounts of noise emissions. The permissible noise emissions of train sets are defined in Directive 2001/16/EC, the Conventional Rail Systems. The Directive covers the noise emitted by trucks, power-driven vehicles, complete units and passenger cars. The Directive is valid for the trans-European rail network. It also describes subsystems and outlines requirements for noise emissions. The basic subsystems are divided according to the emitted noise – road freight vehicles, units and trailers. The TSI noise subsystem contains requirements for acoustic parameters of vehicles while taking into account different types of noise.

## ANALYSIS OF NOISE SOURCES OF PASSING TRAINS

The noise emitted by the train set can be divided into:
— stationary noise (when the vehicle is still),
— noise at the start-up,
— noise emitted by the vehicle at a steady speed,
— noise in the driver's cabin

Stationary noise is mostly caused by vehicle components such as compressors, cooling systems and air conditioning. Start-up noise is a combination of traction noise and rolling noise with the above components in use.

Noise emitted when the vehicle is passing along a fixed point is mostly rolling noise. The noise indicator is the sound level A - noise measured when the train passes, at the distance of 7.5 m from the track centreline, 1.2 m above the track.

In the following table we outline the limits for external noise emitted by a vehicle while passing along a fixed point:

Table 1. Limits for the fixed point

| Type of vehicle | Allowed limits $L_{pAeq}$ [dB] |
|---|---|
| Electric locomotives | 85 |
| Diesel - electric locomotives | 85 |
| Electric units | 81 |
| Diesel-electric locomotives | 82 |
| Personal carriage | 80 |

According to the Directive, the operational and technical specifications of the railway noise are broken down according to the different types of noise.

## MEASUREMENT OF VARIOUS PASSING TRAINS AND EVALUATION OF RESULTS

The measurement conditions were defined by the methodology developed on the basis of the Directive EN ISO 3095 in line with allowed deviations. An asserted descriptor is the sound level A.

─ Placement of measurement points

The sound meters were placed in accordance with the TSI methodology for measuring train passes. The acoustic camera was located 16.5 m from the centre of the track and it was positioned so that the horizontal axis of the acoustic camera was parallel to the track and its centre was approximately 0.5 m above its level.
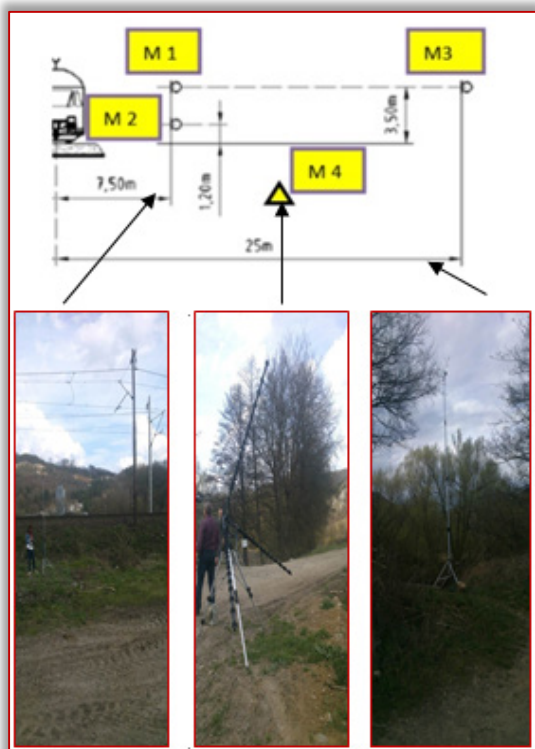


Figure 1. Location of measurement points

The measurement interval was selected according to the TSI parameters - the measurement starts at a moment the weighted sound pressure level A is 10 dB lower than the level found at the moment when the front part of the train is in front of the microphone; the measurement ends at a time the sound pressure level A is 10 dB lower than the level found at the moment the end of the train is in front of the microphone. The following figure shows an example of how a time interval, T, was selected for the entire train or a complete unit.
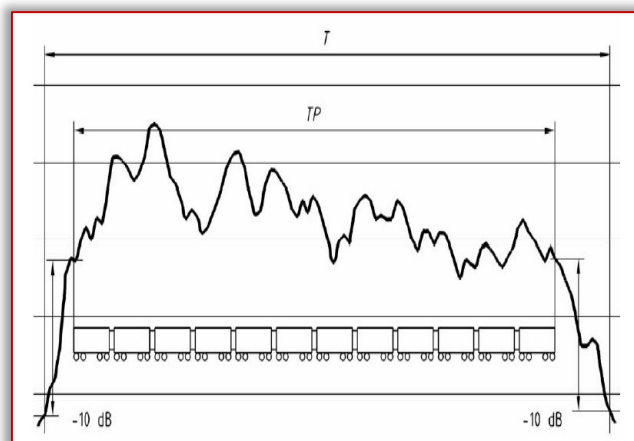


Figure 2. Selecting a time interval

When measuring trailers, the time interval T starts at the moment the centre of the first tested vehicle passes in front of the microphone and ends when the centre of the last tested vehicle passes in front of the microphone. Figure 3 shows the desired measuring time interval T after measuring individual trailer (at least two vehicles of the same type are necessary). In addition, the Figure also shows the time course of the equivalent sound level A when a train is passing.
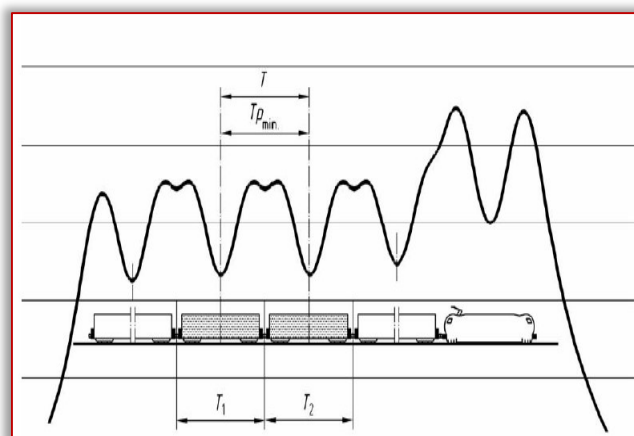


Figure 3. Time course of the equivalent sound level A

The time interval for specific measurements was determined according to the length of the set (number of carriages).

## RESULTS OF THE PASSING TRAIN MEASUREMENTS

A number of measurements has been performed. The paper outlines only the results of one measurement - RegioJet train set. This train is pulled by the locomotive Škoda 163 and behind it are 10 new RegioJet - ASTRA carriages (Relax, Business, Standard and a carriage for parents with children). The track speed is 70 km.h⁻¹.

Figure 4 shows the results of the measurement of the RegioJet train. Figure 5 shows the course of sound pressure at the measuring point M1.
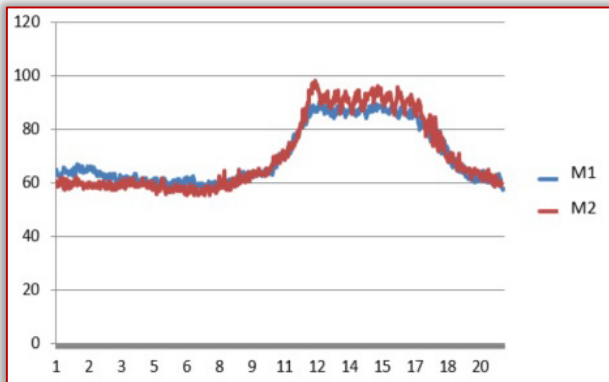


Figure 4. RegioJet passing
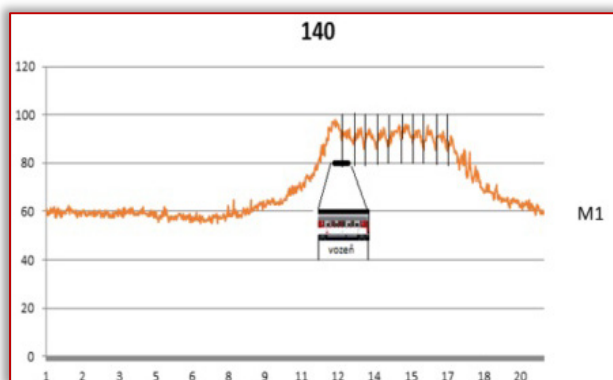


Figure 5. Acoustic pressure at M1

## RESULTS OF SOUND VISUALIZATION

Sound visualization was performed using an acoustic camera. Figure 6 shows the frequency range of the train set.
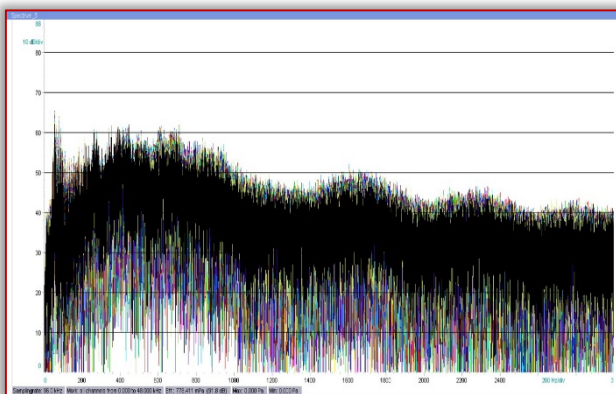


Figure 6. Frequency spectrum of the train set

The spectrum features values up to 65 dB in the frequency range of 40 to 80 Hz, and the subsequent increase in audible levels up to 60 dB in the frequency range from 300 to 600 Hz. These findings are also apparent from the spectrogram in Figure 7.

The highest emission values were recorded for the frequency ranging between 300 to 600Hz. The spectrogram clearly shows the passage of carriages and the locomotive. Interestingly enough, carriage emit different noise levels than the locomotive.

Samples of selected acoustic images are shown in Figure 8 - Figure 10.
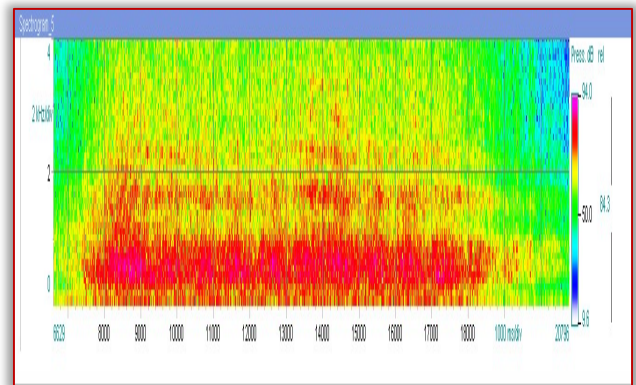


Figure 7. Spectogram of train passing



Figure 8. Acoustic image - rolling noise, 80 Hz
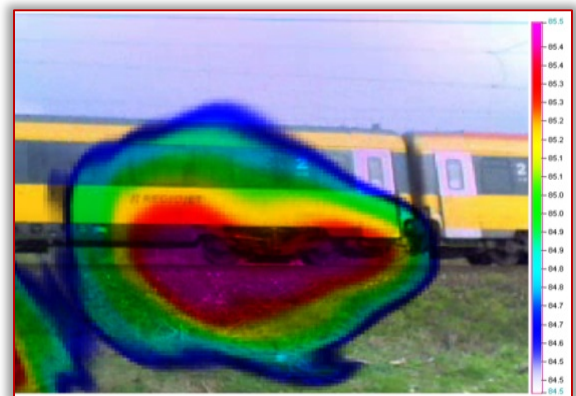


Figure 9. Acoustic image – chassis noise



Figure 10. Acoustic image – 380 – 400 Hz

## CONCLUSION

The measurements showed discrepancies between real values and limit values set by Directives. This discrepancy was noted for passing locomotives as well as carriages. The measurements noted mainly rolling noise.

On the basis of these findings, it is necessary to focus mainly on the railway superstructure when designing measures regarding noise.

## Bibliography

[1] Ervin Lumnitzer, Beata Hricová, Psychoakustické parametre železničného hluku, 2016. In: Fyzikálne faktory prostredia. Roč. 6, mimoriadne č. 1 (2016), s. 46-49.

[2] Ervin Lumnitzer, Beata Hricová, Miriama Piňosová, Acoustical parameters of the sound absorbents, 2015. In: International journal of interdisciplinarity in theory and practice. - 2015 Vol. 2015, no. 3 (2015), p. 16-20. http://www.itpb.eu/

[3] Úradný vestník Európskej únie, SMERNICA 2001/16/ES EURÓPSKEHO PARLAMENTU A RADY Dostupné na internete]: http://eur-lex.europa.eu/legal-content/

[4] Jarosław Zwolski, Noise and Vibration, http://www.zits.pwr.wroc.pl/zwolski/source/CE14_Noise& Vibration.pdf

[5] Petr Karván, Metodika pre meranie akustických parametrov vozidiel podľa TSI, Technická zpráva, Dostupné ma internete, http://www.mdcr.cz/

[6] Strategický plán rozvoja dopravnej infraštruktúry SR do roku 2020, [cit. 2015-3-20], http://www.zeleznicne.info/view

ISSN: 2067-3809

[1.]Abiodun Ayanfemi AYANDELE, [2.]Oluwaseye Moses OLASUNKADE, [3.]Olumuyiwa Idowu OJO

# EFFECTIVENESS OF CARRIER–BASED INDIGENOUS MICROORGANISMS FOR REMEDIATION OF CONTAMINATED SOILS

[1.]Department of Pure & Applied Biology, Ladoke Akintola University of Technology, Ogbomoso, NIGERIA
[2,3.]Department of Agricultural & Environmental Engineering, Ladoke Akintola University of Technology, Ogbomoso, NIGERIA

**Abstract:** Environmental damage due to the oil spills in the past and recent time has focused on the need for the environment friendly strategies for remediation of the contaminated site. Serial dilution pour plate method was employed for the isolation of bacteria and fungi. 1g of each soil sample was suspended in 9ml of double distilled water to make microbial suspensions (10–1 to 10–3). Dilutions of 10–1 and 10–3 were used to isolate both bacteria and fungi. Nutrient agar (NA) and potato dextrose agar (PDA) were used for the isolation of both bacteria and fungi that were used for biodegradation. Minimal salt medium was used for the biodegradation at different concentrations of crude oil (0.015, 0.0225 and 0.0375 ml). Supernatants of different concentrations at every 48 hrs were collected for spectrophometric analysis. The results were plotted into graphs using MATLAB. *Pseudomonas aeruginosa, Bacillus subtilis, Bacillus cereus* and *Pseudomonas putida* bacteria *were* isolated for the experiment. The result indicated that *Pseudomonas aeruginosa* among the bacteria isolates used performed well than other isolates as it gave the highest biodegradation value of 0.342 while *Penicillium chrysogenum* among the fungal isolates used performed well than other isolates as it gave the highest biodegradation value of 0.378. The results obtained showed that all the bacterial and fungal isolates were able to biodegrade crude oil at different concentrations and days. This study therefore shown that *Pseudomonas aeruginosa* and *Penicillium chrysogenum* are good biodegraders and are recommended for oil spillage pollution biocontrol and further molecular work is suggested to enhance their productivities.
**Keywords:** fungi, bacteria, biodegradation, hydrocarbon, crude oil contaminated soils

## INTRODUCTION

Biodegradation generally refers to the breakdown of organic compounds by living organisms eventually resulting in the formation of carbon dioxide and water or methane. Inorganic compounds are not biodegraded, but they can be bio transformed, that is, transformed into compounds having more or less mobility or toxicity than their original form. In many cases, the biodegradation processes involve a particular microorganism that attacks a specific molecular site.

Complete and rapid biodegradation of many contaminants may require not only specific environmental conditions, but also changing conditions to satisfy the needs of the microbe. The mobility of several different metals in soil and the influence of the biodegradation process on that mobility. They have shown that active microorganisms influence the ability of soil to retain or release metals and that cysteine is an effective agent for the release of some metals from soil.

Hydrocarbon contaminants are removed from soils by bioremediation and volatilization.

In this project, bio remediation is the major technique adhered. The potential of hydrocarbon biodegradation depends on the availability of desired microorganisms. Supplementing soils with prepared cultures is practiced when the indigenous content is low.

Environmental conditions such as pH, temperature, oxygen, nutrients, and soil moisture also can influence biodegradation results. Air emissions from the "bio pile" are treated by bio filtration where the pollutants are degraded and mineralized by heterotrophic aerobic microorganisms.

Oil spills, whether on water or soil do disappear, but very little is known about what can be done to accelerate this process. The disappearance of oil from sea water could be accelerated by the addition of deficient nutrients such as nitrogen or phosphorous, or both. Suggestions have also been made for microbial seeding of spills since bacteria and fungi are the only biological species which have the metabolic capability of utilizing petroleum carbon for cell synthesis. Crude oil is essentially a mixture of carbon and hydrogen, and thus spills will result in an imbalance in the carbon–nitrogen ratio at the spill site.

For bacteria to grow efficiently, they require about 10 parts carbon to 1 part nitrogen. If the ratio is greater, e.g. 100:1 or 1,000:1, growth of the bacteria and utilization of carbon source(s) will be retarded. In addition to there being a nitrogen deficiency in oil–soaked soil, other nutrients such as phosphorus may become growth–rate limiting. Therefore, in the experiment described above, urea–phosphate, a fertilizer, was added to oil spilled on soil, thus correcting both deficiencies in one application.

Thus, oil spills were also inoculated with oil–utilizing bacteria with and without a concurrent application of the urea–phosphate amendment.

Environmental damage due to the oil spills in the past and recent time has focused on the need for the environment friendly strategies for remediation of the contaminated site.

For instance, contamination of the environment with crude oil results in pollution, in particular presents a chronic problem to commercial fisheries, recreational resources and public health. Bioremediation is suggested for remediation of contaminated soil sites because of its low cost and its ability to convert contaminants to harmless end products. Other physical and chemical processes have been used to remove spilled oil from environment; however the use of these technologies has not always been successful. Bioremediation, the use of microorganisms or microbial process to degrade environmental contaminants is among these technologies. Numerous microorganisms, including bacteria, fungi, and yeasts are known for their ability to degrade hydrocarbons. Recently, bio augmentation which involves the addition of microorganisms to enhance specific biological activity has been applied in attempts to remediate numerous environmental problems. The potential of using microorganisms for degradation of crude oil and its constituents to minimize contamination have prompted a number of researchers to study the process in laboratories. For instance, augmenting the contaminated site with appropriate bacterial inoculum is a promising technique to enhance the biodegradation of hydrocarbons.

The need for bio remediating of agricultural land have become very essential in view of the high premium placed on it as a veritable source of water, land for agriculture and good environmental/climatic condition for the people living in the community. The study was done to determine the rate of the degradability of a spilled agricultural soil which could further be used for agriculture. This was achieved through developing a conceptual design of experiment with anticipated results, isolation of bacteria and fungi using serial dilution method, purification of bacteria and fungi, characterization of bacteria isolates and determination of the rate of bio degradability potential of both bacteria and fungi on a separate graph using matrix laboratory (MATLAB).

Crude oil is a naturally occurring flammable liquid consisting of a complex mixture of hydrocarbon of various molecular weights and other liquid organic compounds, which are found in geologic formations beneath the Earth's surface (Guerriero et al., 2011). The use of fossil fuels such as crude oil can have a negative impact on Earth's biosphere, releasing pollutants and greenhouse gases into the air and damaging ecosystems through events such as oil spills. Concern over the depletion of the earth's finite reserves of oil, and the effect this would have on a society dependent on it, is a field known as peak oil (WHO, 2004).

Generally any oil spill is most harmful and detrimental to the surrounding environment, but the crude oil toxins that escape into the atmosphere pose a possible health risk for individuals living in and around the affected area. Health risks are most prominent in the very young, the elderly and those who suffer from asthma. After an oil spill, however, contamination is more concentrated and widespread. Oil remediation workers are at a particularly high risk of sickness due to their continued and direct exposure to petrochemicals. In addition, the toxins quickly disperse into the air and are inhaled by individuals living in coastal cities and, if the wind is right, those living several miles inland as well (WHO, 2004).

## ⎯ Components of Crude Oil

Crude oil is essentially a mixture of many different hydrocarbons, all of varying lengths and complexities. In order to separate the individual components that make up the raw natural resource, the crude oil must be fractionally distillated so that chemical components can be removed one at a time according the their boiling points (Matveichuk, 2004).

## ⎯ Composition of Crude Oil

In its strictest sense, petroleum includes only crude oil, but in common usage it includes all liquid, gaseous, and solid such as paraffins hydrocarbons. Under surface pressure and temperature conditions, lighter hydrocarbons methane, ethane, propane and butane occur as gases, while pentane and heavier ones are in the form of liquids or solids. However, in an underground oil reservoir the proportions of gas, liquid, and solid depend on subsurface conditions and on the phase diagram of the petroleum mixture (Itah and Essien, 2005).
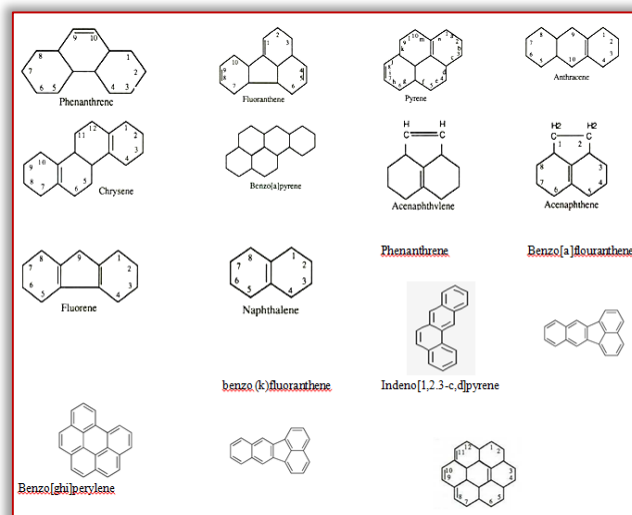


Figure 1: Structure of Health Implicated Polyaromatic Hydrocarbon

The proportion of light hydrocarbons in the petroleum mixture varies greatly among different oil fields, ranging from as much as 97 per cent by weight in the lighter oils to as little as 50 per cent in the heavier oils and bitumen (Leonardo, 2005).

The hydrocarbons in crude oil are mostly alkanes, cycloalkanes and various aromatic hydrocarbons while the other organic compounds contain nitrogen, oxygen and sulphur, and trace amounts of metals such as iron, nickel, copper and vanadium (Aldis and Anne, 2004). There are different types of hydrocarbon present in the composition of crude oil, which are Naphthalene, Acenaphthylene, Acenaphthene, Flourene, Anthracene, Phenanthrene, Fluoranthene, Pyrene, Benzo(a) anthracene, Chyrsene,

Benzo(a) flouranthene, Benzo(k) flouranthene, Benzo(a) pyrene, Dibenzo(ah)perylene, Benzo(ghi)perylene, Indeno (1,2,3–cd)pyrene. (Encyclopedia of Industrial Chemistry, 2002), proportions of chemical element vary over fairly narrow limits as shown in Table 1.

Table 1: Composition of elements present in crude oil by weight Composition by weight

| Element | Percent range |
|---|---|
| Carbon | 83 to 87% |
| Hydrogen | 10 to 14% |
| Nitrogen | 0.1 to 2% |
| Oxygen | 0.05 to 1.5% |
| Sulfur | 0.05 to 6.0% |
| Metals | < 0.1% |

Table 2: Composition by weight of hydrocarbons present in crude oil

| Hydrocarbon | Average | Range |
|---|---|---|
| Paraffins | 30% | 15 to 60% |
| Naphthenes | 49% | 30 to 60% |
| Aromatics | 15% | 3 to 30% |
| Asphaltene | 6% | Remainder |

The oil sands resources are called unconventional oil to distinguish them from oil which can be extracted using traditional oil well methods. Between them, Canada and Venezuela contain an estimated 3.6 trillion barrels (570×109 m3) of bitumen and extra–heavy oil, about twice the volume of the world's reserves of conventional oil (OPEC, 2006).

The heavier crude oils have too much carbon and not enough hydrogen; these processes generally involve removing carbon from or adding hydrogen to the molecules, and using fluid catalytic cracking to convert the longer, more complex molecules in the oil to the shorter, simpler ones in the fuels (Marcel, 1999).

— Air Pollution

About ninety–five percent of waste gases from the production fields and operation are flared. Gas flaring pollutes the air and it is common practice among companies in Nigeria especially in the Niger–Delta region which is hazardous to the ozone layer of the area and leading to climate change (IPCC, 2007). This is the major source of air pollution in the area as well untreated waste disposal on the environment.

According to Uyigue and Agho (2007), there are about 123 flaring sites in the region making Nigeria one the highest emitter of greenhouse gases in Africa and releasing some 45.8 billion kilowatts of heat are discharged into the atmosphere of the Niger–Delta from 1.8 billion cubic feet of gas everyday (Aaron, 2006). This is environmentally unethical and has contributed significantly to the degradation of the environment in the region.

This practice have also altered the vegetation of the area, replacing natural vegetation with stubborn grasses and the presence of these grasses indicates that the soil is no longer fertile for cultivation of crops. A major example could be seen in Opuama and Sekewu communities in the Warri North Local Government Area of Delta State in the region. It is evident that gas flaring has affected the ozone layer of the region leading to climate change that is unhealthy to crops cultivation (IPCC, 2007).

— Major Air Pollutants

Air pollution is a real public health and environmental problem that can lead to other things like global warming, acid rain, and the deterioration of the ozone layer. Table 3 stated some common pollutants, their sources, and their effect on the environment (Levy, 2007).

— Effect of crude oil in Nigeria

The Niger Delta is one of the 10 most important wetland and coastal marine ecosystems in the world and is home to some 31 million people (NDTC, 2008). The Niger Delta is also the location of massive oil deposits, which have been extracted for decades by the government of Nigeria and by multinational oil companies. Oil has generated an estimated $600 billion since the 1960s (Wurthmanm, 2006). Despite this, the majority of the Niger Delta's population lives in poverty. The United Nations Development Programme (UNDP) describes the region as suffering from "administrative neglect, crumbling social infrastructure and services, high unemployment, social deprivation, abject poverty, filth and squalor, and endemic conflict."

The majority of the people of the Niger Delta do not have adequate access to clean water or health–care (UNDP, 2006). Their poverty, in contrast with the wealth generated by oil, has become one of the world's starkest and most disturbing examples of the "resource curse" (UNDP, 2006). For the people of the Niger Delta, environmental quality and sustainability are fundamental to their overall wellbeing and development. According to UNDP, more than 60 per cent of the people in the region depend on the natural environment for their livelihood. For many, the environmental resource base, which they use for agriculture, fishing and the collection of forest products, is their principal or sole source of food (UNDP, 2006). Pollution and environmental damage, therefore, pose significant risks to human rights.

Oil spills, waste dumping and gas flaring are endemic in the Niger Delta. This pollution, which has affected the area for decades, has damaged the soil, water and air quality. Hundreds of thousands of people are affected, particularly the poorest and those who rely on traditional livelihoods such as fishing and agriculture. The human rights implications are serious, under–reported and have received little attention from the government of Nigeria or the oil companies. According to a study carried out by a team of Nigerian and international environmental experts in 2006, (NCF, 2006) the Niger Delta is "one of the world's most severely petroleum–impacted ecosystems". They stated: "The damage from oil operations is chronic and cumulative, and has acted synergistically with other sources of environmental stress to result in a severely impaired coastal ecosystem and compromised the livelihoods and health of the region's impoverished residents."

The Niger Delta has suffered for decades from oil spills, which occur both on land and offshore. Oil spills on land destroy crops and damage the quality and productivity of soil that communities use for farming. Oil in water damages fisheries and contaminates water that people use for drinking and other domestic purposes (NDHD, 2006).There are a number of reasons why oil spills happen so frequently in the Niger Delta. Spills result from corrosion of oil pipes, poor maintenance of infrastructure, spills or leaks during processing at refineries (WB Report, 1995), human error and as a consequence of deliberate vandalism or theft of oil (Richard, 2008).In August and December 2008, two major oil spills disrupted the lives of the 69,000 or so people living in Bodo, a town in Ogoni land in the Niger Delta. Both spills continued for weeks before they were stopped. Three years on, the prolonged failure of the Shell Petroleum Development Company of Nigeria, a subsidiary of Royal Dutch Shell, to clean up the oil that was spilled, continues to have catastrophic consequences for the Bodo community. The lives of tens of thousands of people have been directly affected by the spills and the ongoing pollution. Many are worried about their health and are afraid to eat locally caught fish or drink water from streams or rain water, as they did before the oil spills.

## ▬ Crude Oil's Toxins

Any oil spill is detrimental to the surrounding environment, but the crude oil toxins that escape into the atmosphere pose a possible health risk for individuals living in and around the affected area (WHO, 2003). Crude oil is a complex mixture of chemical constituents including various alkanes (butane, pentane, and hexane); aromatic hydrocarbons (benzene, ethyl benzene, toluene, and xylenes); cycloalkanes; other nitrogen, oxygen, and sulfur compounds (hydrogen sulfide); and trace metals such as iron, nickel, copper and vanadium (LDHH, 2010). Some constituents of crude oil can have significant toxicity. For example, several aromatic hydrocarbons are considered to be human carcinogens (Joseph, 2004).

The International Agency for Research on Cancer (IARC) indicates that for crude oil, there is inadequate evidence for the carcinogenicity in humans, although there is limited evidence for carcinogenicity in experimental animals (Matt, 2005). Hydrocarbon exposures from crude oil constituents will vary based on its exposure to the atmosphere, time in the marine aquatic and coastal environment, treatments with dispersants and interaction of the chemicals, wave action and heat. Generally, the more "aged" or "weathered" crude oil is (by mixing with seawater and traveling long distances from the source), the lower are the concentrations of volatile organic compounds (VOCs) (NIOSH, 2005). Although it generates less VOCs, weathered crude oil still contains harmful chemicals which can cause skin irritation and other irritant reactions. Thus, use of gloves and protective clothing is recommended to minimize skin contact with weathered oil, including oil deposited on the shore (tarballs) (WHO, 2003).

Appropriate hand hygiene facilities should be readily available to clean incidental skin exposures (NIOSH, 2005). Weathered crude oil is unlikely to pose an inhalation risk although a potential risk does exist for it to be aerosolized into respirable airborne droplets or volatilized by activities such as pressure washing. Even though detection of hydrocarbon "odors" is common in areas contaminated by crude oil, odor is not a reliable indication of a health hazard. Some individuals, though, are bothered by odors and can develop symptoms (e.g., may report dizziness, nose and throat irritation, headache and/or nausea) (WHO, 2003). These individuals may need medical evaluation when symptoms occur, especially if severe or persistent. Individuals with severe or persistent symptoms should be relocated to perform tasks where symptoms can be alleviated (NIOSH, 2005).

Studies of tanker oil spill responses have reported adverse health effects in response workers. These studies may underestimate the health effects associated with the Deepwater Horizon Response activities since the magnitude and duration of the Response is unprecedented. In addition, there is an incomplete understanding about the human health toxicity associated with the use of large amounts of dispersant, about the toxicity of the mixed exposure to large amounts of crude oil, dispersants and combustion products together and the cumulative effect of such exposures occurring over a long duration (Mendez, 2010). Since knowledge about potential inhalational exposures to the mixed exposure of crude oil, dispersant and combustion products associated with the Deepwater Horizon Response work is incomplete and still evolving, NIOSH and OSHA believed it was prudent to reduce the potential for adverse health effects by the responsible use of engineering controls, administrative controls and PPE, including respirators when appropriate (NIOSH, 2005). In the absence of comprehensive and coordinated health surveillance among workers and volunteers, and the absence of interpretable, quantitative exposure data, NIOSH and OSHA recommended that employers take precautions sufficient to ensure workers are protected from the chemical, physical and psychological hazards posed by the Deepwater Horizon Response (NIOSH and OSHA, 2005).

Environmental damage due to the oil spills in the past and recent time has focused on the need for the environment friendly strategies for remediation of the contaminated site. For instance, contamination of the environment with crude oil results in pollution, in particular presents a chronic problem to commercial fisheries, recreational resources and public health. Bioremediation is suggested for remediation of contaminated soil sites because of its low cost and its ability to convert contaminants to harmless end products (Rahman et al., 2002; Sathishkumar et al., 2008). Other physical and chemical processes have been used to remove spilled oil from environment; however the use of these technologies has not always been successful (Aldrett et al., 1997). Bioremediation, the use of microorganisms or microbial

process to degrade environmental contaminants is among these technologies (Boopathy, 2000). Numerous microorganisms, including bacteria, fungi, and yeasts are known for their ability to degrade hydrocarbons (Swannell and Head, 1994). Recently, bio augmentation which involves the addition of microorganisms to enhance specific biological activity has been applied in attempts to remediate numerous environmental problems (Vogel, 1996). The potential of using microorganisms for degradation of crude oil and its constituents to minimize contamination have prompted a number of researchers to study the process in laboratories. For instance, augmenting the contaminated site with appropriate bacterial inoculum is a promising technique to enhance the biodegradation of hydrocarbons.

Although pesticides are hydrocarbon pollutants of the soils, the main sources of hydrocarbon pollution are the spills and leaks of petroleum products (Potter, 1993). The Exxon Valdez oil spill in South Central Alaska is an example (Pritchard et al., 1992). In Nigeria, the exploration and exploitation practices and the breaking of oil pipes lead to incessant pollution especially in the Niger Delta area and Southern part of Nigeria (Salu, 1999). These spills have the largest immediate and economic impact as they harm, to a large extent, the ecosystem more than just the isolated location. In many spills involving tankers or offshore oil wells, some of the spills catch fire and consequently their combusting results in emission of large quantities of toxic ash which is detrimental to human health.

In recent times, the number of microbiological research has been devoted to bioremediation of oil–contaminated sites using various microbial species (Atlas, 1981). Notable among them were the bacterial species of Arthrobacter (Edgehill and Finn, 1982), Flavobacterium (Saber and Crawford, 1985), Sphingomonas (a novel Pseudomonas sp) (Radehaus and Schimidt, 1992), Pseudomonas spp. (Leung et al., 1997) and Acinetobacter (George–Okafor et al., 2005). Fungal species such as Trichoderma (Cserjesi and Johnson, 1972) and Phanerochaete (Andrea et al., 2001) have been implicated in hydrocarbon biodegradation.

Fungal bioremediation has been successful for clean–up of pentachlorophenol (PCP), a wood preservative and polycyclic aromatic hydrocarbon (Andrea et al.2001). The advantages associated with fungal bioremediation lay primarily in the versatility of the technology and its cost efficiency compared to other remediation technologies (such as incineration, thermal desorption, extraction) (Aust, 1990).

The use of fungi is expected to be relatively economical as they can be grown on a number of inexpensive agricultural or forest wastes such as corncobs and sawdust. More so, their utilization is a gentle non–aggressive approach. The application of bioremediation capabilities of indigenous organisms to clean up pollutants is viable and has economic values (Bijofp, 2003).

## MATERIALS AND METHODS

### — Materials and Equipments

The materials and equipments used for isolation of bacterial were; Disposable petri dishes, beaker, inoculation loop, Conical flask, measuring cylinder, slant bottles, gin bottles, cotton wool, funnel, foil paper, sieve, test–tube, distilled water, spatula, weighing balances, autoclave, shaker, centrifuge, spectrophotometer, ethanol, paper tape, NA (nutrient agar), (PDA) Potato Dextrose Agar and Incubator.

### — Collection of Soil Samples

Soil sample was collected from local mechanic garage along isale general, Ogbomoso, Oyo–State. The soil sample was taken to Ladoke Akintola University of Technology central Laboratory for analysis.

### — Preparation of nutrient Agar and Potato Dextrose Agar

Potato Dextrose Agar (PDA) and Nutrient Agar (NA) used in this study were prepared according to the manufacturer's specification i.e. 39 g of PDA and 28 g of NA in 1000 ml of distilled water each. Bacterial contamination was inhibited by aseptically adding 2g of tetracycline to 1000 ml of the sterile medium prior to pouring into sterile petri dishes, while fungi contamination inhibition was done by aseptically adding 2 ml of nystatin to 1000 ml of the sterile medium prior to pouring into sterile petri dishes for bacteria plates. The media were prepared, mixed thoroughly and sterilized by autoclaving at $121^0$C for 15 minutes.



Figure 2: Solidified Potatoes Dextrose Agar



Figure 3: Solidified Nutrient Agar

### — Isolation of Bacteria and Fungi

Serial dilution pour plate method was employed for the isolation of bacteria and fungi.1 g of each soil sample was suspended in 9ml of double distilled water to make microbial suspensions ($10{-}1$ to $10{-}3$). Dilutions of $10{-}1$ and $10{-}3$ were

used to isolate both bacteria and fungi. 1ml of microbial suspension of each concentration was added to sterile Petri dishes containing 15ml of sterile Potato Dextrose Agar for fungi isolation and Nutrient Agar for bacteria isolation (Waksman, 1992). After the plates have been solidified, the petri dishes for fungi were incubated at $30^0$C for 4 days while bacteria petri dishes were incubated $37^0$C for 24 hours. After the organisms have grown, both bacterial and fungal colonies were pure cultured.

— Purification of Bacteria and Fungi

Re–streaking on fresh plate containing solidified NA and PDA was done to obtain pure isolates. This sub culturing was continued until pure bacterial and fungal isolates were obtained. After pure isolates have been obtained, they were stored in different slant bottles containing solidified NA and PDA respectively. The storage was done based on their colonial morphology on NA and PDA plates before 24 hours. After pure isolates have been obtained, they were stored in slant bottles for characterization.

— Screening for the Biodegradability of both Bacterial and Fungal Isolates

After the plates have solidified, pure isolates of each organism (i.e. bacteria and fungi) was inoculated into the solidified plates. Bacterial plates were incubated at $37^O$C for 48 hours while fungal plates were incubated at $30^0$C for 6 days. At 48 hours of incubating bacteria, bacteria growth was observed on the plates while no growth was observed on fungal plates after 6 days of incubation. Therefore, bacterial isolates were stored for characterization and biodegradation of Crude Oil at different concentrations.



Figure 4: Bacteria plates incubated at $37^0$C for 48 hour



Figure 5: Fungi plates incubated at $30^o$C for 72 hours

— Inoculum Development

A loopful of the inoculum was taken from the NA slant bottles and inoculated into a sterilized Nutrient broth inside gin bottles. All the gin bottles were incubated in the incubator at $37^0$C for 24 hours.

— Biodegradation Crude Oil and Minimal Salt Medium

Chemically defined minimal salt medium was prepared by weighing different five salts and the crude oil at various concentrations (i.e. 5 ppm, 15 ppm and 25 ppm) into 1500 ml of distilled water in three (3) bowls.

Table 3: The constituents of Crude Oil selective medium

| SALT | CONCENTRATION (g/l) |
|---|---|
| $MgSO_4$ | 2 |
| $NaNO_3$ | 2 |
| $NH_4Cl$ | 2 |
| $KH_2PO_4$ | 2 |
| $CaCO_3$ | 2 |
| Crude Oil | 0.015, 0.0225, 0.0375 |

For the substrate, crude oil concentration was varied as 0.015g, 0.0225 and 0.0375g. After the media had been prepared, 90ml of the each medium was measured into gin bottles each and were sterilized at 121oC for 15 minutes and allowed to be properly cooled.

— Inoculation of Inoculum into Minimal Medium

After sterilization and the bottles had been properly cooled, 10ml of the bacteria isolates was inoculated into the minimal salt medium prepared into the bottles. The bottles were then transferred into the shakers in order to evenly shake or distribute the medium with the inoculum. The bottles were then later stored inside an incubator of 370 C. Supernatant for each of the isolate was harvested at every 48 hours for a period of 4 days.



Figure 6: Inoculation of bacteria into minimal salt medium



Figure 7: Inoculation of fungi into minimal salt medium

— Extraction of Bacterial from Minimal Salt Medium

After the incubation, pH of the minimal salt medium at different hour was determined also, the minimal salt medium at 2 days and 4 days were harvested by the techniques.

— Centrifugation

At 2 days and 4 days after inoculation, the supernatant were collected by centrifugation at 500rpm for 10minutes. The clear supernatant was stored in universal bottle and kept in refrigerator, after which it was subjected to estimate for spectrophotometry analysis.

— Spectrophotometry analysis for the Supernatants Collected

The clear supernatant of the three (3) concentrations collected from the formation media were placed into the universal bottles and spectrophotometric analysis was done with the absorbance read taken as 540 nm.

— Characterization of Bacterial Isolates

Colonial characteristics of the bacterial isolates were determined using parameters such as size, elevation, pigment, surface, opacity, edge and shape. Cellular characteristics of the isolates were determined through the following experiments: Gram's staining, Motility test, Spore staining, Capsule staining, Catalase test, Oxidase test and Methyl red test. Others include Indole test, Starch hydrolysis test, Citrate utilization test, Sugar fermentation test and Oxygen relationship test.

RESULTS AND DISCUSSION

Bacterial strains were isolated from soil samples collected from the site. The pure cultures of all the isolated bacterial strains were used for the biodegradation. The following are the bacteria isolated; Pseudomonas aeruginosa, Bacillus subtilis, Bacillus cereus and Pseudomonas putida. The ability of all the bacterial isolates to degrade the crude oil at different concentrations (0.015 ml/L, 0.0225 ml/L and 0.0375 ml/L) was analyzed spectrophotometrically.

Figures 8 to 15 showed the results obtained from the experiment at every 48 hours for a period of 4 days. All the bacterial and fungal strains moderately degraded the crude oil at different concentrations. Crude oil in the medium was reduced as a result of the biodegradation potential by the various bacterial and fungal isolates compared with the control that has no organism. Biodegradability of the crude oil by the bacterial and fungal isolates irrespective of the concentrations was noted, although some organisms could not biodegrade crude oil at higher concentrations. At the second and fourth day of incubation, the highest rate of biodegradation of crude oil by the bacteria isolate Bacillus subtilis gave 0.27 and 0.341 respectively at 0.0375 mg/ml; this indicates that biodegradation increases as the incubation periods and concentration increase as shown in Figure 8. Also at the second and fourth day of incubation, the highest rate of biodegradation of crude oil by the bacteria isolate Bacillus cereus gave 0.228 and 0.165 respectively at and 0.015 mg/ml and 0.0375 mg/ml respectively but it gave the least of 0.096 and 0.165 at 0.0225 mg/ml and 0.0375 mg/ml respectively,

this indicates that biodegradation increases as the incubation periods increases but decreases as concentration increases as shown in Figure 9.
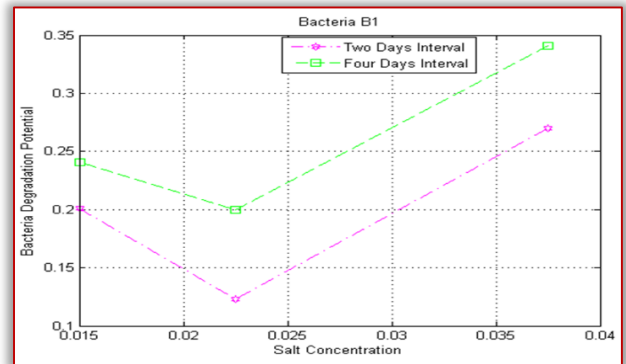


Figure 8: Biodegradation of Crude Oil by Bacillus subtilis at Different concentrations
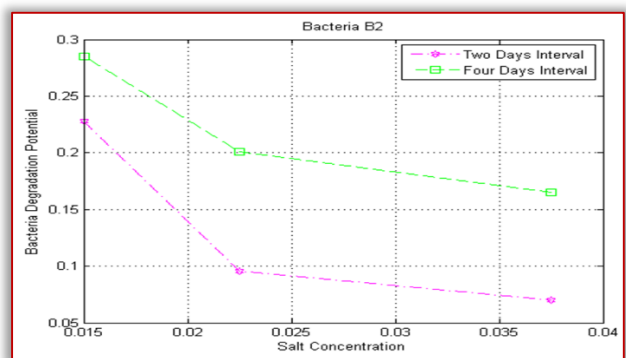


Figure 9: Biodegradation of Crude Oil by Bacillus cereus at Different concentrations
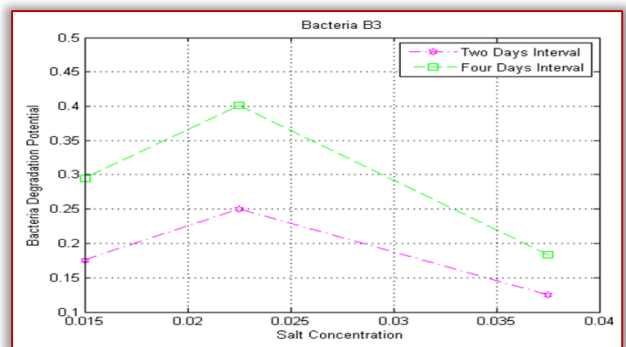


Figure 10: Biodegradation of Crude Oil by Pseudomonas putida at Different concentrations
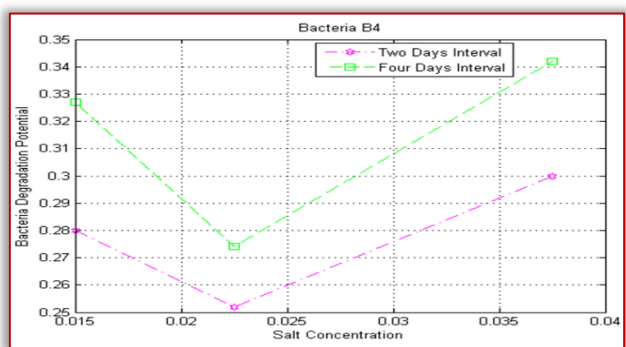


Figure 11: Biodegradation of Crude Oil by Pseudomonas aeruginosa at Different concentrations

In Pseudomonas putida, at the second and fourth day of incubation, the highest rate of biodegradation of crude oil by the bacteria isolate gave 0.176 and 0.165 respectively at 0.015 mg/ml and 0.0375 mg/ml respectively but it gave the least of 0.125 and 0.184 at 0.0375 mg/ml respectively, this indicates that biodegradation increases as the incubation periods increases but decreases as concentration increases as shown in Figure 10. At the second and fourth day of incubation, the highest rate of biodegradation of crude oil by the bacteria isolate Pseudomonas aeruginosa gave 0.300 and 0.342 respectively at 0.0375 mg/ml; this indicates that biodegradation increases as the incubation periods and concentration increase Figure 11.
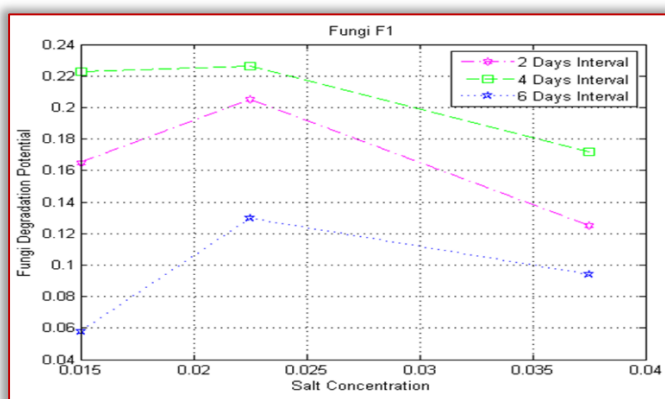


Figure 12:  Biodegradation of Crude Oil by Aspergillus niger at Different concentrations
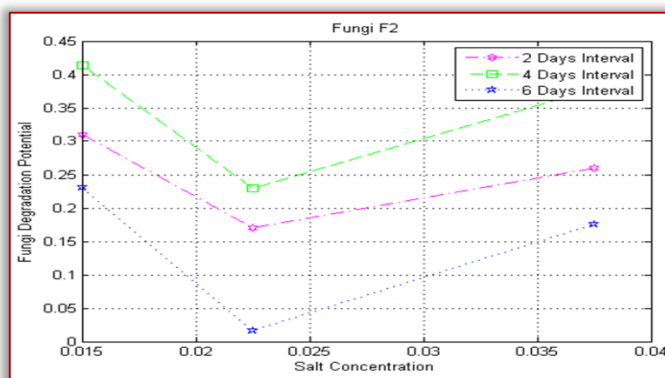


Figure 13:  Biodegradation of Crude Oil by Aspergillus flavus at Different concentrations
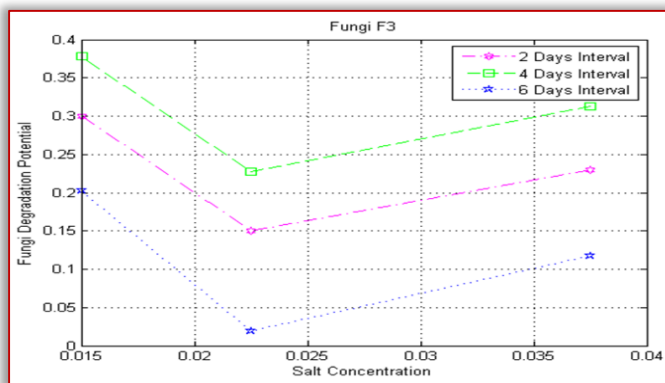


Figure 14: Biodegradation of Crude Oil by penicillium chrysogenum at Different concentrations

In the case of fungal isolates, at the second and fourth day of incubation, the highest rate of biodegradation of crude oil by the fungal isolate Aspergillus flavus gave 0.205 and 0.226 respectively at 0.0225 mg/ml but it gave least of 0.125 and 0.172 at 0.0375 mg/ml respectively, while on the sixth day the results at all concentrations reduced.  This indicates that biodegradation decreases as the incubation periods and concentration increase especially after the fourth day of incubation.

At the second and fourth day of incubation, the highest rate of biodegradation of crude oil by the fungal isolate Aspergillums Niger gave 0.310 and 0.414 respectively at 0.015 mg/ml but it gave least of 0.170 and 0.229 at 0.0225 mg/ml respectively, while on the sixth day the results at all concentrations reduced.  This indicates that biodegradation decreases as the incubation periods and concentration increase especially after the fourth day of incubation. Also, at the second and fourth day of incubation, the highest rate of biodegradation of crude oil by the fungal isolate Peniccilum chrysogenum gave 0.300 and 0.378 respectively at 0.015 mg/ml but it gave least of 0.195 and 0.228 at 0.0375 and 0.228 mg/ml respectively, while on the sixth day the results at all concentrations reduced. This indicates that biodegradation decreases as the incubation periods and concentration increase especially after the fourth day of incubation.

The degradation of crude oil by bacterial and fungal strains isolated from oil contaminated soil; the microorganisms implicated in oil degradation are widely distributed in nature and have been isolated from soil and water ecosystems with their oil degrading potentials (Bello, 2007).

The microorganisms capable of utilizing oil and oil products as a sole source of carbon and energy occur practically everywhere in air, water and soil (Oliver and Magot, 2005). It is estimated that in 1 g of unpolluted soil, there are only 100 to 1,000 cells of hydrocarbon degrading microorganisms, whereas, in 1 g of soil polluted by oil, their number increases to $1 \times 106$ to $5 \times 07$ cells, especially if pollution occurred repeatedly and during a long time (Rosenberg and Ron, 1996). Taxonomic characteristics of these isolates identified them as Bacillus spp and Pseudomonas spp.

## CONCLUSIONS

Bioremediation is a cheap and easy method to reduce oily sludge contamination while the use of microbial inoculants is a common practice, which enhances the rate of biodegradation. The study demonstrated that, if suitably developed, application of a carrier–based indigenous microorganism like Pseudomonas spp and Bacillus spp can be used to remediate soil contaminated with crude oil. Maintenance of proper soil conditions is an essential aspect to be looked into and needs to be studied in further detail when taking up such studies because soil conditions influence the survival of the microorganisms. Bacteria and Fungi show tremendous diversity and adaptability in utilization of different organic molecule as a carbon source; however their abilities to degrade a specific hydrocarbon as a

source of energy and or biomass may differ. The chemical composition of a crude oil may also be a factor in determining the type of bacteria and fungi, which may grow on it.

## References

[1] Akpofure, E. A. (2008). Oil Spillage in the Nigeria's Niger–Delta. Psycho–morphological and Empirical Overview, International Association of Impact Assessment, Opulence Environmental Service Ltd.

[2] Bisina, J. (2006). Environmental Degradation in the Niger–Delta (Unpublished).

[3] Guerriero M. (2011). Quantifying uncertainties in multi–scale studies of fractured reservo analogues: Implemented statistical analysis of scan line data from carbonate rocks". Journal of Structural Geology 32 (9): 1271–1278.

[4] Itah A. Y. and J. P. Essien (2005). Growth Profile and Hydrocarbonoclastic Potential of Microorganisms Isolated from Tarballs in the Bight of Bonny, Nigeria, World Journal of Microbiology and Biotechnology, Volume 21, Numbers 6–7, October, 2005, p 1317–1322.

[5] Khan K. and Ahmad H. M. (2000). Climate Justice Programme and Environmental Rights Action/Friends of the Earth Nigeria, Gas Flaring in Nigeria: A Human Rights, Environmental and Economic Monstrosity.

[6] Marcel, K. (1999). Degradation of pyridines in the environment. CRC Critical Reviews in Environmental Control. 19 (4): 309–340.

[7] Matt, K. (2005). Amnesty International, "Nigeria: Petroleum, Pollution and Poverty in the Niger Delta".

[8] Matveichuk, Alexander A. (2005). Intersection of Oil Parallels: Historical Essays. Moscow: Russian Oil and Gas Institute.

[9] McLennan, K. L. (2005). Nontechnical Guide to Petroleum Geology, Exploration, Drilling, and Production. Penn Well Corporation.

[10] Mendez, K. (2010). U.S. Department of State. Remarks on U.S. and International Cooperation in the Niger River Delta. Retrieved 8 May 2016, fromhttp://www.state.gov/p/af/rls/rm/82010.htm.

[11] National Institute for Occupational Safety and Health (NIOSH) and Occupational Safety and Health Administration (OSHA), 2005.

[12] NIOSH (2005). National Institute for Occupational Safety and Health. Pocket Guide to Chemical Hazards, DHHS (NIOSH) Publication No. 2005–149. http://www.cdc.gov/niosh/npg/ Retrieved 12 May 2016

[13] Norman J. (2001). Nontechnical Guide to Petroleum Geology, Exploration, Drilling, and Production. Penn Well Corporation.

[14] Ofehe, S. (1999). Hope for the Niger–Delta. The Netherlands. HNDC

[15] Omofonmwan, S. I. and Odia, L. O. (2009). Oil Exploitation and Conflict in the Niger–Delta Region of Nigeria. Kamla–Raj. Journal of Human Ecology 26(1): 25–30.

[16] Organization of the Petroleum Exporting Countries (OPEC), 2004

[17] Osuji, L. C. and Ukale, E. E. (2000). Post–oil Spill Fire at Ugbomro (Niger–Delta): A New Vista in Soil–Pollution Studies. Port–Harcourt. Petroleum Chemical Research Group.

[18] Robert; Organization of Petroleum Exporting Countries (2006). Oil in the 21st century: issues, challenges and opportunities. Oxford Press.

[19] United Nations Development Report (UNDP) (2005). Niger–Delta Development Human Report

[20] World Health Organisation, (2004). "Air quality and health", www.who.int. Retrieved 18 April 2016.

[21] Wurthmanm, G. "Ways of Using the African Oil Boom for Sustainable Development", African Development Bank, Economic Research Working Paper Series, No. 84, March 2006

[22] Zabbey, N. (2004). Impacts of Extractive Industries on the Biodiversity on the Niger–Delta Region, Nigeria. Centre for Environment, Human Rights and Development.

# Fascicule 3
## [ July - September ]
## t o m e
## [2018] XI

ACTA Technica CORVINIENSIS
BULLETIN OF ENGINEERING

[1.]Jimit R. PATEL, [2.]G. M. DEHERI

# FERROFLUID SQUEEZE FILM IN CURVED ROUGH POROUS CIRCULAR PLATES WITH SLIP VELOCITY: A COMPARISON OF MAGNETIC FLUID FLOW MODELS

[1.]Department of Mathematical Sciences, PD Patel Institute of Applied Sciences, Charotar University of Science and Technology, Changa–388421, Anand, Gujarat, INDIA
[2.]Department of Mathematics, Sardar Patel University, Vallabh Vidyanagar, Anand, GujaratIndia–388 120, INDIA

**Abstract:** This investigation presents a comparison of all the three magnetic fluid flow models (Neuringer–Rosensweig model, Shliomis model, Jenkins model) concerning the performance of a ferrofluid squeeze film in curved rough porous circular plates considering the slip velocity. The slip model of Beavers and Joseph's has been invoked to study the effect of slip velocity. The stochastic averaging model of Christensen and Tonder has been deployed to evaluate the effect of transverse surface roughness. The pressure distribution is obtained by solving the associated stochastically averaged Reynolds type equation. The expression for load carrying capacity is obtained thereafter. The graphical representations establish that Shliomis model remains more favourable for designing the bearing system. It is also appealing to note that for lower to moderate values of slip, Neuringer–Rosensweig model may be adopted. Besides, Jenkins model may be used when the roughness is at lower level and the slip is at minimum.
**Keywords:** Circular bearing, Ferrofluid, Roughness, Flow models, Load carrying capacity

## INTRODUCTION

It is known that the additives are added to the based lubricants to enhance the bearing characteristics in general. Magnetic fluids are stable colloidal suspensions composed of single–domain magnetic nanoparticles dispersed in a viscous fluid. The main advantage of magnetic fluid as lubricant, over the conventional oil, is that the former can be retained at a desired location by an external magnetic field and still possesses flow ability at the same time. Due to their some important physical and chemical properties the ferrofluids have been attractive in different types of engineering and other fields applications, such as, vacuum sealing, magnetic resonance, imaging, intelligent sensors, buffer solution in chips, drug delivery, grinding, separation, ink–jet printing, damper and so on.

In the last decade, various theoretical models have been put forward to study the continuum description of ferrofluid flow. However, most of the systematic studies about the motion of magnetic fluids are based on the formulation given by Neuringer and Rosensweig [1], Shliomis [2] and Jenkins [3]. Neuringer and Rosensweig [1] proposed a quite simple model where the effect of magnetic body force was measured under the assumption of magnetization vector being parallel to the magnetic field vector. However, Shliomis [2] embarked on a different formulation. He observed that the magnetic particles in the fluid had Brownian motion and their rotation affected the motion of magnetic fluids. Thus, Shliomis developed the equation of motion for ferrofluids by considering internal angular momentum due to the self–rotation of particles. Jenkins [3] modified the idea of Neuringer–Rosensweig to develop a model to describe the flow of a ferrofluid by using Maugin's modification.

A good number of papers (Agrawal [4], Shah and Bhat [5], Shah and Bhat [6], Nada and Osman [7], Deheri and Abhangi [8], Patel el al. [9], Patel and Deheri [10] and Patel el al. [11]) exist in the literature dealing with the theory of different types of bearing using Neuringer and Rosensweig flow model. It was pointed out that Neuringer–Rosensweig model enunciated the pressure and enhanced the performance of bearing system.

Thereafter, many researchers (Kumar et al. [12], Singh and Gupta [13], Lin [14], Patel and Deheri [15]) dealt with the model of Shliomis to examine the performance of different bearing's characteristics. All the above investigations analyze the steady state characteristics of the bearings lubricated with magnetic fluids, resorting to the flow model estimated by Shliomis.

It was concluded that Neuringer–Rosensweig model modified the pressure while Jenkins flow model modified both the pressure and the velocity of the Magnetic fluid. The steady–state characteristics of bearings with Jenkins model based ferrofluids were discussed by Agrawal [4], Ram and Verma [16], Shah and Bhat [17], Ahmad and Singh [18] and Patel and Deheri [19]. It was manifest in all the studies that the load carrying capacity of the bearing system increased with increasing magnetization.

Nowadays, a significant amount of tribology research has been dedicated to the study of the effect of surface roughness or geometric imperfections on hydrodynamic lubrication because the bearings surfaces, in practice, are all rough and the height of the roughness asperities may have the same order as the mean bearing clearance. Under these circumstances, the surface roughness affects the bearing performance noticeably. The deep–rooted stochastic theory

of hydrodynamic lubrication of rough surfaces developed by Christensen and Tonder [20–22] formed the basis of this paper. In a series of works (Ting [23], Praksh and Tiwari [24], Guha [25], Turaga et al. [26], Gururajan and Prakash [27], Gadelmawla et al. [28], Sinha and Adamu [29], Adamu and Sinha [30]). In fact, the model was applied to the study of the surface roughness for various geometrical configurations.

The combined effect of slip velocity and surface roughness on the performance of Jenkins model based magnetic squeeze film in curved rough annular plates was examined by Patel and Deheri [31].

It was concluded that the effect of transverse surface roughness remained adverse in general, Jenkins model based ferrofluid lubrication provided some measures in mitigating the adverse effect and this became more apparent when the slip parameter was at reduced level and negatively skewed roughness occurred. Jao et al. [32] studied a lubrication theory that included the coupled effects of surface roughness and anisotropic slips. It was found that the load ratio increased as the dimensionless slip length decreased (except the case of short bearing) or as the slenderness ratio increased. The effect of a magnetic fluid based parallel plate rough slider bearing with the comparison of all the three magnetic fluid flow models (Neuringer–Rosensweig model, Shliomis model, and Jenkins model)was investigated by Patel and Deheri [33].

However, comparison does not exist for the performance of the circular plates bearing system in all the three models. Thus, this paper investigates the combined effect of surface roughness and slip velocity on squeeze film characteristics of circular plates bearing by considering the comparison of three magnetic fluid flow models, namely, Neuringer–Rosensweig model, Shliomis model and Jenkins model.

## ANALYSIS

Figure 1 presents the formation of the squeeze film circular bearing considering the laminar flow of an incompressible fluid and transversely rough bearing surfaces between two circular plates, each of radius$a$. The upper curved plate approaches the lower curved plate with normal uniform velocity $\dot{h_0}$, where $h_0$ is the central film thickness.

In view of the theory of Christensen and Tonder [20–22], the expression for the film thickness is assumed to be made up of two parts

$$h = \bar{h} + h_s \qquad (1)$$

where $\bar{h}$ denotes the mean film thickness and $h_s$ represents the deviation from the mean film thickness characterizing the random roughness of the bearing surfaces.$h_s$is taken to be stochastic in nature and governed by a probability density function

$$f(h_s) = \begin{cases} \dfrac{35}{32c}\left(1 - \dfrac{h_s^2}{c^2}\right)^3, & -c \leq h_s \leq c \\ 0, & \text{elsewhere} \end{cases}$$

$c$ being the maximum deviation from the mean film thickness. The details of the mean$\alpha$, the standard deviation $\sigma$ and the parameter $\varepsilon$, which is the measure of symmetry of the

random variable $h_s$ are explained in Christensen and Tonder [20–22].
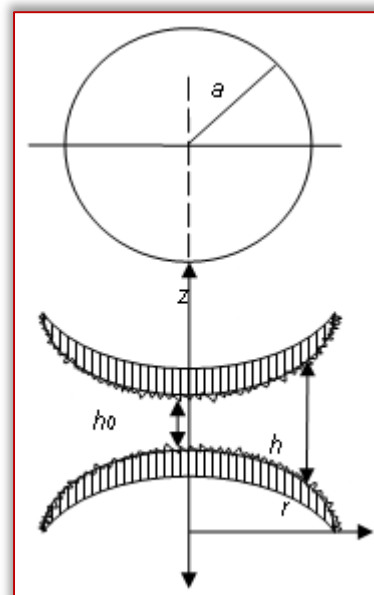


Figure 1: Circular bearing configuration

The deliberations of Bhat [34] and Patel and Deheri [35], discuss that the upper plate lying along the surface determined by the relation

$$z_u = h_0\exp(-\beta r^2); \; 0 \leq r \leq a$$

goes towards the lower plate lying along the surface given by

$$z_l = h_0\left[\frac{1}{1 + \gamma r} - 1\right]; \; 0 \leq r \leq a$$

with normal velocity $\dot{h_0}$. Where $\beta$ and $\gamma$ are the curvature parameters of the respective plates. The film thickness then, is given by (Bhat [34], Patel and Deheri [36])

$$h(r) = h_0\left[\exp(-\beta r^2) - \frac{1}{1 + \gamma r} + 1\right];$$
$$0 \leq r \leq a \qquad (2)$$

A simple flow model proposed by Neuringer and Rosensweig [1] examined the steady flow of magnetic fluids in the presence of slowly changing external magnetic fields. The model was developed by the following expressions

$$\rho(\bar{q}\nabla)\bar{q} = -\nabla p + \eta\nabla^2\bar{q} + \mu_0(\bar{M}\nabla)\bar{H} \qquad (3)$$
$$\nabla\bar{q} = 0 \qquad (4)$$
$$\nabla \times \bar{H} = 0 \qquad (5)$$
$$\bar{M} = \bar{\mu}\bar{H} \qquad (6)$$
$$\nabla(\bar{H} + \bar{M}) = 0 \qquad (7)$$

where $\rho$ is the fluid density, $\bar{q}$ being the fluid velocity in the film region, $\bar{H}$ represents external magnetic field, $\bar{\mu}$ isthe magnetic susceptibility of the magnetic field, $p$represents the film pressure, $\eta$ denotes the fluid viscosity and $\mu_0$ representsthe permeability of the free space. The details can be seen from Bhat [34] and Prajapati [37].

Using equations (4)–(6), equation (3) becomes

$$\rho(\bar{q}\nabla)\bar{q} = -\nabla\left(p - \frac{\mu_0\bar{\mu}}{2}M^2\right) + \eta\nabla^2\bar{q}$$

The Reynolds equation with modification governing the film pressure for Neuringer and Rosensweig model then, is given by

$$\frac{1}{r}\frac{d}{dr}\left[h^3 r\frac{d}{dr}\left(p-\frac{\mu_0\bar{\mu}}{2}M^2\right)\right]=12\eta\dot{h_0} \qquad (8)$$

Shliomis [2] pointed out that magnetic particles of a magnetic fluid could relax in two ways, by the rotation of magnetic particles in the fluid and by rotation of the magnetic moment with in the particles, when the applied magnetic field changed. According to Bhat [34] and Patel and Deheri [35], the modified Reynolds type equation for Shliomis model comes out to be

$$\frac{1}{r}\frac{d}{dr}\left(h^3 r\frac{dp}{dr}\right)=12\eta_a\dot{h_0}$$
$$=12\eta(1+\tau)\dot{h_0} \qquad (9)$$

The details of the derivation of the expression (9) are already discussed in Bhat [34] and Patel and Deheri [35, 31].

Jenkins [3] modified the theory of Neuringer–Rosensweig model and investigated a model to depict the flow of a ferrofluid. Using the Maugin's modification, equation for the model for steady flow becomes (Jenkins [3], Ram and Verma [16], Patel and Deheri [10]).

$$\rho(\bar{q}.\nabla)\bar{q}=-\nabla p+\eta\nabla^2\bar{q}+\mu_0(\bar{M}.\nabla)\bar{H}+\frac{\rho A^2}{2}\nabla$$
$$\times\left[\frac{\bar{M}}{M}\times\{(\nabla\times\bar{q})\times\bar{M}\}\right] \qquad (10)$$

together with equations (4)–(7), A denotes a material constant. From equations (3) and (10) it is found that Jenkins model is a generalization of Neuringer– Rosensweig model with an additional term

$$\frac{\rho J^2}{2}\nabla\times\left[\frac{\bar{M}}{M}\times\{(\nabla\times\bar{q})\times\bar{M}\}\right]$$
$$=\frac{\rho A^2\bar{\mu}}{2}\nabla\times\left[\frac{\bar{H}}{H}\times\{(\nabla\times\bar{q})\times\bar{H}\}\right] \qquad (11)$$

which improves the velocity of the fluid.

In view of the discussions of Bhat [34] and Patel and Deheri [35], the modified Reynolds equation for Jenkins model can be found in the form of,

$$\frac{1}{r}\frac{d}{dr}\left(\frac{h^3}{\left(1-\frac{\rho A^2\bar{\mu}H}{2\eta}\right)}r\frac{d}{dr}\left(p-\frac{\mu_0\bar{\mu}}{2}H^2\right)\right)$$
$$=12\eta\dot{h_0} \qquad (12)$$

Taking into account the usual assumptions of hydrodynamic lubrication (Bhat [34], Prajapati [37], Deheri et al. [38]) and the stochastic modelling of Christensen and Tonder [20–22], the modified Reynolds' equation leading to the pressure distribution takes the form for Neuringer–Rosensweig model, Shliomis model and Jenkins model, respectively as,

$$\frac{1}{r}\frac{d}{dr}\left[g(h)r\frac{d}{dr}\left(p-\frac{\mu_0\bar{\mu}}{2}M^2\right)\right]=12\eta\dot{h_0} \qquad (13)$$

$$\frac{1}{r}\frac{d}{dr}\left(g(h)r\frac{dp}{dr}\right)=12\eta(1+\tau)\dot{h_0} \qquad (14)$$

and

$$\frac{1}{r}\frac{d}{dr}\left(\frac{g(h)}{\left(1-\frac{\rho A^2\bar{\mu}H}{2\eta}\right)}r\frac{d}{dr}\left(p-\frac{\mu_0\bar{\mu}}{2}H^2\right)\right)$$

$$=12\eta\dot{h_0} \qquad (15)$$

where

$$g(h)=(h^3+3h^2\alpha+3(\sigma^2+\alpha^2)h+3\sigma^2\alpha+\alpha^3+\varepsilon$$
$$+12\phi H_0)\left(\frac{4+sh}{2+sh}\right),$$

$\phi$ being the permeability of the porous facing and $H_0$ denotes the thickness of the porous facing.

The following dimensionless quantities are considered

$$\bar{h}=\frac{h}{h_0},R=\frac{r}{a},P=-\frac{h_0^3 p}{\eta a^2 \dot{h_0}},B=\beta a^2,$$
$$C=\gamma a,\bar{\sigma}=\frac{\sigma}{h_0},\bar{\alpha}=\frac{\alpha}{h_0},\bar{\varepsilon}=\frac{\varepsilon}{h_0^3},$$
$$M^2=H^2=kr^2\frac{(a-r)}{a},\mu^*=-\frac{k\mu_0\bar{\mu}h_0^3}{\eta\dot{h_0}},$$
$$\bar{A}^2=\frac{\rho A^2\bar{\mu}\sqrt{ka}}{2\eta},\bar{s}=sh_0,\bar{\psi}=\frac{\phi H}{h_0^3} \qquad (16)$$

The associated boundary conditions are

$$P(1)=0,\left(\frac{dP}{dR}\right)_{R=0}=0 \qquad (17)$$

Using the dimensionless quantities (16), the equations (13–15) convert respectively into,

$$\frac{1}{R}\frac{d}{dR}\left[g(\bar{h})R\frac{d}{dR}\left(P-\frac{\mu^*}{2}R^2(1-R)\right)\right]=-12 \qquad (18)$$

$$\frac{1}{R}\frac{d}{dR}\left(g(\bar{h})R\frac{dP}{dR}\right)=-12(1+\tau) \qquad (19)$$

and

$$\frac{1}{R}\frac{d}{dR}\left(\frac{g(\bar{h})}{(1-\bar{A}^2 R\sqrt{1-R})}R\frac{d}{dR}\left(P-\frac{\mu^*}{2}R^2(1-R)\right)\right)$$
$$=-12 \qquad (20)$$

where

$$g(\bar{h})=\left(\bar{h}^3+3\bar{h}^2\bar{\alpha}+3(\bar{\sigma}^2+\bar{\alpha}^2)\bar{h}+3\bar{\sigma}^2\bar{\alpha}+\bar{\alpha}^3+\bar{\varepsilon}\right.$$
$$\left.+12\bar{\psi}\right)\left(\frac{4+\bar{s}\bar{h}}{2+\bar{s}\bar{h}}\right)$$

With the help of the boundary conditions (16), solving equations (18–20), the non–dimensional pressure for Neuringer–Rosensweig model, Shliomis model and Jenkins model, found respectively as,

$$P=\frac{\mu^*}{2}R^2(1-R)-6\int_1^R\frac{R}{g(\bar{h})}dR \qquad (21)$$

$$P=-6(1+\tau)\int_1^R\frac{R}{g(\bar{h})}dR \qquad (22)$$

and

$$P=\frac{\mu^*}{2}R^2(1-R)$$
$$-6\int_1^R\frac{R}{g(\bar{h})}\left(1-\bar{A}^2 R\sqrt{1-R}\right)dR \qquad (23)$$

One can obtain the dimensionless load carrying capacity for all three cases, respectively as,

$$W = -\frac{h_0^3}{2\pi\eta a^4 \dot{h_0}} w = \int_0^1 RPdR$$

$$= \frac{\mu^*}{40} + 3\int_0^1 \frac{R^3}{g(\bar{h})}dR \qquad (24)$$

$$W = -\frac{h_0^3}{2\pi\eta a^4 \dot{h_0}} w = \int_0^1 RPdR$$

$$= 3(1+\tau)\int_0^1 \frac{R^3}{g(\bar{h})}dR \qquad (25)$$

and

$$W = -\frac{h_0^3}{2\pi\eta a^4 \dot{h_0}} w = \int_0^1 RPdR$$

$$= \frac{\mu^*}{40} + 3\int_0^1 \frac{R^3}{g(\bar{h})}(1 - \bar{A}^2 R\sqrt{1-R})dR \qquad (26)$$

## RESULTS AND DISCUSSIONS

It is noticed that equations (24–26) determine the non–dimensional $W$. It is observed that the $W$ enhances by $\frac{\mu^*}{40}$ in the case of Neuringer–Rosensweig model and Jenkins model while the increase in load carrying capacity for the case of Shliomis model is found to be $3\tau\int_0^1 \frac{R^3}{g(\bar{h})}dR$ as compared to the case of traditional lubricant based bearing system. This is perhaps due to the fact that the viscosity of the lubricant gets increased owing to magnetization, there by leading to increased pressure and hence the load carrying capacity. A glance at the expression of the load suggests that the expressions are linear with respect to the magnetization parameter. This means an increase in the magnetization parameter would always result in enhanced $W$.

The variation of $W$ with respect to magnetization presented in Figures 2–7 ensures that an increase in the magnetic strength leads to enhance $W$, the most increase being in the case of Shliomis model. Although a nominal increase in $W$ is noticed for Neuringer–Rosensweig model and Jenkins model, the effect of $\mu^*$ is more sharp in the case of Shliomis model.
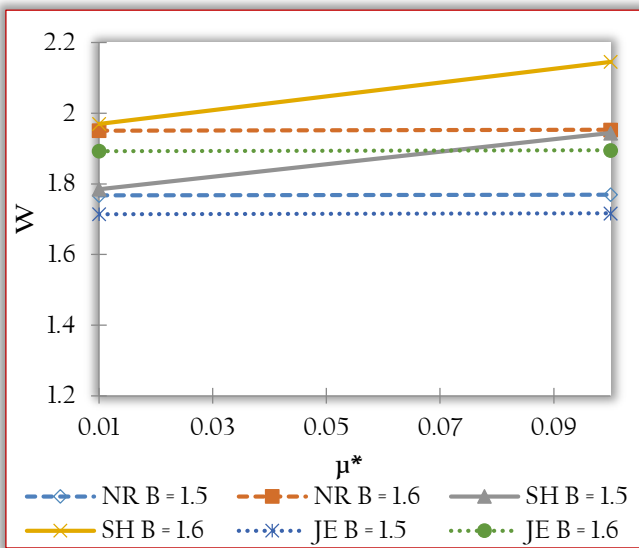


Figure 2: Variation of $W$ with respect to $\mu^*$ and $B$.
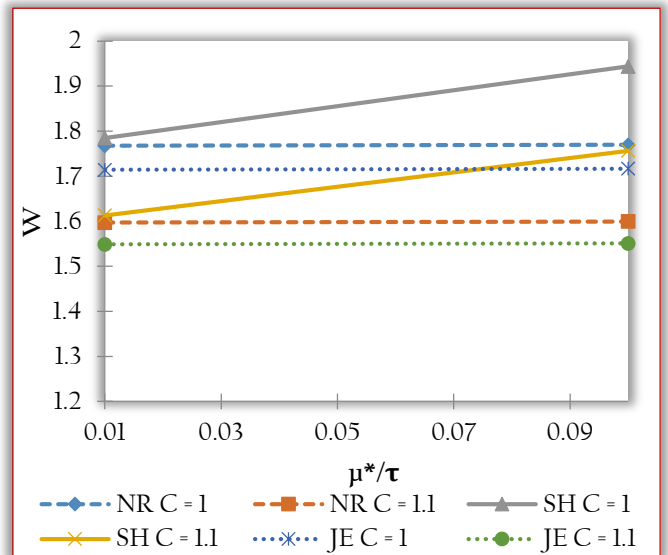


Figure 3: Variation of $W$ with respect to $\mu^*$ and $C$.
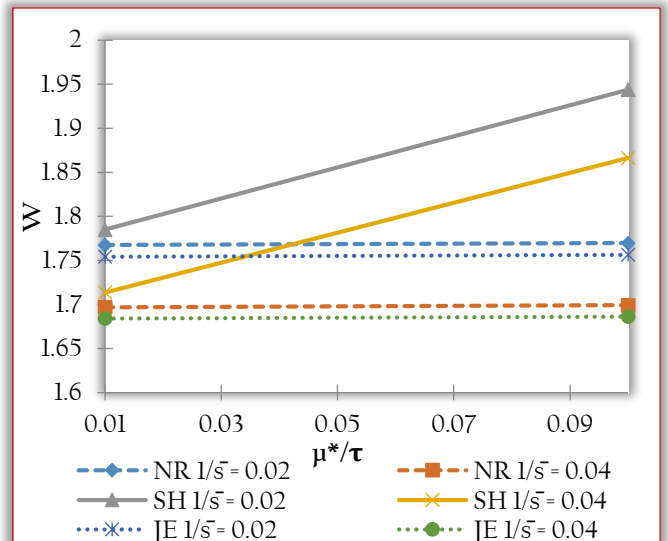


Figure 4: Variation of $W$ with respect to $\mu^*/\tau$ and $1/\bar{s}$.
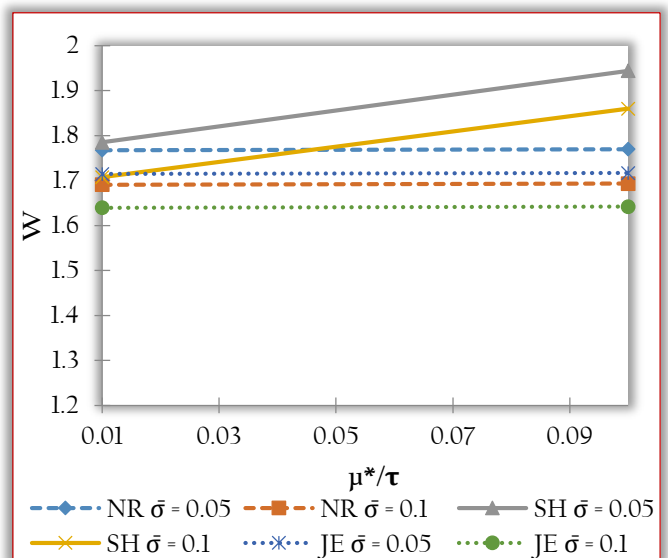


Figure 5: Variation of $W$ with respect to $\mu^*/\tau$ and $\bar{\sigma}$.

The combined effect of curvature parameters given in Figures 8–11 indicates that the lower plates curvature parameters affects the most in the case of Jenkins model.
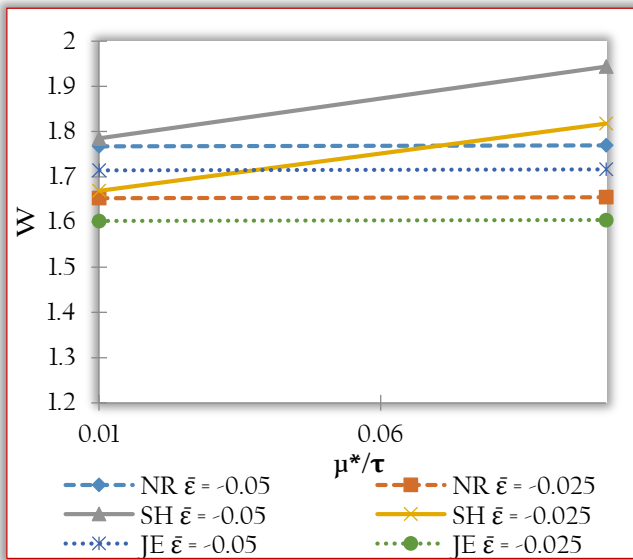


Figure 6: Variation of **W** with respect to $\mu^*/\tau$ and $\bar{\varepsilon}$.
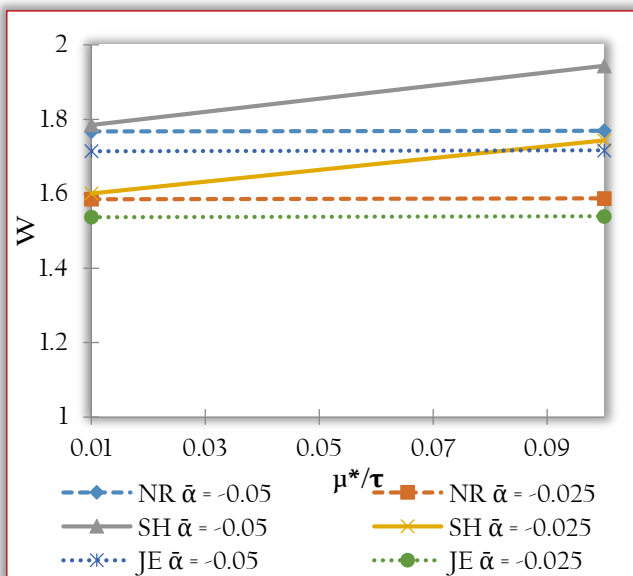


Figure 7: Variation of **W** with respect to $\mu^*/\tau$ and $\bar{\alpha}$.
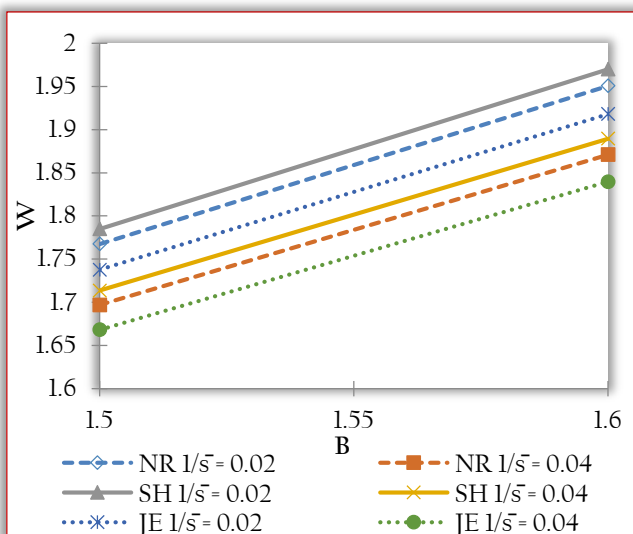


Figure 8: Variation of **W** with respect to **B** and $1/\bar{s}$.
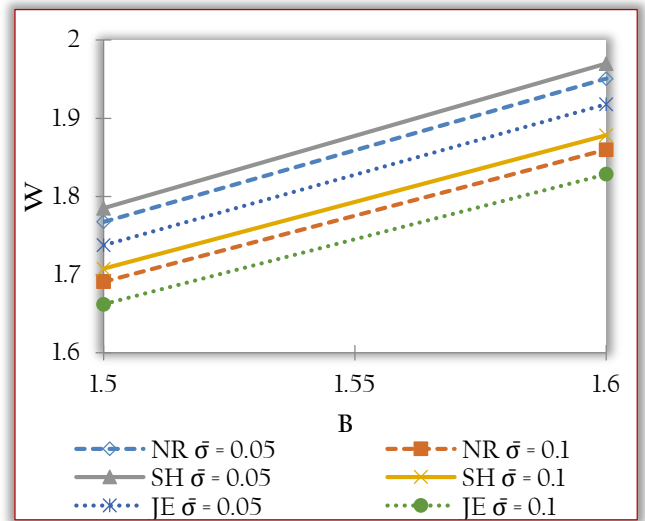


Figure 9: Variation of **W** with respect to **B** and $\bar{\sigma}$.
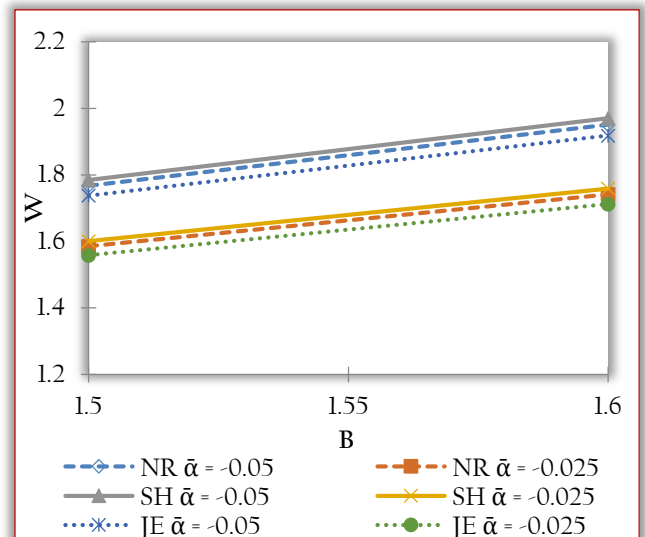


Figure 10: Variation of **W** with respect to **B** and $\bar{\alpha}$.
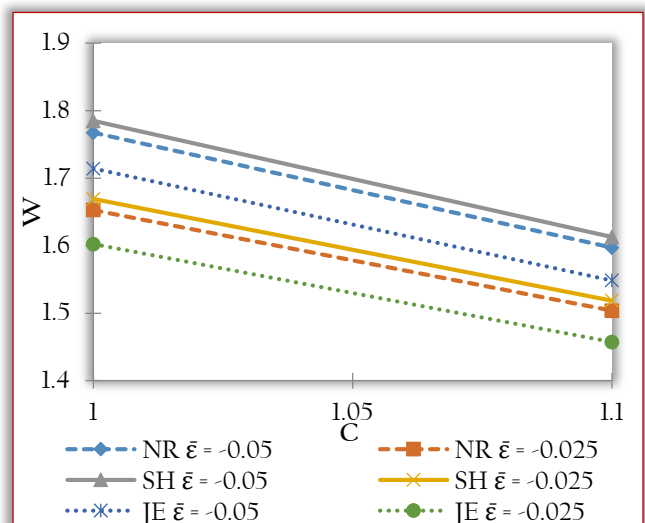


Figure 11: Variation of **W** with respect to **C** and $\bar{\varepsilon}$.

The effect of slip velocity encountered in Figures 12–14 suggests that the slip effect is comparatively more in the case of Jenkins model.
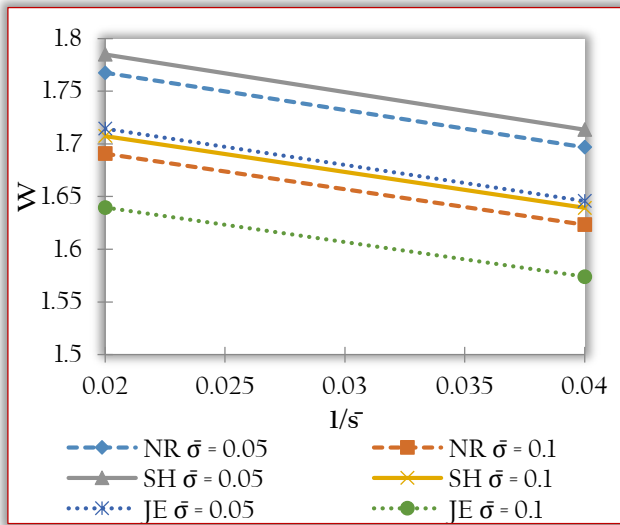


Figure 12: Variation of $W$ with respect to $1/\bar{s}$ and $\bar{\sigma}$.
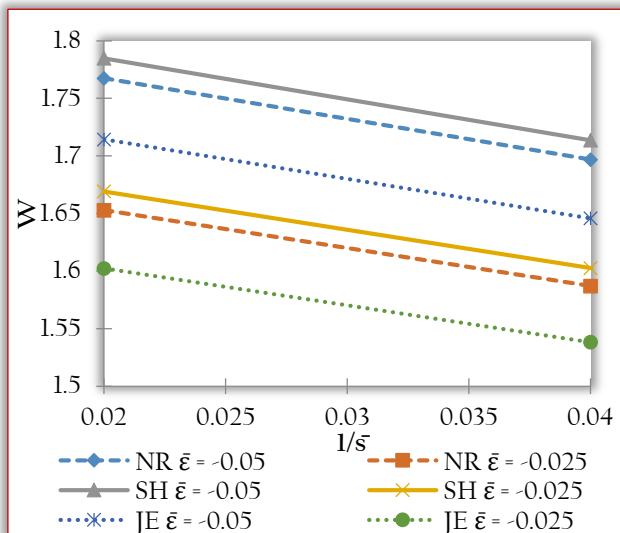


Figure 13: Variation of $W$ with respect to $1/\bar{s}$ and $\bar{\varepsilon}$.
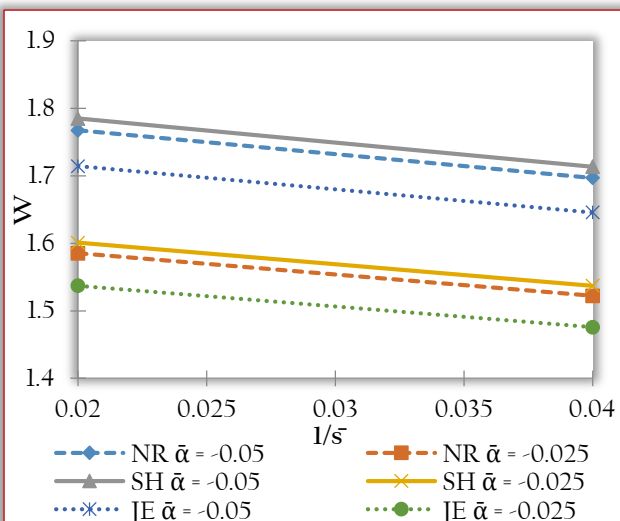


Figure 14: Variation of $W$ with respect to $1/\bar{s}$ and $\bar{\alpha}$.
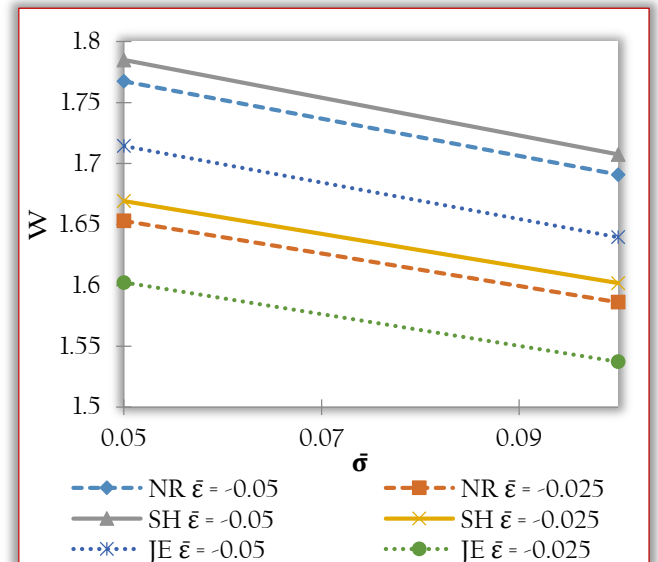


Figure 15: Variation of $W$ with respect to $\bar{\sigma}$ and $\bar{\varepsilon}$.
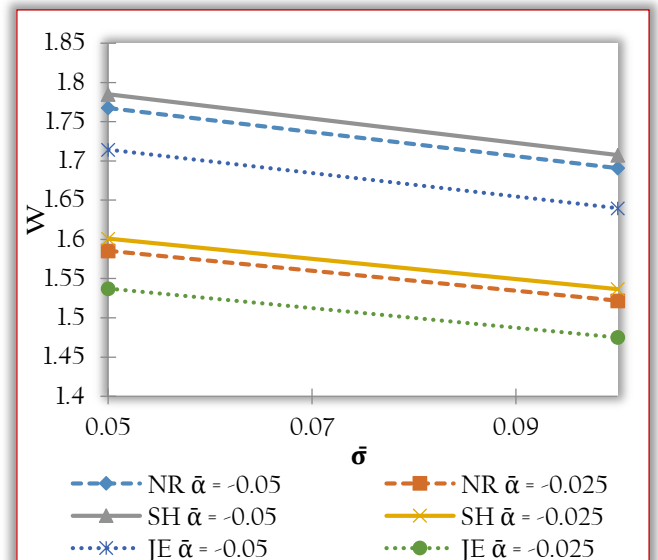


Figure 16: Variation of $W$ with respect to $\bar{\sigma}$ and $\bar{\alpha}$.
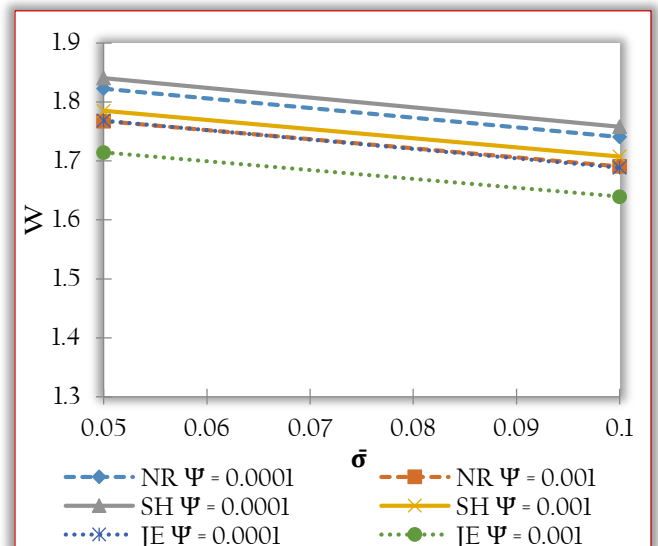


Figure 17: Variation of $W$ with respect to $\bar{\sigma}$ and $\bar{\psi}$.
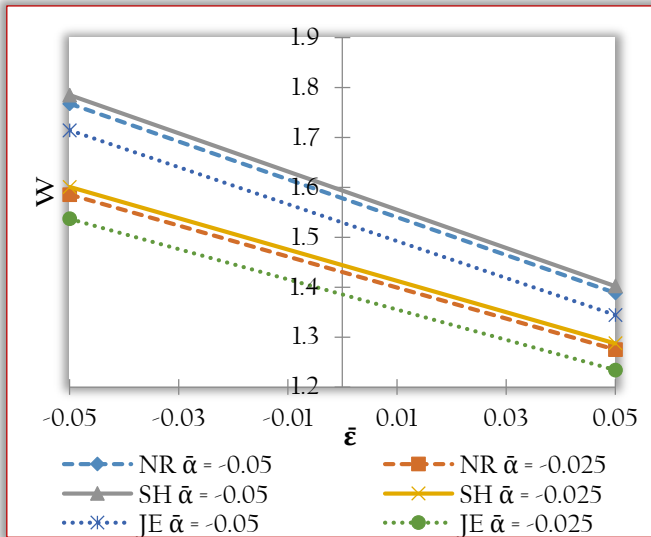
Figure 18: Variation of **W** with respect to $\bar{\varepsilon}$ and $\bar{\alpha}$.
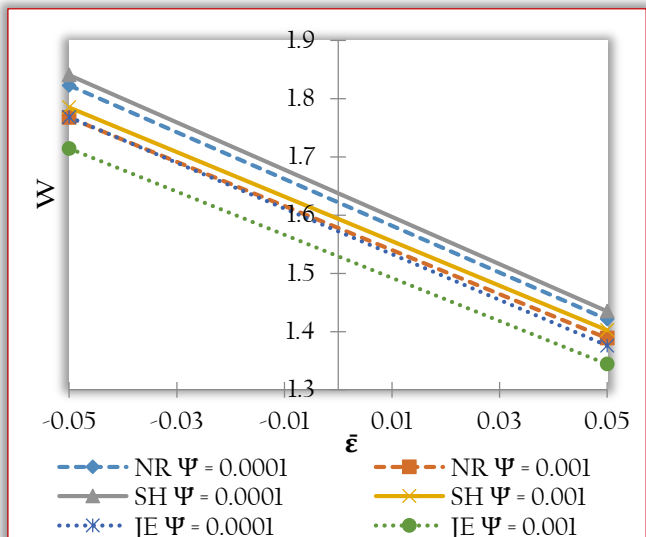


Figure 19: Variation of **W** with respect to $\bar{\varepsilon}$ and $\bar{\psi}$.
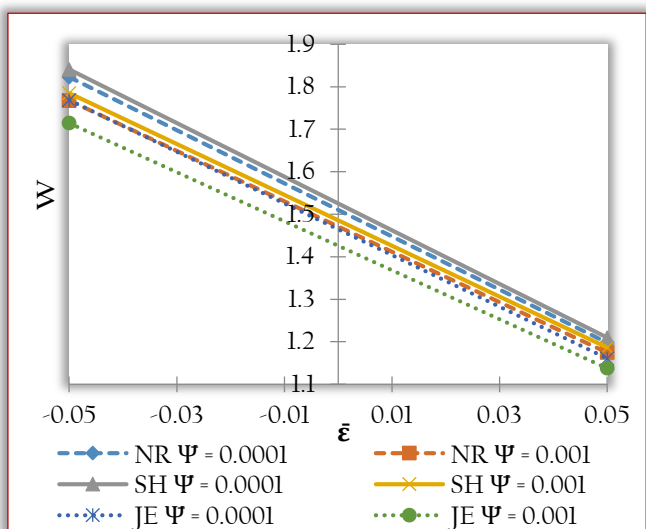


Figure 20: Variation of **W** with respect to $\bar{\varepsilon}$ and $\bar{\psi}$.

The effect of transverse surface roughness on the **W** found in Figures 15–20 establishes that the adverse effect of transverse surface roughness is registered to be more in the case of Jenkins model. It is interesting here to note that for moderate to higher values of roughness the Shliomis model goes past the Neuringer–Rosensweig model in reducing the effect of surface roughness.

As it happens mostly, the porosity leads to decreased **W** and the situation turns out to be worse when the higher values of slip are involved.

In addition, the comparison of graphical representations reveals the following:

— All the three models improve the bearing performance. So far as magnetization is concerned Neuringer–Rosensweig model performs a little better as compared to Jenkins model while the Shliomis model remains the best.

— The Shliomis model comes out to be more effective in comparison with other two models exclusively, from surface roughness point of view. Further, Neuringer–Rosensweig model and Jenkins model differ a little when the combined effect of negative skewness and variance (–ve) is considered.

— A key point to be noted is that the standard deviation reduces the **W** significantly which fails to happen in the case of parallel plate slider bearing in the absence of slip.

— When the slip is at minimum the effect of negatively skewed roughness may provide some amount of help to improve the bearing performance in the case of all the three models when the variance (–ve) occurs.

— If one considers the combined effect of roughness and slip the Shliomis model stays ahead of the other two models for all the values of porosity.

— Up to certain extent the effect of standard deviation remains more manifest in the Neuringer–Rosensweig model as compared to Jenkins model.

— Besides, the Shliomis model scores over the other two models in lowering the adverse effect of porosity and slip.

## CONCLUSION

This study concludes that the load carrying capacity gets increased approximately by 2 to 3 percent as compared to the case of conventional fluid based curved rough porous circular squeeze films with slip velocity. Some of the graphical representations indicate that the Neuringer–Rosensweig model may be deployed to compensate the effect of surface roughness when the slip and porosity are at reduced level. However, for a bearing design point of view Shliomis model may be preferred for moderate to higher loads irrespective of the slip effect.

For nominal roughness and moderate slip velocity Neuringer–Rosensweig model and Jenkins model perform alike. The bearing system always supports certain amount of load even when there is no flow which never happens in the case of traditional lubricant based bearing system. However, the load supported by the bearing system in the absence of flow remains significantly higher in the case of Shliomis

model. At the same time this discussion underlines that the roughness aspect is required to be carefully evaluated while designing the bearing system even if Shliomis model is in force. It is needless to say that a suitable choice of the ratio of curvature parameters may provide augmented performance of the squeeze film bearing system.

References

[1] J.L. Neuringer, R.E. Rosensweig, Magnetic Fluids, Magnetic Fluid, Physics of Fluids. 7(12) (1964)1927.

[2] M.I. Shliomis, Effective viscosity of magnetic suspensions, Sov. Physics JETP. 34(6) (1972) 1291–1294.

[3] J.T. Jenkins, A theory of magnetic fluids, Archive for Rational Mechanics and Analysis. 46(1972) 42–60.

[4] V.K. Agrawal, Magnetic–fluid–based porous inclined slider bearing. Wear 107(2) (1986) 133–139.

[5] R.C. Shah, M.V. Bhat, Squeeze film based on magnetic fluid in curved porous rotating circular plates, Journal of Magnetism and Magnetic Materials. 208(1) (2000) 115–119.

[6] R.C. Shah, M.V. Bhat, Magnetic fluid based porous inclined slider bearing with velocity slip, Int. J. of Applied Mechanics and Engineering. 18(2) (2003) 331–336.

[7] G.S. Nada, T.A. Osman, Static performance of finite hydrodynamic journal bearings lubricated by magnetic fluids with couple stresses, Tribology Letters. 27(3) (2007) 261– 268.

[8] G.M. Deheri, N.D. Abhangi, Numerical modelling of a magnetic fluid–based squeeze film between rotating transversely rough curved circular plates, International Journal of Computational Materials Science and Surface Engineering. 4(3) (2011)185–204.

[9] N.S. Patel, D.P. Vakharia, G.M. Deheri, A study on the performance of a magnetic–fluid–based hydrodynamic short journal bearing, ISRN Mechanical Engineering. 2012 (2012), Article ID 603460.

[10] J.R. Patel, G. Deheri, A study of thin film lubrication at nanoscale for a ferrofluid based infinitely long rough porous slider bearing, Facta Universitatis, Series: Mechanical Engineering,14(1)(2016) 89–99.

[11] N.S. Patel, D.P. Vakharia, G.M. Deheri, H.C. Patel, Experimental performance analysis of ferrofluid based hydrodynamic journal bearing with different combination of materials, Wear. 376–377(2017), 1877–1884.

[12] D. Kumar, P. Sinha, P. Chandra, Ferrofluid squeeze film for spherical and comical bearings, Int. J. Engg. Sci. 30(5) (1992) 645–656.

[13] U.P. Singh, R.S. Gupta, Dynamic performance characteristics of a curved slider bearing operating with ferrofluid, Advances in Tribology. 2012 (2012), Article Id 278723.

[14] J.R. Lin, Fluid inertia effects in ferrofluid squeeze film between a sphere and a plate, Applied Mathematical Modeling. 37(7) (2013) 5528–5535.

[15] J.R. Patel, G. Deheri, Shliomis model–based magnetic squeeze film in rotating rough curved circular plates: a comparison of two different porous structures, Int. J. of Computational Materials Sci. and Sur. Eng. 6(1) (2014) 29–49.

[16] P. Ram, P.D.S. Verma, Ferrofluid lubrication in porous inclined slider bearing, Indian Journal of Pure and Applied Mathematics. 30(12) (1999)1273–1281.

[17] R.C. Shah, M.V. Bhat, Ferrofluid lubrication in porous inclined slider bearing with velocity slip, International Journal of Mechanical Sciences. 44(12) (2002) 2495–2502.

[18] N. Ahmad, J.P. Singh, Magnetic fluid lubrication of porous pivoted slider bearing with slip velocity, Proceedings of the Institution of Mechanical Engineers Part J: Journal of Engineering Tribology. 221(5)(2007) 609–613.

[19] J.R. Patel, G. Deheri, Combined Effect of Surface Roughness and Slip Velocity on Jenkins Model Based Magnetic Squeeze Film in Curved Rough Circular Plates, International Journal of Computational Mathematics. 2014 (2014) Article ID 367618.

[20] H. Christensen, K.C. Tonder, Tribology of rough surfaces: stochastic models of hydrodynamic lubrication, SINTEF. Report No.10/69–18 (1969a).

[21] H. Christensen, K.C. Tonder, Tribology of rough surfaces: parametric study and comparison of lubrication models, SINTEF. Report No.22/69–18 (1969b).

[22] H. Christensen, K.C. Tonder, The hydrodynamic lubrication of rough bearing surfaces of finite width, ASME–ASLE Lubrication Conference. Paper no.70–lub–7, 1970.

[23] L.L. Ting, A Mathematical analog for determination of porous annular disk squeeze film behavior including the fluid inertia effect, J. Basic Engg.Trans.ASME. 94(1972) 417–421.

[24] J. Prakash, K. Tiwari, Roughness effects in porous circular squeeze–plates with arbitrary wall thickness, J. Lubr. Tech. 105(1) (1983) 90–95.

[25] S.K. Guha, Analysis of dynamic characteristics of hydrodynamic journal bearings with isotropic roughness effects, Wear. 167 (2) (1993) 173–179.

[26] Ram, Turaga, A.S. Sekhar, B.C. Majumdar, Stochastic FEM analysis of finite hydrodynamic bearings with rough surfaces, Tribology Transactions. 40(4)( 1997) 605–612.

[27] K. Gururajan, J. Prakash, Effect of surface roughness in a narrow porous journal bearing, J. Tribology. 122(2) (2000) 472–475.

[28] E.S. Gadelmawla, M.M. Koura, T.M.A. Maksoud, I.M. Elewa, H.H. Sollman, Roughness parameters, Journal of materials processing Technology. 123 (1) (2002) 133–145.

[29] P. Sinha, G. Adamu, THD analysis for slider bearing with roughness: special reference to load generation in parallel sliders, Acta Mech. 207 (2009) 11–27.

[30] G. Adamu, P. Sinha, Thermal and Roughness Effects in a Tilted Pad Slider Bearing Considering Heat Conduction Through the Pad and Slider, Proceedings of the National Academy of Sciences, India Section A: Physical Sciences, 82(4) (2012) 323-333.

[31] J.R. Patel, G.M. Deheri, Jenkins model based ferrofluid lubrication of a curved rough annular squeeze film with slip velocity, Tribology in Industry. 37(2) (2015) 129–141.

[32] Hsiang–Chin Jao, Kuo–Ming Chang, Li–Ming Chu, Wang–Long Li, A Modified Average Reynolds Equation for Rough Bearings With Anisotropic Slip, Journal of Tribology. 138(1)(2016)011702–1–14.

[33] J. R. Patel and G. M. Deheri, Performance of a Ferrofluid Based Rough Parallel Plate Slider Bearing: A Comparison of Three Magnetic Fluid Flow Models, Advances in Tribology. 2016(2016) Article ID 8197160.

[34] M.V. Bhat, Lubrication with a Magnetic fluid, Team Spirit (India) Pvt. Ltd, India, 2003.

[35] Patel, J.R. and Deheri, G., Effect of various porous structures on the Shliomis model based ferrofluid lubrication of the film squeezed between rotating rough curved circular plates, FactaUniversitatis, Series: Mechanical Engineering. 12 (3) (2014) 305–323.

[36] J. R. Patel and G. M. Deheri, Numerical modeling of Jenkins model based ferrofluid lubrication squeeze film performance in rough curved annular plates under the presence of slip velocity, FactaUniversitatis, Ser. Math. Inform. 31(1) (2016) 11–31.

[37] B.L. Prajapati, On Certain Theoretical Studies in Hydrodynamic and Electro–magneto hydrodynamic Lubrication, Ph.D. Thesis,S.P. University, VallabhVidya–Nagar, 1995.

[38] G.M. Deheri, P.I. Andharia, R.M. Patel, Transversely rough slider bearings with squeeze film formed by a magnetic fluid, Int. J. of Applied Mechanics and Engineering. 10(1) (2005) 53–76.

# Fascicule 3
## [ July - September ]
## t o m e
## [2018] XI

ACTA Technica CORVINIENSIS
BULLETIN OF ENGINEERING

1.K. AGYEKUM

# STATE-OF-THE-ART REVIEW OF CURRENT LITERATURE AND DEVELOPMENT STUDIES ON RECYCLED AGGREGATE CONCRETE

1.Department of Building Technology, Kwame Nkrumah University of Science and Technology, Kumasi, GHANA

**Abstract:** The expansion of the world's population has given rise to increase in the consumption of natural resources and energy which has consequently led to increased amounts of wastes. In the quest to control such wastes, researchers in the construction industry are looking for alternative materials that could be generated from such materials. One of such materials gotten from waste from construction sites is recycled concrete aggregates (RCAs) which is used in the production of recycled aggregate concrete (RAC). Studies on RACs have been on the rise since time immemorial. This study reviews current research and development studies on recycled aggregate concrete. A similar methodology used by Darko and Chan in their study in 2016 was followed. The paper examined issues related to RAC by analyzing 41 research papers published in 12 selected Construction Materials Journals from 2013 to 2017. The analysis was done based on the current review of related literature, the contributions of various countries, research institutions/universities and authors. The findings revealed that there has been a good number of RAC research papers published between 2013 and 2017. During the studied periods, researchers from developed countries like USA, UK, Spain, Portugal, China and Canada had made major contributions to studies on RACs. Researchers from developing countries like India and Turkey had also made good efforts at carrying out studies on RACs. The findings further revealed that such researchers have currently focused their attention on partially replacing virgin aggregates with recycled aggregates to determine some physical, mechanical and durability properties of concrete produced. This study has shed light on the current state of RAC research, which should be of immense benefit to both industry practitioners and academic researchers worldwide.
**Keywords:** recycled concrete aggregate, recycled coarse aggregate, recycled fine aggregate, recycled aggregate concrete

## INTRODUCTION

Increase in the world's population has given rise to an increase in the use of natural resources and energy which has consequently led to the increased amounts of wastes of such resources [1]. For several decades now environmental concerns has been a hot issue amongst professionals within the construction industry, and this has given rise to finding ways to make the industry more sustainable [2, 3, 4]. According to DEFRA [5], the construction industry contributes around 100 million tonnes of waste a year, out of which 60 million tonnes of such waste is generated from concrete. This point was buttressed by Somani et al. [6] who revealed in their study that in every 100 parts of construction waste, 40 parts are made up of concrete, 30 parts of ceramics, 5 parts of plastics, 10 parts of wood, 5 parts of metals, and 10 parts of other mixed compounds, making concrete the most wasted material on construction sites worldwide. Although about 46 million tonnes of this waste is recycled [2], approximately 127 million tonnes of natural aggregates are quarried per year [7]. This does not only deplete the environment, but also consumes about 209.5 million kWh of energy [7]. It is therefore evident that reducing the environmental impact of aggregates will provide an opportunity to reduce the overall environmental impact of concrete and the construction industry [8,9].

An attractive way to ensure sustainability of the virgin aggregates is to recycle concrete from construction and demolition wastes into recycled/crushed concrete aggregates (R/CCAs). According to Deng et al. [10], replacing virgin aggregates with recycled aggregates in construction applications is considered as an approach that can contribute to a greater sustainability in construction. Replacing virgin aggregates with RCAs has gained recognition in the construction industry over the last few decades. This is mainly because of some of its associated advantages which include but are not limited to: opening up the possibility of providing a sustainable end use to concrete waste; providing a solution to the scarcity and depletion of virgin aggregates; and conservation of the natural aggregate resources [11]. These advantages associated with RCAs based on previous findings have recently motivated researchers to turn their attention towards investigating more into the potential use of RCA as a constituent material in concrete [11]. These recent studies have also been tailored towards determining the level of performance/applications of the concrete that results from RCAs (commonly called recycled aggregate concrete, RAC). The American Concrete Institute [12] reported that the use of RCA in structural concrete has specifically gained interest because it also enables closed-loop recycling.

From these reports it has become very necessary to examine the current research trend and development studies on recycled/crushed aggregate concrete to pave way for future research in the area. This study seeks to conduct a state-of-the-art review of current literature on recycled/crushed aggregate concrete. On a more specific note, the study assesses current development studies on RACs and the contributions of authors and institutions or universities to RAC research. The review is based on selected studies

conducted from 2013 to 2017. Studies conducted in these years were considered because detailed review of literature on previous studies had been conducted by [13,14,15]. There is therefore the need to know the current development studies in the area after these studies had been conducted.

## LITERATURE REVIEW

Recycled Concrete Aggregates (RCAs) became an increasingly popular construction material for replacing virgin aggregates from the beginning of the 1980s. Several factors have contributed to the promotion of RCAs in the construction industry. These factors include increased environmental concerns, scarcity of landfill sites, and the rapid depletion of sources of virgin aggregates in some countries [16].

### ▬ Definitions of recycled concrete aggregate and recycled aggregate concrete

Over the last decade a significant volume of research in the area of RCA concrete and its possible application in the construction industry has been carried out [17]. Recycled Concrete Aggregate (RCA) has been defined in several ways by several authors worldwide. The Structural Engineer [18] revealed that the terminology that relates to recycled aggregates varies between users, and it is often used to describe all non-primary aggregates.

According to the British Standard, BS 8500-1[19], RCA is an aggregate that principally comprise of crushed concrete, or which results from the processing of inorganic materials previously used in construction. Rao et al. [20] threw more light on the definition by BS 8500-1 by stating the processes involved in the generation of RCAs. According to the researchers, RCA is mainly composed of construction waste materials that have been taken through the processes of sorting, screening and crushing, and used to replace virgin aggregate in concrete production [20]. In their definition, The World Business Council for Sustainable Development, WBCSD, [21] also stated clearly that when concrete is diverted from waste streams and recycled for use in a new concrete product, a recycled aggregate concrete is obtained. The Structural Engineer [18] agreed to the definitions provided by BS 8500-1 and WBCSD [21] by indicating that RCAs are generally formed from crushed construction wastes or byproducts of industrial processes. In 2013, Clear expounded these definitions by iterating that RCA is an aggregate that is obtained from the disintegration of inert construction and demolition waste. According to Clear [22], for it to be classified as RCA, it should basically be made up of crushed concrete, and for it to be classified as recycled aggregate (RA), it should contain some substantial amount of materials other than crushed concrete. Ismail and Ramli [23] agreed to this definition, but added a bit of a touch by indicating that such RCAs are made up of virgin aggregates but are encompassed with some specific amount of adhered mortar. The BSI [24] then came in again, but shifted their attention a bit from the crushing of the concrete to the aggregates obtained from the crushed concrete. Now the emphasis was no more on the concrete that had been crushed, but on the properties of the aggregates obtained from the crushed concrete. According to the BSI [24], recycled aggregates result from the processing of inorganic materials previously used in construction. It was further specified that the RA that is obtained from the RAC should possess certain key qualities. Despotovic [25] added on to the definitions given by the BSI [24] and Ismail and Ramli [23], and stated that RCA is derived from concrete and demolition wastes generally consisting of natural coarse aggregates adhered to mortar, and which makes it porous, inhomogeneous and less dense due to higher mortar contents. Looking as though the definitions of RCAs have been exhausted, Awoyera et al. [26] did not have much to add to that already known. In their study, RCA was defined as concrete that is generally produced with the inclusion of construction and demolition wastes.

RCA can be classified into three groups [27]. The groups include aggregates that are mainly composed of masonry rubbles (Group 1), aggregates gotten from concrete rubbles (Group 2), and aggregates which are made up of a mixture of virgin aggregates and rubbles from Groups 1 and 2 (Group 3). According to Katz [27], the third group is more appropriate for producing all kinds of concrete. However, there are limitations to the use of the other two groups [27].

### ▬ Properties of RAC

Concrete made with RCA may have its mechanical properties like that of a conventional concrete produced with virgin aggregates [28, 29]. This notwithstanding, a very important property of recycled aggregates is their capacity to highly absorb water as a result of the old mortar adhered to the surface of the aggregate extracted from the recycling [28].

Key properties of RAC have been reported in literature. Among such properties are: durability [30, 31, 32]; compressive strength [33]; workability and moisture content [34, 35]; flexural strength [33, 36]; modulus of elasticity [33, 37]; split tensile strength [31, 36]; specific gravity and bulk density [38]; shrinkage and creep [1, 33, 32]; rapid chloride migration and accelerated corrosion among other things.

## RESEARCH METHODOLOGY

To be able to understand the current research trends of studies in a particular area, a methodical presentation and analysis of published papers in more reputable scholarly journals is important for the research community [39, 40]. This study sought to conduct a state of the art review of current literature on recycled/crushed aggregate concrete. To achieve this aim, studies related to the topic published in some selected Construction Materials Journals (CMJ) from 2013 to 2017 were retrieved and systematically analyzed to gain insight into the area under study.

A three-stage approach was adopted to conduct the review. These included searching and collecting the relevant papers (which further involved identifying or selecting the CMJ), classifying or selecting the relevant papers, and analyzing or assessing the contribution of the relevant papers. The approaches are discussed to include the following:

— Searching and collecting the relevant papers

In identifying reputable academic journals that have published issues related to RACs from 2013 to 2017, search engines such as SCOPUS, Google Scholar, ResearchGate, Academia.edu, among others were used. These search engines were agreed on because most research publications within the chosen area of study have been archived in them. They also form majority of the key search engines for academic publications in the area of construction materials. Because the focus of this study was to explore current studies on RACs, several keywords were used to identify and search for the journals and papers. Studies on RACs are very broad with quite a number of keywords in literature. Using all the keywords related to RACs will mean that the size of literature obtained would be bulky.

Because it is not possible for a single study to report on all the complexities involved in selecting majority of the potential RAC research keywords, the researchers were posed with a major challenge of obtaining a workable number of RCA related papers. This challenge was controlled by making the assumption that some of the top key words used in RAC research include recycled concrete aggregate, recycled coarse aggregate, recycled fine aggregate and recycled aggregate concrete. Since these four keywords encompass almost everything about RACs, they were used to search for the papers. The search revealed a number of construction journals that had published issues relating to RACs. However, only those journals that showed current papers (2013-2017) as well as those published by reputable publishing houses were considered.

Based on the initial search results, about 20 related journals were obtained. However, a total number of twelve journals: Construction and Building Materials, CBM, (Elsevier); Journal of Cleaner Production, JCP, (Elsevier); Magazine of Concrete Research, MCR; Case Studies in Construction Materials, CSCM, (Elsevier); Materials and Design, MD, (Elsevier); Archives of Civil Engineering, ACE, (DE GRUYTER OPEN); European Journal of Environmental and Civil Engineering, EJECE, (Taylor and Francis);  Journal of Materials in Civil Engineering, JMCE, (ASCE),  International Journal of Concrete Structures and Materials, IJCSM, (Springer),  International Journal of Smart and Nano Materials IJSNM, (Taylor and Francis), Materials De Construction, MDC and Journal of Building Engineering (JBE, Elsevier) were selected for this study. These journals were selected because they contained papers that were of relevance to the current study.

It is very important to note that there are other equally reputable and important CMJs within this area. However, these few numbers were due to the fact that the papers searched were within a limited time interval (2013-2017).

— Classifying or selecting the relevant papers

Of the twelve CM journals that were selected for this study, a total number of 84 current papers (2013-2017) were obtained. These 84 papers were obtained because the keywords used for the search appeared in their titles,

abstracts or keywords sections. These keywords have been widely used in general construction materials research journals.

As a result of that, there was the possibility of irrelevant papers still appearing. Because of this perceived problem, all the 84 papers were critically scrutinized by reading through their abstracts to rule out all papers that did not meet the search criteria. The results from the inspection showed that only 41 out of the 84 papers were valid for the study. Table 1 summarizes the papers together with the journals from which they were retrieved.

Table 1. Summary of search results and number of relevant papers

| Selected Journals | Number of relevant papers for the study |
|---|---|
| Construction and Building Materials (CBM) | 28 |
| Magazine of Concrete Research (MCR) | 2 |
| Journal of Cleaner Production (JCP) | 2 |
| Case Studies in Construction Materials (CSCM) | 1 |
| Archives of Civil Engineering (ACE) | 1 |
| Materials and Design (MD) | 1 |
| European Journal of Environmental and Civil Engineering (EJECE) | 1 |
| Journal of Materials and Civil Engineering (JMCE) | 1 |
| Concrete Structures and Materials (CSM) | 1 |
| International Journal of Smart and Nano Materials (IJSNM) | 1 |
| Materials De Construction (MDC) | 1 |
| Journal of Building Engineering | 1 |
| TOTAL | 41 |

— Analyzing or assessing the relevant papers

Through research, industrial practice is affected [39]. According to Hong et al. [41] as cited in [39], the greater the number of published scholarly works in a particular discipline within a given country, the greater the extent to which people pay attention to the area, both industrially and innovatively. According to Yuan and Shen [42], once the active contributors within a given research discipline are identified, it becomes easier to understand the main stream of research within that particular discipline in different regions [39].

The identification will help researchers to track the contributions made previously in the chosen area of research to assist in further studies within the area [39].

In examining the current literature within the area of study, this study additionally sought to provide insights into the current development studies on RACs in different countries. The contributions of researchers located within institutions of several countries are presented and discussed in Section 4.0. To assist in calculating the contributions from researchers to RACs, a formular proposed by [43] and used by several researchers to conduct studies in other areas:

≡ to conduct research trends in green buildings [39];

≡ research trend in construction labour productivity [44]; and

≡ demolition waste management [42]

was used. According to Darko and Chan [39], the formular has been widely adopted and used in studies of similar nature, and this guarantees its suitability for the current study. The formular as proposed by [43] is as follows:

$$Score = \frac{1.5^{n-i}}{\sum_{i=1}^{n} 1.5^{n-i}}$$

where 'n' represents the number of authors and 'i' represents the order of a specific author [43]. To apply the formular, the scores given to authors in a multi authored paper should be proportionally divided [43]. Table 2 therefore presents a detailed score matrix for authors. This Table was adopted from that proposed by [43]. Based on Table 2, the contribution of authors (from institutions within various countries) to RAC research were computed, ranked and discussed.

Table 2. Score matrix for multi-authored papers

| Number of authors | Order of specific author | | | | |
|---|---|---|---|---|---|
| | 1 | 2 | 3 | 4 | 5 |
| 1 | 1.00 | | | | |
| 2 | 0.60 | 0.40 | | | |
| 3 | 0.47 | 0.32 | 0.21 | | |
| 4 | 0.42 | 0.28 | 0.18 | 0.12 | |
| 5 | 0.38 | 0.26 | 0.17 | 0.11 | 0.08 |

(Source: [39])

## RESULTS AND DISCUSSION

This study sought to conduct a state of the art review of current literature on recycled/crushed aggregate concretes. The study was based on a review of research papers selected from some construction material journals. The results presented and discussed in this section are based on the analysis performed on the RAC research papers that were obtained based on the specific sampling approach as discussed in Section 3.0. It is worth noting that the study only considered current papers which the authors deemed as significant. As a result, there may be research papers which were published either in 2013, 2014, 2015, 2016 or 2017, but may not be included in the current study. The results are presented in terms of the current studies on RACs, research contributions by various institutions/universities, as well as various authors.

### — Current studies on RACs

For many years now, researches in the area of RCAs have focused on the influence of the composition and quality of these secondary materials on the properties of recycled concrete in the fresh and hardened states [45]. Two broad properties of RACs that have recently gained attention are mechanical and durability properties. Compressive strength, split tensile strength, flexural strength and modulus of elasticity are mechanical properties of RACs that have been thoroughly researched. Carbonation depth, deformation, permeability, chloride penetration and freeze thaw resistance are among the durability properties which have been widely researched.

### ⊞ Mechanical properties

According to Wingrove [2], in an attempt to bridge the knowledge gap in the use of RCA multiple studies have been conducted to investigate its performance. For the studies that investigate the impact of RCA on the properties of concrete, majority of them focus on the mechanical properties [2].

The mechanical properties as used here refers to those properties that deal with the strength of concrete both in tension and compression, density, modulus of elasticity, bond strength between concrete and steel, amongst others [14 p. 724]. The discussion on the mechanical properties will be centered on compressive strength, split tensile strength, flexural strength and modulus of elasticity.

### » Compressive strength

Compressive strength is the key mechanical property considered in concrete design. Kisku et al. [14] indicated that comprehensive strength is the most important property of hardened concrete because it has the tendency to influence the strength, durability and performance of concrete. Factors that affect compressive strength of concrete are well researched and summarized in literature.

According to Çakir [46], the compressive strength of concrete is influenced by the strength of the aggregates, the cement matrix and the interfacial transition zone. Kisku et al. [14] expounded this assertion and reported that the water binder ratio, different properties of RAC, properties of adhered mortar, mixing approach and properties of admixtures used all affect the strength properties of concrete.

Majority of research have been conducted in different countries using different sources of RCAs together with different materials to produce RACs. It has been well established that increasing the quantity of RCAs and the water cement ratio decreases the compressive strength of RACs [14, 47, 48, 49, 50, 51, 52]. It is therefore very prudent to agree with [53] who opined that the inclusion of RCA in any replacement ratio will weaken the hardened concrete.

Yildirim et al. [54] analyzed the effect of internal curing on the strength of concrete containing RCAs and found that after 7 and 28 days, the compressive strength was strongly affected by the water cement ratio, the substitution levels of RCA and the degree of saturation. This finding agreed with the assertion by [14] and [53]. Lotfi et al. [55] also postulated that depending on the concrete mix produced, there is always a loss in the compressive strength when the water cement ratio and the recycled aggregate contents are increased.

Also, Laserna and Montero [56] found that the values of compressive strength was approximately 40.42 N/mm$^2$ for those mixtures that had a replacement ratio of 50%, 300 kg/m$^3$ cement and 0.5% water cement ratio. An important contribution from their study was that different dosages of cement may influence the compressive strength of concrete produced with RAs.

Seara-Paz et al. [57] further stated that 100% replacement of natural aggregates (NAs) with RCAs will reduce the compressive strength by 22.31%, a confirmation of the assertion that there is a decrease in the compressive strength when the RCA content is increased. McGinnis et al. [58] found something that was almost closer to that found by [57].

According to the researchers, compressive strength of mixes made with RCAs decrease from NA mixes by an average of 16.6% at 50% replacement and 26.4% at 100% replacement. Liu et al. [59] and Gonzalez-Taboada et al. [60] were also in agreement with the fact that at different replacement levels, the compressive strength of RAC will decrease with an increase in the water cement ratio.

Deng et al. [61] chipped in an interesting issue by iterating that when the coarse aggregate replacement rate is 50%, the compressive strength of the RCA specimens with different water to cement ratios are relatively close. In examining the properties of pervious concrete that contains natural limestone aggregates replaced with RC block aggregates and RCAs, Zaetang et al. [62] realized that the use of RCA in these mixtures improved on the compressive strength of the concrete produced. An optimum compressive strength of 15.0 MPa was produced with an optimum replacement level of 60% of RCA. This strength was achieved because of the good bonding between the RCA and the cement paste.

Kurad et al. [63] felt that there had been enough studies on coarse recycled aggregate concretes. Therefore, basing their studies on that carried out in 2016, they examined the effect of using supplementary cementing materials (SCMs) and recycled concrete fine aggregate (RCFA) on the compressive strength of concrete and found that an increase in the RA content caused a decrease in the compressive strength.

Kumar et al. [68] further conducted a similar study using fine recycled aggregates (FRA) and found that the compressive strength still decreased as the replacement level of the RFA increased. This further strengthened the findings of [63]. The explanation given for the reduction in the compressive strength was based on the porous microstructure of concrete made with RFA. It was also realized from the study that the incorporation of FRCA in concrete mixes still decreased the compressive strength of concrete.

In other studies, which involved a mixture of lime stone aggregates with RAs [64], and a mixture of new earth concrete with various volumes of RCAs [65], similar findings were observed where the compressive strength of the resultant concrete decreased with the different replacement levels of RCAs. In the study by McGinnis et al. [58], it was revealed that compressive strength of mixes made with RCA decrease from the normal aggregate mixes by an average of 16.6% at 50% replacement and 26.4% at 100% replacement. These findings as presented by the authors are great, however, all the authors mentioned above were silent on the reaction of RCAs with Ordinary Portland Cement or the cement types used in their studies. Parthiban et al. [66] indicated that the compressive strength of Alkali Activated

Slag Concrete is higher than OPC mixes. Kurda et al. [15] summed all the issues up through a comprehensive review of literature and concluded that using up to 30% of RCA does not significantly affect the properties of concrete. Their study concluded that the difference between compressive strength at 90 days of a conventional concrete mix and concrete made with about 50% RCA and 50% FA is not significant, and in most cases may be classified in the same strength class.

» **Split tensile strength**

The split tensile strength of concrete produced with RCAs is observed to be dependent on the aggregate replacement levels, water binder ratio, mixing methods, type of cement, curing age and the quality of the recycled aggregate [14]. Literature has indicated that an increase in the RAC decreases the split tensile strength [14, 49, 50, 47, 48, 52]. However, not much of the current studies undertaken on RCAs have focused on this area.

The few studies that have been conducted on split tensile strength of RACs agree with [14] findings. Laserna and Montero [56] observed the influence of two different types of natural aggregates on the tensile strength properties of RCAs, and found that in both cases, the tensile strength reduced by up to 25% compared to the concrete without RCAs. However, they stressed that different dosages of cement do not affect the tensile strength of RAC.

Seara-Paz et al. [57] observed that recycled concrete (RC) experienced reductions in split tensile strengths by between 23 and 31% for a 100% replacement rate of NAs. According to the researchers, the reduction could be attributed to the weaker paste aggregate interface of RCs. These findings were further buttressed by the study of [60] who also revealed that increase in RCAs decreases the split tensile strength of recycled aggregate concretes. Sahoo et al. [67] revealed that though these decreases exist, adding bacteria (*Bacillus Subtilis*) to the mix has the potential to increase the split tensile strength of recycled aggregate concrete.

Parthiban et al. [66] further conducted a study to examine the engineering and durability characteristics of alkali activated slag concrete made with RCAs and concluded that the tensile strength of the concrete produced was higher than that of the OPC mixes. This difference in findings probably stemmed from the fact that a different kind of cement was used in the study [66].

In investigating the fresh and hardened mechanical properties of a high performance concrete mix produced with different percentages of RCAs, [64] observed that the average reductions in split tensile strengths for all mixes were 13.5% and 10.3% respectively for both normal strength and high strength concrete mixes.

These findings were the case for the mixes with natural and recycled coarse aggregates. However, [68] in conducting a similar study with fine recycled aggregates revealed that split tensile strength only decreased by 6.46% with an increase in the content of RFA. The researchers indicated that for such concrete, the porous microstructural characteristics of the

concrete produced caused the decrease in the split tensile strength.

» **Flexural strength and modulus of elasticity**

Flexural strength (FS) and modulus of elasticity (MOE) are two other mechanical properties that affect the strength of concrete. Studies have shown that both FS and MOE are negatively affected by an increase in the RCA level. Flexural strength for any RCA depends on the aggregate replacement ratio, moisture conditions of aggregate, curing and water cement ratio [14]. An increase in the RA content will decrease the FS of concrete [48, 52].

Hamad and Dawi [64] found that for several mixes of 0, 20, 40, 60, 80 and 100% replacement levels of RCA, the average reduction in the FS relative to the control mix is 9.2%. They went on to further stress that for normal and high strength concretes produced with RCA, the FS relative to the control mixes are 10.8% and 9.2% respectively.

However, [14] had earlier on reported that recycled concrete aggregates made with 25% and 50% recycled aggregates had their FS to be around 6-13% less than that of normal concrete. Their study further reported that 100% replacement of NA with RAs yielded a reduction in FS of about 26%. These characteristics were attributed to RCAs used to replace natural coarse aggregates (NCAs). In a similar study, [68] partially replaced fine aggregates (FAs) with FRAs and realized that the FS of the resulting concrete decreased by about 22.62%. This finding is roughly around the range of that found by [14]. Based on these comparisons it can be said that the decrease in FS of RACs with partial replacement of both coarse and fine recycled aggregates are roughly around the same percentages as reported in literature.

It has further been reported that the incorporation of RCAs also decreases the MOE of RACs [69]. Pedro et al. [70] examined the mechanical strength properties of concrete produced with RAs from different sources and found that the MOE of the concrete produced decreased by 22%, 18% and 15% for 20 MPa, 45 MPa and 65 MPa concrete families. These decreases were attributed to the use of the RAs and supplementary cementitious materials (SCMs).

Rodriguez-Robles et al. [71] examined the effect of mixed recycled aggregates on MOE and also found that 50% replacement of natural aggregates yielded values of 23.43 GPa and 23.57 GPa for both recycled aggregates used. They indicated that the strength values obtained only accounted for a small reduction as compared to the natural aggregates. According to Laserna and Montero [56], for 50% replacement ratio of RAs, the MOE reduces by 10-15%, and for 100%, the reduction is in the order of 20-25%. However, contrary to that reported by [56], [64] revealed in their study that the average reduction in MOE was 11%. The reduction was only 3.52% for the 20% replacement mix, but jumped above 10% for the other larger replacement percentage mixes.

Seara-Paz [57] was also in agreement with these findings as she also found that 100% replacement of recycled aggregate reduced the MOE by 22-31%. Liu et al. [59] attested to the fact that at different replacement levels, the MOE decrease with the increase in water cement ratio.

Contrary to the conclusions of all the other researchers, Kanema et al. [65] investigated the shrinkage behavior of a new earth concrete amended with various volume percentages of recycled concrete aggregates and found that the MOE increased with the percentages of the RCA which were added linearly. A similar result was also obtained by [72] when they examined different mixtures of structural concretes with different degrees of substitutions of coarse aggregates by RAs. Their study revealed that the addition of RA increased the MOE of the concrete produced. The impression that is obtained from the studies of [65] and [72] is that the addition of extra materials to the RAs in the concrete had positive influence on the MOE of the concrete produced. Kurda et al. [15] postulated that percentages of FAs that exceed the standard limit which is above 35% but below 50% will not significantly affect the results of a concrete's MOE both with NA and RCA.

» **Summary of interventions to improve on mechanical properties of RACs**

It is of importance to note that most of the current research trends on RACs are now shifting from just determining the mechanical and durability properties to finding ways to improve on these properties.

With all these conclusions about compressive strength of RACs, [67] realized that as an important property of hardened concrete, it is better to increase the compressive strength of concrete, especially if it is to be manufactured with RCAs. The researchers tried to enhance the properties of recycled coarse aggregate concrete (RCAC) by introducing bacteria (*Bacillus Subtilis)* into the mix, which was the first of its kind. It was revealed that increasing the content of the RCA decreased the compressive strength of the concrete. However, with the addition of the bacteria to the mix, the compressive strength increased by 20%. Anastasiou et al. [73] embraced the fact that using RCAs will reduce the compressive strength of concrete, however, they stressed that with the introduction of steel slag aggregate, there is the possibility of recovering some of the lost strength. They further stressed that 50% cement replacement, with high calcium fly ash and use of only steel slag and recycled aggregates can result in concrete of adequate strength. In the opinion of [74] however, coarse RCAs from precast concrete elements has the potential to be used to produce new concrete up to 100% content without losses in terms of most of the properties (mechanical and durability) of the concrete.

Kisku et al. [14] also posit that the use of super-plasticizers is reported to minimize the negative influence of RCAs on split tensile strength of concrete. This assertion was confirmed by [1] in their study. Katkhuda and Shatarat [75] further investigated how to improve the mechanical properties of RACs by adding chopped basalt fibres, and realized that its inclusion significantly enhances the split tensile strength of the concrete produced. Silva et al. [1] postulated that despite

the tensile strength loss with increase in RA content, the use of proper mixing approaches could control this problem. An important thing to note is that several studies have also reported that as the RCA replacement ratio approaches 100%, the tensile strength becomes constant [14]. This is a confirmation of the finding from [1] who revealed that concrete with increasing coarse RCA content may achieve equal or higher tensile strength a year after casting.

## Durability properties

Durability with regards to concrete has been defined in several ways. According to [76], durability is *'Capability of a structure or any component of it to satisfy, with planned maintenance, the designed performance requirements over a specified period of time under the influence of environmental actions, or as a result of self-ageing process'*. Domone [77, p.175] also defined durability to mean a material or structure which remains in an acceptable state for use throughout the period for which it has been designed.  A critical examination of literature suggests that these definitions are in agreement to that provided in literature. Though per the views of these authors the precise definition of a durable concrete may vary, there is the common agreement on the significance of designing for durability [53].

Kisku et al. [14, p. 729], defined durability with regards to RAC to mean its *'ability to withstand external environmental, physical action and chemical reactions'*. The properties of concrete constituents, mixing proportions, curing conditions, admixtures used, amongst other things may influence the durability properties of RACs [14, 3, 78, 79]. A concrete's durability is usually characterized by its permeability and deformation [14]. Carbonation depth, deformation, permeability, chloride penetration and freeze thaw resistance are among the durability properties of RACs that have been widely studied.

### » Permeability

The ease or difficulty with which water flows through concrete is a measure of its permeability. Bertolini et al. [8, p. 21] defined permeability as the flow of fluids through concrete as a result of differing pressures between the concrete surface and the internal pore structure. According to [14], several parameters can be used to measure permeability. Key amongst such parameters are water permeability, oxygen permeability, capillary water absorption, and air permeability [14].

Anastasiou et al. [73] indicated that the use of fine construction and demolition waste (CDW) aggregates increase the porosity of concrete produced and render it susceptible to several penetrations. Such materials increase capillary water absorption because they are rich in hydrophobic products like brick fragments and lime. Behera et al. [14] further attested to this fact and suggested that the permeability characteristics of RAC is associated with the poor quality of RA due to the presence of cracks, fissures and pores present in the aggregates.

The microstructure of RAC is also porous in nature due to the presence of old adhesive mortar around the RA, which also contributes to the permeability characteristics of RAC [14]. The permeability of RAC increases with an increase in RA content, water to cement ratio and age [14, 31]. With regards to water absorption, Pedro et al. [70] observed that water absorption in RAC increased between 23% and 50% for various target strengths of concrete.

The researchers were in agreement with [13] and [73] and suggested that the adhered mortar in the RA was responsible for the increased porosity. This finding was again confirmed in a later finding reported by [50] who had indicated that when it happened that way, the absorption capacity of the RA could increase by as much as 7 times that of the NA. Soares et al. [74] also agreed to the findings of the previous researchers when they realized that replacing coarse natural aggregates with coarse recycled aggregates increased the water absorption capacity of RAC by as much as 29%. Though they believed that the percentage obtained in their RAC was slightly lesser than that reported in other studies, they were in agreement that the high water absorption capacity of the CRCA resulting from its increased porosity was a major contributory factor to the finding.

In a similar study, [55] also found that increase in the content of RA in RAC increased its susceptibility to permeability, a finding which was also agreed on by [66], [80] and [31]. What made Lofti et al. [55] work unique was their finding which revealed that of all the various characteristics of permeability, the effect of the water cement ratio is very dominant. Evangelista et al. [81] indicated that for fine recycled aggregates, their apparent density which is 10% to 15% lower than that of fine natural aggregates may result from its higher porosity.

## Carbonation depth

Carbonation in concrete usually occurs as a result of the interaction between carbon dioxide (that is present in the air and water) and unhydrated calcium hydroxide on the set cement in concrete [14]. Studies have shown that it is influenced by water cement ratio, the contents of the binder, the presence of recycled aggregates, admixtures and the conditions of curing [14]. Again, it has been reported that increase in the contents of RA increases the carbonation depth [15, 14, 55, 1, 29].

Pedro et al. [70] evaluated the capacity of producing concrete with a pre-established performance by incorporating RCAs from different sources. The authors produced concrete of three different strength classes (15-25 MPa, 35-45 MPa, and 65-75MPa). It was found that for the high strength concrete produced, the depth of carbonation increased with the replacement of virgin aggregates by the RCAs. It was also realized that the carbonation depth increased with a decrease in the target strength of the concrete manufactured. The authors attributed this to the lower water cement ratio as well as the increased cement contents. Soares et al. [74] evaluated the effect of incorporating RCAs from

crushed elements produced by the precast concrete industry into the production of new concrete. At all the different ages tested, the coarse recycled crushed concrete aggregate showed similar carbonation depths. The authors therefore concluded that the CRCA had no significant influence on the concrete carbonation resistance. This finding differs from that obtained by [70]. The difference in the finding is attributed to the very good quality of the CRCA that was sourced from high-strength precast elements and used in the study [74]. After a series of tests conducted on recycled aggregate concrete of different strength properties, Lotfi et al. [55] were in agreement with [15] and [14] that, the depth of carbonation of RAC increases with an increase in the RAs. The depth of carbonation achieved in their concrete also corresponded to that achieved by [74]. Another important finding from Lotfi et al. [55] work was its correspondence with the finding of [70] who reported that the depth of carbonation increases with a decrease in the target strength of the concrete.

Silva et al. [1] examined the effect of incorporating recycled aggregates sourced from construction and demolition wastes on the carbonation behavior of concrete. The authors examined several factors that may in one way or the other influence the depth of carbonation of RACs. Their study revealed that 100% incorporation of CRCA in concrete may cause up to 2 times the depth of carbonation of that of the corresponding normal aggregate concretes (NACs). In several reviews carried out by [29], it was revealed that the depth of carbonation was 1.3-2.5 times that of the NAC, and in another study, 3 times that of the NAC. The finding from the study was also in agreement with that of [15], [14], [55], [74], and [70]. Singh and Singh [82] examined the carbonation and electrical resistance of self-compacting concrete (SCC) made with CRCAs. In agreement to the findings of [15, 14, 55, 1], it was revealed that when the RCA content used to replace the NAs increased, the carbonation resistance of the SCC decreased. After 28 days of curing the concrete and 16 weeks of exposure, the depth of carbonation of the SCC mix produced with 100% RCA increased by nearly 58% as compared to that made with 100% of NAs.

Singh and Singh [82] further investigated the carbonation resistance of Low Volume Fly Ash (LVFA) and High Volume Fly Ash (HVFA) based SCC produced with CRCA. Accelerated carbonation tests were further conducted for exposure periods of 4, 12 and 16 weeks. The carbonation resistance of LVFA and HVFA based SCC was found to decrease with increase in RCA contents. The depth of carbonation reached its peaks of 63% and 53% in the LVFA and HVFA respectively after exposure for 12 weeks. Even with the introduction of fly ash, the findings obtained were still closer to the findings as obtained in their earlier study.

An evaluation of the real influence of a commercial densified silica fume and RAs on the behavior of high performance concrete was carried out by [83]. It was realized that the depth of carbonation increased with the increase in RAs incorporated into the mix. This increase was attributed to the higher porosity and the lower water to cement ratio of the mixes made with them. This finding is in agreement with the findings obtained from their earlier study in which [50] analyzed the effect of different types of recycled concrete aggregate on structural concrete.

» **Chloride penetration/migration**

'*Chloride penetration refers to the depth to which chloride ions from the environment penetrate concrete*' [14, p. 732]. The ability of chloride ions to penetrate concrete cover is a key factor in the service life of any reinforced concrete structure. The presence of the ions can lead to corrosion of reinforced concrete elements; this therefore makes it an important property of a durable concrete. The penetration of chloride ions into concrete normally results from absorption by capillary action, diffusion and permeation [14]. From an extensive review of literature, [14] reported that the ability of chlorides to penetrate RACs depends on the natural aggregate replacement level, water cement ratio, and the period of curing. Increasing the natural aggregate replacement as well as the water cement ratio increase the chloride ingress.

Anastasiou et al. [73] examined the possibility of producing concrete with the incorporation of large volumes of industrial by-products and secondary materials. Several mixes were produced and tested for chloride ion penetration. Chloride concentration was measured at 40-50 mm depth for the different test concrete mixtures. When the mixture containing the construction and demolition waste (CDW) alone was tested, a decreased chloride ion penetration resistance was recorded. The combination of CDW and electric arc furnace (EAF) slag aggregate had no effect on chloride penetration resistance.

However, the combination which had CDW and 50% of cement substitution with high calcium fly ash (HCFA) improved the chloride ion penetration resistance. In comparing the chloride ion penetration resistance between a reference concrete (RC) and a CRAC, Pedro et al. (2014) reported that the penetration rate was higher in the RAC than the RC. This finding was very well in agreement with that reported by [29] who indicated that RA has a negative effect on chloride ion penetration resistance, and the resistance declines with the increase in quantity of RA.

The reason assigned was as a result of the more permeable nature of the RAC that was caused by the adhered mortar in the RA. The greater chloride penetration rate that was exhibited was attributed to the paste/aggregate interfacial effects and the presence of more internal cracks in the RA. The researchers recommended that if the transition zone of the microstructure is improved, its chloride penetration resistance will be improved.

Soares et al. [74] perfectly agreed with the findings of [73] and [70]. However, they made a very important argument concerning the source of the CRAC. They conducted their study using CRAC from precast concrete elements and

realized that because such CRAC members have more improved properties than other CRAC elements, the penetration is not very severe. They further stressed that the use of superplasticizers in concrete is beneficial for all properties of concrete. Both mechanical and durability properties of the RAC are improved, thereby offsetting any negative effects of the RACs.

De Brito et al. [81] agreed with the findings of the other researchers [14, 73, 70, 74], by iterating that since RAC is more permeable, there is the tendency for higher chloride ingress when they are compared to the conventional concrete. Buttressing the comments of Pedro et al. [70], [80] indicated that the effect of RA incorporation on chloride ion penetration depends on the quality and adhered mortar. When [66] investigated the effect of RCA on the durability properties of alkali activated slag concrete under ambient curing conditions, similar conclusions were drawn as in the case of previous researchers.

It was revealed that there was a slight increase in the maximum depth of chloride penetration with an increasing volume of RCA. This increase was attributed to the pores present at the ITZ between the new mortar and the RCA, a confirmation of the findings of [80] and [70]. [83] provided further enlightenment on the situation by indicating that chloride diffusivity tests observed at 91 days for RC and RAC indicated low chloride diffusivity values. It was further found that increasing the replacement ratio of normal aggregates with recycled aggregates led to a decrease in the resistance to chloride penetration. This still buttressed the assertions of earlier researchers that increasing the RA content increases chloride ingress. In a follow up study, [83] indicated that there is an increase in the chloride diffusion coefficients when there is a simultaneous increase in the incorporation of fine and coarse recycled concrete aggregates.

» **Summary of interventions to improve on durability properties of RACs**

Because the use of recycled aggregates in new concrete structures is limited due to the high water absorption and weak bonding to new matrix, Qiu et al. [84] conducted a study to investigate a novel approach (microbial carbonate precipitation, MCP) that can be used to treat the surface of RCAs. The researchers examined the factors that influenced MCP on RCA and found that the surface modification of RCA through MCP is feasible, and it was evidenced by the increase in weight as well as a reduced water absorption of the RCAs. Behera et al. [13] shifted from concentrating on the properties of the RCAs to working on improving the durability properties of RACs. The researchers suggested that to improve on the durability properties of RACs, it is very important to modify the weak ITZ of the RAC and the bulk matrix of the concrete. They suggested that it is better to improve on the microstructure of the RAC by incorporating mineral admixtures such as fly ash, meta kaolin, silica fume, GGBS, and Nano silica. According to Behera et al. [13], such mineral admixtures will act as micro fillers, thereby filling the ITZ

between the aggregate surface and the matrix. Soares et al. [74] added that the use of superplasticizers in concrete is very beneficial for improving the mechanical and durability properties of RACs. They indicated that when such superplasticizers are used, any negative effects induced by the RCAs on the RACS will be offset. Emphasis was however, laid on the fact that the superplasticizers together with coarse recycled aggregates generated from precast elements give an excellent result for RACs.

Lotfi et al. [55] made an important assertion by indicating that all durability properties of RACs can be influenced by the choice of cement and the amount of mixing water used in the concrete mixture. More importantly, the authors agreed with [13] that the addition of superplasticizers can greatly enhance the durability properties of RCAs. However, in their case, the issue of RCAs from precast concrete elements did not arise.

Silva et al. [1] also indicated that decreasing the porosity by increasing the quantity of cement, decreasing the water cement ratio as well as using superplasticizers in the mix should all improve on the durability properties of RACs. This indicates that the authors agree very well with [84], [13] and [55].

Thomas et al. [31] also agreed on the use of superplasticizers to enhance the durability properties of RACs. Singh and Singh [82] further agreed with [13] on the use of meta kaolin and fly ash in improving on the durability properties of RACs. Parthiban et al. [66] sighed to the use of alkali activated slag to improve on the durability properties of RACs. SCMs greatly assist in improving on the chloride resisting abilities of RACs.

— **Contributions made by countries, institutions/ universities and researchers to RCA research**

Table 2 is a score matrix (adopted from [39] which was used to assess the contributions of various researchers and institutions to RAC research. The ultimate contribution score of an author was calculated by summing the various scores of all authors within the same country and institution [39]. For instance, if an author based in a particular country and institution, is associated with the first and second authorship in two separate papers respectively, the author scores one point (i.e. 0.6+0.4) each for their country and institution/university [39].

Based on this assertion, the countries of origin of the papers selected, the total number of researchers and institutions/universities involved, and the contribution score of each author are summarized in Table 3.

Table 3 shows that during the period under investigation (2013-2017), studies on recycled aggregate concrete had been carried out in both developed and developing countries. This clearly shows that studies on RAC are of interest to researchers worldwide. Researchers from 24 countries had contributed their quota to studies on RACs. However, per the criteria used in this study, only studies from 8 countries qualified to be included for further analysis.

Table 3. Origins of selected RCA research papers

| Country | Number of Institutions involved in RCA Research | No of Researchers Involved in RCA Research | Number of Papers Generated from the Research | Score |
|---|---|---|---|---|
| USA | 7 | 13 | 5 | 3.92 |
| Spain | 5 | 17 | 6 | 3.72 |
| India | 5 | 23 | 6 | 6.00 |
| UK | 4 | 6 | 3 | 1.42 |
| China | 3 | 8 | 2 | 2.00 |
| Turkey | 3 | 4 | 3 | 2.47 |
| Portugal | 2 | 13 | 10 | 7.95 |
| Canada | 2 | 3 | 1 | 1.00 |

From Table 3, it can be seen that close to 70% of the countries where research on RAC has been conducted are developed, with the least coming from developing countries. USA, Spain, UK, China, Portugal and Canada are among the developed countries that have currently contributed to research on RCA. These countries have contribution scores of 3.92, 3.72, 1.42, 2.00, 7.95 and 1.00 respectively.

Table 3 further suggests that the contributions from UK, China and Canada were low. The lowest scores as obtained from these developed countries may be attributed to other reasons. Research on RCAs started after the Second World War, and all these countries have contributed their quota from that time to date. The slow pace as seen in Table 3 indicates that such countries may have exhausted majority of the issues there are to consume on the subject area, hence the research interests are being moved to other areas. Also, considering the limited nature of papers that were considered in this current study, there could be the possibility that there may be other studies which have been conducted within the said period under investigation but were not included in the current paper because such studies may be out of scope depending on the criteria used by the researchers of this study.

The UEPG 2005 and 2006 statistics published in 2008 indicated that the greatest users of RCAs were the UK, Netherlands, Belgium, Switzerland and Germany [21]. In 2000, it was also reported that 5% of aggregates in the US was recycled aggregates. This report shows that studies on RCAs have been dominant in most developed countries over the years [21].

Among the developing countries involved in studies on RACs, only India and Turkey were among the top with scores of 6.00 and 2.47 respectively. It is seen from Table 3 that though researches on RACs have been in existence for many years, quite a number of researchers from different parts of the world are still dedicating their time and efforts at conducting RCA studies.

Table 4 further shows the top 4 institutes and universities that have currently published a number of papers on RACs. The University of Lisbon in Portugal, University of Cantabria in Spain, CSIR-Central Building Research Institute in India and the University of A Coruña in Spain, have contributed most to

studies on RACs currently. The contribution scores of those institutes/universities are 8.40, 1.81 and 1.79 and 1.54 respectively.

Table 4. Top 4 Institutes/universities that have published RCA related papers in CMJs (2013-2017)

| University/ Institution | Country | Number of Papers | Score | Rank |
|---|---|---|---|---|
| University of Lisbon | Portugal | 16 | 8.4 | 1st |
| University of Cantabria | Spain | 3 | 1.81 | 2nd |
| CSIR-Central Building Research Institute | India | 7 | 1.79 | 3rd |
| University of A Coruña | Spain | 6 | 1.54 | 4th |

Table 5. Contributions made by researchers to RCA research

| Researcher | No. of papers | Affiliation | Country | Score |
|---|---|---|---|---|
| de Brito, J. | 10 | University of Lisbon | Portugal | 2.93 |
| Çakir, Ö. | 2 | Yildiz Technical University | Turkey | 1.32 |
| Silva, R.V. | 2 | University of Lisbon | Portugal | 0.94 |
| Thomas, C. | 2 | University of Cantabria | Spain | 0.85 |
| Soares, D. | 2 | University of Lisbon | Portugal | 0.59 |

The contributions of various authors to RCA research were also analyzed and it is shown in Table 5. Per the calculations done, several authors were identified. However, the study only limited itself to authors who obtained contribution scores of 0.5 and above. The contribution score was pegged at 0.5 because few research papers were considered in the current study. This implies that there would not be many papers for several authors to obtain higher contribution scores.

As a result, for a contribution score of 0.5, it would be easier for an author to use at least a single paper to obtain such a mark. It is also very important to note that some prominent researchers (especially those with a given number of scholarly publications) in RAC research area may have been omitted because of the formular that was used in the current study to calculate the contribution scores. It is worth noting that the formular takes into consideration the position of the authors on the research paper, together with the number of authors. So, the higher the authors, the smaller the mark and vice versa.

From Table 5, it is seen that the authors with the highest contributions were de Brito, J. from University of Lisbon (Portugal), Çakir, Ö. From Yildiz Technical University (Turkey), Silva, R.V. from University of Lisbon (Portugal), Thomas, C. from

University of Cantabria (Spain) and Soares, D. from University of Lisbon (Portugal). This looks very reasonable and convincing because Portugal and Spain were all among the countries that have currently contributed much to research on RACs as per Table 3. This information may be of value to individuals, especially those from developing nations who may want to conduct studies into recycled concrete aggregates. Furthermore, once active authors are identified in RCA research area, other researchers who are interested in such areas can form active collaborations with other active researchers and practitioners for future research opportunities.

## CONCLUSIONS

The depletion of virgin aggregates and the subsequent pollution of the environment as a result of aggregate mining activities have made the recycling of aggregates a major concern to the construction industry. For many years past until now, there have been a number of useful studies on the applications of RCAs in making more sustainable concrete for the construction industry. This study sought to explore current research and development studies on recycled concrete aggregates. To achieve this aim, RCA research papers published in twelve construction materials journals (i.e. CBM, JCP, MCR, CSCM, MD, ACE, EJECE, JMCE, IJCSM, IJSNM, MDC, JBE) from 2013-2017 were systematically analyzed. A total of 41 papers from the selected journals were analyzed. The review revealed an increasing trend in the number of RCA research papers. Developed countries such as USA, Spain, UK, China, Portugal and Canada are among those countries that have currently made the most contributions to RAC research through the publication of most of the papers. Developing countries such as India and Turkey have also made good efforts at carrying out studies on RACs. With regards to research institutions/universities, it was revealed that researchers from the University of Lisbon (Portugal), CSIR-Building Research Institute (India), University of Cantabria (Spain) and University of A Corũna in Spain, have currently contributed most to studies on RCAs. The researchers who have currently made the most contribution to RAC research include de Brito, J from University of Lisbon in Portugal, Çakir, Ö. from Yildiz Technical University (Turkey), Silva, R.V. from University of Lisbon (Portugal), Thomas, C. from University of Cantabria (Spain) and Soares, D. from University of Lisbon (Portugal). The review of the related literature on RCAs further revealed that researchers have currently focused their attention on: the partial replacement of NAs with RAs to determine some physical and mechanical properties of concrete; and adding volumes of fly ash, waste glass, steel fibres, among others to concrete produced with RCAs. Though the objectives set out in this paper were duly achieved, it would not be very academic to say that the paper was without limitations. Key amongst the limitations was the relatively small sample size of the papers used (in this case 41 papers). This small sample size is attributed to the limitation in the search keywords that were used. Although this is a limitation, it was not practically possible to consider all RCA keywords in a single review study. This therefore means that though the selected papers can reflect the current state of RCA research, the review did not cover all relevant studies. Future review could be done to include other relevant papers which may have been excluded from the current study. Another limitation is the fact that not all authors who have greatly contributed to research on RAC were included in this study. The reason is that there is the possibility that most of such studies did not fall within the scope of the current years under study (i.e from 2013-2017), or the search keywords that were used did not permit the papers of such authors to be included in the number of chosen papers for the study. Probably in the future, a catalogue of all such authors together with their studies could be compounded for further analysis. There is also a limitation in the method that was used to rank the authors and their institutions. This is because there are highly reputable journals which consider the main authors to an article to be listed at the last position, in that order. There could therefore be the possibility that some of the journals considered in this study used that system, however, this was not considered in the current study. This study has shed light on the current state of RAC research, which should be of immense benefit to both industry practitioners and academic researchers worldwide.

## References

[1] Silva, R.V., de Brito, J. and Dhir, R.K. (2015). Tensile strength behaviour of recycled aggregate concrete. Construction and Building Materials, Vol. 83 (2015), pp. 108-118.

[2] Wingrove, E.J. (2015). Durability of structural concrete with recycled concrete aggregates and ground granulated blast-furnace slag. A dissertation submitted in partial fulfilment of the requirements for the award of Masters of Civil Engineering of Loughborough University.

[3] Matthews, S. (2014). Design of Durable Concrete Structures, Watford: IHS Global Limited & BRE Trust.

[4] Mehta, P.K. and Monteiro, P.J. (2006). Concrete: Microstructure, properties and materials. Third Edition, McGraw-Hill, New York.

[5] DEFRA (2015). Digest of waste and resources statistics-2015 Edition.

[6] Somani, P., Dubey, B., Yadav, L., Kumar, J., Kumar, A. and Singh, M. (2016). Use of demolished concrete waste in partial replacement of coarse aggregate in concrete. International Journal of Civil Engineering, Vol. 3 No. 5; pp. 117-121.

[7] Lowndes, I.S. and Jeffrey, K. (2008). Optimising the efficiency of primary aggregate production, Nottingham.

[8] Bertolini, L. et al. (2013). Corrosion of Steel in Concrete: Prevention, Diagnosis, Repair Second, Weinheim: Wiley-VCH.

[9] Manzi, S., Mazzotti, C. and Bignozzi, M.C. (2013). Short and long-term behavior of structural concrete with recycled concrete aggregate. Cement and Concrete Composites, 37(1), pp.312–318.

[10] Deng, X.H., Lu, Z.L., Li, P. and Xu, T. (2016). An investigation of mechanical properties of recycled coarse aggregate

concrete. Archives of Civil Engineering, Vol. LXII No. 4(2); pp. 19-34.

[11] Wijayasundara, M., Mendis, P., Crawford, R.H. (2017). Methodology for the integrated assessment on the use of recycled concrete aggregate replacing natural aggregate in structural concrete. Journal of Cleaner Production, 166 (2017), pp. 321-334.

[12] merican Concrete Institute, ACI, (2015). Recycled Concrete- A Sustainable Choice.

[13] Behera, M., Bhattacharrya, S.K., Minocha, A.K., Depoliya, R. and Maiti, S. (2014). Recycled aggregates from construction and demolition wastes and its use in concrete-A breakthrough towards sustainability in construction sector: A review. Construction and Building Materials, Vol. 68 (2014), pp. 501-516.

[14] Kisku, N., Joshi, H., Ansari, M., Panda, S.K., Nayak, S. and Dutta, S.C. (2017). A critical review and assessment for usage of recycled aggregate as sustainable construction material, Construction and Building Materials, Vol. 131 (2017), pp. 721-740.

[15] Kurda, R., de Brito, J. and Silvestre, J.D. (2017). Combined influence of recycled concrete aggregates and high contents of fly ash on concrete properties. Construction and Building Materials, Vol. 157 (2017), pp. 554-572.

[16] Nassar, R.U.D. and Soroushian, P. (2012). Strength and durability of recycled aggregate concrete containing milled glass as partial replacement for cement. Construction and Building Materials, Vol.29 (2012); pp. 368-377.

[17] Junak, J. and Sicakova, A. (2017). Concrete containing recycled concrete aggregate with modified surface. International High Performance Built Environment Conference - A Sustainable Built Environmental Conference 2016 Series (SBE16), iHBE 2016, Procedia Engineering 180 (2017), pp. 1284-1291.

[18] The Institution of Structural Engineers Sustainable Construction Panel (2010). Sustainability Briefing: Recycled and Secondary Aggregates in Concrete. The Structural Engineer, Vol. 88 No. (15/16), pp. 1-13.

[19] British Standard, BS, 85001 (2006). Concrete-Complementary British Standard to BS EN 206-1-Part 1: Method of Specifying and Guidance for Specifier.

[20] Rao, A., Jha, K.N. and Misra, S. (2017). Use of aggregates from recycled construction and demolition waste in concrete. Resources. Conservation and Recycling, Vol. 50 No. 1, pp. 71-81.

[21] World Business Council for Sustainable Development, WBCSD, (2009). Concrete recycling: The cement sustainability initiative, available http://www.wbcsdcement.org/pdf/CSI-RecyclingConcreteFullReport.pdf, accessed 15/12/2017.

[22] Clear, C.A. (2013). Use of recycled aggregates in concrete. MPA Cement Fact Sheet 6. Available http://cement.mineralproducts.org

[23] Ismail, S. and Ramli, M. (2014). Mechanical Strength and Drying Shrinkage properties of concrete containing treated coarse recycled concrete aggregates. Construction and Building Materials, 68 (2014), pp. 726-739.

[24] British Standards Institution (BSI), 2015b. BS 8500-2:2015, Concrete – Complementary British Standard to BS EN 206 - Part 2: Specification for constituent materials and concrete. London: BSI.

[25] Despotović, I. (2016). The improvement of recycled concrete aggregate- A review paper. In Procs, 4th International Conference on Contemporary Achievements in Civil Engineering, April 22, 2016, Subotica, Serbia.

[26] Awoyera, P.O., Akinmusuru, J.O. and Moncea, A. (2017). Hydration mechanism and strength properties of recycled aggregate concrete made using ceramic blended cement. Cogent Engineering (2017), 4: 1282667.

[27] Katz, A. (2003). Properties of concrete made with recycled aggregates from partially hydrated old concrete. Cement and Concrete Research, Vol. 33 No. 5; pp. 703-711.

[28] Wardeh, G., Ghorbel, E. and Gomart, H. (2014). Mix design and properties of recycled aggregate concretes: Applicability of Eurocode 2. International Journal of Concrete Structures and Materials, Vol. 9 No. 1, pp. 1-20.

[29] McNeil, K. and Kang, TH-K. (2013). Recycled Concrete Aggregates-A review. International Journal of Concrete Structures and Materials, Vol. 7 No. 1, pp. 61-69.

[30] Yehia, S., Helal, K., Abusharkh, A., Zaher, A. and Istaitiyeh, H. (2015). Strength and durability evaluation of recycled concrete aggregate concrete. International Journal of Concrete Structures and Materials, Vol. 9 No. 2; pp. 219-239.

[31] Thomas, C., Setien, J., Polanco, J.A., Alaejos, P. and Sanchez de Juan, M. (2013). Durability of recycled concrete aggregate. Construction and Building Materials, Vol. 40 (2013), pp. 1054-1065.

[32] Fathifazl, G. and Razaqpur, A.G., Isgor, O.B., Fournier, B. and Foo, S. (2011). Creep and drying shrinkage characteristics of concrete produced with coarse recycled concrete aggregate. Cement and Concrete Composites, Vol. 33 No. 10; pp. 1026-1037.

[33] Xiao, J., Fana, L.Y. AND Huang, X. (2012). An overview of studies on recycled aggregate concrete in China (1996-2011). Construction and Building Materials, Vol. 31 (2012); pp. 364-383.

[34] Medina, C., Zhu, W., Howind, T., Sanchez de Rojas, M.I. and Frias, M. (2014). Influence of mixed recycled aggregate on the physical-mechanical properties of recycled concrete. Journal of Cleaner Production, Vol. 68 No. 1; pp. 216-225.

[35] Qasrawi, H. and Marie, I. (2013). Towards better understanding of concrete containing recycled concrete aggregate. Advances in Materials and Science Engineering, Vol. (2013); pp. 1-8.

[36] Malešev, M., Radonjanin, V. and Marinković, S. (2010). Recycled concrete as aggregate for structural concrete production. Sustainability, Vol. 2 No. 5; pp. 1204-1225.

[37] Corinaldesi, V. (2010). Mechanical and elastic behavior of concretes made of recycled-concrete coarse aggregates. Construction and Building Materials, Vol. 24 No. 9; pp. 1616-1620.

[38] Padmini, A.K., Ramamurthy, K. and Mathews, M.S. (2009). Influence of parent concrete on the properties of recycled aggregate concrete. Construction and Building Materials, Vol. 23 No. 2, pp. 829-836.

[39] Darko, A. and Chan, A.P.C. (2016). Critical analysis of green building research trend in construction journals. Habitat International, 57(2016); 53-63.

[40] Tsai, C.C. and Wen, M.C.L. (2005). Research and trends in Science Education from 1998 to 2002: A Content Analysis of Publications in Selected Journals. International Journal of Science Education, Vol. 27 No. 1; pp. 3-14.

[41] Hong, Y., Chan, D.W.M., Chan, A.P.C. and Yeung, J.F.Y. (2014). Critical analysis of partnering research trend in construction journals. Journal of Management in Engineering, Vol. 28 No 2; 82-95.

[42] Yuan, H. and Shen, L. (2011). Trend of the research on construction and demolition waste management. Waste Management, 31 (2011); pp. 670-679.

[43] Howard, G.S., Cole, D.A. and Scot, M.E. (1987). Research productivity in psychology based on publication in the Journals of the American Psychological Association. American Psychologist, Vol. 42 No. 11; 975-986.

[44] Yi, W. and Chan, A.P. (2014). Critical review of labour productivity research in construction journals. Journal of Management in Engineering, Vol. 30 No. 2, pp. 214-225.

[45] Rodríguez-Robles, D., García-González, J. Juan-Valdés, A., Morán—del Pozo, J.M. and Guerra-Romero, M.I. (2017). Effect of mixed recycled aggregates on mechanical properties of recycled concrete. Magazine of Concrete Research, Vol. 67 No. 5; pp. 1-10.

[46] Çakır, Ö. (2014). Experimental analysis of properties of recycled coarse aggregate (RCA) concrete with mineral additives. Construction and Building Materials, Vol. 68 (2014), p.17–25.

[47] Khodair, Y. and Bommareddy, B. (2017). Self-consolidating concrete using recycled concrete aggregate and high volume of fly ash, and slag. Construction and Building Materials, Vol. 153 (2017), pp. 307-316.

[48] Zhang, Z., Zhang, Y., Yan, C. and Liu, Y. (2017). Influence of crushing index on properties of recycled aggregates pervious concrete. Construction and Building Materials, Vol. 135 (2017), pp. 112-118.

[49] Bui, N.K., Satomi, T. and Takahashi, H. (2017). Improvement of mechanical properties of recycled aggregate concrete basing on a new combination method between recycled aggregate and natural aggregate. Construction and Building Materials, Vol. 148 (2017), pp. 376-385.

[50] Pedro, D., de Brito, J. and Evangelista, L. (2017a). Evaluation of high performance concrete with recycled aggregates: use of densified silica fume as cement replacement. Construction and Building Materials, Vol. 147 (2017), pp. 803-814.

[51] Andal, J., Shehata, M. and Zacarias, P. (2016). Properties of concrete containing recycled concrete aggregate of preserved quality. Construction and Building Materials, Vol. 125 (2016), pp. 842-855.

[52] Akça, K.R., Özgür, C. and ipek, M. (2015). Properties of polypropylene fiber reinforced concrete using recycled aggregates. Construction and Building Materials, Vol. 98 (2015), pp. 620-630.

[53] Snowden, P. (2015). The durability performance of concrete containing recycled concrete aggregate and ground granulated blast furnace slag. A dissertation submitted in partial fulfilment of the requirements for the award of a Masters of Civil Engineering of Loughborough University.

[54] Yidirim, S.T., Meyer, C. and Herfellner, S. (2015). Effects of internal curing on the strength, drying shrinkage and freeze-thaw resistance of concrete containing recycled concrete concrete aggregates. Construction and Building Materials, Vol. 91(2015); pp. 288-296.

[55] Lotfi, S., Eggimann, M., Wagner, E., Mróz, R. and Deja, J. (2015). Performance of recycled aggregate concrete based on a new concrete recycling technology. Construction and Building Materials, Vol. 95(2015), pp. 243-256.

[56] Laserna, S. and Montero, J. (2016). Influence of natural aggregates typology on recycled concrete strength properties. Construction and Building Materials, Vol. 115(2016); pp. 78-86.

[57] Seara-Paz, S., Corinaldesi, V., González-Foteboa, B. and Martínez-Abella, F. (2016). Influence of recycled coarse aggregates characteristics on mechanical properties of structural concrete. European Journal of Environmental and Civil Engineering, Vol. 20 No. 1; pp. 123-139.

[58] McGinnis, M.J., Davis, M., de la Rosa, A., Weldon, B.D. and Kurama, Y.C. (2017). Strength and stiffness of concrete with recycled concrete aggregates. Construction and Building Materials, Vol. 154 (2017), pp. 258-269.

[59] Liu, Z., Cai, C.S., Peng, H. and Fenghong, F. (2016). Experimental study of the geopolymeric recycled aggregate concrete. Journal of Materials in Civil Engineering, Vol. 28 No.9; pp. 04016077-1-9.

[60] González-Taboada, I., González-Fonteboa, B., Martínez-Abella, F. and Carro-López, D. (2016). Study of recycled concrete aggregate quality and its relationship with recycled concrete compressive strength using database analysis. Materials De Construction 66 (323); pp. 1-18.

[61] Deng, X.H., Lu, Z.L., Li, P. and Xu, T. (2016). An investigation of mechanical properties of recycled coarse aggregate concrete. Archives of Civil Engineering, Vol. LXII No. 4(2); pp. 19-34.

[62] Zaetang, Y., Sata, V., Wongsa, A. and Chindaprasirt, P. (2016). Properties of pervious concrete containing recycled concrete block aggregate and recycled concrete aggregate. Construction and Building Material, Vol. 111 (2016), pp. 15-21.

[63] Kurad, R., Sivestre, J.D., de Brito, J. and Ahmed, H. (2017). Effects of incorporation of high volume of recycled concrete aggregates and fly ash on the strength and global warming potential of concrete. Journal of Cleaner Production, 166 (2017); pp. 485-502.

[64] Hamad, B.S. and Dawi, A.H. (2017). Sustainable normal and high strength recycled concrete aggregates using crushed tested cylinders as coarse aggregates. Case Studies in Construction Materials, 7(2017); pp. 228-239.

[65] Kanema, J.M., Eid, J. and Taibi, S. (2016). Shrinkage of earth concrete amended with recycled aggregates and superplasticizer: Impact on mechanical properties and cracks. Materials and Design, 109 (2016); pp. 378-389.

[66] Parthiban, K. and Mohan, K.S.R. (2017). Influence of recycled concrete aggregates on the engineering and durability

properties of alkali activated slag concrete. Construction and Building Materials, Vol. 133 (2017), pp. 65-72.

[67] Sahoo, K.K., Arakha, M., Sarkar, P., Davis, R.P. and Jha, S. (2016). Enhancement of properties of recycled coarse aggregate concrete using bacteria. International Journal of Smart and Nano Materials, Vol. 7 No. 1; pp. 22-38.

[68] Kumar, R., Gurram, S.C.B. and Minocha, A.K. (2017). Influence of recycled fine aggregate on microstructure and hardened properties of concrete. Magazine of Concrete Research, (2017); pp. 1-8.

[69] Silva, R.V., de Brito, J. and Dhir, R.K. (2016). Establishing a relationship between modulus of elasticity and compressive strength of recycled aggregate concrete. Journal of Cleaner Production, Vol. 112(2016), pp. 2171-2186.

[70] Pedro, D., de Brito, J. and Evangelista, L. (2014). Influence of the use of recycled concrete aggregates from different sources on structural concrete. Construction and Building Materials, Vol. 71 (2014), pp. 141-151.

[71] Rodríguez-Robles, D., García-González, J. Juan-Valdés, A., Morán—del Pozo, J.M. and Guerra-Romero, M.I. (2017). Effect of mixed recycled aggregates on mechanical properties of recycled concrete. Magazine of Concrete Research, Vol. 67 No. 5; pp. 1-10.

[72] Thomas, C., Setién, J. and Polanco, J.A. (2016). Structural recycled aggregate concrete made with precast wastes. Construction and Building Materials, Vol. 114 (2016), pp. 536-546.

[73] Anastasiou, E., Filikas, K.G. and Stefanidou, M. (2014). Utilization of fine recycled aggregates in concrete with fly ash and steel slag. Construction and Building Materials, Vol. 50 (2014), pp. 154-161.

[74] Soares, D., de Brito, J., Ferreira, J. and Pacheco, J. (2014). Use of coarse recycled aggregates from precast concrete rejects: Mechanical and durability performance. Construction and Building Materials, Vol. 71 (2014), pp. 263-272.

[75] Katkhuda, H. and Shatarat, N. (2017). Improving the mechanical properties of recycled concrete aggregate using chopped basalt fibres and acid treatment. Construction and Building Materials, Vol. 140 (2017), pp. 328-335.

[76] ISO 13823: 2008 (en). General principles on the design of structures for durability. Available https://www.iso.org/

[77] Domone, P.L. (2010). Self-compacting concrete: An analysis of 11 years of case studies. Construction and Building Materials, Vol. 24 No. 1, pp. 113-117.

[78] Dyer, T. (2014). Concrete Durability, Boca Raton, FL: CRC Press, Taylor & Francis Group.

[79] Bapat, J.D. (2013). Mineral admixtures in cement and concrete, CRC Press.

[80] de Brito, J., Ferreira, J., Pacheco, J., Soares, D. and Guerreiro, M. (2016). Structural, Material, mechanical and durability properties and behaviour of recycled aggregate concrete. Journal of Building Engineering, Vol. 6 (2016), pp. 1-16.

[81] Evangelista, L., Guedes, M., de Brito, J., Ferro, A.C. and Pereira, M.F. (2015). Physical, chemical and mineralogical properties of fine recycled aggregates made from concrete waste. Construction and Building Materials, 86 (2015); pp. 178-188.

[82] Singh, N. and Singh, S.P. (2016). Carbonation and electrical resistance of self-compacting concrete made with recycled concrete aggregates and metakoalin. Construction and Building Materials, Vol. 121 (2016), pp. 400-409.

[83] Pedro, D., de Brito, J. and Evangelista, L. (2017b). Structural concrete with simultaneous incorporation of fine and coarse recycled concrete aggregates: Mechanical, durability and long term properties. Construction and Building Materials, Vol. 154 (2017), pp. 294-309.

[84] Qiu, J., Tng, D.Q.S. and Yang, E.H. (2014). Surface treatment of recycled concrete aggregates through microbial carbonate precipitation. Construction and Building Materials, Vol. 57 (2014), pp. 144-150.

[1.]O.O. FAGBOLU, [2.]A.O. ATOLOYE

# MOBILE RECRUITMENT SYSTEM FOR NIGERIAN CIVIL SERVICE COMMISSION VIA CLOUD COMPUTING

[1,2.]Department of Computer Science, School of Computing and Information Technology,
Kampala International University, Kampala, UGANDA

**Abstract:** Traditional recruitment procedures are replaced in order to overcome most of its attendant challenges such as time-consuming and tiresome nature of recruiting a larger number of applicants into Civil Service from different parts of Nigeria considering multifaceted nature of the nation. This research work obliterate favoritism, nepotism and other corrupt means that were the usual practice in shortlisting prospective candidate for job, electronic recruitment system are enhanced with the availability of mobile platform that improve accessibility with emerging computing paradigm over the internet. Finite State Transducer (FST) in Machine Learning is used to learn from the pool of candidates for employment, GIATI (Grammar Inference and Alignment for Transducers Inference) are efficiently applied that is prospective candidates are offered job on a deductive rule-based Machine Learning. It is implemented with Android Studio and WAMP server. Its performance was tested using Ogun State as a pilot in the Federation and User Satisfaction was evaluated.
**Keywords:** recruitment, e-recruitment, mobile recruitment, finite state transducer, GIATI

## INTRODUCTION

E-recruitment is done on web and other media, it is a practice in which technology are deployed to attract, find, evaluate and hire people. Suitable candidate are searched for, assess, interview and hire personnel based on the vacancies but the accessibility of mobile phones, PDA, tablets and other portable gadgets will encourage, invigorate and support the Mobile Recruitment (m-Recruitment). Mobile gadgets are commonly used and readily available for easier use than other electronic gadgets because of its portability and availability, the growing use of mobile technologies couple with the evolution of technologies has opened up novel opportunities, contributed to the way of life of people and how endeavors are better tackled which invariably bring about the need to develop m-recruitment system for Nigerian Civil Service.

Considering the mobile deployment in business and banking (m-business and m-banking) and its ease of use coupled with the wider acceptability then this concept can be used in government agencies and parastatals to recruit qualified candidates to various vacancies (CRR, 2015). The remarkable use of mobile technologies has brought great changes, not only to individuals but also to several companies including their service, hence mobile technologies is stretching into shortlisting and recruiting prospective jobs seeker into Nigerian public sector on cloud. M-Recruitment on cloud will avail diverse resources to both applicant and the government which include software, hardware, data storage, power consumption and so on. In this system, computing needs are accessed, stored and occur over the internet. Hardware resources such as processing power, memory are replicable so as to efficiently utilize these hardware resources that is, memory and processing power can be multiplied and moved from server to server at any time. The storage of data is done online (cloud storage) which means as data are stored, it will be accessed from different distributed terminals.

Power consumption could be saved by moving and processing recruitment process in Nigerian Civil Service into the cloud and consequently saved electricity. Although there are many ways by which the Nigerian Civil Service recruit talents for their organization which can be internal (it is vacancies for staff that were on previous appointment with a particular government agency but desire upward movement which can be promotion, transfer, employment exchanges, employee recommendation and others) and external vacancies (it is done for fresh applicant that were not on previous employment of government parastatals) (Sharma, 2014). Recruitment is an essential part of any organization as it includes the way of drawing or harnessing critical assets for example, human capacity and skills into an organization (Amusan, 2016) and Government as well as individuals are aware that lack of employee may impede their growth and compromise their success. In 2014, 3.6 billion people had a mobile subscription, accounting for 50 percent of the world population. In that same year, 2.6 billion people had a smartphone, a penetration rate just under 40 percent (GSMA, 2015).

The Nigerian Civil Service has been undergoing gradual restructuring and systematic reforms since May 29, 1999 after decades of military era (Babaru, 2003). Government have made effort to transient from archaic and traditional ways of handling their activities to better, sophisticated and electronic approach but recruitment processes is still adjudged to be grossly unfair, ethical, costly and time-consuming hence need for m-Recruitment will proffer solutions to problems such as filling of forms, time

consuming manual screening and reviewing of resumes which is often fuelled by sectionalism, nepotism and favouritism. These issues has become very critical and spread from the Federal Civil Service to the State Civil Service Commissions(Briggs, 2007). Recruitment process in Nigeria has become nightmare as indicated by 2014 report of Nigeria Immigration Service where 15 unemployed youth died in a stampede, 200 injured including pregnant women.

The country experienced a terrible situation in which 6.5 million people applied for 4000 vacancy positions (administration news, 2014). Although government has introduced e-recruitment as the recruitment strategy in some ministries, departments and agencies but still with some flaws while the m-recruitment is proposed and developed to cater for these inadequacies.

## WHY DO WE NEED TO GO MOBILE?

The total number of mobile subscribers has increased rapidly over the past decade; at the end of 2005 there were 19,519,154 subscribers, but by the end of 2015 there were 151,017,244 subscribers which is equivalent to an increase of 13,149,809 subscribers every year. However, this increased population of subscribers will help recruiters (Government or Individual) in employing best fit and most suitable candidates in terms of quality and quantity through mobile technologies.

## STATISTICAL FRAMEWORK FOR M-RECRUITMENT SYSTEM

Finite State Transducers have proved to be useful in Machine Learning, Stochastic Finite State Transducer (SFST) is used to automatically learn from the database or pool of prospective candidates for employment by using efficient algorithms called GIATI (Grammar Inference Alignments for Transducer Inference).

The candidates are offered job on a rule-based Machine Learning which is deductive and involve knowledge domain of the employer. GIATI models the shortlisting once the basic requirement such as WAEC (West African Examination Council) or Bachelor Degree/Higher National Diploma are met.

GIATI Algorithm provides a probabilistic finite state transducer that performs the following:

(1) Given a list of prospective applicant, find the status of the applicant by assigning an output sequence to their basic requirement.

(2) Deduce probabilistic finite state automation from the database by promoting the use of k-testable in the strict sense (k-TSS) model instead of n-gram models, since k-TSS model keep the rules of shortlisting any qualified applicant

(3) Split the status of the applicant such as Offered employment, Denied employment or Indifferent

Once we have the transducer and prospective applicant submit their application as input $r \in \Sigma^+$, the recruitment process implies searching the applicant details which will include Academic, Personal and Medical to determine the status of their job requirement $s$ where $d(r, s)$ represents a path in SFST which is compatible with the applicant requirement, status and joint probability is

$$s = \arg\max_{s} (P(r, s) \approx \arg\max_{s} \max_{d(r,s)} P(d(r, s))$$

This research work handles an efficient e-recruitment framework to deal with all phase of the e-recruitment process such as multi-job posting, organization channel administration and candidate filtering to distinguish the most qualified candidates. The system is developed using macromedia dream weaver (a professional HTML editor for designing, coding, and developing websites, web pages, and web applications), SWISHmax (for creating graphics and animations), Structured Query Language (SQL) database creation for the website, creation of different tables and the storage of data sent from the website).

## EXISTING SYSTEM

The existing system for recruitment in Ogun State Civil Service has been traditional mode of recruitment since the creation of the state in 1976. Traditional civil service recruitment is centralized but relies on formal examinations and leaves government officials with low discretion and little or no flexibility. Increasingly, this method of recruitment is however with its own attendant flaw which is challenged by faster and more flexible private sector practices to avail prospective job seekers with more effective, high discretion and greater flexibility. The traditional process of recruitment includes submission of job request and its approval, recognition of recruitment needs, application or resumption of screening, job posting, pre-employment screening, interviewing and employment contract and job offers (Sundell, 2013).

## IMPLEMENTATION

Recruitment system via cloud computing was developed with Android Studio Development Platform, for execution and debugging Android Emulator with SDK and Nexus 5_API_21 on Android 4.4 and a 4-inch screen HDPI was used. The mobile recruitment system was designed to be user friendly, easy to navigate and all what the prospective user needs to apply for job is to download the application from the publisher store. This is achieved by offering data privacy, index privacy, keyword privacy and many others, the cloud enable search service which is of utmost paramountcy to mobile recruitment system and eliminate local storage management, storing data into the cloud does not serve a purpose unless they can be searched and utilized easily, conveniently and efficiently. By considering the larger population of Nigeria, search service will eliminate unnecessary network traffic by sending back only most relevant data that are desirable in the pay-as-you-use cloud paradigm.

The various modules were integrated together in different interfaces, the modules were packaged and install on the testing machine, each module having some specific requirements but certain minimum specifications were met. Mobile Recruitment System for Nigerian Civil Service Commission was configured and implemented.

The configuration of the application was done in the Android Studio using Java Programming Language, PHP (Hypertext

ACTA TECHNICA CORVINIENSIS – Bulletin of Engineering
Tome XI [2018] | Fascicule 3 [July – September]

processor) was used to connect Android Studio Platform of Mobile Recruitment Application to a database and validate the table designed in the WAMP. MySQL connector was used to link Android Studio and WAMP server at the backend.



Figure 1: Mobile app for prospective job seekers



Figure 2: Mobile app with a typical drop-down menu

## RESULT AND DISCUSSION
By experimenting with the system, it afforded us to determine whether the system is capable of accepting applicant data for job processing. Conclusive validation was done to test, evaluate and measure the usability of the developed mobile application.

The first stage of the evaluation was the self-evaluation and technical testing which was carried out without the help of external users, and this part included validating and dry running the java code, xml code, testing the system with different kinds of inputs, debugging, and other design issues. After that, the system was tested using android virtual device (emulator). At this stage the system was said to be valid.

At the second stage of evaluation, a survey was conducted using questionnaire with prospective applicants, Twenty-eight (28) was used to pick sample size from population of Thirty (30) in sample size determinant table (Krejcie and Morgan, 1970) in Abeokuta, Ogun State of Nigeria. Table 1, shows the responses for the multiple choice questions, along with each question, the percentage of user satisfaction of the system is 60% positive feedback for that question according to our success criteria.

Table1: Results from questionnaire that show evaluation of the user satisfaction of the developed application.

| Responses | Number of Applicant | Count | Percentage |
|---|---|---|---|
| Very Satisfied | 28 | 5 | 17.9 |
| Satisfied | 28 | 17 | 60.7 |
| Not Satisfied | 28 | 6 | 21.4 |

It is shown from Table 1 that user satisfaction for prospective job seekers randomly selected is 78.6% while only 21.4% were not satisfied with the mobile app.

Table2: Results from questionnaire that show evaluation of the user interaction of the developed application.

| Responses | Number of Applicant | Count | Percentage |
|---|---|---|---|
| Excellent | 28 | 16 | 57.1 |
| Good | 28 | 6 | 21.4 |
| Bad | 28 | 6 | 21.4 |

Table 2 shows that interactivity of the mobile application is satisfactorily okay with 78.5% and 21.4% is the percentage of dissatisfaction with the developed mobile application and from this result, it was deduced that the developed mobile recruitment system attain satisfactory level when compare with the existing system in terms of satisfaction and interaction.

## CONCLUSION
This research work introduced a new mobile application for recruitment that can facilitate many recruitment in 24 hours in a week without any limitations and make larger storage capacity available in cloud hence irrespective of the population of any nation, this recruitment system can be employed. Shortcomings of other online job portals were enhanced after thorough analysis of their limitations.

At the end, the use of a mobile recruitment application will greatly enhance Civil Service Commission responsibilities by improving flexibility, enhancing transparency, promoting equity among different applicants and upsurge accessibility, portability and availability to applicants and Nigerian government. Cloud services will ensure that mechanism for accountability, tracking and transparency are obtainable while valuable information can therefore be centralized, stored and redistributed so as to avoid data redundancy and unnecessary duplication and the recruitment processing time will consequently be reduced.

137 | Fascicule 3

## References

[1] Ahmad, S. and Ahmad, M: Good Governance as a Yardstick to Measure the Effectiveness of E-recruitment in Nigerian Public Service, Journal of US-China Public Administration, volume(9), pp. 1-7, ISSN 1548-6591, January 2012.

[2] Aloisa, N: E-recruitment systems: A theoretical model, DWU Research Journal Contemporary PNG Studies, volume (23) November 2015.

[3] Amusan, D. G: Development of Efficient E-Recruitment System for University Staff in Nigeria, Vol 1(1), pp. 10–14, 2016.

[4] Babaru, A.S: Leading public service innovation, in New Zealand Agency for International Development (NEAID), Monday, February 24th – 26th March, pp. 26, 2003

[5] Briggs, B. R: Problems of recruitment in civil service -Case of the Nigerian Civil Service, volume (1) pp. 142–153, September, 2007.

[6] Caudill, J.G: The growth of m-learning and the growth of mobile computing: Parallel developments, 2007. Retrieved on 17/01/2017.

[7] Consumer Requirement Regulation: Mobile Update and Mobile commerce- Percentage of total e-commerce in select global markets in 2015, Workshop 2015. Retrieved January 2, 2017.

[8] Du Plessis, A.J: Effectiveness of e-recruiting: empirical evidence from the Rosebank business cluster in Auckland, New Zealand, Science Journal of Business Management, pp.1-19, 2012.

[9] Emma, O and Paul, M: Politics of Recruitment and Selection in the Nigerian Civil Service – An Ebonyi State Experience, volume 5 (2), pp. 92–100, 2015.

[10] Fagbolu, O.O; Alese, B.K and Adewale, O.S: Development of a Digital Yorùbá Phrasebook on a Mobile Platform, Nigerian Computer Society (NCS) 25th Annual Conference Building a knowledge-based economy in Nigeria: The Role of Information Technology Nike Lake Resort Enugu, volume (25), pp. 13 – 19, 2014.

[11] Global System Mobile Association (GSMA): The Mobile Economy, 2015.

[12] Krejcie, R. V., Morgan, D. W: Determining Sample Size for Research Activities, Educational and Psychological Measurement, volume (30), pp. 607-610, 1970.

[13] Kuyoro, S. O; Okolie, S. O and Abel, S. B: Design and Implementation of an Automated Personnel Recruitment System, volume 2 (3), pp. 313–318, 2012.

[14] Niklas, S. and Böhm, S: Applying Mobile Technologies for Personnel Recruiting – An Analysis of User - sided Acceptance factors, volume 3 (1), pp. 169–178, 2011.

[15] Nigerian Telecommunications Services Sector Report: 2016.

[16] Shahila D: E-Recruitment Challenges, International Journal of Social Science and Interdisciplinary Research IJSSIR, volume. 2 (5), pp.118-12, May 2013.

[17] Sharma, N: Recruitment Strategies -A Power of E-Recruiting and Social Media, volume 1 (5), pp. 15–35, 2014.

[18] Sundell, A: The Conditional Relationship Between Traditional Civil Service Recruitment and Meritocracy, September 2013.

[19] Wolswinkel, J; Fuertmueller, E and Wilderom, C: Reflecting on E-Recruiting Research Using Grounded Theory, 18th European Conference on Information Systems, University of Twente, Netherlands, 2010.

[20] Yadav, A. K: A Study of Recruitment and Selection of Employees in Public Sector Enterprises of India, volume 9 (2), pp. 39–43, 2014.

[1.]Salahaldein ALSADEY, [2.]Abdelnaser OMRAN

# EFFECT OF SUPERPLASTICIZER ON PROPERTIES OF MORTAR

[1.]Department of Civil Engineering, Faculty of Engineering, Bani Waleed University, Bani Waleed, LIBYA
[2.]College of Engineering, Bright Star University, Elbrega City, LIBYA

**Abstract:** Superplasticizers are chemical admixtures used where well-dispersed particle suspension is required. They have become indispensable constituents of any designed cement mortar mix today. Property of fresh and hardened cement mortar is strongly influenced by the interaction of superplasticizers and cement which is essentially requiring a careful selection of SP dosage. The performance of superplasticizers in cementitious system is known to depend on cement fineness, cement composition mode of introduction to the mixture etc., as well as on the chemical composition of superplasticizers. This present study examined the effect of Plastiment –BV 40 and the effect of SP dosage on the properties of cement mortar was investigated. The test samples were subjected to elevated temperatures ranging from 200°C to 400°C. After exposure compressive strength test was conducted. The strength properties of cement mortars at different dosage of SP cement mortars were also investigated. The results show that 0.4-0.8 % more than dosage required to exhibits better workability and also strength for cement mortar.
**Keywords:** mortar, cement, superplasticizer, temperature, saturation dosage, strength

## INTRODUCTION

Superplasticizers are chemical admixtures used where well-dispersed particle suspension is required (Ramachandran, 1995, Wikipedia, 2018). They have become indispensable constituents of any designed cement mortar mix today. Property of fresh and hardened cement mortar is strongly influenced by the interaction of superplasticizers and cement (Maheshwarappa et al., 2014) which is essentially requiring a careful selection of SP dosage (Ronneberg and Sandvik, 1990; Aitcin et al., 1991; Maheshwarappa et al., 2014).

The term cement-SP compatibility is used to represent the ability to achieve the desired result from a cement-SP combination in a concrete mix viz., improved workability for a given w/c or reduction in free water for a target workability (Maheshwarappa et al., 2014). An extensive literature had been carried out to study the effect of superplasticizer on the compressive strength of concrete and its workability. A study by Franklin (1976) reported that superplasticizers are organic polyelectrolytes, which belong to the category of polymeric dispersants.

The performance of superplasticizers in cementitious system is known to depend on cement fineness, cement composition mode of introduction to the mixture etc., as well as on the chemical composition of superplasticizers. Ozkul and Dogan (1999) carried out a study on the effect of an N-vinyl copolymer superplasticizer on the properties of fresh and hardened concretes.

Workability of concrete was measured by slump flow test and in situ tests were undertaken to find out the pumping ability of super plasticized concrete. The coarse aggregate was crushed stone with the maximum size of 25 mm. By using this chemical admixture, which was a little bit different from the conventional ones, the ability of water reduction was increased along with the retention of high workability for a longer time.

Roncero et al. (1999) evaluated the influence of two superplasticizers (a conventional melamine based product and a new-generation comb-type polymer) on the shrinkage of concrete exposed to wet and dry conditions. Tests of cylinders with embedded extensometers have been used to measure deformations over a period of more than 250 days after casting. In general, it was observed that the incorporation of superplasticizers increased the drying shrinkage of concretes when compared to conventional concretes, whereas it did not have any significant influence on the swelling and autogenous shrinkage under wet conditions.

Aitcin et al. (1991) reported that by choosing carefully, the combination of Portland cement and superplasticizer, it was possible to make a 0.17 water/binder ratio concrete with 230mm slump after an hour of mixing which gave a compressive strength of 73.1MPa at 24 hours but failed to increase more than 125MPa after long-term wet curing. During 1980s, by increasing the dosage of superplasticizers little by little over the range specified by the manufacturers, it is realized that superplasticizers can be used as high range water reducers (Ronneberg and Sandvik, 1990). In this current study, the strength properties of mortar have used as criteria for evaluating its performance. In the absence of proper quality control measures, the batch to batch variations in SPs can also add to the problems. Clearly, this is only a short-term solution.

For a more comprehensive approach, a thorough understanding of the causes and remedies of incompatibility is necessary. Since the problem is often region specific and project specific, it is necessary to identify possible source of variability and address the problem of incompatibility that can arise.

The chemical admixtures are very important components of modern concretes and mortars; they make it possible to

modify certain properties of the mortar in the fresh or hardened state (Alsadey, 2015). Conventionally, researchers have used strength properties of mortar as criteria for evaluating its performance. A mortar having high strength does not necessarily imply that it will have a long- service life. Thus, it is clearly well known that mortar performance should be determined in terms of both strength and durability under anticipated environmental conditions. Various definitions exist for high-performance mortar (HPM). The objective of this current study is to investigate the effects of high temperatures on Superplasticizer Mortar performance. High-temperature resistance is defined as the ability of a structural element to withstand its load-bearing function under a high-temperature condition.

The mortar behaviour at high temperature is of concern in predicting the safety of building and construction in response to certain accidents or particular service conditions. The behaviour of mortar with respect to a high temperature where tested on groups of specimens to identical testing condition. Such investigation is aimed at studying the influence of exposing to high temperatures on some mechanical properties of mortar containing admixtures.

Most of the past studies had discussed the effect of temperature on concrete and the effect of admixtures on concrete independently but none of these studies had taken into consideration the effect of temperature on mortar containing admixtures which became the intention of the researchers to consider in this current study where it is expecting that each admixture dosage which will be added to mortar will have a different effect on the mechanical properties, under the influence of high temperatures.

## METHOD AND MATERIALS
### ─ Materials Used and Properties
The experimental investigation was carried out in the Concrete Laboratory of the faculty of Engineering at Bani Waleed University.

The cement used in mortar mixtures was the ordinary Portland cement type I manufacture in Zlitan. The fine aggregate was sea sand, with a fineness modulus of 2.86 and maximum size of less than 5 mm, and Ordinary drinking (tap) water from Bani Walid area was used in all cement mortar mixes of this study water.

Plastiment –BV 40 is the superplasticizer used in this study. Plastiment –BV 40 complied with requirements of ASTM (ASTM C494/C494M-04, 2004).

### ─ Mix Proportions and Mixing Method
Five mortar mixes were prepared using the water-cement ratio as 0.42. The sea sand was used as fine aggregate. The mix design of the control mix (M1) was carried out according to the absolute volume method given by the ACI (ACI Committee 211, 1993) to achieve the criteria of flowing cement mortar.

The superplasticizer used in this study is Plastiment-BV 40. It is suitable for all types of cement mortar. One of its benefits is that it can improve both early and final strength. The superplasticizer dosages 0.4%, 0.8%, 1.2%, and 1.6% were used to prepare mixes: M2, M3, M4 & M5, respectively. Each batch of mortar was produced in a pan mixer.

The cement, sand, water and Plastiment-BV 40 were added to the mixer and mixed for 3 minutes. Each batch of cement mortar was produced in a pan mixer. Then after mixing process, the slump test was done. Then the mix was immediately poured into moulds by means of a scoop. Casting of the samples was carried out in two layers; each layer was compacted by using a small steel bar.

The complete compaction was determined by appearance of a film of cement mortar on the top, and the air void was no longer appearing. After compaction, the top surfaces of specimens were trowelled level for obtaining a smooth surface.

After casting, all specimens were kept under nylon sheets inside the laboratory for (24±2) hours to assure a humid air around the specimens and to prevent fast evaporation of water from the specimens, and then they were demoulded and cured until they were tested.

All specimens prepared for compressive were stored in tap water tanks until testing age of 28 days it was three cube samples of 50 mm were used for each mix. The compressive strength test was done immediately according to ASTM (ASTM C 192/C 192M, 2002) for each test mix.

### ─ Mortar Heating and Cooling Process
The mortar specimens were heated to different levels of high temperatures; using an electrical furnace with a maximum temperature of $(2400^0C)$. The furnace consists of wide chamber of a double metal containing auto-control thermal probes; with built in thermocouples.

The temperature of the furnace increases by an average value of $(5^0C/min)$ at its primary stage up to $(200^0C)$, becoming faster to about $(10^0C/min)$ at the required temperature.

The mortar specimens were then placed inside the furnace for ten mints at a constant temperature; after that, the specimens were left for (10 min) to be air cooled.

## RESULTS AND DISCUSSION
### ─ Effect of Superplasticizer Compressive Strength
The change of the residual compressive strength in mortar mixes at an age of (28) days during the temperatures rise is shown in Figure (1).

In general, the compressive strength of different mortar mixes is decreased by various proportions as a result of exposure to high temperatures. As shown in Table (1), the highest stress was that for mortar containing the superplasticizer additive at $0^0C$ compared with reference mortar mix.

For reference mortar mix M1 at (28) days, the residual compressive strengths are about (41 N/mm$^2$, 40 N/mm$^2$) at a temperature of $(200, 400)^0C$ respectively. The residual stresses for mortar containing additives are about (33 N/mm$^2$, 32 N/mm$^2$, 28 N/mm$^2$, and 27 N/mm$^2$) for (M2, M3, M4 and M5) respectively at a temperature of $(200^0C)$. At a temperature of $(400^0C)$, the residual compressive strength for mortar

containing additive are about (32 N/mm$^2$, 30N/mm$^2$, 26 N/mm$^2$, and 24 N/mm$^2$) for (M2, M3, M4, & M5) respectively.

Table 1. Effect of temperature
on different properties of mortar

| Mixture | Superplasticizer (SP) % | Slump (mm) | Compressive Strength (N/mm$^2$) | | |
|---|---|---|---|---|---|
| | | | 0 C$^0$ | 200 C$^0$ | 400 C$^0$ |
| M1 | 0 | 145 | 43 | 41 | 40 |
| M2 | 0.4 | 170 | 47 | 33 | 32 |
| M3 | 0.8 | 173 | 49 | 32 | 30 |
| M4 | 1.2 | 180 | 31 | 28 | 26 |
| M5 | 1.6 | 210 | 31 | 27 | 24 |
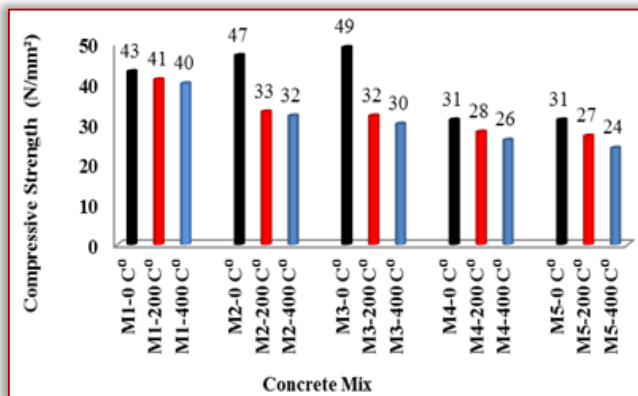


Figure 1. Effect of Temperature
on Compressive Strength of Mortar

## CONCLUSION

Based on these obtained results, this study concluded that the existence of additive in the mortar mix exposed to high temperatures resulting variable changes in compressive strength compared to the reference mix.

These changes –in general–varied from additive dosages for different temperatures; however it was limited to 200°C but was clear at 400°C.

It has also concluded that the mix containing a superplasticizer maintained the higher residual proportion of the compressive strength at a temperature of 0°C, while the mix containing the superplasticizer additive maintained the lowest residual compressive strength at temperatures of (200, 400)°C.

## Acknowledgement

## References

[1] ACI Committee 211 (1993). Guide for selecting proportions for HSC with Portland cement and fly ash, ACI material journal, 90 (3): 273-283.
[2] Aitcin, P.C., Sarkar, S.L., Ranc, R., and Levy, C. (1991). A high silica modulus cement for high-performance concrete - advances in cementitious materials. Vol.16 (Ed. by J. Mindess), American Ceramic Society, Westerville, OH, USA, pp. 103-120.
[3] Alsadey, S.M.K. (2015). Effect of Superplasticizer on Fresh and Hardened Properties of Concrete" Journal of Agricultural Science and Engineering, 1(2): 70-74.
[4] ASTM C 192/C 192M. (2002). Standard Practice for Making and Curing Concrete Test Specimens in the Laboratoryǁ. ASTM International.
[5] ASTM C109 (2002). Standard Test Method for Compressive Strength of Hydraulic Cement Mortars Using 50mm Cube Specimens. Annual book of ASTM standard.
[6] ASTM C230 (2002). Standard Specification for Flow Table for Use in Tests of Hydraulic Cement. Annual book of ASTM standard; PA, www.astm.org.
[7] ASTM C494/C494M-04 (2004). Standard and Specification for chemical admixtures for concrete, Annual Book of ASTM Standards, Vol.04.02.2004.
[8] Franklin A.J. (1976). Cement and mortar Additives. Noyes Data Corporation USA, pp. 308.
[9] Maheshwarappa, S.M., Madhuvan, S., Chetan Kumar, K.M., & Dattatreya, J.K. (2014). Effect of Superplasticizers Compatibility on the Workability, Early Age Strength and Stiffening Characteristics of OPC, PPC, AND PSC Pastes and Mortar, International Journal of Research in Engineering and Technology, 3 (3), 419-425.
[10] Ozkul, M. H., and Dogan, A. (1999). Properties of fresh and hardened concrete prepared by N-vinyl copolymers", International Conference on Concretes, Dundee, Scotland.
[11] Ramachandran, V.S. (1995). Concrete Admixtures Handbook – Properties, Science, and Technology, 2$^{nd}$ Edition, William Andrew Publishing.
[12] Roncero, J., Gettu, R., and Carol, I. (1999). Effect of chemical admixtures on the shrinkage of cement mortars, ACI SP-189, 273-294.
[13] Ronneberg, H., and Sandvik, M. (1990). High strength concrete for North Sea platforms. Concrete International, 12, 29-34.
[14] The American Concrete Institute (ACI 211.1-91), (2000). Standard P "Standard Practice for Selecting Proportions for Normal, Heavyweight, and Mass Concrete", ACI Manual of Concrete Practice 2000, Part 1: Materials and General Properties of Concrete.
[15] Wikipedia (2018). General information on Superplasticizer, https://en.wikipedia.org/wiki/Superplasticizer [24/3/2018].

# Fascicule 3
## [ July - September ]
## t o m e
## [2018] XI

ACTA Technica CORVINIENSIS
BULLETIN OF ENGINEERING

ACTA TECHNICA CORVINIENSIS BULLETIN OF ENGINEERING

## ISSN: 2067-3809

¹·J. ABUTU, ²·S.A. LAWAL, ³·M.B. NDALIMAN, ⁴·R.A. LAFIA ARAGA

# AN OVERVIEW OF BRAKE PAD PRODUCTION USING NON–HAZARDOUS REINFORCEMENT MATERIALS

1-4.Department of Mechanical Engineering, Federal University of Technology, Minna, NIGERIA

**Abstract:** An overview of brake pad production using non–hazardous reinforcement materials is carried out with assessment of various production methods and mechanical and tribological properties produced from these non–hazardous materials. Suggestion of new research directions with respect to the combination of these non–hazardous materials in different proportion is made. This paper concludes by advocating for commercial or industrial application of these brake pads that has been developed from these non–hazardous materials.
**Keywords:** material, mechanical properties, tribological properties, environment, friction

## INTRODUCTION

Brake pad material is a heterogeneous substance composed of different elements. Each constituent element has its own functions which include improvement of frictional properties at low and high temperature, reduce noise, prolong life, increase strength and rigidity as well as reduce porosity. Changes in the weight percentage or types of elements in the formulation may result to the alteration of the chemical, mechanical and physical properties of the brake pad materials developed (Jang *et al.,* 2004; Cho *et al.,* 2005 and Mutlu *et al.,* 2005; Zaharudin *et al.,* 2012). Early researchers have concluded that no simple correlation exist between wear and friction properties of frictional materials with the mechanical and physical properties (Talib *et. 1al.,* 2006; Todorovic, 1987 and Tanaka *et al.,* 1973).

As a result, each new formulation developed requires to be subjected to several tests to evaluate its wear and friction properties using on–road braking performance test as well as abrasion testing mechanism to ensure that the developed friction pad material meets the minimum requirements of its intended use (Talib *et al.,* 2006). Modern brake pad development has history spanning over the past 100 years. Herbert Frood was credited to be the first to invent brake pad materials in 1897. This pad was a cotton–based material that was used for wagon wheels as well as early automobiles and coupled with bitumen solution. This invention led to the formation of the manufacturing company known as Ferodo Company, a firm which still supplies frictional materials till date. Bertha Benz, the wife of Carl Benz was the first to invent patented automobile friction pads. This invention came during her first long and historic distance trip by a car in 1888 (Blau, 2001).

The earliest brake pad material was woven, but in the early 1920's, moulded materials which were made of crysotile asbestos fibres, a plentiful mineral were used to replace it. In the 1950's, metallic pads that were resin–bonded were introduced, and semi–metals which contain higher amount of metal additives were developed in the 1960s (Nicholson, 1995). Industrial brake pads usually contain many constituents such as ceramic particles and fibres, metallic chips, minerals solid lubricants and elastomers in a matrix material like phenolic resin. Also, Ole–Von et al. (2005) investigated the use of antimony in brake pads. The results show that the use antimony (Sb) in friction materials should be suspended as it posed a human cancer risk due to considerable concentrations of Sb in the material. Agricultural products are also emerging as inexpensive and new materials in the development of brake pad material with commercially viability and environmental acceptability (Bledzki and Gassan, 1999). Cyras *et al*. (2001) reported that among the different kinds of agricultural products investigated, lignocellulosic fillers are most times considered as attractive materials to be utilised as fillers of thermoplastic polymers due to its excellent properties.

It is possible to obtain composite materials with properties very similar to the existing synthetic–filler reinforced plastics with their superior properties such as low density, energy recovery, low cost, enhanced recyclability and biodegradability. Garcia *et al*. (2007), Bledzki and Gassan (1999) and Seki, (2006), also reported the use of rice husk that one of the agricultural products which can be potentially utilised as fillers in friction pad production is the. It was stated that rice is the most important food crop grown and planted in the world today and they can be grinded and burned at low temperature. This burning and grinding process produced white ashes which consist of about 80% silica. The rice straw comprises of 20% hemicelluloses, 30% cellulose and lignin, 10% water and about 15% mineral ash. This mineral ash is composed mainly of 95% silica, insoluble silicates of iron, aluminium, calcium and magnesium (Van–Hoest, 2006).

Concerted efforts have been channelled towards replacing asbestos and other carcinogenic materials in the production of brake pads. In the work of Nakagawa et al. (1986), metal fibres were used in the production of brake pads so as to counter the environmental pollution caused by asbestos.

During this study, a semi–metallic type of pad material was developed from chattered–machined metal fibres as it exhibits good properties in line with brake characteristics and also good wear resistance. This pad contained close to 60 % by weight of the steel fibres having 60 microns (μm) in diameter and length of 3mm. Dagwa and Ibhadode (2008) and Deepika *et al*. (2013), also developed a non–asbestos–containing friction pad material using an agro –waste material base, palm kernel shell (PKS) as a reinforcement material. It was reported in their work that palm kernel shell was selected because it exhibited more favourable properties than the other agro–waste they investigated. Aigbodion *et al.* (2010); Bashar *et al*. (2012) and Ruzaidi *et al,* (2011), also developed a non–asbestos brake pad by utilizing bagasse, coconut shell and palm ash respectively as reinforcement materials. The result of their study showed that the selected reinforcement materials were comparable with other commercially available brake pad materials. Similarly, Naemah (2011) reported that a good brake pad material must meet the following criteria:

— It must be environmentally acceptable and be safe for use.
— The contact materials must exhibit good resistance to wear effects
— The materials must have a good high heat capacity, thermal conductivity, and good thermal properties and also be able to withstand higher temperatures and high contact pressures
— The materials must exhibit a high frictional coefficient.
— The frictional value must be stable over a temperatures and pressures range.
— The materials must have a good resistant to environmental effects which arises from dust, pressure and moisture, and
— Must possess excellent shear strength of transferring frictional forces to structure.

Blau (2001) and Bashar *et al*. (2012) observed that brake pad additives serve different functions and a difference of two or three percent of additive can alter the performance of the friction material. Therefore, the control of the composition is of great important. Blau (2001) also stated that friction materials and additives based on their expected functions are categorised into the following:

— fillers and reinforcement,
— abrasives,
— friction modifiers, and
— binder materials.

## NON–HAZARDOUS REINFORCEMENT MATERIALS

Medical research carried out has shown that asbestos fibres can lodge in the lungs thereby inducing adverse respiratory conditions. Environmental protection agency (EPA) in 1986, announced a proposed ban on asbestos. This proposed ban by EPA may have required all new automobile vehicles to possess non–asbestos brakes and clutches by 1993, and the aftermarket would have had until 1996 to convert to non–asbestos which is non–hazardous (Blau, 2001).

Though the use of asbestos in brake pads has not been fully banned, but most brake pad producing industries are moving away from the use of asbestos as reinforced material to using non–hazardous reinforced material in friction pad production. This is because of the concerns regarding airborne particles in the factories and disposal of asbestos containing wastes (Dagwa and Ibhadode, 2006). Several studies have been carried out using different reinforced materials to find a possible replacement for asbestos whose dust has been reported to be carcinogenic (cancer causing). Some of these studies are discussed in the following section.

— Palm Kernel Shell and Fibre
Ndoke (2006), reported that palm kernel shell as shown in Figure 1, has an average dry density of 0.65mg/m³, porosity of 28% and an impact value of 4.5%. The report suggested that the dry density, porosity and impact value of palm kernel shell place it in the same category as lightweight aggregate and a good substitute for asbestos.



Figure 1: Palm kernel Shell (Source:  Mayowa *et al.,* 2015)

Fono–Tamo and Koya, (2013), developed brake pad materials for automobile using standard factory procedure from palm kernel shell. Mechanical properties of the material developed were studied. The results showed that the developed pad has an average hardness of 32.34 and average shear strength of 40.95 MPa. The coefficient of friction of the product was also tested and the result indicated that the pad possessed a frictional coefficient of 0.43. This result was in agreement with the work of Koya *et al*. (2004) in which it was stated that the coefficients of friction of palm kernel shell on metal surfaces are in the range of 0.37–0.52. In contrast, friction coefficient that falls within the range of 0.30–0.70 is desirable when using brake pad material (Roubicek *et al.,* 2008). The bonding of the material to the back plate was also tested and the result indicates a value of 3375 N/s. All the values of the responses though not as excellent as asbestos–based brake pads whose coefficient of friction falls within 0.37–0.41 as the recommended by SAE was reported to be good and can be applied as automotive friction material therefore making palm kernel shell a good substitute for asbestos and suitable for brake friction pads production.

Ikpambese *et al*. (2014) also developed asbestos–free automobile brake pads from palm kernel fibers together with epoxy resin as binder. The fibers (PKFs) were soaked in caustic soda solution (sodium hydroxide) for 24 hours to get rid of

the remnant of red oil in fiber. The fibers were then washed with water to remove the caustic soda and then dried under the sun for a period of one week. The binder used during the study was varied in formulations during production. The physical, morphological and mechanical properties of the composite were investigated to examine the effect of composition on the friction material.

The results obtained from the study indicated that the coefficient of friction, temperature, wear rate, stopping time and noise level of the pads increases with increasing speed. The results also show that moisture content, porosity, surface roughness, hardness, specific gravity, water and oil absorption rate remained stable with increasing speed. From the microstructure analysis it was observed that worm surfaces wear where the asperities ploughed were characterized by abrasion thereby exposing the white region of the fibers and increasing the smoothness of the composite material. The report showed that the brake pad sample with composition of 10% palm wastes, 40% epoxy–resin, 15% calcium carbonate, 6% $Al_2O_3$, and 29% graphite gave optimum properties. Therefore, it was concluded that palm kernel fibers can be used effectively as a good replacement for asbestos in friction pad production.

Ibhadode and Dagwa, (2008), also studied the feasibility of using agro–waste material, palm kernel shell (PKS) as replacement for asbestos in brake pad production. The material was used along with other constituents. Taguchi optimization technique was utilised in achieving the optimal formulation and manufacturing variables. The value of experimental parameters selected includes moulding pressure (16.74–27.90 MPa), moulding temperature (150–170°C), curing time (6–10 minutes) and heat treatment time (1–3 hour). The composition used during their study includes 56% reinforcement, 24% binder, 14% abrasives and 6% friction modifier. The brake pads produced were tested on a test rig and on a car (Toyota Carina II) in order to examine its effectiveness and wear properties. The results of the test conducted on the produced brake pad samples indicates that the surface hardness falls within 64–89 Rockwell scale B while the coefficient of friction falls within 0.35–0.44 and wear values falls within 0.017–0.170. The results compared well with asbestos–based brake pad and also performed satisfactorily. However, it was also reported that more pad wear was observed on the PKS pad at high vehicular speeds beyond 80km/hour.

— Coconut Shell

Coconut shells shown in Figure 2 are agricultural wastes used in the preparation of various attractive articles (antiques) and also applied in the production of activated charcoal as well as reinforcement material in the production of composites. Salmah (2013) reported that coconut shell is a lignocellulosic filler which exhibits excellent properties compared to mineral fillers (kaolin, calcium carbonate, mica and talc). Some of the outstanding properties reported by Salmah (2013) include minimal health hazard, high–specific strength–to–weight ratio, low cost, biodegradability, environmental friendly and renewability. Matthew (2012) reported that moisture desorption of coconut shells takes place between 25 and 150°C and at 150°C, degradation of sclerenchyma cells, which are responsible for holding water in the shell occurs. Further heating of the shells between 190°C to 260°C may result to the degradation of hemicellulose present in the shell and at 240°C to 350°C, degradation of cellulose take place. The final stage of thermal degradation involves the breakdown of lignin which occurs between 280°C and 500°C (Matthew, 2012).



Figure 2: Coconut shells

Bashar et al. (2012) conducted a study with the aim of finding a possible replacement for asbestos, used coconut shell powder to develop brake pad material. This material was mixed with other ingredients such as catalyst, epoxy resin, cast iron fillings, silica, and accelerator. The coconut shell was dried in the sun for some days in order to get rid of the shell moisture and then reduced into smaller sizes using anvil and hammer and then pounded using mortar and pestle. Finally, a grinding machine was used to ground it into powder and sieved with a mesh size of 710 µm. In the study, the weights of epoxy resin and the coconut shell powder were varied while the weight of the other ingredients remained unchanged. Mechanical (tensile, hardness, compressive, wear and impact) and corrosion tests were conducted to study the effect of process on the products. The results show that as the percentage of the coconut shell powder increases, the hardness, breaking strength, compressive and impact strength reduces. Therefore, it was reported that higher percentage of coconut powder results to brittleness and that brake pad samples with 50% matrix and 10% reinforcement as well as samples with 60 % matrix and 10% reinforcement can be adopted in friction pad production since they are far lighter and possesses better properties when compared with the other compositions. The report also suggested that the coconut shell reinforced brake pad possessing this composition may be a better alternative to asbestos as it possesses lower wear resistance though; the presence of iron filings in the samples causes poor resistance to corrosion.

Darlington et al. (2015) in their study also produced an asbestos–free brake pad from locally sourced raw materials using coconut shell powder and palm kernel shell as reinforcement materials, graphite as lubricant, polyester resin as binder material, carbides and metal chips as the abrasives.

According to the report of their study, three different samples of brake pads were produced by varying mass compositions of coconut shell and palm kernel shell while the composition of the binder, lubricant and abrasive materials remained unchanged throughout the experiment. The tests results obtained shows that developed samples have density which falls between 2.55–2.78 g/cm$^3$, wear rate of 0.2007–0.2733 g/min, percentage water absorption of 0.0399–0.0522% and hardness of 3.00 –3.41.

Samples of commercial brake pads were also tested and it was found that the commercial pads possesses a density of 3.36 g/cm$^3$, wear rate of 0.1873 g/min, water absorption of 0.0327% and hardness of 2.53. These results indicate that the developed samples though could not meet up with properties of commercial brake pads due to its high density and wear rate but compared well with commercial brake pads and can serve as an alternative to commercial products. Therefore the study concluded that locally sourced palm kernel and coconut shell can be used as a replacement for commercial pad.

— Palm Ash

Ruzaidi *et al* .(2011) conducted a study to produce a non–asbestos brake pad at varying composition of palm ash and polychlorinated biphenyls (PCB) waste along with thermoset resin as a binder and metal filler as abrasive. Five samples were produced using moulding pressure, moulding temperature and curing time of 122 MPa, 150℃ and 5 minutes respectively and were tested to examine its compression strength, water absorption rate, wear rate, and morphological properties.

The test results showed that the brake pads with higher percentage of palm ash gave the best mechanical and wears properties. This indicates that the wear properties of the produced brake pads are comparable with conventional brake pad. The study also concluded that brake pads can be developed by replacing asbestos with other reinforcement materials such as palm ash and PCB waste which could lower the cost of producing brake pad.

It was also suggested that compressive strength of the product can be increased if the percentage of palm ash in the composition is also increased while the samples with higher palm ash content may give optimum wear properties and water absorption rate which will lead to better properties of brake pad application (Ruzaidi *et al.,* 2011).

— Rice Husk and Rice Straw

Rice husks and rice straw are agricultural wastes which are abundantly available mostly in rice producing countries like Nigeria. Rice husk dust (RHD) and rice straw dust (RSD) shown in Figure 3 are known to have high silica and low lignin content which gives friction materials a ceramic–like behaviour (Ibrahim, 2009). These materials are used as filler or reinforcement materials in the development of composites like friction pads.



(a)



(b)

Figure 3: Rice straw (a) and Rice husk (b)

Acharya and Samantrai (2012) studied the wear and friction behaviour of rice husk using randomly oriented unmodified and modified rice husk as reinforcement in epoxy matrix (Araldite LY556 and hardener HY 951). A pin on–disc apparatus was used to study the wear behaviour of rice husk composites reinforced with 5–20 wt%. The pin of each sample was attached to a holder and then abraded under different loads of 5, 7.5,10 and 15N. Each test was conducted for duration of 5 minutes.

The results of the coefficient of friction and wear rate of the composite were found to be the functions of sliding velocities, normal load and the filler volume fraction. Scanning electron microscope (SEM) was used to also study the morphology of the worn surface of the composites. According to the report of Acharya and Samantrai (2012), the test result shows that wear rates decreases with increase in the rice husk fibres addition under all testing conditions. It was then concluded that the addition of the rice husk fibres in epoxy is very effective in the improvement of the composite wear resistance and the optimum fibre fraction which gave the optimum wear resistance to the composite is found to be 10 w%.

The morphologies of scanning electron micrograph of worn surface for the untreated rice husk composite and the benzoyl chloride treated rice husk composite showed that surface damage and cracking of the matrix (longitudinal and transverse crack) are more pronounced for the untreated composite. Reverse is the case for the benzoyl chloride–treated composite as the surface damage seems to be minimal and only longitudinal cracks are observed on the surface of the material in the rolling direction. It was therefore concluded that the treatment of the surface of the fibre restricts the propagation of the cracks in the transverse direction thereby improving the wear resistance of the composite.

Mutlu (2009) also conducted a study with the aim of finding a possible replacement for asbestos whose dust is hazardous. Investigation was carried out using rice husk dust (RHD) and rice straw dust (RSD) to study the tribological properties of brake pads. The study was conducted for four different mixtures of brake pads which were coded $RS_4$, $RS_{20}$, $RH_4$ and $RH_{20}$. The materials in each brake pad were composed of rice husk dust (RHD), rice straw dust (RSD), copper particles, barite, brass, cashew, steel fibres, graphite and alumina and production of samples was done using moulding temperature, curing time and heat treatment time of 180 ℃, 15 minutes and 4 hours respectively.

The newly formulated brake pads were tested and examine to study their performance and determine the coefficient of friction, wear rate and morphological properties. The results of the study shows a mean coefficient of friction of 0.315–0.381 which is very low to be applied in heavy duty automobiles brake pads as specified in the work of Dagwa and Ibhadode (2008). The result of the wear rate varies from 0.000853–0.001041 $g/mm^2$. Therefore, considering the wear rate of all the samples, $RS_4$ has a little better wear rate than $RH_4$ which can be ignored. The coefficient of friction variations with test time are shown in Figure 4.
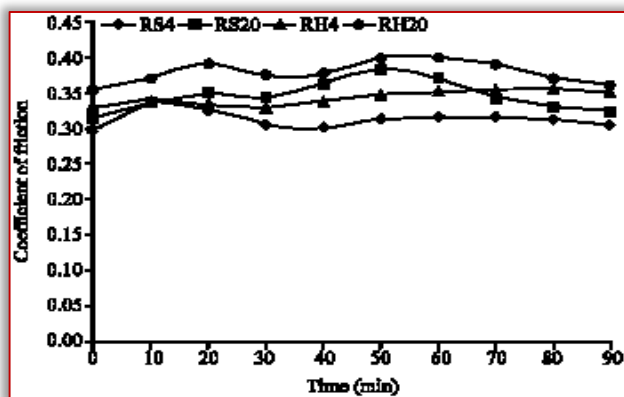


Figure 4: Change of coefficient of friction as a function of time for the four samples (Source: Mutlu, 2009)

From Figure 4, it was observed that the coded samples $RH_4$ and $RS_4$ showed a continuous initial rise in coefficient of friction (μ) between the 10th and 20th minutes of test. It was then concluded that such increase can often be attributed to the adhesion of metal chips in the brake pad to the friction surface of the cast iron disc. Also, the SEM micrographs of each coded samples was conducted and the results showed that there was homogenous distribution of the silica particles in the body (white points). It was also reported that the micro–voids on the surface of each sample were bigger and smaller in size which was reported to be due to the falling of the metal particles during friction. In addition to the micro–voids observed in the sample, it was also stated that there were some micro cracks on the surface which stayed as effective in the friction surface. The study then concluded that RHD and RSD can be used effectively in brake pad formulations when combined properly with other additives and that the use of RHD significantly improved the overall performance of the formulated material. It was also established that the sample with 20 % rice husk ($RH_{20}$) will provide a better friction coefficient and wear rate when used in brake pad formulation.

─ Banana Peels

Banana peels shown in Figure 5 are also known as banana skin. They are the outer covering of the banana fruit. It is a popular fruit consumed Worldwide with a yearly production of over 145 million tonnes. Once the peel is removed, the fruit can be eaten raw or cooked and the peel is generally discarded. Because of this removal of the banana peel, a significant amount of organic waste is generated (Babatunde, 1992).



Figure 5: Banana peel (Source: Idris et al., 2013).

The coefficient of friction of banana peel on a linoleum (a tough washable floor covering) surface was measured at just 0.07. This is about half that of lubricated metal on metal surface. Several researchers have attributed this to the crushing of the natural polysaccharide follicular gel, releasing a homogenous sol (Kiyoshi et al., 2012). It has been reported that at increased temperature, banana peel powder becomes more gelatinous and at much higher temperatures, the hardness increases. Therefore, because of these properties of banana peel, it is recommended for use in the formulation of new friction pad material as it increases the binding ability of resin at higher temperatures (Idris et al., 2013).

Bashir et al, (2015), with the aim of establishing the general behaviour of a newly developed friction material to serve as light weight automotive friction pad material when subjected to high temperature and significant compression loads studied the wear and friction behaviour of disc brake pad material using banana peel powder. The newly formulated brake pad was composed of thirteen ingredients (phenolic resin, banana peel, $CaCO_3$, $Ca(OH)_2$, graphite, $Sb_2S_3$, $MoS_2$, $Al_2O_3$, MgO, SiC, Steel wool, PAN fiber and $CaSiO_3$). During the experiment, eleven of the ingredients were kept constant while two ingredients (phenolic resin and banana peel) were varied. To ensure homogeneity, an organic solvent, ethanol was utilised to mix the ingredients in a beaker using magnetic stirrer while samples were produced using moulding pressure (15MPa), moulding temperature (150 ℃), curing time (10 minutes) and heat treatment time (8 hours) as process parameters. A reciprocating friction monitor was used to study the wear and friction properties of the newly formulated brake pad. The machine is a digitally controlled versatile device used in the evaluation of wear and friction

properties of the material under lubricated and dry conditions. New set of disc of 14mm diameter was designed and fabricated to be suitable for area contact testing. The new disc was used as an upper specimen while the brake pad material serves as the lower specimen and the experimental results showed that at higher temperature, a breakdown of the efficiency of the brake occur which was termed as brake fade. Mutlu (2009) reported that the possible reason for brake fade is due to phenolic resin degradation.

Also, it was observed that with increase in temperature, the wear of the pads reduces. This was attributed to the binding ability of the resin used in the study which was retained because of the presence of the banana peel powder which led to the attainment of higher coefficient of friction. It was therefore concluded in the study that proper bonding can be achieved in brake pad formulation with the banana peel powder, which will result in increase in coefficient of friction. Idris *et al.* (2013) carried out a study with the aim of finding a possible replacement for asbestos and phenolic resin (phenol formaldehyde) binder, formulated a new brake pad using banana peels waste. The composition of the resin varied from 5 to 30 wt% with interval of 5 wt%. The banana peels used in the study was dried and ground into powder (uncarbonized, BUNCp). Analysis of the particle size of the peel particles was carried out in accordance with BS1377:1990.

Table 1: Summary of findings compared Asbestos based Brake Pads.

| Properties | Asbestos based | New (Banana peel carbonized at 30% resin) | New (Banana peel uncarbonized at 25% resin) |
|---|---|---|---|
| Flame Resistance (%) | Charred ash 9% | Charred ash 12% | Charred ash 24.67% |
| Specific gravity (g/cm$^3$) | 1.89 | 1.20 | 1.26 |
| Coefficient of Friction | 3.80 | 0.35 | 0.40 |
| Thickness swells in water (%) | 0.3–0.4 | 3.0 | 3.21 |
| Wear rate (mg/m) | 3.80 | 4.15 | 4.15 |
| Hardness values (HRB) | 101 | 71.6 | 98.8 |
| Compressive strength (N/mm$^2$) | 110 | 61.20 | 95.6 |

Source: Idris *et al.* (2013).

During the study, two sets of samples were produced using the carbonised and uncarbonised banana peels particles. Physical, wear, morphology and mechanical properties of the formulated brake pads were investigated. During the tests, the samples contain 30 wt% carbonised (BCp) and 25 wt% in uncarbonised banana peels (BUNCp) gave the better properties in all. Table 1 shows the summary of the results findings compared with asbestos based friction pads.

From Table 1, it was observed that the results obtained are in close agreement with commercial brake pads. Therefore, it was concluded that taking into consideration all the desired dimensions of the brake pad, a prototype of Peugeot 504 brake pad of length 77 mm, width of 65 mm and depth of 12 mm asbestos–free brake pads can be produced with these formulations. Hence, banana peels particles can be used effectively as a replacement for asbestos in brake pad production.

— Bagasse

Bagasse as shown in Figure 6 is a fibrous residue that remains after crushing the stalks. It is composed of fibers, water and little amounts of soluble solute. The percentage contribution of each of these components in bagasse depends on the maturity, variety, efficiency of the crushing plant and the harvesting techniques. Bagasse contains about 30% hemicelluloses, 40% cellulose, and 15% lignin (Punyapriya, 2007).



Figure 6: Bagasse (Source: Punyapriya, 2007).

Aigbodion *et al.* (2010), with the conducted a study using bagasse to produce brake pads in the ratio of 30% resin and 70% bagasse using compression moulding machine. The bagasses used in the study were sieve into grades of 100, 150, 250, 350 and 710µm. The binder used during the study was phenolic resin (phenol formaldehyde). During the experiment, the compression moulding machine was set to a moulding temperature of 140ºC, moulding pressure of 100 KN/cm$^2$ pressure and a curing time of 2 minutes and the final product was cured in an oven for 8 hours. The optimal values of the properties examined during the study include hardness (92 at 3000 kgf), density (1.65 g/cm$^3$), microstructure analysis, compressive strength (103.5 MPa), flame resistance (charred with 46% ash), water and oil absorption (5.04 and 0.44 %). From the result obtained, it was reported that the compressive strengths of the produced samples followed similar trend with that of the values of the hardness as each of the properties increases with decreasing sieve sizes. The microstructure of each sample was reported and the results showed that as the particles size of the bagasse decreases, there was more uniform distribution of the resin with the bagasse which was attributed to the proper bonding between the resin and the bagasse as the sieve grade decreases. It was therefore concluded in the study that better properties of friction pad can be achieved using a lower sieve grade of 100µm of bagasse with a composition 70% and 30% of resin.

— Maize Husk

Maize husks as shown in Figure 7 are the outer covering of maize. For most applications, the husks need to be soaked in hot water to become flexible. This type of husk is commonly

used to encase foods for baking or steaming thereby imparting light maize flavour.



Figure 7: Maize husk

Ademoh and Adeyemi (2015) conducted a study using maize husks as reinforcement material to produce automotive brake pads. Three friction composite compositions were developed using the maize husks as strengthening material with varied epoxy resin binder. Maize husks were grounded and sieved to a mesh size of 300µm. Other ingredients used during the study include silica sand, epoxy resin, calcium carbonate, anhydrous iron oxide, talc as release agent and powdered graphite.

Three samples were produced using curing time of 80–120 minutes and varying percentage weight of maize husk and binder (epoxy resin and hardener at 1:2) while the weight of friction modifier (graphite powder), abrasives (silica and iron oxide), and fillers (calcium carbonate) were kept constant throughout the experiment. To ascertain suitability of the formulated composites for brake pad application, the samples were subjected to tests to determine its mechanical, physical and tribological properties. Some of the tests conducted include water and oil absorption, density, friction coefficient, wear resistance, thermal conductivity, hardness, compressive and tensile strengths. The optimal values of the developed brake pad compared with asbestos–based brake pads are shown in Table 2.

Table 2: Optimal values of developed brake pad compared with Asbestos–based Brake Pad

| Properties | Newly Formulated Maize Husk Based | Asbestos based |
|---|---|---|
| Specific gravity (g/cm$^3$) | 0.853 | 1.890 |
| Wear rate (mg/m) | 2.146 | 3.800 |
| Friction Coefficient | 0.37 – 0.40 | 0.30 – 0.40 |
| Thickness swell in H$_2$O (%) | 0.91 | 0.9 |
| Thickness swells in SAE oil (%) | 0.58 | 0.30 |
| Hardness | 127.8 | 101.0 |
| Compressive strength (MPa) | 103 | 110.0 |
| Tensile strength (MPa) | 20.22 | 7.00 |
| Thermal conductivity (W/mK) | 0.251 – 0.372 | 0.539 |

Source: Ademoh and Adeyemi, 2015.

As shown in Table 2, it can be observed that the newly formulated brake pads has slight higher thickness swell in water as well as SAE oil compare to asbestos based brake pads. The authors therefore concluded that maize husks are suitable eco–friendly replacement for asbestos and other agro–biomass friction materials in automobile brake pads application.

─ Periwinkle Shell

Periwinkles shown in Figure 8 are small marine snails belonging to the family *Littorinidae* (class Gastropoda, phylum Mollusca). They are widely distributed shore snails which are usually found on stones, rocks or pilings. Some are found on mud flats while some tropical forms are found on the prop roots or mangrove trees. The shell of periwinkles is the outer casing of the animal which is usually discarded after the flesh inside is consumed. They are usually considered as agricultural waste products in riverine area of southern Nigeria (Yawas *et al.,* 2013).



Figure 8: Periwinkle shells

Yawas *et al.,* (2013) developed an asbestos–free brake pad using periwinkle shell as reinforced material. The periwinkle shells used during the study was grounded and sieved into grain sizes of 125, 250, 335, 500 and 710 µm, and was mixed with 35% phenolic resin binder. Five test samples were produced using compression moulding machine at a pressure of 40 kg/cm$^2$, a moulding temperature (160ºC) and a curing time (1.5 hours). All the samples were post cured in an oven of temperature 140 ºC for 4 hours. The microstructure (surface morphology) of the developed friction materials was analysed using scanning electron microscope (SEM) and the results indicate that the microstructures of the developed samples showed a homogeneous distribution as the periwinkle shell particles sieve size decreases. Mechanical, physical and tribological properties of the periwinkle shell based brake pads were also investigated and compared with the properties of asbestos–based brake pads.

It was reported that the hardness, compressive strength and density of the formulated brake pads increases as the particle size of periwinkle shell decreases from 710 to 125 µm while the oil absorption, wear rate and water absorption rate decreases as the particle size of the periwinkle shell decreases. Therefore, the results obtained for the sieve size of 125 µm of periwinkle shell particles compared well with that of commercial brake pad. The optimal values of the test results reported include specific gravity (1.01 g/cm$^3$), coefficient of friction (0.41), hardness (116.7 HRB), Compressive strength (147 N/mm$^2$), and thickness swell in water (0.39 %) and thickness swell in SEA oil (0.37 %). It was therefore concluded that periwinkle shell particles can

effectively serve as a replacement for asbestos in the production of brake pads.

━ Cow bone

Due to large number of cows being slaughtered daily in the Nigeria, cow bones as shown in Figure 9 are abundantly available. These natural fibers are obtained from cow wastes which causes environmental pollution. Isiaka and Temitope (2013) reported that cow bone exhibit excellent structural compatibility in addition to the surface compatibility requirements as biomaterials. Mayowa *et al.* (2015) also reported that cow bone consists of living cells which are renewed constantly in the bone and widely scattered within a non–living material known as the matrix formed by osteoblasts cells. It was also reported that this osteoblasts in the bone secrete and makes protein collagen, which gives the bones elastic property which help it withstand stresses generated by lifting, walking, and other related activities.



Figure 9: Cow Bones (Source: Mayowa *et al.,* 2015).

Isiaka and Temitope (2013) investigated the influence of particle size distribution of cow bone powder on the mechanical properties of polyester matrix composites with the aim of considering how suitable it is to be applied as biomaterials. During the study, the cow bone used was thoroughly washed to get rid of unwanted materials and then crushed into smaller particles sizes using hammer. Sieve size analysis was conducted on the crushed bones and was sieved into three sieve sizes of 300, 106 and 75μm.

Other materials used during the experiment include unsaturated polyester resin which serves as the binder, a catalyst known as methyl ethyl ketone peroxide (MEKP), polyvinyl acetate which serves as the mould releasing agent, 2% cobalt solution (accelerator) and a cleaning agent known as ethanol.

During the production of the composite, 120 g of the polyester resin was mixed with 1.5 g each of catalyst and accelerator while the particulate of the cow bone was varied in 2, 4, 6, and 8 wt% predetermined proportion. The developed composites were tested using standard testing methods to determine its mechanical properties.

The test results indicate that the sample reinforced with 8 wt% from sieve size of 75 μm gave a better tensile strength than others polyester matrix while hardness results show that the 300 μm particle size gave the optimal result as the 300 μm particle reinforcement increases the hardness as the fibre content rises from 2 to 8 wt%. Also, the flexural strength

results specify a peak improvement with the addition of cow bone particles.

The study further concluded that the optimal reinforcement can be obtained by the addition of 6 % of cow bone powder from 106 μm particle size. Though, from the results obtained, the authors reported that cow bones can serves as a reinforcement material in polyester matrix as well as a good replacement for asbestos but tribological properties such as wear resistance and friction coefficient which majorly affect the frictional behaviour of a brake pad was not investigated. Mayowa *et al.* (2015) also formulated a new friction material using cow bone and palm kernel shell (PKS) as reinforced materials. Both the cow bone and the palm kernel shell were washed, dried, grounded into fine powder and subjected to sieve analysis. The retained fractions which were below the 100 μm, on 100 μm and 120 μm, were used in the production of the friction material. About 60% epoxy resin and 10% hardener along with 30% of different grade sizes of amount retained on 120, 100 and grading below 100 (–100%) was used for the production.

The manufacturing parameters used during the study include a preform pressure which was varied between 0.40 MPa and 0.60 MPa for a period of 2–4 seconds. A hot pressing pressure of 0.27 MPa at a temperature of 200℃ and breathing at 30 and 45 second after a minute of hot pressing. After which the curing is continued at 0.90 MPa for another 10 minutes. Post curing of the samples was done for 2 hours in an electric oven at a temperature of 200℃. The formulated friction materials were characterized based on the requirements for its application in automobile vehicles. The experimental test results obtained during the study showed that density of the palm kernel shell and cow bone reinforced composites falls between 1.03–1.2 g/cm$^3$ and 1.3–1.5 g/cm$^3$ respectively while the impact energy ranges between 0.5–1.0 J and 0.8–1.5 J correspondingly and the tensile strength for the two composites ranges between 9–23 J/mm$^2$ and 12–24 J/mm$^2$ respectively.

The study also reported that as the particle size increases, the density decreases. This was due to fact that smaller particle size occupies higher surface area (Isiaka and Temitope, 2013). Also, the result of the impact energy showed that samples with higher sieve size gave a relative increase in impact strength when compared to samples with finer particle sizes and that cow bone composition tends to absorb more water than palm kernel shell composition. Mayowa *et al.* (2015) reported that this was due to the closer packing in palm kernel shell as compare to cow bone. This close packing makes it difficult for water to pass through as a result of the stronger binding properties.

Finally, themogravimetric analysis (TGA) was conducted and a rise in weight loss with increasing temperature in the range of 200–500℃ was observed. The percentage weight loss rises as the sieve size rises. The study therefore concluded that palm kernel shell and cow bone reinforced material can serve as a good replacement for asbestos in the production of

friction materials. Though tribological properties such as wear resistance and friction coefficient which majorly affect the frictional behaviour of friction materials were not investigated.

─ Fly Ash

Fly ash shown in Figure 10 is the finely divided residue obtained from the combustion of pulverized coal and is transported from the combustion chamber by exhaust gases. It is generally captured by a particle filtration equipment such electrostatic precipitators before the flue gases reach the chimneys of coal fired power plants. This waste generated by thermal power plants poses a great environmental concern (Anushree & Alka, 2009).



Figure 10: Fly ash (Source: Natarajan et al., 2012)

Natarajan et al. (2012) conducted a study on the effect of ingredients on the tribological and mechanical properties of different brake pad materials. A non–asbestos organic based friction material was utilized in developing brake pads which was applied in automobile brake system. Two different types of frictional materials having different combinations were developed. The first consist of fly ash range (10–60%) and the second was developed without fly ash. Fly ash according to the study is composed of substantial amounts of silica, calcium sulphate, alumina, and un–burnt carbon. These two materials were studied to investigate the effect of ingredients on the tribological (wear) and mechanical properties of different brake pad materials.

The result of the experiment showed that the presence of fibers in the phenolic matrix improved the tensile strength and hardness of the friction material. It was reported that this result was expected because soft resin matrix is reinforced by the hard fibers.

The results of the study also indicated that the coefficient of friction of the fly–ash was in the range of 0.35 to 0.48. It was reported that these results were better when compared barites based (without fly–ash) and asbestos based brake pads. Also, the results showed that wear resistance of the friction material was greatly influenced by the amounts of rockwool, ceramic wool, zirconium silicate (zircon) and calcium hydroxide in the samples and the presence of friction dust powder, potassium titanate (terraces) and wollastonite ($CaSiO_3$) strongly influence the friction coefficient of the product. Similarly, the increasing strength of the friction material was achieved by the presence of para–aramid fiber and glass fiber. It was therefore concluded in the

report that the presence of ingredients posed a great impact on the properties of frictional materials. Though, according to National Precast Concrete Association (NPCA) of 2010, some fly ash, especially those produced in power plant are usually compatible with engineering material, while some other needs to be beneficiated and few other types cannot actually be improved for use in engineering application. Thus, the use of fly ash in friction material may pose some negative effects on the properties of friction material.

─ Cocoa Beans Shells

Cocoa bean shells as shown in Figure 11 also called cocoa bean mulch or cocoa bean hull mulch are shells of cocoa bean which come off the beans during roasting process and are separated from the beans by strong air action, therefore insuring a dry weed–free product. Oliver, (2013) reported that the waste shells of cocoa bean are rich in anti–oxidants and fiber which constitute a great potential as brake pad ingredients.



Figure 11: Cocoa beans shells (Source: Foodbev Media, 2015)

Adeyemi et al. (2016) developed asbestos–free brake pad materials using cocoa bean shells (CBS). The materials used for the production of the samples include calcium carbonate, silica sand, anhydrous iron oxide, epoxy resin and graphite. The base material, coco bean shells were prepared by washing, sun–drying, grinding into a fine powder and sieving of grinded powder using a sieve of aperture 300 μm. Three samples were produced by varying the epoxy resin (50–60%) and Cocoa beans shells powder (21–31%) while keeping the calcium carbonate ($CaCO_3$), silica, iron oxide and graphite constant at 4, 7, 3 and 5% respectively.

Experimental tests were conducted on the samples to determine the physical, mechanical and tribological properties of the material and to ascertain the feasibility of applying the product on automobile brake pad. The experimental results shows that the specimen labelled as sample 3 (60% epoxy resin and 21% Cocoa beans shells powder) gave the optimum performance compared to other experimental samples. The responses obtained were compared with asbestos–based brake pad as shown in Table 4.

From Table 4, it can be observed that the optimal values of the experimental results compared favourably with that of commercial brake pad (asbestos based). Though the samples performed well as reported by the authors but the presence of iron in the composition may result to poor corrosion

resistance which was not investigated by the researchers. Lawal *et al.* (2016) reported that poor corrosion resistance of brake pads may lead to poor braking performance.

Table 4: Experimental Test Results Compared with Existing Ones

| Properties | Newly formulated (CBS at 325 µm) | Asbestos based (Commercial) |
|---|---|---|
| Specific gravity (g/cm$^3$) | 1.010 | 1.890 |
| Wear rate (mg/m) | 3.934 | 3.800 |
| Friction Coefficient | 0.32 – 0.35 | 0.30 – 0.40 |
| Thickness swells in water (%) | 1.19 | 0.9 |
| Thickness swells in SAE oil (%) | 0.28 | 0.30 |
| Hardness Values (MPa) | 120.3 | 101.0 |
| Compressive strength (MPa) | 23.2+ | 110.0 |
| Tensile strength (MPa) | 16.88 | 7.00 |
| Thermal conductivity (W/mK) | 0.239 – 0.338 | 0.539 |

Source: Adeyemi *et al.* (2016)

— Cow Hooves

Cow hooves shown in Figure 12 are the horny covering protecting and encasing the foot of a cow.



Figure 12: Cow Hooves (Bala *et al.,* 2016)).

Bala *et al.* (2016) conducted a study using cow hooves with the aim of replacing asbestos whose presence in brake pad was reported to be carcinogenic. The cow hooves used during the experiment were washed thoroughly to remove impurities and then properly dried in the sun. Other processes involved in preparing the pulverised hooves powder include drying it in an electric vacuum oven for 180 minutes at 250°C in order to remove contaminating oil, crushing using pestle and mortar, grinding into powder using a milling machine and finally sieving the powder using sieve size of 710 µm. Other materials used along with the pulverized hooves powder include graphite, aluminium oxide, barium sulphate and epoxy resin.

Seven different samples were produced by varying the epoxy resin (10–40 %) and pulverized cow hooves (10–40 %) while keeping the barium sulphate, alumina and graphite constant at 30, 10, and 10 % respectively. The production of the samples was done using a moulding temperature of 70 °C, a moulding pressure of 30 MPa and a curing time of 10 minutes. The produced samples were post–cured in an electric oven for one hour at a temperature of 180°C.

Tests were conducted on the products to determine the mechanical, tribological and physical properties of the developed friction materials. The test results obtained shows that sample composed of 15 % pulverized cow hooves, 35% epoxy resin and sample 7 with 10% pulverized cow hooves, 7% epoxy resin gave the optimum results and were compared with commercially available brake pads as shown in Table 5.

Table 5: Comparison of developed brake pads with Asbestos based Brake pads

| Property | Commercial (Asbestos based) | Sample 6 (Pulverized cow hooves) |
|---|---|---|
| Oil absorption (%) | 0.30 | 1.30 |
| Hardness (Shore D) | – | 71 |
| Relative density | 1.89 | 1.66 |
| Coefficient of friction | 0.3 – 0.4 | 0.41 |
| Water absorption (%) | 0.90 | 2.00 |
| Wear rate (mg/m) | 0.38 | 0.176 |
| Compressive strength (MPa) | 110 | 75.53 |

Source: Bala *et al.* (2016)

From the summary of the results presented in Table 5, it was concluded that pulverized pulverised cow hooves is a suitable reinforcement material for brake pad production. Though, some of the results obtained during the study compared well with commercially available brake pads but the use of a design of experiment technique instead of trial and error method of design may have given a better comparable result as trial and error method are sometimes characterised by repeated, varied attempts which are continued until success is achieved.

— Seashell

Natural materials such as seashell (exoskeletons of mollusks) is made up of three distinct layers which include the smooth inner layer composed mainly of calcium carbonate, intermediate layer (calcite) and the outer layer of horny substance known as conchiolin (Schaeffer, 2014). Norazlina *et al.* (2015) reported that seashell as shown in Figure 13 primarily consist of calcium carbonate (CaCO$_3$), been naturally above 80% CaCO$_3$ by weight with only about 2 % protein content and no complex extraction process is needed to use it for composite production.



Figure 13: Seashells (Norazlina *et al.*, 2015)

Seashells exhibit significant combinations of low weight, toughness, stiffness and strength which are in some cases

unrivaled by mineral fillers (Vignesh *et al.,* 2015). Table 6 shows the chemical composition of a commercial calcium carbonate and calcium carbonate obtained from seashell as reported by Michele *et al.* (2012). The seashell powder used in the study was utilised as filler by the authors to produce a composite using polyester binder. The test results indicate that the commercial $CaCO_3$ based composite possesses an impact and tensile strength of 918 MPa and 3.2 $kJm^{-2}$ respectively while seashell based composite exhibit an impact and tensile strength of 904 MPa and 3.4 $kJm^{-2}$ correspondingly.

The authors therefore concluded that seashell can be used in place of commercial $CaCO_3$ to produce composites since commercial $CaCO_3$ and seashell (mussel or oyster shells) produces similar results regardless of their variation in distribution of particle size and particle sizes.

Table 6:  Chemical composition of seashell and commercial $CaCO_3$

| Oxides | $CaCO_3$ from seashell (%) | Commercial $CaCO_3$ (%) |
|---|---|---|
| CaO | 95.7 | 99.1 |
| $SO_3$ | 0.7 | – |
| $SiO_2$ | 0.9 | – |
| $K_2O$ | 0.5 | 0.4 |
| $Fe_2O_3$ | 0.7 | – |
| $Al_2O_3$ | 0.4 | – |
| MgO | 0.6 | – |
| SrO | 0.4 | – |

Source: Michele *et al., (*2012)

Albert *et al.* (2006) conducted a comparative study on the mechanical properties and structure of haliotis rufescens, tridacna gigas and strombus gigas sea shells. The study shows that seashells are made of crystals of $CaCO_3$ interwoven with viscoelastic proteins layers as well as dense–tailored structures that produce tremendous mechanical properties. The mechanical test conducted include compressive and flexural (three–point bending) strength test. The test results indicate that the red abalone (haliotis rufescens), conch (strombus gigas*)* and giant clam (tridacna gigas*)* has compressive strength values of 233–540 MPa, 166–218 MPa and 87–123 MPa respectively.

The authors reported that the differences in the compressive strength of the shells was attributed to an optimisation of microstructural design form of 2–D laminates which enables the development of higher stresses before fracture as well as improving the toughness of the shell material. The flexural test results also show that the red abalone seashell exhibited the highest value. Therefore, it was concluded that the macro and microstructure of seashells play an important role in increasing the toughness of a brittle–based material like $CaCO_3$.

Abiodun *et al.* (2014) also evaluated the properties of seashell reinforced unsaturated polyester composite using seashell particle size of 250 µm at varying percentage composition together with unsaturated polyester resin.  Tensile, hardness,

impact, flexural and water absorption tests were conducted to determine the properties of the material.

The test results show that bending strength varies from 0.077–30.85 MPa, tensile strength, 90.70 –262.05 MPa, impact strength, 3.54–4.76, Brinell hardness, 20.10–24.87 and percentage water absorption, 0.908 –1.211%. Also, it was concluded that the seashell–reinforced sample of 10 % seashell powder provided that optimal properties thereby making seashell suitable for production of seashell reinforced unsaturated polyester composite.

Vignesh *et al.* (2015) carried out an experimental analysis of the mechanical properties of seashell particles– polymer matrix composite. The particles of the seashell were separated into five sieve sizes (75, 150, 300, 425 and 600 µm) and used to produce a composite. Mechanical test was conducted to evaluate the properties (hardness, impact. flexural and tensile strength) of the material.

The experimental results showed that particle size of 75µm seashell exhibit better properties compared to other particle sizes and can act as a reinforcement material in polymer matrix composites.

─ Lemon Peel Powder

Ramanathan *et al.* (2017) investigated the use of lemon peel powder as a filler material in brake pad production. Two samples composed of lemon peel particles (10–20%), epoxy resin (40 %), aluminium oxide (7.5–12.5 %), graphite (15%), iron oxide (7.5–12.5%) and calcium hydroxide (10 %) were produced by varying the composition of lemon peel powder, iron oxide and aluminium oxide. The process parameters reported by the authors shows a curing time of 24 hours while other production parameters were not reported. Samples produced were also tested to study the wear rate, hardness, density, water and oil absorption.

The test results showed that the brake pad samples possess a density of 1.55–2.00 $g/cm^3$, hardness of 26–32 (barcol hardness), percentage wear loss, water and oil absorption of 13.45–19.14%, 0.96 –1.38% and 0.01– 0.02% respectively. The authors therefore concluded that the sample composed of 10% lemon peel powder, 15% graphite, 12.5% Aluminium oxide, 12.5 % iron oxide and 40% epoxy resin, 10% calcium hydroxide gave the optimum properties and can be applied in brake pad applications.

Though some of the results compared well with asbestos based brake pads but the high rate of wear (13.45–19.14%) experienced by the samples represent a limitation and also, in reality, conclusion cannot be drawn by producing only two samples for automobile application and subjecting them to testing.

## CHALLENGES AND FUTURE RESEARCH DIRECTION

Production of brake pad from non–hazardous materials to replace asbestos is receiving serious attention in the laboratory and a lot have been achieved, but these achievements have not been translated into commercial application.

Again, there is need for utilisation of these combinations of non–hazardous materials (hybrid) in different ratios to further study their effect on mechanical, physical and tribological properties of brake pad produce from such hybrid.

## CONCLUSION
A comprehensive review of application of non–hazardous reinforcement materials as possible replacement for asbestos has been highlighted in this study. The physical, mechanical and tribological properties of these brake pads compared favorably with the commercial brake pad.

The need for results obtained from these research works to evolve from laboratory will address the current gap in making available eco–friendly and low–cost brake pads for commercial consumption.

## Acknowledgement

## References
[1] Jang, H., & Kim, S. J. (2000). The Effects of Antimony Trisulfide and Zirconium Silicate in the automotive. Wear, 239:229–36.

[2] Cho, M., Kim, D., &Kim S. J. (2005). Effects of ingredients on tribological characteristics of a brake pad, An experimental case study, Wear, 258(11–12): 1682–1687.

[3] Mutlu, I., Eidogan, O., Findik, F. (2005). Production of ceramic additive automotive brake pad and investigation of its braking characteristics, International journal of Tribology, 84–92.

[4] Zaharudin A.M., Tali R.J., Berhan M.N., BudinS., & Aziurah R. (2012).Taguchi method for optimizing the manufacturing parameters of friction materials, Faculty of Mechanical Engineering, Universiti Teknologi MARA, 40450, Penang, Malaysia Kedah, Malaysia.

[5] Todorovic, J. (1987). Modelling of the tribological properties of friction materials used in motor vehicles brakes. Processing Instn. Mechanical Engineers. 226, 911–916.

[6] Talib, R. J., Mohmad, S. S., Ramlan, K.. (2012). Selection of best formulation for semi–metallic brake friction materials development. Powder metallurgy (accessed at www.intechopen.com), 1–30.

[7] Tanaka, K., Ueda, S., & Noguchi, N. (1973). Fundamental studies on the brake friction of resin–based friction materials. Wear, 23, 349–365.

[8] Blau, P. J., (2001). Compositions, Testing and Functions of Friction Brake Materials and their Additives: A report by Oak Ridge National Laboratory for U.S Dept. of Energy. Retrieved from www.0rnl.gov/webworks/cppr/y2001/rpt/11 2956.pdf.

[9] Nicholson, G. (1995). Facts about Friction. P&W Price Enterprises, Inc., Croydon, PA.

[10] Ole–Von U., Staffan, S., Reed, D., Michael, B. (2005). Antimony in brake pads–a carcinogenic component?, Journal of Cleaner Production, 13, 19–31

[11] Blesdzki, A. K., & Gassan J. (1999). Composite Reinforced with Cellulose based Fibres, Progress in Polymer Science, 24(2), 221–274. doi: 10.1016/S0079–6700(98)00018–5.

[12] Cyras, V. P., Iannace, S., Kenny J. M., & Vazquez, A. (2001). Relationship between processing and properties of biodegradable composites based on PCL/starch matrix and Sisal fibers. Polymer Composites, 22: 104–110.

[13] Garcia, D., Lopez, J., Balart, R., Ruseckaite, R. A., & Stefani, P. M. (2007). Composites based on sintering rice husk–waste tire rubber mixtures, Material Design, 28: 2234–2238.

[14] Seki, Y. (2006). Rice and its waste, Science and Technical. The Science Technology Resources Council, Turkey, 464: 30–30.

[15] Van–Hoest, P. J., (2006). Rice Straw, The Role of Silica and Treatments to Improve Quality. Journal of Animal Feed Science Technology, 130: 137–171.

[16] Nakagawa, T., Ishi, M. Suzuki, K., Yanada, M., and Ito, K. (1986). Development of Technology for producing Short–Length Metal Fiber by Chatter Machining, Research and Development in Japan, The Okochi Memorial prize, 45–50.

[17] Dagwa I. M., & Ibhadode A. O. A. (2008). The Development of Asbestos–Free Friction Pad Material from Palm Kernel Shell:a Journal of the Braz. Soc. of Mech. Science and Engineering, 2(154).

[18] Deepika, K., Bhaskar, R. C., & Ramana, R. D. (2013). Fabrication and Performance Evaluation of a Composite Material for Wear Resistance Application. International Journal of Engineering Science and Innovative Technology. (2)6.

[19] Aigbodion, V. S., Agunsoye, J. O., Hassan, S. B., Asuke, F., & Akadike, U. (2010). Development of Asbestos–free Brake pad using Bagasse: Tribology in industry, 32(1).

[20] Bashar D., Peter B. M., and Joseph M., (2012). Effect of Material Selection and Production of a Cold–Worked Composite Brake Pad, Journal of Engineering of aPure and Applied Science, 2(3)154.

[21] Ruzaidi, C.M., Mustafa, A. B., Shamsul, J.B., & Alida A., & Kamarudin, H. (2011). Morphology and Wear Properties of Palm Ash and PCB Waste Brake Pad., International Conference on Asia Agriculture and Animal IPCBEE vol.1, IACSIT Press, Singapore.

[22] Naemah, B. A. (2011), Application of Palm Waste Product for Raw material in organic brake friction materials. Department of Mechanical Engineering, UTem, Melaka, Malaysia.

[23] Dagwa, I. M., & Ibhadode, A. O.(2006). Determination of Optimum Manufacturing conditions for Asbestos–free Brake Pad using Taguchi optimization Method. Nigeria Journal of Engineering Research and Development, 5(4), 1–8.

[24] Ndoke N. P. (2006). Performance of Palm Kernel Shells as a Partial replacement for Coarse Aggregate in Asphalt Concrete. Leonardo Electronic Journal of Practices and Technologies, Issue 9, 145–152.

[25] Fono–Tamo,R. S., & Koya, O. A. (2013). Evaluation of Mechanical properties of Friction Pad developed from Agricultural Waste. International Journal of Advancements in Research & Technology. 2(154), 2278–7763.

[26] Koya, O. A., & Fono, T. R., (2011). Palm kernel Shell in the Manufacture of Automotive Brake pad. Department of Mechanical Engineering, OAU, Ile–Ife. Nigeria.

[27] Roubicek, V., Raclavska, H., Juchelkova D., & Filip, P. (2008). Wear and Environmental aspects of Composite Materials for Automotive Braking Industry. Wear, 265: 167–175.

[28] Ikpambese, K. K., Gundu, D. T., & Tuleu, L. T. (2014). Evaluation of palm kernel fibers (PKFs) for production of asbestos–free automotive brake pads. Journal of King Saud University – Engineering Sciences, 28 (1), 110–118.

[29] Ibhadode, A. O. A., & Dagwa, I. M. (2008). Development of asbestos–free friction pad material from palm kernel shell, Journal of the Brazilian Society of Mechanical Sciences and Engineering. 30(2), 166173.

[30] Salmah, H., Koay, S. C., & Hakimah, O. (2013). Surface modification of coconut shell powder filled polylactic acid biocomposites, Journal of Thermoplastic composite material, 26(6), 809–819.

[31] Matthew L. K. (2012). "Thermal Degradation as a Function of Time and Temperature in a Coconut Shell Powder Polypropylene Composite," Master's Thesis, Baylor University, Waco, Texas.

[32] Darlington E., Chukwumaobi O., & Patrick O. (2015). Production of Eco–Friendly Brake Pad Using Raw Materials Sourced Locally in Nsukka. Journal of Energy Technologies and Policy, 5(11), ISSN 2224–3232. Retrieved from http://www.iiste.org/Journals/index.php/JETP/article/view File/27197/27876

[33] Ibrahim, M. (2009). Investigation of Tribological Properties of Brake Pads by Using Rice Straw and Rice Husk Dust. Journal of Applied Sciences, 9(2), 377–381.

[34] Mayowa, A., Abubakre, O. K., Lawal, S. A., & Abdulkabir, R. (2015). Experimental Investigation of Palm kernel shell and Cow bone Reinforced polymer composites for Brake pad Production. International Journal of Chemistry and Material Research, 3(2), 27-40.

[35] Acharya S. K., & Samantrai S. P. (2012). The Friction and Wear behaviour of Modified Rice Husk filled Epoxy Composite. International Journal of Scientific and Engineering Research. 3(6), 180–184.

[36] Babatunde, G. M. (1992). Availability of banana and plantain products for animal feeding. Proceedings of the FAO Expert Consultation held in CIAT, Cali, Colombia: FAO Animal Production and Health Paper 95, Fao, Roma. Retrieved from http://www.fao.org/docrep/003/T0554E/T0554E17.htm.

[37] Idris, U. D., Abubakar, I. J., Nwoye, C. I., &Aigbodiun, V. S., (2015). Eco–friendly Asbestos free Brake–pad: Using Banana Peels". Journal of Engineering Sciences, 1018–3639.

[38] Kiyoshi, M., Kensei, T., Daichi, U., & Rina, S. (2012). Frictional coefficient under banana skin. Tribology Online 7 (3): 147–151. doi:10.2474/trol.7.147.

[39] Bashir, M., Saleem, S. S.,& Bashir, O. (2015).Friction and Wear Behavior of Disc Brake pad Material using Banana peel powder. International Journal of Research in Engineering and Technology, eISSN: 2319–1163, pISSN: 2321–7308.

[40] Punyapriya M. (2007). Effect of Environment on Mechanical Properties of Bagasse fibre Reinforced Polymer Composite. M.Tech Thesis, National Institute of Technology, Rourkela.

[41] Ademoh A. N., & Adeyemi I. O. (2015). Development and Evaluation of Maize Husks (Asbestos–Free) Based Brake Pad. Industrial Engineering Letters –IEL, 5(2), 67–80.

[42] Yawas D. S., Aku S. Y., & Amaren S. G. (2016). Morphology and properties of periwinkle shell asbestos–free brake pad. Journal of King Saud University– Engineering Sciences, 28, 103–109.

[43] Isiaka, O. O., & Temitope, A. A. (2013). Influence of Cow Bone Particle Size Distribution on the Mechanical Properties of Cow Bone–Reinforced Polyester Composites. Biotechnology Research International, Volume 13, Article ID 725396. Retrieved from http://dx.doi.org/10.1155/2013/725396.

[44] Anushree M. & Alka T., (2009). Eco–friendly Fly Ash Utilization: Potential for Land Application. Journal of Critical Reviews in Environmental Science and Technology,39(4), 333–366. Retrieved from http://dx.doi.org/10.1080/10643380 701413690.

[45] Natarajan, M. P., Rajmohan, B., & Devarajulu, S. (2012). Effect of Ingredients on Mechanical and Tribological Characteristics of Different Brake Liner Materials. International Journal of Mechanical Engineering and Robotic research,1(2), IJMERR, ISSN 2278 – 0149.

[46] Oliver N. (2013). The cocoa shell is a magnificent piece of material that hasn't been exploited. Retrieved from http://www.confectionerynews.com/Ingredients/The–cocoa–shell–is–a–magnificent–piece–of–material–that–hasn–t–been–exploited–Daintree–Estates.

[47] Foodbev Media, (2015). Ferrero develops Packaging from Waste Hazelnuts and Cocoa Beans. Retrieved from, http://www.foodbev.com/news/ferrero–develops–packaging–from–waste–hazelnuts–and–cocoa–beans/.

[48] Adeyemi, I. O., Ademoh, N. A., & Okwu, M. O. (2016). Development and Assessment of Composite Brake Pad Using Pulverized Cocoa Beans Shells Filler, International Journal of Materials Science and Applications, 5(2), 66–78.

[49] Lawal, S. A., Ugwuoke, I. C., Abutu, J., Lafia–Araga, R. A., Dagwa, I. M., & Kariim, I. (2016). Rubber Scrap as Reinforced Material in the Production of Environmentally Friendly Brake Pad. Reference Module in Materials Science and Materials Engineering. Oxford: Elsevier; 1–10.

[50] Bala, K. C., Okoli M., & Abolarin M. S., (2016). Development of automobile brake pad using pulverized cow hooves, Leonardo Journal of Sciences, 15(28) 95–108.

[51] Schaeffer, H. (2014), Seashell, retrieved from www.brittanica.com/EBchecked/ topic/5310 21/seashell

[52] Norazlina, H., Fahmi, A. R. M., & Hafizuddin, W. M. (2015). CaCO3 from Seashells as a Reinforcing Filler for Natural Rubber, Journal of Mechanical Engineering and Sciences, 8, 1481–1488.

[53] Vignesh K., Anbazhagan K., Ashokkumar E., Manikandan R., & Jayanth A. (2015). Experimental Analysis of Mechanical Properties of Sea Shell Particles– Polymer Matrix Composite, International Journal of Mechanical and Industrial Technology, 3(1)13–21.

[54] Michele, R. R., Hamestera, P. S. B. & Daniela, B. (2012). Characterization of Calcium Carbonate Obtained from Oyster and Mussel Shells and Incorporation in

Polypropylene. Journal of Materials Research, 15(2), 204–208.

[55] Albert, Y. M. L., Marc, A. M. & Kenneth, S. V. (2006). Mechanical properties and structure of Strombus gigas, Tridacna gigas, and Haliotis rufescens sea shells: A comparative study. Journal of Materials Science and Engineering, C 26, 1380 – 1389.

[56] Abiodun, A. O., Babatunde, B. & Chioma, I. M. (2014). Property Evaluation of Seashell Filler Reinforced Unsaturated Polyester Composite. International Journal of Scientific and Engineering Research, 5(11), 1343 – 1349.

[57] Ramanathan, K., Saravanakumar, P., Ramkumar, S., Pravin, K. P. & Surender, S. R. (2017). Development of Asbestos–Free Brake Pads using Lemon Peel Powder. International Journal of Innovative Research in Science, Engineering and Technology, 6(3), 4449 – 4455.

[1]Annamária BEHÚNOVÁ, [2]Marcel BEHÚN, [3]Lucia KNAPČÍKOVÁ

# ECONOMICAL POTENTIAL OF RECYCLED POLYVINYL BUTYRAL

[1,3]Technical University of Košice, Faculty of Manufacturing Technologies with a seat in Prešov, Prešov, SLOVAKIA
[2]Technical University of Košice, Faculty of Mining, Ecology, Process Control and Geotechnology, Košice, SLOVAKIA

**Abstract:** The European Union is planning to significantly reduce the landfill of plastic waste from the year 2020. Measures in Slovakia should be launched today, especially in the building industry sector.  It is necessary to prepare solutions for the recycling or energy utilization of used plastics materials, including plastic insulating materials. The building industry in Europe consumes up to 1/5 of the total volume of plastics production, it means up to 11 million tonnes. Waste plastics make up to a third of municipal waste in Europe, with nowadays ending in landfills. Up to 80% of plastic products are used once and then discarded. The landfills subsequently occupy a considerable area and inductive of air, water and soil pollution. This is why the measures should start as soon as possible.
**Keywords:** Economy, used plastics, recycled polyvinyl butyral

## INTRODUCTION

One of the basic tasks before launching a new product is to assess its prospective development, in terms of participants and dynamics, to identify:

—　key success factors,
—　current trends,
—　potential risks and
—　opportunities. [1]

The starting point is to determine an estimate of the actual size of the market, through various statistics, publicly published financial documents, marketing agency research or own research.

Revenues of primary end-users of plastics waste are dependent on the performance of the general economy, especially for safety glass, which is very important in the automotive and construction industry and in architecture (Figure 1).
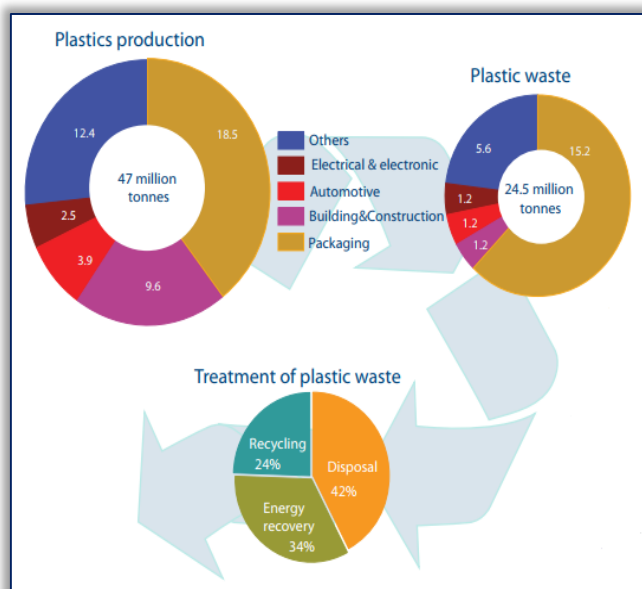


Figure 1. Total plastics waste in the Europe (year 2016) [2]

The European Commission report on the thematic strategy on the prevention and recycling of waste signals a move towards material-specific targets to meet the Europe 2020 objective of promoting a resource-efficient economy. However, an urgent revision, as much as better enforcement of the existing waste and packaging directives seems necessary, to address specific issues concerning plastic waste. Plastic waste could become a valuable resource if separate collection circuits were designed to ensure that single-use plastic packaging could be phased out through an effective roadmap towards the circular economy. In the market, polyvinyl butyral (PVB) resins are highly concentrated and are the domain of four companies - Eastman, Sekisui, DuPont and Kuraray. [2]

PVB is exported to countries with expanded car production. In most advanced countries, such as the United States, Western Europe and Japan, but also in the Middle East, demand for PVB is still high. In the context of the use of the security foil, PVB was especially preferred for architectural areas, such as laminated safety glass. PVB is a huge potential for the emerging market as a safety glass. [1], [2]

Figure 2 shows the location of the polyvinyl butyral sheet between the glass sheets and the safety glass.
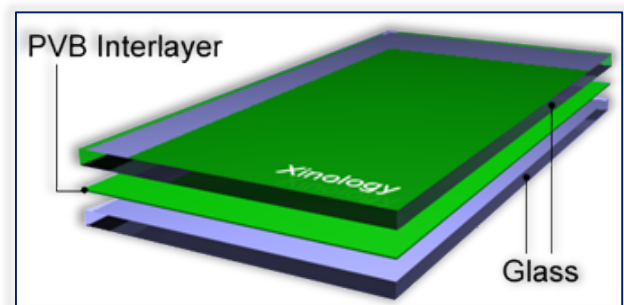


Figure 2. Polyvinyl butyral interlayer in the safety glass [3]

PVB film is one of the most important parts in the interlayer of a car glass or safety glass. Laminated glass, commonly used in architecture and the automotive industry, contains a

protective interlayer, most of which is a PVB that forms a fuse between two glass sheets. [3]

In terms of solar energy, there is a prediction that the fastest growing area of the PVB end-user, with regard to the compound annual growth rate, is projected to increase by more than 6% between 2015 and 2015 2023. [1], [3], [5] In terms of volume of PVB produced, the Asian region in 2014 contributed to more than 35% of the share of PVB use in the global market. The use of PVB film on the market in Latin America, the Middle East and Africa is expected to increase significantly over the next 8 years, mainly due to the increase in land transport and construction as end users [6].

The key producers of PVB are Eastman Chemical Company, Kuraray CO., LTD., Sekisui Chemical Co., Ltd., Li & Fung Group Co., Ltd., Kingboard Chemical Holdings Ltd., Huakai Plastic (Chongqing) Co., Ltd., Zhejiang Decent Plastic Co., Ltd., Tiantai Kanglai Industrial Co., Ltd., and Zhejiang Pulijin Plastic Co., Ltd. [4] These companies are working to actively research and develop new applications for the usability of PVB films and also to improve polyvinyl butyral itself, which are the composition and the subsequent properties. General areas of application are:

— coatings and primers
— printing inks for packaging
— films for laminated safety glass
— binders for ceramics and metal powders
— adhesives
— retroreflective coatings for traffic signs and road markings
— binders for a wide range of special applications
— use in thermoplastic applications

Polyvinyl butyrals meet the requirements for an enormous number of applications, e.g. interlayers for safety glass, paints, lacquers, varnishes, printing inks, temporary binder for ceramics and adhesives.

The PVB [8] application is mainly implemented in automotive industry, building industry - in architecture, solar energy and other areas.

## RECYCLED POLYVINYL BUTYRAL

Polyvinyl butyral, which forms a safety interlayer in windscreens or building glasses, by material recovery takes the form of flakes having a size of 2-20 mm and a thickness of 0.5 mm to 1.5 mm (see Figure 3).



Figure 3. Recycled polyvinyl butyral [8]

The granulate form is a more convenient alternative to the preparation for the next usability. Polyvinyl butyral, as thermoplastic material, is soluble in ethanol, butanol, ethyl acetate, butyl acetate, in a mixture of chlorinated hydrocarbons and insoluble in aliphatic hydrocarbons (in gasoline). The density of polyvinyl butyral is about 1.07 g.cm$^3$, and the recyclable sales price is 0.25 € to 0.50 € per kilogram.

— Application of recycled polyvinyl butyral

The laboratory preparation of recycled polyvinyl butyral is an important step to the successful end of the stated goal. Since polyvinyl butyral is loosely stored in big bags after recycling, there is of course the absorption of ambient moisture by the material itself. Recycled polyvinyl butyral contains impurities that are still present at the end of the recycling process, due to processing, packaging, storage. [5], [7] It is therefore necessary to get the material to the most suitable processing state before starting the process.

— Recycled Polyvinyl butyral used by laboratory experiments

Recycled polyvinyl butyral used in research has the following parameters (Table 1).

Table 1. Basic characterization of recycled polyvinyl butyral

| Recycled polyvinyl butyral (PVB) | |
|---|---|
| Form | flakes |
| Colour | clear |
| Size | 20-30 mm |
| Purity | more as 97% |
| Impurities | less as 3% |
| Humidity | ca. 2% |
| Glass particle | less as 2% |
| Fire point | - |
| Softening temperature | 130 ℃ - 170℃ |
| Viscosity (dynamic) | 100 – 175 m Pa*s (DIN 53015) |
| MVR (Melt Volume Rate) | 6 – 7 cm$^3$ / 10 min |
| MFR (Melt Flow Rate) | 5 – 6 g / 10 min |

## CONCLUSIONS

From the economic point of view, the use of this raw material is advantageous compared to the use of the primary raw material, since the price per kilogram ranges from 0.25€ to 0.50€ per kilogram. From a technological point of view, the consumer's properties of the material are not diminished (with the respect of selected application).

From the environmental point of view, minimization of waste material and its accumulation in waste dumps was achieved. In the area of exploring new materials, it is first and foremost important to understand and respond to the basic economic issues:

— What to produce?
— How to produce?
— For whom to produce?
— Why manufacture?
— What price to produce?

If these questions are answered and the solution options are worked out, then the work is successful. Nowadays, this is

evidenced by companies that have been on the market for decades.

References

[1] CRAWFORD R.J.: Plastics Engineering, Pergsmon Press, England. 1987Barry, C.M.F.-Orroth, S.A.:Processing of thermoplastics, In: Harper, CH.A.: Modern Plastics Handbook, USA,2000, ISBN 0-07-026714-6

[2] Plastic waste, Available on https://epthinktank.eu/2013/11/07/plastic-waste/

[3] PVB Film Available on http://www.xinology.com

[4] DIN Taschenbuch 18, Kunststoffe- Mechanische und thermische Eingeschaften, s. 251, ISBN 3-410-13421-2

[5] BEHÚNOVÁ A., a kol.: Znižovanie environmentálneho a ekonomického dopadu na životné prostredie využitím druhotných surovín (2016). In: Fyzikálne faktory prostredia. Roč. 6, mimoriadne č. 2 s. 14-17. - ISSN 1338-3922

[6] CHMIELEWSKA, E.: Odpady: Vysokoškolské skriptá. Bratislava: Prírodovedecká fakulta UK 1997, s. 129-130, ISBN 80-967774-3-2

[7] CRAWFORD R.J. : Plastics Engineering, Pergsmon Press, England. 1987Barry, C.M.F.-Orroth, S.A.:Processing of thermoplastics, In: Harper, CH.A.: ModernPlastics Handbook, USA,2000, ISBN 0-07-026714-6

[8] KNAPČÍKOVÁ, L, PEŠEK L.: Kompozitný materiál z recyklovaných textílií, úžitkový vzor č. 6907 : Vestník ÚPV SR č.: 052014 - Banská Bystrica : ÚPV SR - 2014. - 8 s..

# Fascicule 3
## [ July - September ]
## t o m e
## [2018] XI

ACTA Technica CORVINIENSIS
BULLETIN OF ENGINEERING

# MANUSCRIPT PREPARATION – GENERAL GUIDELINES

Manuscripts submitted for consideration to **ACTA TECHNICA CORVINIENSIS – Bulletin of Engineering** must conform to the following requirements that will facilitate preparation of the article for publication. These instructions are written in a form that satisfies all of the formatting requirements for the author manuscript. Please use them as a template in preparing your manuscript. Authors must take special care to follow these instructions concerning margins.

## INVITATION

We are looking forward to a fruitful collaboration and we welcome you to publish in our **ACTA TECHNICA CORVINIENSIS – Bulletin of Engineering**. You are invited to contribute review or research papers as well as opinion in the fields of science and technology including engineering. We accept contributions (full papers) in the fields of applied sciences and technology including all branches of engineering and management.

**ACTA TECHNICA CORVINIENSIS – Bulletin of Engineering** publishes invited review papers covering the full spectrum of engineering and management. The reviews, both experimental and theoretical, provide general background information as well as a critical assessment on topics in a state of flux. We are primarily interested in those contributions which bring new insights, and papers will be selected on the basis of the importance of the new knowledge they provide.

Submission of a paper implies that the work described has not been published previously (except in the form of an abstract or as part of a published lecture or academic thesis) that it is not under consideration for publication elsewhere. It is not accepted to submit materials which in any way violate copyrights of third persons or law rights. An author is fully responsible ethically and legally for breaking given conditions or misleading the Editor or the Publisher.

**ACTA TECHNICA CORVINIENSIS – Bulletin of Engineering** is an international and interdisciplinary journal which reports on scientific and technical contributions. Every year, in four online issues (fascicules 1–4), **ACTA TECHNICA CORVINIENSIS – Bulletin of Engineering [e-ISSN: 2067-3809]** publishes a series of reviews covering the most exciting and developing areas of engineering. Each issue contains papers reviewed by international researchers who are experts in their fields. The result is a journal that gives the scientists and engineers the opportunity to keep informed of all the current developments in their own, and related, areas of research, ensuring the new ideas across an increasingly the interdisciplinary field. Topical reviews in materials science and engineering, each including:

─ surveys of work accomplished to date
─ current trends in research and applications
─ future prospects.

As an open-access journal **ACTA TECHNICA CORVINIENSIS – Bulletin of Engineering** will serve the whole engineering research community, offering a stimulating combination of the following:

─ Research Papers – concise, high impact original research articles,
─ Scientific Papers – concise, high impact original theoretical articles,
─ Perspectives – commissioned commentaries highlighting the impact and wider implications of research appearing in the journal.

**ACTA TECHNICA CORVINIENSIS – Bulletin of Engineering** encourages the submission of comments on papers published particularly in our journal. The journal publishes articles focused on topics of current interest within the scope of the journal and coordinated by invited guest editors. Interested authors are invited to contact one of the Editors for further details.

## BASIC INSTRUCTIONS AND MANUSCRIPT REQUIREMENTS

The basic instructions and manuscript requirements are simple:

─ Manuscript shall be formatted for an A4 size page.
─ The all margins (top, bottom, left, and right) shall be 25 mm.
─ The text shall have both the left and right margins justified.
─ Single-spaced text, tables, and references, written with 11 or 12-point Georgia or Times Roman typeface.
─ No Line numbering on any pages and no page numbers.
─ Manuscript length must not exceed 15 pages (including text and references).
─ Number of figures and tables combined must not exceed 20.
─ Manuscripts that exceed these guidelines will be subject to reductions in length.

The original of the technical paper will be sent through e-mail as attached document (*.doc, Windows 95 or higher). Manuscripts should be submitted to e-mail: redactie@fih.upt.ro, with mention **"for ACTA TECHNICA CORVINIENSIS".**

## STRUCTURE

The manuscript should be organized in the following order: Title of the paper, Authors' names and affiliation, Abstract, Key Words, Introduction, Body of the paper (in sequential headings), Discussion & Results, Conclusion or Concluding Remarks, Acknowledgements (where applicable), References, and Appendices (where applicable).

## THE TITLE

The title is centered on the page and is CAPITALIZED AND SET IN BOLDFACE (font size 14 pt). It should adequately describe the content of the paper. An abbreviated title of less than 60 characters (including spaces) should also be suggested. Maximum length of title: 20 words.

## AUTHOR'S NAME AND AFFILIATION

The author's name(s) follows the title and is also centered on the page (font size 11 pt). A blank line is required between the title and the author's name(s). Last names should be spelled out in full and succeeded by author's initials. The author's affiliation (in font size 11 pt) is provided below. Phone and fax numbers do not appear.

## ABSTRACT

State the paper's purpose, methods or procedures presentation, new results, and conclusions are presented. A nonmathematical abstract, not exceeding 200 words, is required for all papers. It should be an abbreviated, accurate presentation of the contents of the paper. It should contain sufficient information to enable readers to decide whether they should obtain and read the entire paper. Do not cite references in the abstract.

## KEY WORDS

The author should provide a list of three to five key words that clearly describe the subject matter of the paper.

## TEXT LAYOUT

The manuscript must be typed single spacing. Use extra line spacing between equations, illustrations, figures and tables. The body of the text should be prepared using Georgia or Times New Roman. The font size used for preparation of the manuscript must be 11 or 12 points. The first paragraph following a heading should not be indented. The following paragraphs must be indented 10 mm. Note that there is no line spacing between paragraphs unless a subheading is used. Symbols for physical quantities in the text should be written in italics. Conclude the text with a summary or conclusion section. Spell out all initials, acronyms, or abbreviations (not units of measure) at first use. Put the initials or abbreviation in parentheses after the spelled-out version. The manuscript must be writing in the third person ("the author concludes… ").

## FIGURES AND TABLES

Figures (diagrams and photographs) should be numbered consecutively using Arabic numbers. They should be placed in the text soon after the point where they are referenced. Figures should be centered in a column and should have a figure caption placed underneath. Captions should be centered in the column, in the format "Figure 1" and are in upper and lower case letters. When referring to a figure in the body of the text, the abbreviation "Figure" is used Illustrations must be submitted in digital format, with a good resolution. Table captions appear centered above the table in upper and lower case letters.

When referring to a table in the text, "Table" with the proper number is used. Captions should be centered in the column, in the format "Table 1" and are in upper and lower case letters. Tables are numbered consecutively and independently of any figures. All figures and tables must be incorporated into the text.

## EQUATIONS & MATHEMATICAL EXPRESSIONS

Place equations on separate lines, centered, and numbered in parentheses at the right margin. Equation numbers should appear in parentheses and be numbered consecutively. All equation numbers must appear on the right-hand side of the equation and should be referred to within the text.

## CONCLUSIONS

A conclusion section must be included and should indicate clearly the advantages, limitations and possible applications of the paper. Discuss about future work.

## Acknowledgements

An acknowledgement section may be presented after the conclusion, if desired. Individuals or units other than authors who were of direct help in the work could be acknowledged by a brief statement following the text. The acknowledgment should give essential credits, but its length should be kept to a minimum; word count should be <100 words.

## References

References should be listed together at the end of the paper in alphabetical order by author's surname. List of references indent 10 mm from the second line of each references. Personal communications and unpublished data are not acceptable references.

**Journal Papers:** Surname 1, Initials; Surname 2, Initials and Surname 3, Initials: Title, Journal Name, volume (number), pages, year.

**Books**: Surname 1, Initials and Surname 2, Initials: Title, Edition (if existent), Place of publication, Publisher, year.

**Proceedings Papers:** Surname 1, Initials; Surname 2, Initials and Surname 3, Initials: Paper title, Proceedings title, pages, year.

**ACTA TECHNICA CORVINIENSIS – Bulletin of Engineering** is an international and interdisciplinary journal which reports on scientific and technical contributions.

The **ACTA TECHNICA CORVINIENSIS – Bulletin of Engineering** advances the understanding of both the fundamentals of engineering science and its application to the solution of challenges and problems in engineering and management, dedicated to the publication of high quality papers on all aspects of the engineering sciences and the management.

You are invited to contribute review or research papers as well as opinion in the fields of science and technology including engineering. We accept contributions (full papers) in the fields of applied sciences and technology including all branches of engineering and management. Submission of a paper implies that the work described has not been published previously (except in the form of an abstract or as part of a published lecture or academic thesis) that it is not under consideration for publication elsewhere. It is not accepted to submit materials which in any way violate copyrights of third persons or law rights. An author is fully responsible ethically and legally for breaking given conditions or misleading the Editor or the Publisher.

The Editor reserves the right to return papers that do not conform to the instructions for paper preparation and template as well as papers that do not fit the scope of the journal, prior to refereeing. The Editor reserves the right not to accept the paper for print in the case of a negative review made by reviewers and also in the case of not paying the required fees if such will be fixed and in the case time of waiting for the publication of the paper would extend the period fixed by the Editor as a result of too big number of papers waiting for print. The decision of the Editor in that matter is irrevocable and their aim is care about the high content-related level of that journal.

The mission of the **ACTA TECHNICA CORVINIENSIS – Bulletin of Engineering** is to disseminate academic knowledge across the scientific realms and to provide applied research knowledge to the appropriate stakeholders. We are keen to receive original contributions from researchers representing any Science related field.

We strongly believe that the open access model will spur research across the world especially as researchers gain unrestricted access to high quality research articles. Being an Open Access Publisher, Academic Journals does not receive payment for subscription as the journals are freely accessible over the internet.

## GENERAL TOPICS

### ENGINEERING
- ✔ Mechanical Engineering
- ✔ Metallurgical Engineering
- ✔ Agricultural Engineering
- ✔ Control Engineering
- ✔ Electrical Engineering
- ✔ Civil Engineering
- ✔ Biomedical Engineering
- ✔ Transport Engineering
- ✔ Nanoengineering

### CHEMISTRY
- ✔ General Chemistry
- ✔ Analytical Chemistry
- ✔ Inorganic Chemistry
- ✔ Materials Science & Metallography
- ✔ Polymer Chemistry
- ✔ Spectroscopy
- ✔ Thermo-chemistry

### ECONOMICS
- ✔ Agricultural Economics
- ✔ Development Economics
- ✔ Environmental Economics
- ✔ Industrial Organization
- ✔ Mathematical Economics
- ✔ Monetary Economics
- ✔ Resource Economics
- ✔ Transport Economics
- ✔ General Management
- ✔ Managerial Economics
- ✔ Logistics

### INFORMATION SCIENCES
- ✔ Computer Science
- ✔ Information Science

### EARTH SCIENCES
- ✔ Geodesy
- ✔ Geology
- ✔ Hydrology
- ✔ Seismology
- ✔ Soil science

### ENVIRONMENTAL
- ✔ Environmental Chemistry
- ✔ Environmental Science & Ecology
- ✔ Environmental Soil Science
- ✔ Environmental Health

## AGRICULTURE
✓ Agricultural & Biological Engineering
✓ Food Science & Engineering
✓ Horticulture

## BIOTECHNOLOGY
✓ Biomechanics
✓ Biotechnology
✓ Biomaterials

## MATHEMATICS
✓ Applied mathematics
✓ Modeling & Optimization
✓ Foundations & Methods

**ACTA TECHNICA CORVINIENSIS – Bulletin of Engineering** has been published since 2008, as an online, free-access, international and multidisciplinary publication of the Faculty of Engineering Hunedoara.

We are very pleased to inform that our international and interdisciplinary journal **ACTA TECHNICA CORVINIENSIS – Bulletin of Engineering** completed its ten years of publication successfully [**issues of years 2008 –2017, Tome I–X**]. In a very short period it has acquired global presence and scholars from all over the world have taken it with great enthusiasm.

Every year, in four online issues (**fascicules 1 – 4**), **ACTA TECHNICA CORVINIENSIS – Bulletin of Engineering** [**e-ISSN: 2067-3809**] publishes a series of reviews covering the most exciting and developing fields of science and technology. Each issue contains papers reviewed by international researchers who are experts in their fields. The result is a journal that gives the scientists and engineers the opportunity to keep informed of all the current developments in their own, and related, areas of research, ensuring the new ideas across an increasingly the interdisciplinary field.

Now, when we celebrate the tenth years anniversary of **ACTA TECHNICA CORVINIENSIS – Bulletin of Engineering**, we are extremely grateful and heartily acknowledge the kind of support and encouragement from all contributors and all collaborators!

On behalf of the Editorial Board and Scientific Committees of **ACTA TECHNICA CORVINIENSIS – Bulletin of Engineering**, we would like to thank the many people who helped make this journal successful. We thank all authors who submitted their work to **ACTA TECHNICA CORVINIENSIS – Bulletin of Engineering.**

**ACTA TECHNICA CORVINIENSIS – Bulletin of Engineering** exchange similar publications with similar institutions of our country and from abroad.

# INDEXES & DATABASES

We are very pleased to inform that our international scientific journal **ACTA TECHNICA CORVINIENSIS – Bulletin of Engineering** completed its ten years of publication successfully [2008–2017, Tome I–X].
In a very short period the **ACTA TECHNICA CORVINIENSIS – Bulletin of Engineering** has acquired global presence and scholars from all over the world have taken it with great enthusiasm.
We are extremely grateful and heartily acknowledge the kind of support and encouragement from all contributors and all collaborators!

**ACTA TECHNICA CORVINIENSIS – Bulletin of Engineering** is accredited and ranked in the **"B+" CATEGORY Journal** by **CNCSIS – The National University Research Council's Classification of Romanian Journals**, position no. 940 (http://cncsis.gov.ro/).
ACTA TECHNICA CORVINIENSIS – Bulletin of Engineering is a part of the **ROAD, the Directory of Open Access scholarly Resources** (http://road.issn.org/).

ACTA TECHNICA CORVINIENSIS – Bulletin of Engineering is also indexed in the digital libraries of the following world's universities and research centers:

WorldCat – the world's largest library catalog
https://www.worldcat.org/
National Lybrary of Australia
http://trove.nla.gov.au/
University Library of Regensburg – GIGA German Institute of Global and Area Studies
http://opac.giga-hamburg.de/ezb/
Simon Fraser University – Electronic Journals Library
http://cufts2.lib.sfu.ca/
University of Wisconsin-Madison Libraries
http://library.wisc.edu/
University of Toronto Libraries
http://search.library.utoronto.ca/
The University of Queensland
https://www.library.uq.edu.au/
The New York Public Library
http://nypl.bibliocommons.com/
State Library of New South Wales
http://library.sl.nsw.gov.au/
University of Alberta Libraries - University of Alberta
http://www.library.ualberta.ca/
The University of Hong Kong Libraries
http://sunzi.lib.hku.hk/
The University Library - The University of California
http://harvest.lib.ucdavis.edu/

ACTA TECHNICA CORVINIENSIS – Bulletin of Engineering is indexed, abstracted and covered in the world-known bibliographical databases and directories including:

INDEX COPERNICUS – JOURNAL MASTER LIST
http://journals.indexcopernicus.com/
GENAMICSJOURNALSEEK Database
http://journalseek.net/
DOAJ – Directory of Open Access Journals
http://www.doaj.org/
EVISA Database
http://www.speciation.net/
CHEMICAL ABSTRACTS SERVICE (CAS)
http://www.cas.org/
EBSCO Publishing
http://www.ebscohost.com/
GOOGLE SCHOLAR
*http://scholar.google.com*
*SCIRUS* - Elsevier
http://www.scirus.com/
ULRICHSweb – Global serials directory
http://ulrichsweb.serialssolutions.com
getCITED
http://www.getcited.org
BASE - Bielefeld Academic Search Engine
http://www.base-search.net
Electronic Journals Library
http://rzblx1.uni-regensburg.de
Open J-Gate
http://www.openj-gate.com
ProQUEST Research Library
http://www.proquest.com
Directory of Research Journals Indexing
http://www.drji.org/
Directory Indexing of International Research Journals
http://www.citefactor.org/